Ultimate strength of a large wind turbine blade

Jensen, Find Mølholt

Publication date:
2009

Document Version
Publisher's PDF, also known as Version of record

Risø-PhD-thesis

Ultimate strength of a large wind turbine blade

Find Mølholt Jensen

Risø-PhD-34(EN)
ISBN 978-87-550-3634-5
DTU BYG R-205-
ISBN=9788778772831

Risø National Laboratory for Sustainable Energy &
Department of Civil Engineering
Technical University of Denmark
Roskilde & Kgs. Lyngby, Denmark

Submission date May 2008

Author: Find Mølholt Jensen

Title: Ultimate strength of a large wind turbine blade

Department: Division of Wind Energy

Risø-PhD-34(EN)
Submission date May 2008

ISBN 978-87-550-3634-5

Contract no.:

Group's own reg. no.:
(Føniks PSP-element)

Sponsorship: Risø DTU, SSP-Technology and DAWE (Danish Academy of Wind Energy)

Cover :

Pages:
Tables:
References:

Information Service Department
Risø National Laboratory for Sustainable Energy
Technical University of Denmark
P.O.Box 49
DK-4000 Roskilde
Denmark
Telephone +45 46774004
bibl@risoe.dk
Fax +45 46774013
www.risoe.dtu.dk

Abstract

The present PhD project contains a study of the structural static strength of wind turbine blades loaded in flap-wise direction. A combination of experimental and numerical work has been used to address the most critical failure mechanisms and to get an understanding of the complex structural behaviour of wind turbine blades. Four failure mechanisms observed during the full-scale tests and the corresponding FE-analysis are presented. Elastic mechanisms associated with failure, such as buckling, localized bending and the Brazier effect, are studied.

In the thesis six different types of structural reinforcements helping to prevent undesired structural elastic mechanisms are presented. The functionality of two of the suggested structural reinforcements was demonstrated in full-scale tests and the rest trough FE-studies.

The blade design under investigation consisted of an aerodynamic airfoil and a load carrying box girder. In total, five full-scale tests have been performed involving one complete blade and two shortened box girders. The second box girder was submitted to three independent tests covering different structural reinforcement alternatives. The advantages and disadvantages of testing a shortened load carrying box girder vs. an entire blade are discussed. Changes in the boundary conditions, loads and additional reinforcements, which were introduced in the box girder tests in order to avoid undesired structural elastic mechanisms, are presented.

New and advanced measuring equipment was used in the full-scale tests to detect the critical failure mechanisms and to get an understanding of the complex structural behaviour. Traditionally, displacement sensors and strain gauges in blade tests are arranged based on an assumption of a Bernoulli-Euler beam structural response. In the present study it is shown that when following this procedure important information about distortions of the cross sections is lost. In the tests presented here, one of the aims was to measure distortion of the profile, also called 'local deformations', to verify a more complex response than that of a Bernoulli-Euler Beam. A large number of mechanical displacement sensors and strain gauges were mounted inside and outside the structure. These measurements further proved highly useful when validating Finite Element based analysis and failure mechanisms should be decided.

Finally, comparisons of the ultimate failure loads observed in the full-scale tests are presented and conclusions are drawn based on the mechanisms found.

The thesis consists of a comprehensive summary and a collection of three papers and four patent applications.

Synopsis

Det foreliggende Ph.d.-projekt indeholder et studie af strukturel statisk styrke af vindmøllevinger belastet i flapvis retning. En kombination af eksperimental og numerisk arbejde er blevet brugt til at adressere de vigtigste kritiske svigtmekanismer og at få en forståelse af den komplekse strukturelle opførsel af vindmøllevinger. 4 svigtmekanismer er blevet observeret i fuldskala forsøgene og de tilsvarende FE-analyser er præsenteret. Elastiske mekanismer relateret til svigt, som eksempelvis buling, lokal bøjning og Brazier effekt er studeret.

I afhandlingen er 6 forskellige strukturelle forstærkninger som modvirker uønsket strukturelle elastiske mekanismer præsenteret. Funktionen af de to foreslået strukturelle forstærkninger er blevet demonstreret i fuldskalatest og de resterende igennem FE-studier.

Vingen som er undersøgt består af et aerodynamisk profil og en bærende boksbjælke. I alt er der udført 5 fuldskalatests bestående af en komplet vinge og to afkortet boksbjælker. Den anden boksbjælke var benyttet i 3 uafhængige forsøg med uafhængige strukturelle forstærkninger indsat i bjælken. Fordele og ulemper ved at teste en afkortet boksbjælke mod versus en fuld vinge er diskuteret. Ændringer i randbetingelser, laster og ekstra forstærkninger som var introduceret til boksbjælke forsøgene var for at undgå uønsket strukturelle elastiske svigtmekanismer er præsenteret.

Nyt og avanceret måleudstyr var benyttet i fuldskalaforsøgene til at opdage kritiske svigtmekanismer og til at få en forståelse af den komplekse strukturelle opførsel. Traditionelt set benyttes kun strain gauges og globale deformationssensorer i vingeforsøg, baseret på en antagelse af Bernoulli-Euler bjælke strukturel gensvar. I det foreliggende studie det er vist at denne procedure medføre at vigtig information omkring distortion af tværsnittet er tabt. I forsøgene som er præsenteret, er et af formålene at måle distortion af tværsnittet også kaldet 'lokale deformationer', til at verificere et mere kompleks gensvar end en Bernoulli-Euler bjælke. Et stort antal af mekaniske deformationsfølere og strain gauges var monteret inde og uden på strukturen. Disse målinger viste sig at være meget værdifulde da FE-modellerne skulle valideres og svigtmekanismer bestemmes.

Til slut er sammenligninger af de ultimative svigtlaster præsenteret og konklusioner er draget.

Afhandlingen består af en uddybende sammendrag og samling af 3 videnskabelige artikler og 4 patentansøgninger.

Preface and acknowledgements

This thesis is submitted as partial fulfilment of the requirements for obtaining the PhD-degree at the Technical University of Denmark (DTU). The work has been carried out at the Wind Energy Department (VEA) at Risø DTU and the Department of Civil Engineering at DTU Byg. The PhD-project was funded by SSP-Technology, Risø DTU and DAWE (Danish Academy of Wind Energy).

The project has been supervised by Professor Henrik Stang from DTU Byg, Jakob Wedel-Heinen from DNV (Det Norske Veritas) and senior scientist Kim Branner from Risø DTU. I would like to acknowledge with appreciation the help, support, numerous and valuable comments, suggestions, criticism of my work.

As part of the PhD-programme at DTU a stay at a foreign university is encouraged. In the present study six months were spent at Imperial College-London, Department of Aeronautics in the period of 1st May-1st November 2004, under the supervision of Dr Brian Falzon and Dr Jesper K. Ankersen. I would like to express my gratitude to Brian and Jesper for many fruitful discussions and their help and inspiration particularly with respect to obtaining knowledge from the aeronautical industry. At my 6 months stay in the UK, I also met Dr Paul Weaver and Dr Luca Checchini from the University of Bristol, Department of Aerospace Engineering, with whom I have had (and still have) a fruitful cooperation. I want to acknowledge the many interesting discussions we have had about what lessons the wind turbine industry can learn from the aeronautical industry. In the last year I have also had interesting research cooperation with Dr John Dear and his group at Imperial College- Department of Mechanical Engineering and Andy Morris from E.ON UK. They have performed a significant amount of relevant experimental work on test specimens from wind turbine blades provided by SSP-Technology.

I also want to thank Peter Hjuler Jensen, Head of programme, Wind turbines in VEA and Søren Larsen, Head of the VEA educational programme at Risø DTU. Without their support – personal as well as financial – it would not have been possible to carry out the substantial experimental programme associated with my study. Furthermore, their support allowed for the half year stay abroad with my family. My many other colleagues have also been a great help and encouragement and without them it would not have been possible to do the five time-consuming full-scale tests, submit four patent applications with many drawings, etc.

Finally, I wish to express my gratitude to Flemming Sørensen and Rune Schytt-Nielsen from SSP-Technology. I am very grateful for their qualified guidance and the many inspiring discussions during my participation in their development and certification work during the first part of my PhD study.

Finally, I wish to express my deepest gratitude to my lovely wife who has been an extremely valuable support during the entire PhD-study. Without her, I would never have finished this thesis.

Find Mølholt Jensen
May 2008

"Preface to the published version of the thesis.

The thesis was defended at a public defense on Friday 13th, February 2009.

Compared to the original submitted version of the thesis a number of minor editorial corrections and clarifications have been implemented."

Table of Contents

Publications

Definitions and symbols

1 Introduction 1

1.1 Scope and motivation 1

1.2 State of the art 2

1.3 Discussion of state of the art 5

1.4 Current work and organization of the PhD-thesis 8

1.5 Organization of the PhD-thesis 9

2 Full-scale tests 11

2.1 Overview of full-scale tests 11

2.2 Loads in the full-scale tests 13

2.3 Test setup 15

3 Measurement equipment used for full-scale tests 18

3.1 Strain gauge measurements in the full-scale tests 18

3.2 Mechanical displacement sensors in a cross section 20

3.3 DIC-system used for measuring deformation panels on a local scale 22

3.4 Structural health monitoring 24

4 FE-model 25

4.1 Calibration of stiffness in the FE-model based on experimental results 26

4.2 Realistic combined load scenario 27

5 Elastic response of a blade box design 29

5.1 Brazier load – Geometrically non-linear phenomena 29

5.2 Buckling – Geometrically non-linear phenomena 31

5.3 Localized bending - Linear phenomena 33

6 Failure mechanism in a blade box design 37

6.1 Skin peeling – Debonding of the aerofoil from the box girder 37

6.2 Interlaminar shear failure in the cap caused by Brazier loads 38

6.3 Web failure 40

6.4 Transverse shear distortion of the cross section 45

7 Design reinforcements 47

7.1 Rib/Bulkhead reinforcement 47

7.2 Invention: ‘Cap reinforcement’ (Patent A) 50

7.3 Invention ‘Web coupling reinforcement’ (Patent B) 54

7.4 Invention: ‘Floor reinforcement’ (Patent B) 55

7.5 Invention: 'Shear cross reinforcement' (Patent C) 59
7.6 Invention: 'U-design' (Patent D) 60
7.7 Future blade design – Use of combined reinforcements 62

8 Summary of ultimate loads obtained in the full-scale tests 64

9 Conclusions and future work 65

9.1 Conclusions and discussions 65
9.2 Future work 67

10 References 70

Appendix A – Key papers .....

Appendix A2 – "Full-scale testing and finite element simulation of a 34 metre long wind turbine blade". Find M. Jensen, Andy Morris .....

Appendix A3 – "Structural testing and numerical simulation of a 34m. composite wind turbine blade". Find M. Jensen, Brian G. Falzon, Jesper Ankersen, Henrik Stang .....

Appendix B - Patents .....

Appendix B1 - "WO 2008-071195 Reinforced aerodynamic profile"(cap reinforcement- patent A). Find M. Jensen .....

Appendix B2 - "WO 2008-086805 Reinforced blade for wind turbine (floor- patent B)". Find M. Jensen .....

Appendix B3 - "WO 2008-089765 Reinforced blade for wind turbine (shear cross- patent C)". Find M. Jensen, Per H. Nielsen .....

Appendix B4 - " WO 2008-092451 Wind turbine blade(U-profile-patent D ". Find M. Jensen .....

Publications

Several parts of the work done in the present PhD-study have been published. Three key papers and four patent applications are an integrated part of the PhD-thesis. They can be found in appendix A and B, respectively.

Several other conference papers and data reports from experimental work have been prepared during the study. Furthermore, three other patent applications related to the work in study have been submitted. A list of these papers, data reports and patent applications can be found below. The conference papers prepared together with John Dear's group are related to experimental work performed by PhD-students at Imperial College – London, Department of Mechanical Engineering. These papers are referred to but not included in the thesis. The two data reports report on the 5 full-scale tests, but no conclusions are drawn in these reports. The data reports can be provided upon request.

Key papers – attached in appendix A

Jensen, F.M., Weaver, P.M, Cecchini, L.S, Stang, H., Nielsen, R.F. "*The brazier effect in wind-turbine blades and its influence on design*" (Submitted "Strain – An international Journal for Experimental Mechanics, June 2008).

Jensen, F.M., Morris, A. NAFEMS world congress. "*Full-scale testing and finite element simulation of a 34 metre long wind turbine blade*". (April 2007).

Jensen, F.M., Falzon, B.G., Ankersen, J., Stang, H.. "*Structural testing and numerical simulation of a 34m. composite wind turbine blade*". Composite structures 76 (2006).

Patent applications – attached in appendix B

Jensen, F.M. *"WO 2008-071195 Reinforced aerodynamic profile" (cap reinforcement- patent A)*

Jensen, F.M.*"WO 2008-086805 Reinforced blade for wind turbine (floor- patent B)"*

Jensen, F.M., Nielsen, P.H. *"WO 2008-089765 Reinforced blade for wind turbine (shear cross- patent C)"*

Jensen, F.M. *"WO 2008-092451 Wind turbine blade(U-profile-patent D)"*

Other publications published in the PhD-period

Conference papers:

Jensen, F.M., Falzon, B.G., Ankersen, J., Stang, H. "*Structural testing and numerical simulation of a 34m. composite wind turbine blade*". ICCM15-paper, conference in Durban (June 2005).

Jensen, F.M.. *"Bending behaviour of a wind-turbine blade under full-scale testing"*. Keynotepresentation. NAFEMS-UK seminar in UK, 5-pages abstract (November 2006).

Jensen, F.M., Weaver, P.M, Cecchini, L.S., Stang, H. *" On aspects of non-linear bending behaviour of a wind-turbine blade under full-scale testing"*. Abstract for COMPTEST 2006 conference in Porto (April 2006).

Branner, K., Jensen, F.M., Berring, P., Puri, A., Morris, A., Dear, J.P. "*Effect of sandwich core properties on ultimate strength of a wind turbine blade*". 8th edition. International conference on sandwich structures. (April 2008).

Puri, A., Dear, J. P., Morris, A., Jensen, F.M. *"Analysis of Wind Turbine Material using Digital Image Correlation"*. EWEC conference (2008).

Puri, A., Fergusson, A., Dear, J.P., Morris, A., Jensen, F. M. "*Digital image correlation and finite element analysis of wind turbine blade structural components*". 2007 european offshore wind energy association conference. Germany, (December 2007).

Dear, J.P., Puri, A., Fergusson, A., Morris, A., Dear, I., Branner, K., Jensen, F.M. "*Digital image correlation and finite element analysis of wind turbine blade structural components*". International conference on sandwich structures. (April 2008).

Data reports:

Jensen, F. M., K. Branner, P. H. Nielsen, P. Berring, T. S. Antvorskov, M. Nielsen, B. Lund, C. Jensen, J. H. Reffs, R. F. Nielsen, P. H. Jensen, M. McGugan, K. Borum, R. S. Hansen, C. Skamris, F. Sørensen, R. S. Nielsen, J. H. Laursen, M. Klein, A. Morris, A. Gwayne, H. Stang, J. Wedel-Heinen, J. P. Dear, A. Puri, A. Fergusson. "*Full-scale Test of a SSP34m box girder 1 – Data Report*". Risø-R-RIS88(EN). (March 2008).

F. M. Jensen, K. Branner, P. H. Nielsen, P. Berring, T. S. Antvorskov, M. Nielsen, J. H. Reffs, P. H. Jensen, M. McGugan. C. Skamris, F. Sørensen, R. S. Nielsen, J. H. Laursen, M. Klein, A. Morris, H. Stang, J. Wedel-Heinen, J. P. Dear, A. Puri, A. Fergusson. "*Full-scale Test of a SSP34m box girder 2 – Data Report*". Risø-R-1622(EN) (May 2008).

Other related patent applications:

Jensen, F. M.*"080701 P12735 DK Soft Floor (patent B2)"* Submitted March 2008

Jensen, F. M. *"080623 P12736 DK Angled Girders (patent C2)"* Submitted March 2008

Jensen, F. M., Nielsen, P. H. *"080624 P12737 DK Coupling of trailing edge panels (patent E)"* Submitted March 2008

Definitions and symbols

Definitions:

AE : Acoustic Emission
Blade root: Part of the rotor blade that is closest to the hub
Box girder: Primary, lengthwise structural member of a wind turbine rotor blade
Design loads: Loads that the turbine is designed to withstand. They are obtained by applying the appropriate partial load factors to the characteristic values
DIC: Digital Image Correlation
Edgewise: Direction that is parallel to the local chord of the blade
Failure Mechanism: A structural response of a structure that is the key driver for strains leading to failure
FEM: Finite Element Method
Flapwise: Direction that is perpendicular to the surface swept by the non-deformed rotor blade axis
NDT: Non Destructive Testing
Trailing edge: Aft portion of a blade normally pointed
Ultimate strength: Measure of the maximum (static) load-bearing capacity of a material or structural element

List of symbols:

E: Young's modulus
h: Box girder's depth
I: Second moment of area
l : Segment length
κ: Bending curvature of beam
M: Bending moment
ν : Poisson's ratio
P_{crush}: Crushing pressure acting on each shear web, per unit length of the blade
R: Bending radius of the box girder
w : Local width of the box girder
z: Distance to the neutral axis
δ: Local deflection
ε: Local strain
ψ_{braz} : Brazier crushing force
$1/A_{11}$: In-plane laminate stiffness in 1-direction

1 Introduction

1.1 Scope and motivation

We currently notice a substantial growth in the wind energy sector worldwide. This growth is expected to be even faster in the coming years. By the end of 2006 almost 1% of the world's electricity generation was produced by wind turbines. According to BTM consult ref. [11] the forecast for 2011 is 2% of world's electricity generation and the estimation for 2016 is 4%. This means that a massive number of wind turbine blades will be produced in the forthcoming years. There is a large potential for materials savings in these blades. The scope of the present work is to investigate the structural, static strength of a particular type of wind turbine blade and through this to assess the potential for materials savings and consequent reductions of the rotor weight. The entire wind turbine can benefit from such weight reductions through decreased dynamics loads and thus leave room for further optimization. Figure 1 shows the positive effect of the reduced rotor weight (with a possible reduced cost) on the cost of other components in the wind turbine.

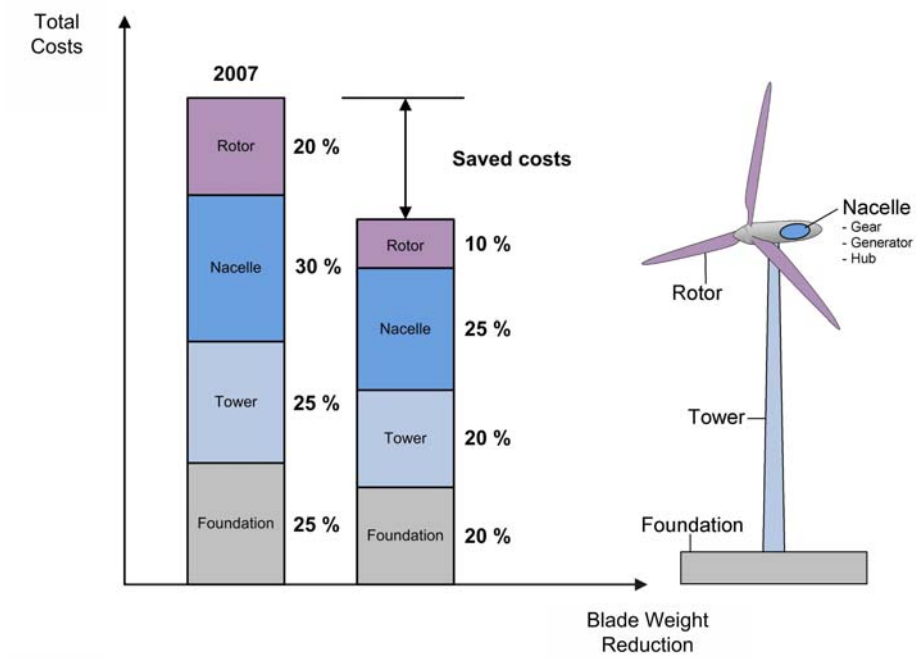

Figure 1. The figure shows the influence of blade optimization on the cost of an entire wind turbine. The components in an entire wind turbine are shown on the far right. The left column shows the relative costs of the various components of a current wind turbine. The column to the right indicates the relative costs of a future wind turbine with reduced weight of the blades. The numbers are estimated based on experience.

The cost of the rotor represents only a lower percentage (approx. 20%) of the entire wind turbine, but as shown in the figure reductions in this part will have a significant favourable effect on other components.

1.2 State of the art

Blade design

The design of the aerofoil of a wind turbine blade is a compromise between aerodynamic and structural (stiffness) considerations. Aerodynamic considerations are dominating the design of the outer two thirds of the blade while structural considerations are more important for the design of the inner one third of the blade.

Structurally the blade is typically hollow, with the outer geometry formed by two shells: one on the suction and one on the pressure side. To transfer shear loads, one or more structural webs are fitted to join the two shells together, see Figure 2a and Figure 2b.

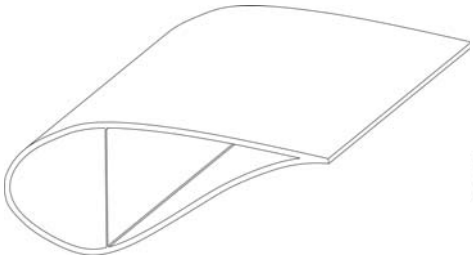

Fig. 2a

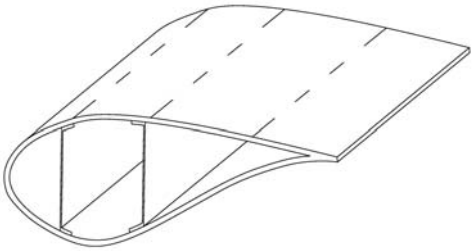

Fig. 2b

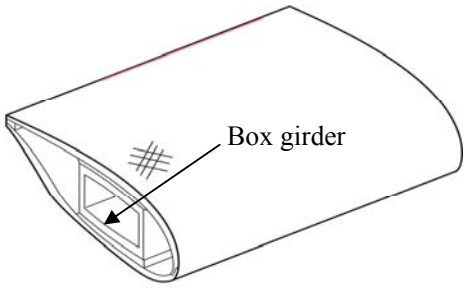

Fig. 2c

Figure 2. Sketches of different blade concepts a) Blade design with one shear web b) Blade design with two shear webs c) Blade design with a load carrying box girder.

A load carrying box girder is used in some blade designs, see Figure 2c. Such designs correspond to blades with two webs.

In Figure 3, three blade designs from different manufacturers (LM Glasfiber, SSP-Technology and Vestas) are shown. In the blade from LM Glasfiber an upper shell, a lower shell and two webs are bonded together to form the blade structure as shown in Figure 3a. In the blade from SSP-Technology a box girder is created of two half parts bonded together, Figure 3b, while Vestas uses a box girder which is manufactured on a mandrel, Figure 3c.

Fig. 3a Fig. 3b Fig. 3c

Figure 3. Different wind turbine blade designs. a) LM-Glasfiber design. b) SSP-Technology design. c) Vestas box girder design.

In Figure 4 rib/bulkhead solutions from 2 different blade manufacturers are shown.

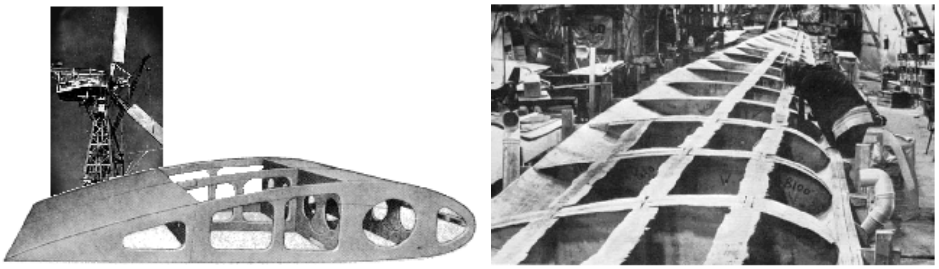

Fig. 4a Fig. 4b

Figure 4. Ribs/Bulkheads used in wind turbine blades. a) Photo of a 200 foot diameter wind turbine from United States Plywood Corporation, see ref. [73]. b) Sketch of a Tvind Wind turbine blade from ref. [90].

The blade design from 1948, shown in Figure 4a, was used in a 200 foot diameter wind turbine which was the first to implement ribs in a wind turbine blade. The blade was manufactured by plywood with ribs of stainless steel. Current blade manufacturing technology based on thermo-setting composites is not suitable for producing rib reinforced blades in an economically sound manner, see ref. [75],[76]. However rib/bulkhead blade design using a thermoplastic with a reactive processing together with vacuum infusion is currently under development, see [75], [76]. Today there are limitations in the melt processing and consequently the size and the thickness is limited. However, if current research in materials technology is successful, ribs/bulkhead design could be re-introduced in the wind turbine blades, see ref. [44].

Materials and manufacturing

There is a wide range of materials and manufacturing techniques utilized in the wind turbine industry today. The material combinations used are predominantly composite laminates with embedded threaded steel rods in the root section connecting the blade to the hub in a bolted connection Polyester, vinyl ester and epoxy resins are common, matched with reinforcing wood, glass, and carbon fibres. Some designs integrate carbon- and glass fibre as well as birch and balsa wood, see ref. [51], [52]. A general overview of materials used in wind turbine blades can be found in ref. [10], [75]. A wide range of manufacturing processes are also utilized in blade manufacturing, encompassing: wet lay-up, pre-preg, filament winding, pultrusion, and vacuum infusion (with and without secondary adhesive bonding). More details can be found in ref. [17].

Finite Element modelling and structural design optimization

Only a limited number of publications on Finite Element (FE) modelling and structural analysis of wind turbine blades are available in current literature, [7], [28], [39], [40], [41], [43], [44], [53], [68]. Most available research done on FE-analysis of wind turbine blades are global FE-models of the entire blade where strains, global deflections and eigenfrequencies are found, see e.g. ref. [48], [49].

Buckling is one of the areas where most research relevant for structural design optimization has been done, see e.g. ref. [18], [37], [51], [54], [55].
Another important problem which has received much attention is the bend-twist couplings of the wind turbine blade, see ref. [3], [6], [19], [44], [57], [58]. This research field is becoming increasingly important as the blades gradually become large enough to cause flutter instability as known from helicopter design.

There has been comprehensive research in failure modelling which take interlaminar crack growth into consideration [65], [66], [91]. In ref. [2], [4], [5], [15], [27], [46], [61], [72], sections, panels and beams from wind turbine blades were analysed. Interlaminar crack growth has been studied very intensively in other industries the last two decades, and has recently become an important area of the research related to the wind turbine industry.

Testing approach

In Figure 5 a pyramid representing a multi-scale approach to testing is shown. The pyramid in Figure 5 is a collection of tests which have been performed at Risø DTU or at DTU Campus over the last 4-5 years. Only full-scale tests (level 1) and the small specimen tests (level 5, right) are required by the certifying agencies when preparing the documentation forming the basis for type certification, see ref. [17], [24], [26].

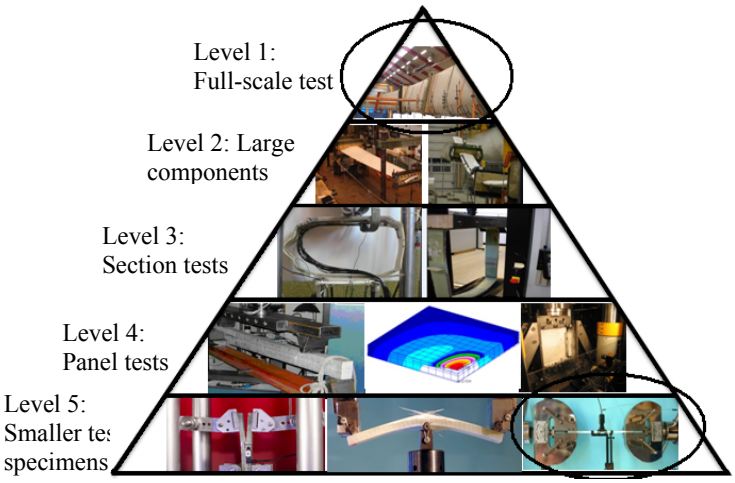

Figure 5. Multi-scale approach for testing and analysis of wind turbine blades used at Risø DTU. The experiments are performed either at Risø DTU or at DTU Campus.

Risø DTU and DTU Campus are trying to systemize subcomponent testing (levels 2-5) so that such testing can be used in a design and certification process. This approach has also been used in recent years at numerous wind turbine manufacturers, see ref. [50], [87]. The approach is expected to be adopted in the certification process in the future, see ref. [17], [87]. In the latest version published in 2008 of "DNV-Risø Guideline for design of wind turbines' a description of this approach, called "Building block approach', can be found, see ref. [17]. In ref. [77] stochastic models for strength of wind turbine blade using experimental results on different levels are presented. Load application in level 1 testing is traditionally very simplistic and today, only separate flap- and edgewise load cases are required by the certification bodies, see ref. [16], [24]. Examples of more sophisticated load applications can be found in [3], [6].

Measurement equipment used for full-scale test of wind turbine blades

Traditionally, only very few measurement techniques have been used in full-scale testing of wind turbine blades; at least very little has been published, see ref. [37], [38], [45], [78]. No full scale tests utilizing advanced equipment have been reported in the available literature. Displacement sensors and strain gauges are used in certification tests to monitor and verify that the global bending stiffness and that the local strains stay within the design limits and design calculations, see e.g. ref. [88]. Guidance in blade certificate testing is given in [16], [26].

Acoustic Emission has been used several times before, see ref. [46], [60], and mainly for research purposes. In Chapter 3 some of the measuring techniques used in the full-scale tests presented in this thesis are described. An overall picture of state of the art in measuring techniques can be found in ref. [37].

1.3 Discussion of state of the art

Design

Due to the fact that current wind turbine blade designs are not thoroughly optimized with regards to structural strength, large differences can be found in the safety against various types of failure modes. The safety against different failure modes including material, structural and buckling failure in current design is illustrated in Figure 6. Buckling and structural strength have been separated, even though both relate to the structural aspect. This is done in order to illustrate the difference in unused capacity.

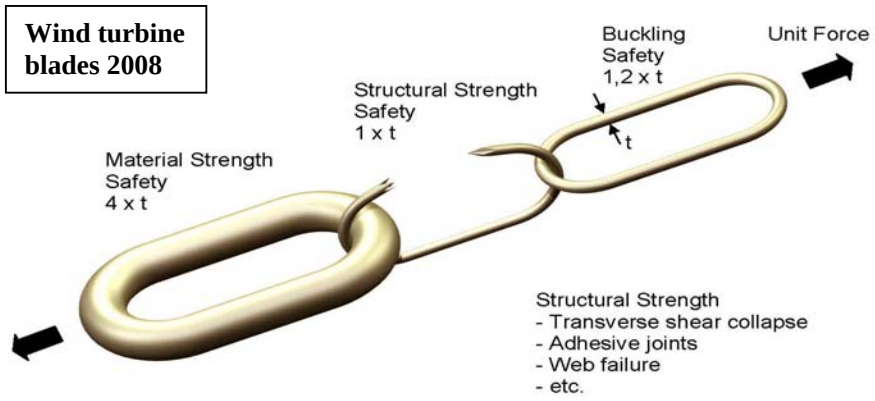

Fig. 6a

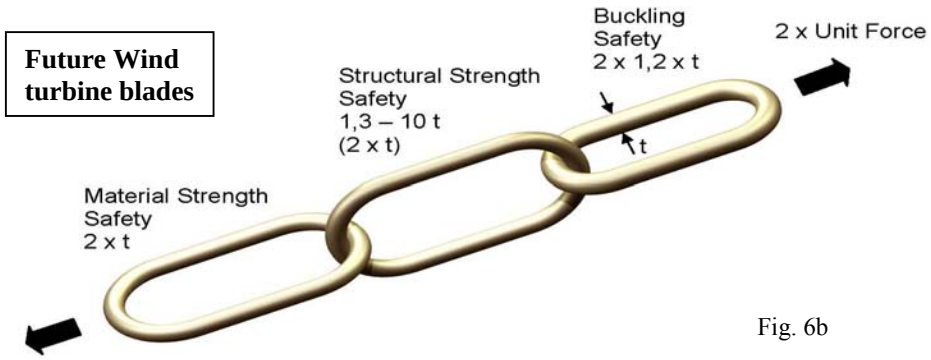

Fig. 6b

Figure 6. Illustration of the safety margins for current (a) and future (b) wind turbine blades. The parameter 't' representing the thickness of the chain links illustrates the safety against ultimate failure. The figures are estimated based on experience in this PhD-project and panel tests prepared by colleagues at DTU-Campus and Risø DTU, see ref. [2], [5], [27], [61]. The arrows represent the safety of the chain illustrated by unit forces. In Figure 6b the chain can carry two times the unit force while the Figure 6a only one unit force can be carried.

Figure 6a illustrates that the material strength enjoys a very large safety margin in modern wind turbine blades. This assumption is based on experimental work [2], [5], [7], [27], [61] where panels from three blade manufacturers have been tested in compression. The experimental setup and the materials, layups and the production methods were similar to the actual blade. Strains measured in the panel tests, with large defects, were in the range of 20-25000μS, which is a factor of 4-5 times higher than those measured in full-scale tests, see ref. [37], [38], [88]. For panels with a large embedded defect the strain levels were in the range of 10-15000μS, which is a factor 2-3 higher than obtained in the full-scale tests.

Figure 6 also illustrate that the safety margin (or reliability) of the optimized (Figure 6b) chain can carry double the load of the chain shown in Figure 6a representing current wind turbine blades.

Testing and Finite Element Analysis

Subcomponent testing (level 2 and 3 in Figure 5) will be of increasing importance in the future since the size of the blades, the number of manufactured blades and the

general cost increase. Full-scale testing is a very costly and time consuming final verification of the design and all technical risks associated with the full-scale testing are sought minimized through testing on coupon and component level as well as non-linear FE-analysis. Finite Element Analysis (FEA), however, has certain limitations. FE analysis does not take defects from the manufacturing process into account and failure criteria of composites are inaccurate particularly under non in-plane loading conditions. Failure criteria may be improved by taking fracture mechanical failure into account, but today it is unrealistic to include all types of interlaminar crack growth in an analysis of an entire wind turbine blade or a larger section, mainly due to computational limitations. Furthermore, the input to fracture mechanics models e.g. the cohesive opening laws (ref. [23], [81], [91]) still need further development before they are reliable at all load conditions. Particularly the mix mode opening problems are not fully understood, see ref. [78], [79], [81], [91].

As mentioned, more systematised experimental testing should be used in connection with large numerical non-linear FE-models which do not necessarily take failure into account, but which take more complex loading into consideration. The increasing complexity of the FE-models, including the non-linearity and the complex load cases, will introduce new elastic failure mechanisms which have not received much attention today. This is explained more in details in Chapter 5.

The main purpose of rotor blade testing is to verify its structural strength for static and fatigue loading. The main advantage of full-scale testing, compared with numerical FE-simulation, is that it gives a 'true' picture of the blade's capacity (fatigue and ultimate strength), including defects from production. This, however, only holds for the load case tested, and unfortunately only a few simple load cases are tested on one or a few blade samples. These are typically two flapwise and two edgewise load cases. The combination of these loads should also be considered in the future, since this is a realistic load scenario, see Figure 7. Here, a typical distribution of the aerodynamic pressure is illustrated resulting in combined flap- and edgewise load cases.

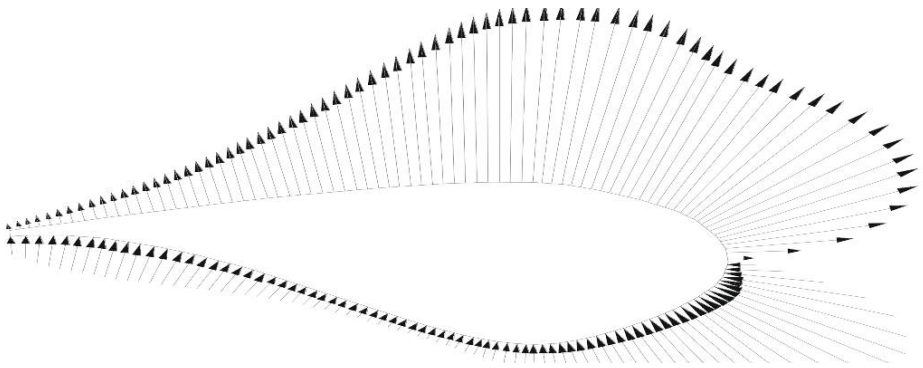

Figure 7. Aerodynamic loads on a wind turbine blade (pressure and drag) including gravity loads result in combined flap- and edgewise load case.

FE-studies, presented in Section 6.4, have shown that this should be considered more carefully in the future. Failure mechanisms and stress distributions different from

those of the traditional load cases tested have been observed when combined loads are applied. Also, the way in which loads are applied in the full-scale test should be reconsidered since the contour of the typical clamps used for load application prevent the blade from distorting in a realistic manner, see Figure 8a. The influence of the non-realistic load introduction is analysed in Section 6.4 and 7.4.

Fig. 8a

Fig. 8b

Figure 8. Different ways to apply load to the blade structure a) Loading clamp used at Blaest test centre b) Anchor plates are used in the full-scale tests at Risø DTU.

New clamps currently being developed at Risø DTU (called anchor plates, see Figure 8b) will allow transverse shear distortion and are used in the coming full-scale tests, see Section 9.2

1.4 Current work and organization of the PhD-thesis

In the present PhD-project, the structural strength of large wind turbine blades with a load carrying box girder has been studied. A combination of experimental and numerical work has been used to address the most critical failure mechanisms, and to get an understanding of the complex structural behaviour. Focus has been placed on level 1-2 in the pyramid shown in Figure 5. Especially the load carrying box girder has received attention as it is the most important structural member. Results from levels 3-4 have – to a smaller extent – been included in the work. The experimental work on these scales have mainly been performed by master students at DTU, Department of Mechanical Engineering and PhD-students at Imperial College – London, Department of Mechanical Engineering, see ref. [15], [37], [63], [71], [72]. All the tested specimens in the references are from SSP-Technology and related directly to the 34m SSP-blade tested in this PhD-project.

Five full-scale tests have been performed investigating the performance of an original design as well as improved designs with various types of structural reinforcements. New, advanced measuring equipment has been employed to detect the critical failure mechanisms. The full-scale tests are compared and a discussion of failure mechanisms and influence of the implemented structural reinforcement is presented.

The knowledge gained from the full-scale tests, FE-analysis and studies on aeronautical structures resulted in the proposal of six structural reinforcements. The suggested reinforcements prevent different structural elastic failure mechanisms. The effect of some of the suggested reinforcements were demonstrated experimentally and others through FE-analysis. The focus was on the blade design from the industrial partner (SSP-Technology), but most of the addressed failure mechanisms and suggested reinforcements are expected to have relevance for other blade designs as well.

In the present PhD-project only the static strength was studied. However, the majority of failure mechanisms, as well as suggested reinforcements, are also relevant for dynamic fatigue loads. Buckling is one of the elastic mechanisms, which sometimes are found critical for wind turbine blades, but in this thesis other elastic mechanisms have been found to be more critical for the current SSP-blade design.

1.5 Organization of the PhD-thesis

This thesis is composed as follows.

Chapter 2. An overview of the full-scale tests is presented. Advantages and disadvantages of testing a load carrying box girder vs. an entire blade are discussed.

Chapter 3. Measuring equipment used in the full-scale tests is presented.

Chapter 4. One of the FE-models is presented and a calibration approach used in the FE-studies is discussed. The chapter ends with a description of how the combined loads are included in the FE-studies.

Chapter 5. Elastic structural phenomena observed during full-scale tests and in the numerical analysis are presented. Elastic responses such as buckling, localized bending and the Brazier effect are studied.

Chapter 6. Four failure mechanisms observed during the full-scale tests and the FE-modelling are presented. The relevance of observed failures to future blade designs is discussed.

Chapter 7. Based on the knowledge of the elastic responses and the observed failure mechanisms, six structural reinforcements are suggested and presented in this chapter. Two of the suggested reinforcements (ribs and cap reinforcement) are validated in full-scale tests, and the test results are given. Another type of reinforcement is validated by experiments on a component level. The three last structural reinforcements have not been verified by experimental tests; only numerical work has been performed, but plans for experimental work (proof of concept) are presented. Future blade designs utilizing combined reinforcement are presented at end of the chapter.

Chapter 8. Conclusions based on comparisons of experimental full-scale tests are presented.

Chapter 9. Conclusions and future work are presented.

2 Full-scale tests

In the present PhD-project one blade and two box girders have been tested. The blade and the box girders are manufactured by the industrial partner, SSP-Technology. The second box girder was subjected to three full-scale tests with different reinforcements inserted. Results from full-scale tests are presented in Chapter 6-8 and in three data reports, see ref. [37], [38], [88]. The experimental results are analysed in Chapter 6-8 and in following papers [7], [28], [39], [41], [42], [43].

This chapter starts with an overview of the full-scale tests and the introduced reinforcements.

2.1 Overview of full-scale tests

The five full-scale tests performed in the present PhD-project are listed in Table 1.

Full-scale test	Blade/Box girder	Additional reinforcement	Test period	Figure reference
Test 1	Blade 1	No additional reinf.	Spring 2005	Figure 9
Test 2	Box girder 1	Web+Tophat reinf.	August 2006	Figure 10
Test 3	Box girder 2	Web reinforcement	March 2007	Figure 11
Test 4	Box girder 2	Web + Cap reinf.	March 2007	Figure 66
Test 5	Box girder 2	Web + Rib reinf.	April 2007	Figure 60

Table 1. List of full-scale tests performed in the PhD-project. The additional reinforcements mentioned are described in detail in Chapter 7.

The first full-scale test was done on the blade without any additional reinforcement. It was a part of a certification test, which the blade passed without any problems. See ref. [88]. After the certification test, destructive testing was performed; still without additional reinforcement, but with extra measuring equipment. The destructive testing and the extra measurement equipment setting is a part of this PhD-project, see Figure 9.

Figure 9. Photo of the first full-scale test of a 34m SSP-blade with extra measuring equipment.

The four following full-scale tests were conducted with the load carrying box structure, mainly to minimise costs, but other advantages were also taken into account. An explanation of this is given later in this chapter. The tip section from 25-34m was not important for the scope of this test. Therefore it was cut off. This reduced the cost, since two load stations in the tip are neglected, see Figure 10 and Figure 11.

Figure 10. Photo of the first shortened 34m SSP-box girder (test 2). The box girder has been shortened to 25.5m.

The second box girder (test 3-5) was tested with the same load distribution and boundary conditions as the first box girder test (test 2). The only difference is that the second box girder had no top hat reinforcement, see explanation later in this chapter. Both box girders had reinforcement on the shear web connections, because the first full-scale test had revealed a weak point here, see Section 6.3.

Figure 11. Photo of the second box girder test (test 3-5). The second box girder has also been shortened to 25.5m

The second box girder tested was involved in three independent full-scale tests where two different types of reinforcement were investigated. The first test with the second box girder (test 3) was performed to be a good reference for comparison for the following test as it had no wire reinforcement in the cap area. Hence, the three tests for the second box girder were:

1) Without cap reinforcement (test 3)
2) With cap reinforcement (test 4)
3) Without cap reinforcement but with rib reinforcements (test 5)

The cap and rib reinforcements are presented in chapter 7.

2.2 Loads in the full-scale tests

The first blade was part of a certification process and the flap-load distribution was based on an extreme load situation including safety factors. The same load distribution was used in the ultimate failure test, except that the tip region did not have much load as there was limited space when the blade had a tip deflection in the area of 4-5m. The 4 other loading stations had enough space and here the loads were up-scaled until the blade collapsed, see Figure 12. The load values shown in Figure 12 correspond to blade failure. The safety margin from the certified loads to failure loads is confidential.

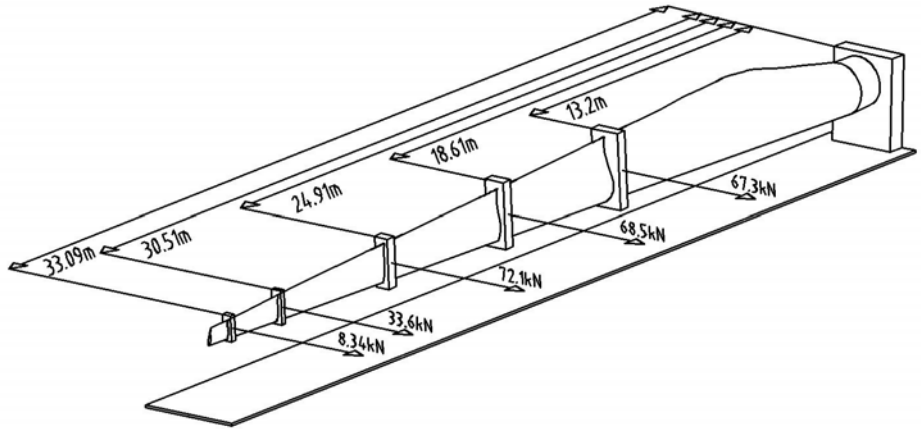

Figure 12. Sketch of the 34m SSP-blade. The load values shown correspond to blade failure.

In the tests of the shortened box girders, the three clamps have similar positions as for the first full-scale test, see Figure 13.

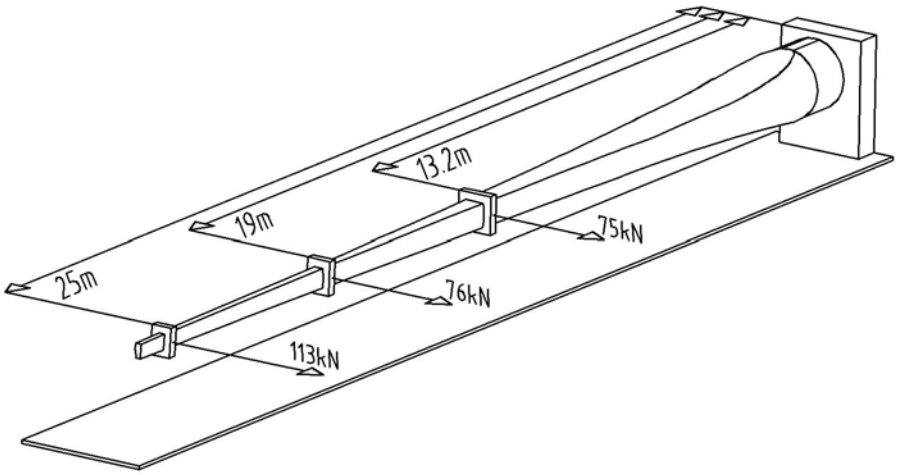

Figure 13. Sketch of a shortened box girder with applied forces. The loads shown represent 100% load, referring to the failure load observed in the first full-scale test, see loads in Figure 12.

In full-scale tests 2-5 (box girder tests) the loads in tip region (25m-34m) have been substituted by a single load at 25m. This causes the maximum moment to be reduced and the moment distribution to change. Extra forces were distributed to the 13.2m and 19m clamps to compensate for the reduced moment. The moment distribution is then changed, compared with the first full-scale test, see Figure 14a.

In region 0-13.2m., which is of major importance in this PhD-project, the moment distribution is similar to the first full-scale test. The shear force distribution has also changed, but is higher for tests 2-5 than for test 1, see Figure 14b. This makes the comparisons between test 1and tests 2 to5 conservative. The comparisons are made in Chapter 8.

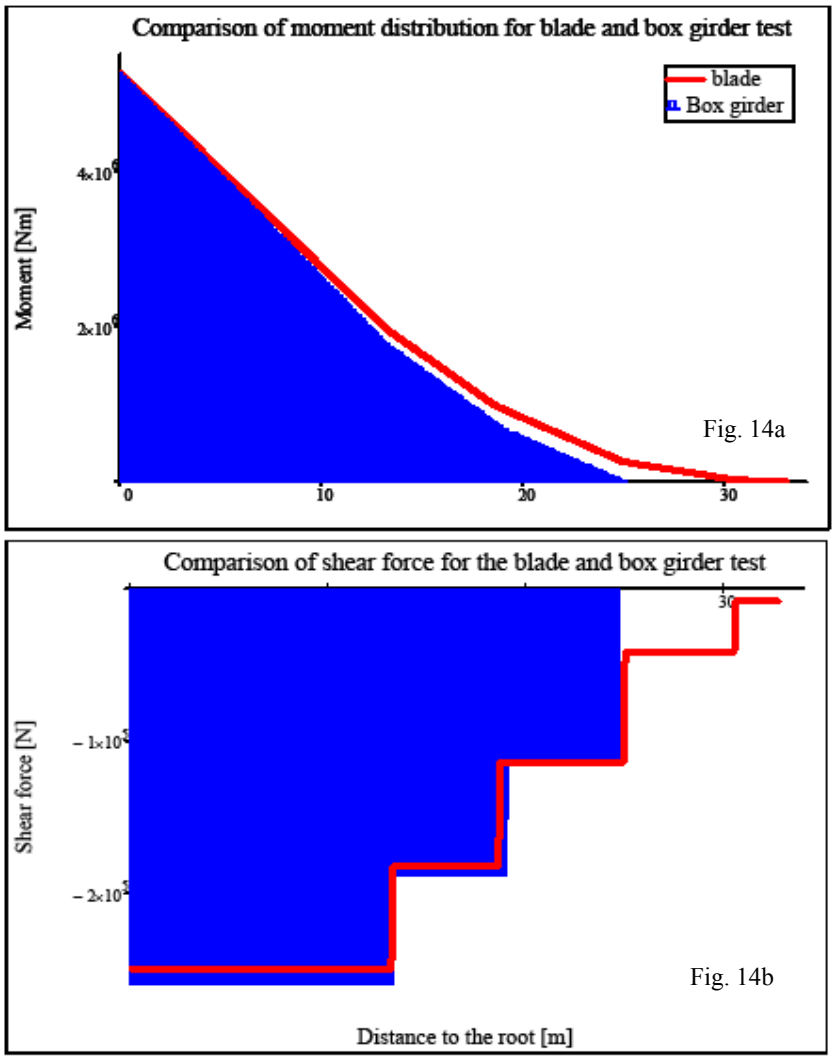

Figure 14. Comparison of moment and shear force distribution for 34m blade test (test 1) and shortened box girder tests (test 2-5) a) Moment distribution b) Shear force distribution.

The loads applied from test 1 and the resulting root moment are used as a reference for all other tests (test 2-5) in this thesis.

2.3 Test setup

Considerations on selecting either a full blade or only the box girder for testing are given in the following.

Apart from savings in manufacturing cost there are other advantages associated with testing only the load carrying box girder. For instance, such testing allows measurement equipment to be mounted on the outer faces of the box girder, since the aerofoil section not is included in the full-scale test. The largest difference in testing a full blade and a box girder is that buckling and transverse shear distorsion becomes important issues.

Buckling becomes critical in the root section when the aerofoil is removed

Even though the aerofoil on average carries approximately 10% of the flapwise bending load, the flexural bending stiffness of the load carrying caps decreases with a larger amount. Consequently, the buckling capacity is reduced by 30-40% due to the aerofoil not being represented in the load carrying cap, see Figure 15.

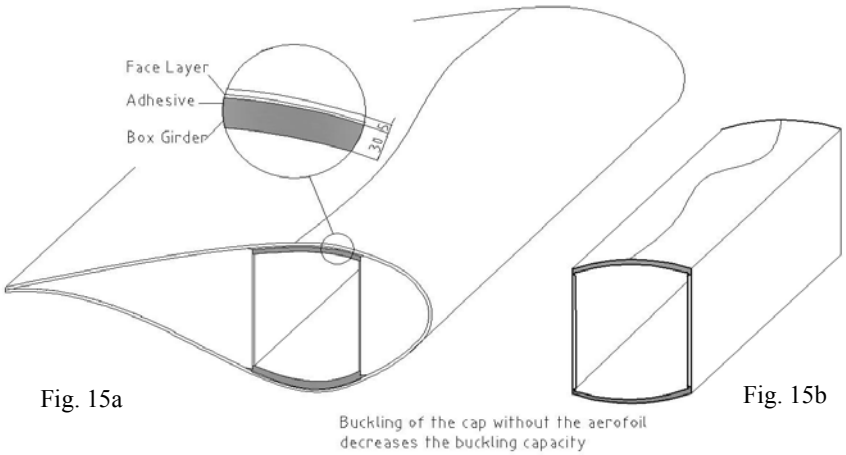

Figure 15. Buckling capacity of a blade and a box girder a) Sketch of a blade b) Sketch of a box girder cap is buckled due to reduction in buckling capacity when the aerofoil is removed.

In the area close to the root section, where the span of the blade is much larger, the aerofoil contributes much more to the flapwise bending stiffness than the 10% referenced above. As a precaution against buckling a tophat girder has been added to the first box girder in the first 9m of the blade. In this area buckling is normally not critical; however when the aerofoil is removed FE analyses have shown that this area can be sensitive to buckling failure on a low (50%) load level, see ref. [41]. This failure mode is unrealistic (and unwanted) since it would never occur on a blade that includes the aerofoil. Consequently, a top-hat girder section has been added to the box girder in order to compensate for the removal of the aerofoil, see Figure 16.

Figure 16. Tophat girder added to the first box girder structure to compensate for the removed aerofoil and eliminate an unrealistic buckling failure in the area (2-9m), where the removed aerofoil carries a large part of the flapwise loads due to the wide cord in this area.

The aim is to increase the flexural bending stiffness so no buckling failure is observed in this area. The tophat girder had an extension from 2-9m from root and the box girder failed at 10m, see Section 6.3 and ref. [41]. The second box girder had no tophat reinforcement, but longitudinal bulkheads were used at different positions depending on the purpose of the test. In test 3-4 the purposes were to identify localized bending or buckling even though it was happening in a region where buckling typically would not occur. Further explanation is given in Section 7.2, and a more comprehensive description is given in ref. [38].

Transverse shear collapse is critical when box is tested without aerofoil

Another unwanted (and unrealistic) failure mode, which is critical when the aerofoil has been removed, is the transverse shear distortion of the box section, see Figure 17a.

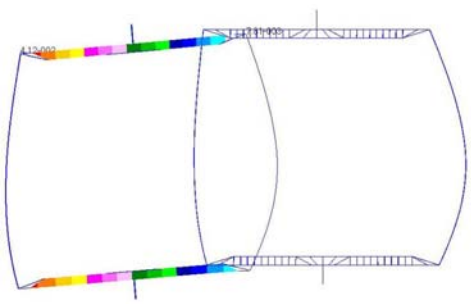

Fig. 17a

Fig. 17b

Figure 17. Transverse shear distortion of a box girder in a flapwise test a) FE-study performed before the experimental test showed that the box girder might fail in a transverse shear collapse b) Supports used in the full-scale tests eliminate transverse movement (perpendicular to the load direction) and transverse shear collapse was prevented.

The transverse shear collapse is unrealistic because the outer skin to a certain extent prevents this failure mode.

This unwanted structural failure mechanism has been prevented in test 2-5 by including extra supports to avoid this unwanted shear distortion failure, see figure 17b. In figure 18 a sketch shows where the three supports, which have been placed in the test and it is important to notice that no supports has been added in the 10-12m section, which has to be the critical area.

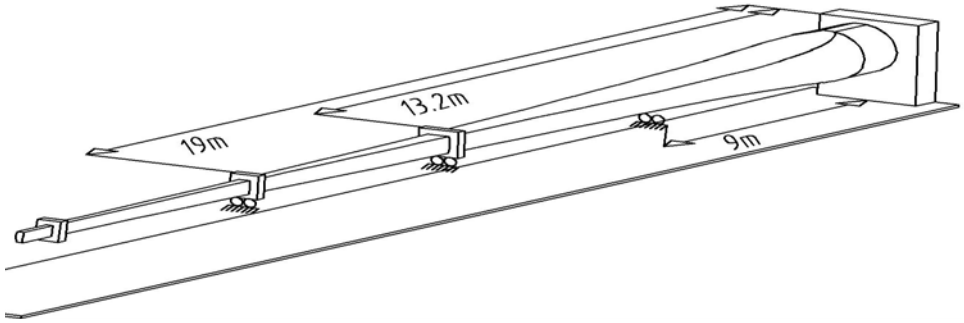

Figure 18. Sketch revealing positions of three supports applied to avoid transverse shear collapse.

3 Measurement equipment used for full-scale tests

In the five full-scale tests performed in the present PhD-work different measuring techniques have been used. This chapter describes some of the measuring techniques very briefly. In this thesis mainly the results from the Aramis system, strain gauges and displacement sensors are used. The results are presented in chapter 5-7. More comprehensive descriptions of the test equipment and the results can be found in ref. [37], [38], [88].

The methods used in the full-scale tests are:
- Strain gauge measurements – Section 3.1
- Mechanical displacement measurements – Section 3.2
- Aramis (Digital Image Coloration - DIC) – Section 3.3
- Fringe projection (Digital Image Coloration-DIC) – Not presented in this thesis, see ref. [37]
- Acoustic emission – Section 3.4
- Vacuum hood (NDT-technique) – Section 3.4
- Ultrasonic scanning – Air coupled (NDT-technique) – Section 3.4

The Author has only been responsible for the strain gauges and the mechanical displacement measurements. Experts were invited to the full-scale tests, and they performed the NDT scans of the blade as well as the DIC-measurements. In this thesis the focus will be on the measurements performed by the Author, but all measurements have contributed to the conclusions in Section 5-9.

3.1 Strain gauge measurements in the full-scale tests

In the certification test of the 34m blade, performed before test 1, 65 strain gauges were used. They were all orientated in the longitudinal direction, see Figure 19, taken from ref. [88].

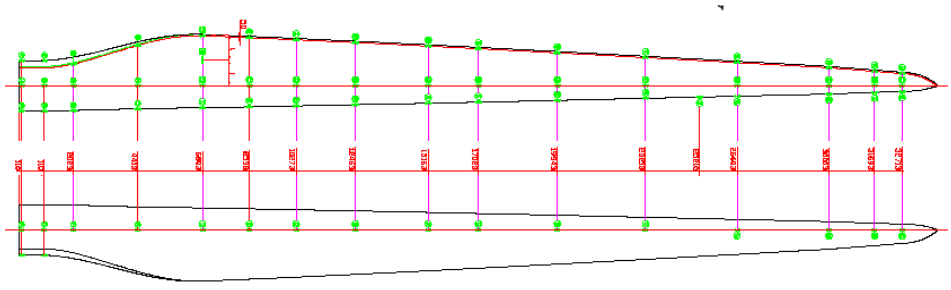

Figure 19. Strain gauge locations on the outer surface of the blade in the first full-scale test. The figure is taken from ref. [88].

Additional strain gauges were put inside the box girder, based on preliminary FE-study of the Author, see Figure 20.

Distance from root [m]	SG Nr.	Strain Direction	Description of the Position
6.803	73	Longitudinal	Cap centre - Suction side
8.538	74	Longitudinal	Cap centre - Suction side - Suction side
10.273	75	Longitudinal	Cap centre - Suction side - Suction side
10.273	76	Longitudinal	Top of web towards leading edge - Suction side
10.273	77	45°	Top of web towards leading edge - Suction side
10.273	78	Transverse	Top of web towards leading edge - Suction side
10.273	79	Longitudinal	Top of web towards trailing edge - Suction side
10.273	80	45°	Top of web towards trailing edge - Suction side
10.273	81	Transverse	Top of web towards trailing edge - Suction side
10.273	82	Longitudinal	Cap corner towards leading edge - Suction side
10.273	83	Transverse	Cap corner towards leading edge - Suction side
10.273	84	Longitudinal	Cap corner towards trailing edge - Suction side
10.273	85	Transverse	Cap corner towards trailing edge - Suction side
12.463	86	Longitudinal	Cap centre - Suction side
12.463	87	Longitudinal	Cap corner towards trailing edge - Suction side
12.463	88	Transverse	Cap corner towards trailing edge - Suction side
15.163	89	Transverse	Cap centre - Suction side
17.023	90	Longitudinal	Cap centre - Suction side

Figure 20. Additional strain gauges inserted inside the box girder in the first full-scale test. The table is from ref. [88].

The strain gauges on the cap are all positioned in longitudinal direction, and one of the purposes is to detect buckling or localized bending, see explanation in Section 5.2 and 5.3, respectively. In the actual case there is no guarantee that a buckling wave would have been identified since the wave length (2 half waves) is typically 1-1.5m long, and the distance between the strain gauges are approx. 2m, see Figure 19. According to the guidelines of ref. [51], six strain gauges per wave length are used.

In the first box girder test (test 2), a much larger number (330 strain gauges) of strain gauges were used compared to the first test. Most of the strain gauges were located in the small area, where the box girder was expected to fail. The box girder failed in 10m, and in Figure 21 it is shown how the 31 strain gauges which were placed in that section.

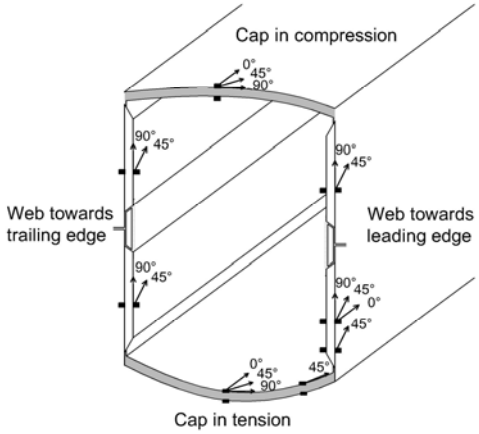

Figure 21. 31 Strain gauges in section (10m), which failed in the first box girder test (test 2). All strain gauges were placed 'back to back'.

Thanks to the measurements from the large numbers of strain gauges and from the other equipment it was rather easy to find and document the failure mechanisms for this first box girder test (test 2), see chapter 5 and 6.

3.2 Mechanical displacement sensors in a cross section

Displacement sensors are used in certification tests to verify global bending of the blade, but in the full-scale tests performed in this PhD-study the aim of using displacement sensors has been totally different. The aim has been to measure distortion of the profile, also known as 'local deformations'. Local deformations are measured using displacement transducers mounted as shown in Figure 22.

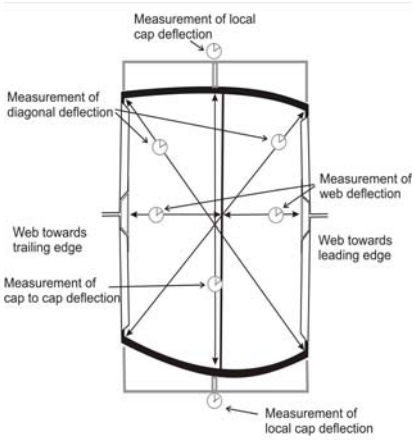

Figure 22. Mechanical displacement sensors in the first box girder test (test 2). Displacement sensors in the 10m cross section are shown.

On the outer side of the box girder, displacement sensors were mounted in order to measure local deflections of the compression cap centreline. This equipment has been used in both the first full-scale test of the SSP34m blade and the following box girder test, see Figure 23.

Fig. 23a Fig. 23b

Figure 23. Displacement sensors measuring the local (relative to the box corner) deformation of the out of plane deformation of the cap centreline a) Cap deflection sensors on the first full-scale test b) Cap deflection sensors on the first box girder test (test 2).

Cap deflections were measured in 7 sections for both full-scale tests, shown in Figure 23. Results are analysed in chapter 5+6, but a more comprehensive description of the test setup is presented in ref. [37].

Displacement sensors were also mounted inside the box girder at both shear webs, see Figure 22 and Figure 24. The sensors measured individual deflection between the webs and the reference frame in the centreline. Measurements of web deflections were preformed in 3m, 4m, 8.6m, 10.1m, 10.6m, 11.1m and 12.1m.

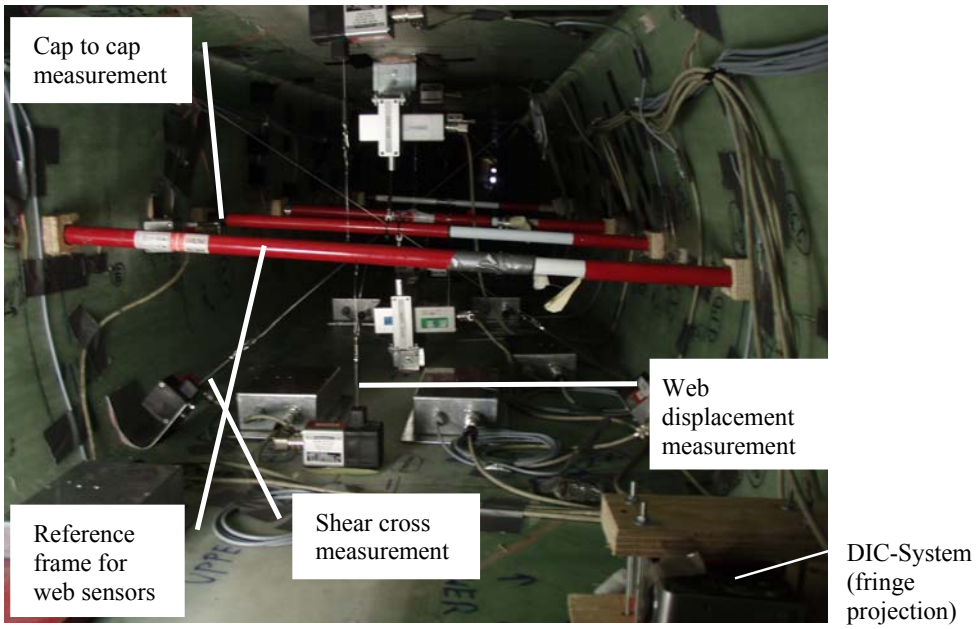

Figure 24. Displacement sensors mounted inside the box girder looking towards the tip. The sketch of measuring equipment in Figure 22 is rotated by 90° with respect to this photo. Details regarding the installed measuring equipment are given in ref. [37].

Diagonal displacement sensors were also mounted inside the box girder, so any transverse shear distortion could be observed. In 10.4m a cap to cap displacement sensor was mounted, measuring from compression cap to tension cap, so the reduction

in profile height could be found, see Figure 22 and Figure 24. All results from the box girder tests be found in ref. [37],[38] and the blade test in ref. [88]. In this thesis, only few relevant results are presented, see chapter 4-7, but almost all measurements have been used to get a full picture of the failure event.

The numerous mechanical displacement sensors have also been used for validation and calibrations of the FE-models, see Section 4.1.

The deformation measurements have also been used for the verification of new advanced measurement equipment such as two DIC-measuring systems.

3.3 DIC-system used for measuring deformation panels on a local scale

In order to measure surface deformation on a local scale, two DIC-measuring systems (Fringe projection and Aramis system) have been used. In this thesis, only the Aramis system, which gave the most accurate results, is presented. The Aramis system is an optical measurement system which is able to measure 3D deformation and surface strain of an object by DIC of images taken with two cameras. In the full-scale tests, only the local out-of-plane deformation had a sufficient tolerance, as the large flap-wise bending of the box girder structure was disturbing the accuracy of the results. Details regarding the two measuring systems can be found in ref. [37], [59]. The Author has no knowledge of others, who have used DIC-systems in full-scale tests of wind-turbine blades before. Markus Klein and Jeppe Laursen from Gom/Zebicon were invited to do the full-scale tests, and they performed the Aramis measurements.

The deformation, which has been measured, is the out-of-plane deformation of the compression cap. This local deformation is determined by subtracting the global deflection (rigid body movement) from all measured points/coordinates (the entire measuring area) and thereby getting a fairly good estimation of local deformation. In Figure 25 the measuring equipment is shown from behind, facing the compression side of the box girder.

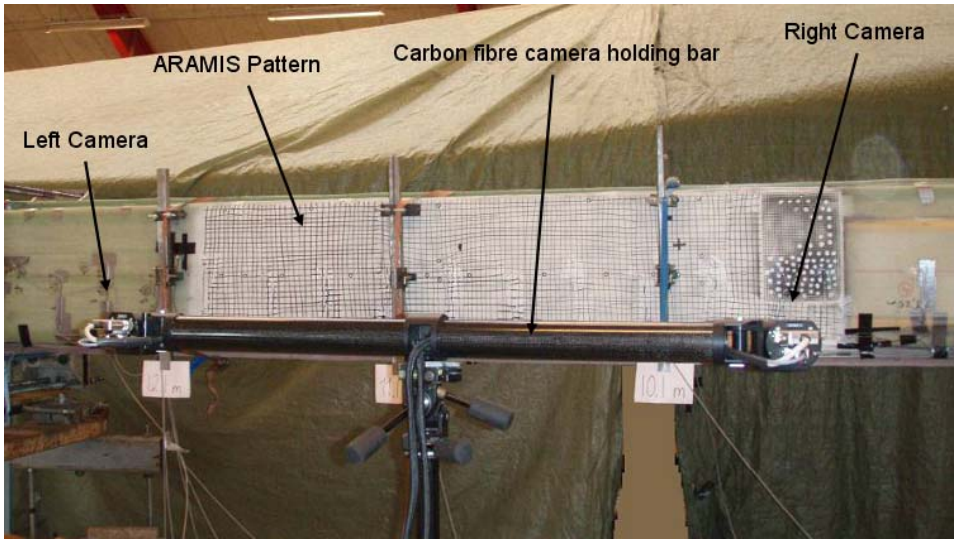

Figure 25. Aramis equipment positioned in front of the measuring area. Test setup for the first box girder (test 2) is shown.

During full-scale test 2, measurements were performed using Aramis on the box girder's compression side in the distance of 9m to 12m from the root, see Figure 25.

In full-scale test 3 and 4 the Aramis system was used to perform measurements in a larger area, i.e. between 5 and 12m from the root, see Figure 26.

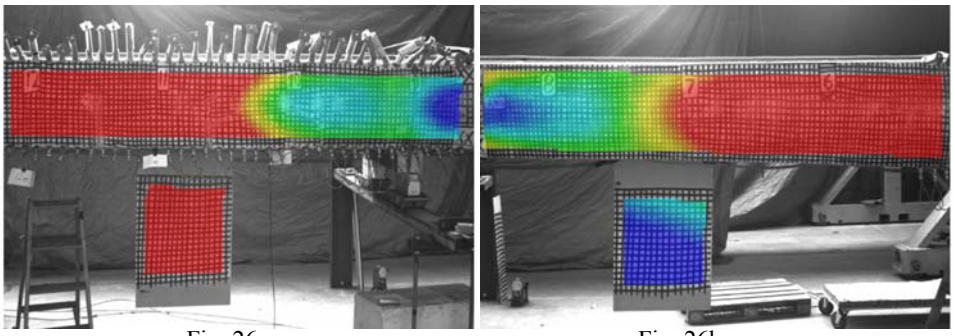

Fig. 26a Fig. 26b

Figure 26. In full-scale test 3 and 4 the Aramis system was measuring surface deformations in a larger area by measurement in two steps (unload and move the Aramis system and load again).

This was done by diving the area into two, one located between 5-8.5m and one located between 8.5-12m, since the Aramis system (4MB) is not able to measure deformations on a larger surface than 3.5x3.5m without large measuring uncertainty on the local deflection on the cap surface. Since two Aramis systems were not avaiable, measurements had to be done in two steps, first measure in one area and then unload, move the Aramis system and upload again. Details about the measurements can be found in ref. [37], [38]. The measured results from the two box girder tests are discussed in chapter 5-7.

3.4 Structural health monitoring

In the full-scale tests experts in structural health monitoring techniqes were invited, see ref. [37]. The structural health monitoring techniques used included:
- Acoustic emission
- Vacuum hood (Non Destructive Test (NDT-technique))
- Ultrasonic scanning - air coupled ultrasonic (also NDT-technique)

In the Acoustic Emission method the damage in the blade structure is recorded with microphones. When certain dynamic processes occur in the material, some of the released energy generates elastic stress waves, we might say vibrations. These stress waves are propagated from the source and can be detected by sensitive transducers. Once amplified, the signal from these transducers is available for further analysis. Information about the location, severity and nature of the event causing the stress wave emission can be deduced from the received signals.

The vacuum hood and ultrasonic scanning are two NDT-techniques which can scan a composite lamina (or another material) and detect flaws, voids and defects in general. Vacuum hood is a method which induces a small force (8-14 kilo) onto the test area utilising a vacuum hood system. The small out of plane deformations can then be measured and flaws etc. can be detected. The details about this measuring method can be found in ref. [37] or at www.laseroptical.co.uk.

Acoustic emission and the vacuum hood methods were used during the test and ultrasonic scanning was performed after the blade has been cut up in pieces, since it was not possible to bring the scanning system to the full-scale test facility and scan large structures during the testing. This was possible for the vacuum hood system, but unfortunately the accuracy of the scanning results were not satisfactory, so improvements must be done before the technique can be used to detect delaminations with a sufficient accuracy, see ref. [37].

The acoustic emission measurements were performed by Malcolm McGugan from the Department of Materials Research at Risø DTU, and the system was used in full-scale tests 2-4. The main purpose of this system is to detect when cracks start to progress, and especially to give an early warning, when the cracks start to grow in an unstable manner. When this is the case, it is time to stop the test and verify the local damage progression. With this technique it is also possible to quickly move or add extra measurement (sensors) in the area, where the increased acoustic noise has occurred. The method and the results from the full-scale test are described in details in ref. [37],[38].

4 FE-model

In the first part of the FE-work, a sub modelling technique with non-linear boundary conditions has been used, see ref.[39], but in the last part of the PhD-work no sub modelling approach has been used. Instead a very efficient cluster has been used, which makes it possible to solve the complete non-linear (geometry) models.

Results from different FE-models are presented in Chapter 5-7 depending of the purpose of the analysis, e.g. investigations of reinforcement, blade or box etc. In this Chapter the FE-model of the load carrying box girder containing both shell and solid elements is presented, see Figure 27.

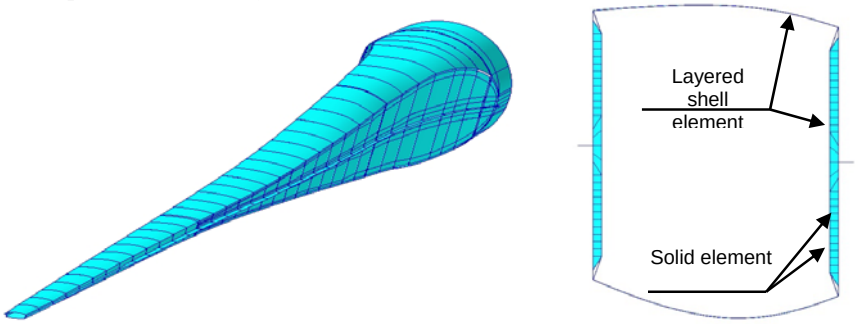

Fig. 27a Fig. 27b

Figure 27. FE-model a) Entire model (no elements shown) of the shortened (25m) box girder b) Section of finite element model.

The cross-section of the box girder, see Figure 27b, can be divided into:

- Caps (flanges)
- Shear webs

The caps are made from thick laminates and are modelled with 4-noded layered shell elements (Quad4), using a thick shell formulation (taking shear deformation into account). The elements are located at the mid-thickness of the caps, and shell offsets are therefore not needed.

The webs are modelled with a combination of shell and solid elements. The thin skins on each side of the webs consisted mainly of bi-axial lamina and are modelled with 4-noded layered shell elements placed in the mid-thickness of the material. The core material in the shear webs is modelled with 8-noded orthotropic solid brick elements (Hex8), with one element through the thickness. Furthermore, the reinforcement of the webs (see Figure 3b) consists of adhesive and is modelled with 8-noded solid brick elements (Hex8).

MSC-Patran and the laminate modeller module were used for pre- and post processing. MSC-Marc was used as non-linear FE-solver. A relatively coarse mesh density is furthermore applied at the first 6 meters and the last 5 meter of the box girder to minimize the degrees of freedom. From 6 to 21 meters the FE-model consists

of a mesh with 128 elements circumferentially and an element aspect ratio no bigger than 2. The entire model has 150000 nodes. The computations were carried out on a computer cluster with up to 240 nodes (one processor machines). In this particular case, 12 nodes were used. The computational time was approx. 1 hour with 40 load steps.

The numerical work has been useful in order to obtain a comprehensive understanding of the structural mechanisms, while the full-scale tests have acted as a tool for identifying failures.

4.1 Calibration of stiffness in the FE-model based on experimental results

Working with large wind turbine blades made of fibre composites, a large margin of manufacturing tolerances must be accepted. SSP-Technology uses a relatively high quality production method (prepreg without autoclaving), but still there are manufacturing defects, which must be taken into account in the evaluation of the strength. Manufacturing tolerances are most pronounced in areas, where prepreg layers terminate, such as the corner of a box girder, see Figure 28a and b which shows the variability of the box girder corner. In the FE-work an approach is used which calibrates the FE-model before accurate predictions of strains and deformations on a local scale can be predicted. In Figure 28c the shell elements in the box corners are used to calibrate the corner stiffness thus indirectly taking the variability into account.

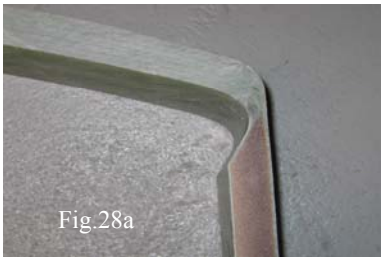

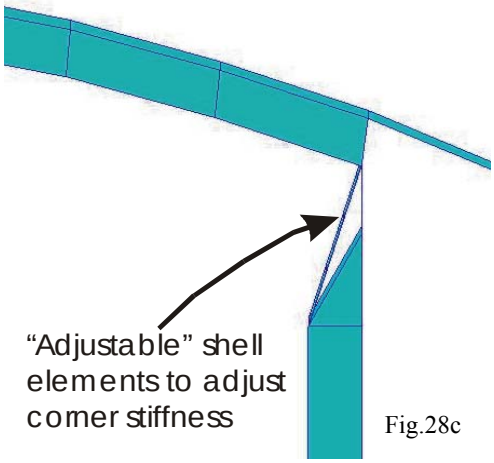

Figure 28. Design and manufacturing tolerances influence the corner stiffness of a box girder a) and b) Box girder corner with different thicknesses due to manufacturing tolerances c) Section of a FE-model which shows a shell element, which can adjust the corner stiffness.

These areas have been adjusted so the FE-model shows the right deformations. This is only necessary for simulating the complex non-linear geometry behaviour on the local scale. Global results, such as tip deflection and eigenfrequencies etc., are generally easy to predict, and a coarse linear shell model is often sufficient.

The stiffness of the corner used in the FE-model, is adjusted so the deformation measured during the testing fits satisfactorily. In Figure 29, cap and web deflections have been compared. More details can be found in ref. [39].

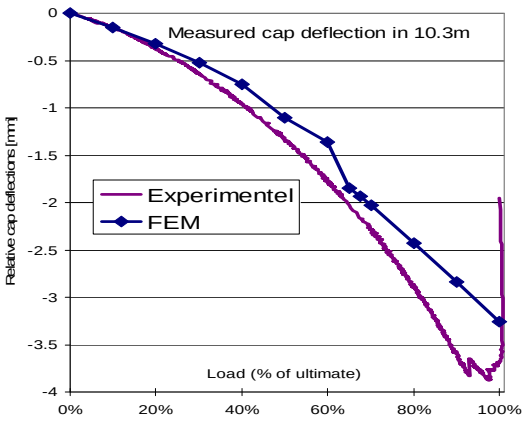

Fig. 29a

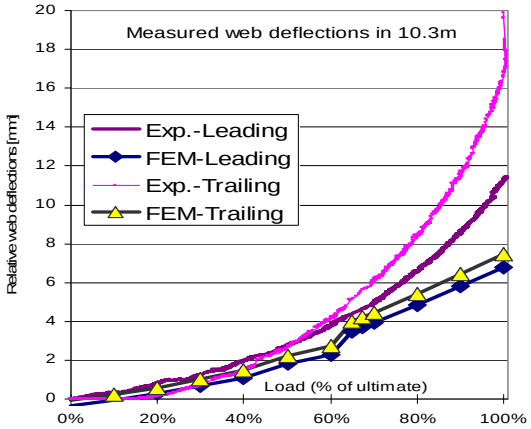

Fig. 29b

Figure 29. Comparison of measured deflections and numerical results in 10.3m after calibration of the box corner stiffness a) Comparison of cap deflection b) Comparison of web deflections

Experiences from the different full-scale tests with the same type of blade (SSP34) have shown that the corner stiffness found in the first full-scale test also represents the following blades corner stiffness satisfactorily. This means that a representative stiffness only has to be determined once. Of course, if the design, materials, lay-up or production methods change dramatically, new corner stiffness must be considered.

4.2 Realistic combined load scenario

In Figure 30, the aerodynamic drag and pressure (shown in Figure 7) are simplified with single forces. This solution is used in the FE-calculations presented in Chapter 5-7.

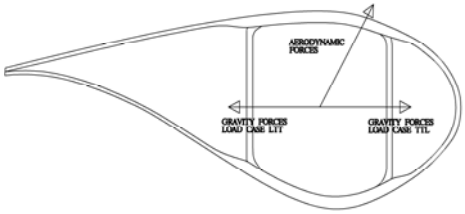

Fig. 30a

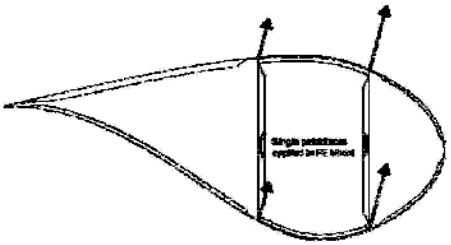

Fig. 30b

Figure 30. Aerodynamic and gravity loads applied to the FE-model a) Aerodynamic and gravity loads represented by single force vectors b) In the FE-model the aerodynamic pressure is distributed in the box corners, and the gravity is included as inertia forces.

In Figure 30b, the aerodynamic drag and pressure (shown in Figure 7) are simplified with single forces. This solution is used in the FE-calculations presented in Chapter 5-7. In the FE-analyses the gravity forces are also taken into account in two separate load cases; one where the blade has the trailing edge towards the ground, and the other one in the opposite position. This is simplified in Figure 7b by two single forces, but in the FE-model, gravety is represented by volume forces.

5 Elastic response of a blade box design

Three elastic phenomena have been found to be of great importance for the structural response and strength. They are presented in the following sections:

Section 5.1: Brazier load – Geometrically non-linear phenomena
Section 5.2: Buckling – Geometrically non-linear phenomena
Section 5.3: Localized bending - Linear phenomena

5.1 Brazier load – Geometrically non-linear phenomena

When a wind turbine blade bends in the flapwise direction, the compressed panel produces a downward crushing load normal to the surfaces. The opposite occurs on the lower panel, see Figure 31 and Figure 33. This nonlinear deformation or 'flattening' of the cross section is also known as the Brazier effect [9], [12], [13] and is most pronounced for long thin hollow beams subjected to bending.

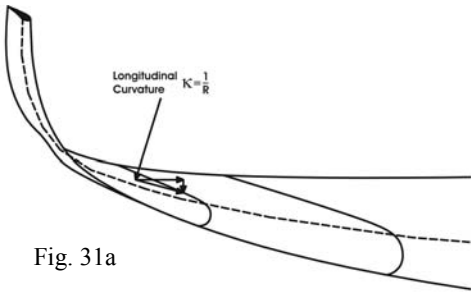

Fig. 31a

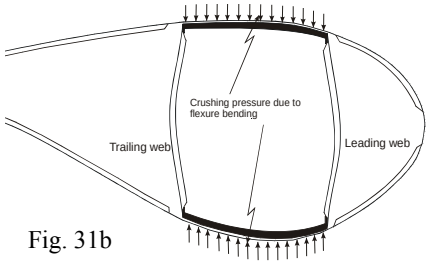

Fig. 31b

Figure 31. Flapwise bending results in crushing pressure a) Longitudinal curvature results in an inward crushing force b) Crushing pressure on a wind turbine blade section.

Since von-Karman [84], it has been recognized that thin-walled, hollow structures under bending suffer a flattening of the cross-section. This flattening manifests itself as an ovalisation in circular sections and a 'sucking in' for squared tubes, see Figure 32.

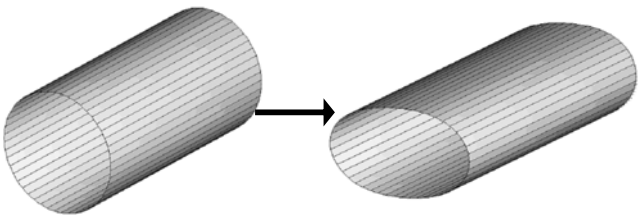

Fig. 32a

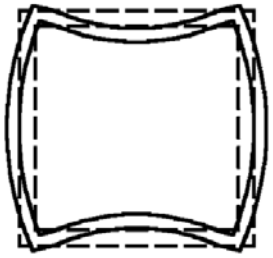

Fig. 32b

Figure 32. Inward crushing forces on a thin walled structure subjected to bending, leading to flattening of the cross-section. a) Ovalisation of a circular section. Figure from ref. [12] b) 'Sucking in' of a squared tube - figure from [69].

The flattening effect is caused by internal forces and appears when large deformations are taken into account. When large deformations of e.g. a box girder cross section

subjected to a bending moment are taken into account, the forces in the flanges can be resolved in transversal and longitudinal components, see Figure 33. The transversal components are responsible for the flattening effect. Only structures with a longitudinal bending curvature have these resulting forces.

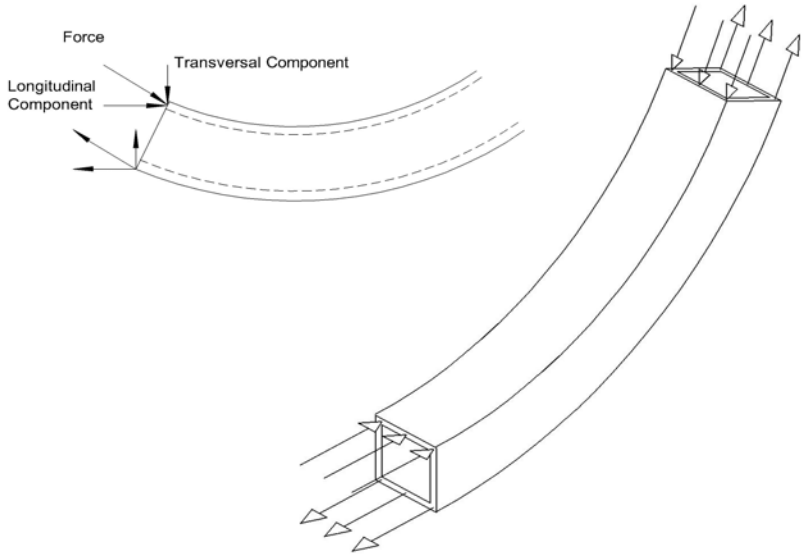

Figure 33. When large deformations of a box girder cross section subjected to a bending moment are taken into account, the forces in the flanges can be resolved in transversal and longitudinal components. The transversal components are responsible for the flattening effect.

The distortion reduces the section's second moment of area and thus it's bending stiffness. Brazier [8], [9], however, was the first to realize, that such a reduction in the second moment of area would lead to a non-linear bending response and eventual structural collapse. Since this time, the analysis of this non-linear response has progressed into the investigation of composite structures [47], non-circular cross-sections (e.g. ref. [12], [13], [74]) and aerofoil sections. From Brazier, the crushing pressure acting on a local section of the cross-section (per unit length) is given by:

$$\psi_{braz} = \frac{1}{A_{11}} \varepsilon_x \cdot \kappa = \frac{1}{A_{11}} z \cdot \kappa^2 \qquad (1)$$

where κ denotes the longitudinal curvature of the cross-section, z the distance to the neutral axis, ε the local strain and $1/A_{11}$ is the laminate's axial, in-plane stiffness (for isotropic materials it is the Young's modulus multiplied by the wall thickness). As a result, the crushing pressure increases with the square of the curvature of the section, and thus (before large cross-sectional deformations occur) with the square of the bending moment:

$$\psi_{braz} = \frac{1}{A_{11}} \frac{z \cdot M^2}{(E \cdot I)^2} \qquad (2)$$

As will be shown later, the Brazier effect as simplistically described in eqs. (1) and (2) is included in both the non-linear FE-analysis and in the experiments, see Section 6.2 and 6.3.

5.2 Buckling – Geometrically non-linear phenomena

Buckling is a structural instability phenomenon for structures, which are loaded in compression. The behaviour of shell-like structures under buckling is characterized by limit points rather than a bifurcation point. With linear buckling analysis, the bifurcation point is obtained as the solution to an eigenvalue problem. Accordingly, linear buckling analysis is a guideline for the design load, to which a suitable reduction factor is called for. The size of the reduction factor may be obtained by further analysis and/or substantial testing. In the analysis of shell imperfection sensitivity it is necessary to investigate the geometrically non-linear structural response. This is done in ref. [51] including a comprehensive analytical buckling theory study. In this thesis no buckling theory is included, and only non-linear geometrical FE-studies and experimental results are used to decide, whether buckling is critical or not.

Figure 15 and Section 2.3 discusses the reduction in the flexural stiffness of the caps, when the aerofoil is removed. FE-studies showed that the root section in particular is critical to buckling, when the aerofoil has been removed. This was solved by implementing tophat reinforcement in the first 9m, see Figure 16 and explanation in Section 2.3. In the present context, only the sections important for relevant (realistic) failure mechanisms are studied. In these areas DIC measurement has been used including mechanical deflection sensors and strain gauges, see Chapter 3. The photo with a coloured fringe pattern, shown in Figure 34, is a typical result generated by the DIC measuring system from the first box girder test (test 2).

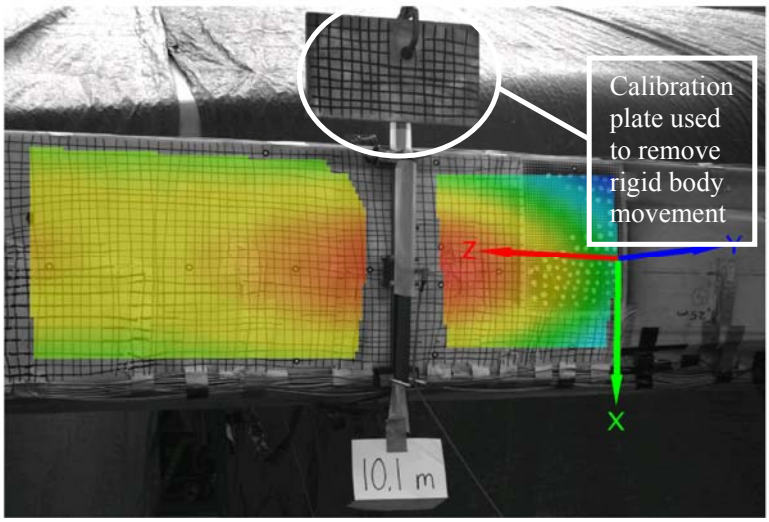

Figure 34. Measurement of the local cap deformations (out-of-plane) in the first box girder test (test 2). The results from DIC measurement are superimposed to a picture of the cap surface.

A special technique was developed in order to remove ridig body movement from the displacement measurements on the cap surface. This involved use of a so-called calibration plate, see Figure 34. This calibration issue is only briefly discussed in this thesis; more details can be found in [37], [59]. The cap deflections shown in Figure 34 are also plotted in Figure 35 (blue curve), but with a calibrated deformation compensating for the 'error' in the local deformation. 'Error' means that the global deformations are deducted from deformations of the box girder so only the local deformation of the centreline is plotted. This compensation is made by taking the two corner deformations and subtracting them from the centreline value, see ref. [59]. The results from the FE-calculations are also plotted (red curve), and a good match was found with the experimentally measured cap deformations, see Figure 35.

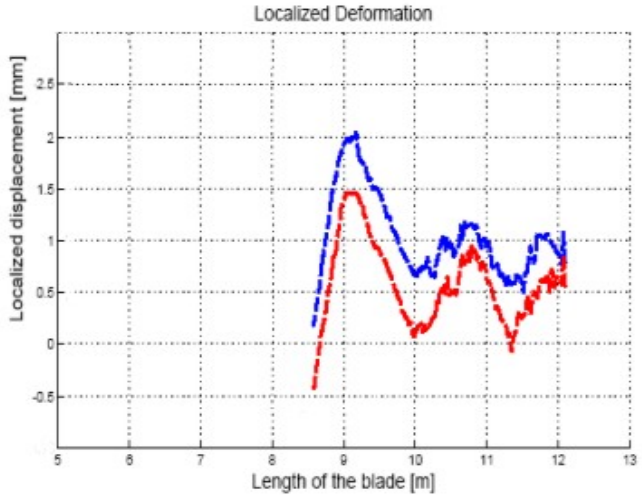

Figure 35. Local deformation of the cap centreline in the 8.5m-12m area, show a 'waving' deformation behaviour measured in the first box girder test (test 2). The blue curve is experimental measurement using the DIC system and the red curve is the numerical FE-results. The graphs are plotted with a load (78%) close to the failure load (80 %).

The waving behaviour in Figure 35 does not reveal whether this is buckling or localized bending, but strain behaviour at a point gives information about the changes in the structural behavior, see Figure 36. Buckling is a non-linear phenomenon while the localized bending is linear, see explanation in section 5.3. A plot of the 'back to back' longitudinal strains on the compressive side in 10m shows that the non-linear buckling behaviour starts at approx. 70% load, see Figure 36.

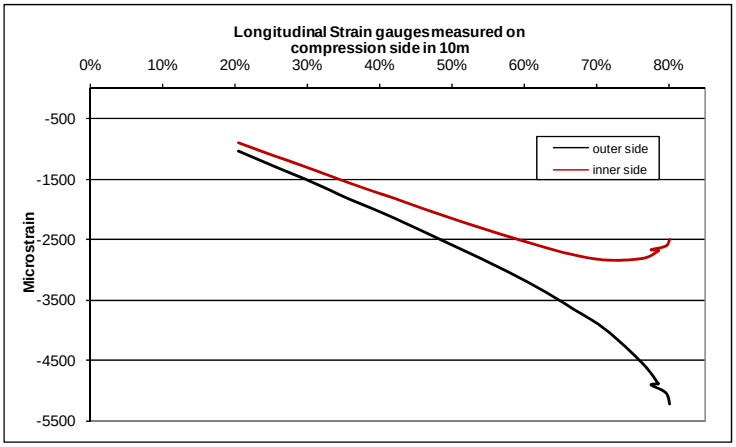

Figure 36. 'Back to back' strain measurements in 10m, showing buckling behaviour at 70% load. The results are from the first box girder test (test 2).

The difference in strain levels in the linear range is not caused by buckling, and the next section will elaborate on this linear behaviour.

5.3 Localized bending - Linear phenomena

The term *localized bending* is used in this thesis when the cap bends locally, but without showing buckling behaviour. The localized bending phenomenon is identified both at caps in compression and in tension. The localized bending may be caused by several reasons e.g. asymmetric layup, non-in-plane loads, non-smooth geometry, see Figure 37.

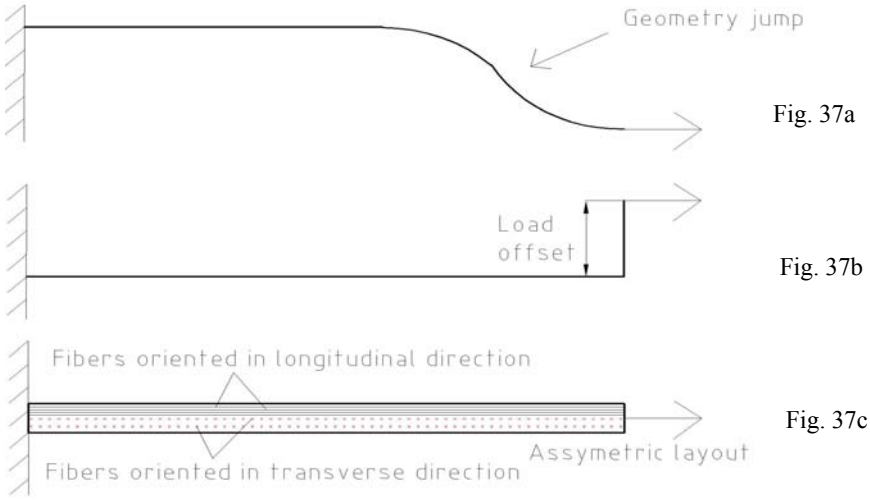

Figure 37. Sketch which illustrate potential reasons for localized bending a) Non-smooth geometry b) Offset in applied loads c) Non-symmetric layup. The arrows indicate sectional forces.

For the box girder in question, the localized bending is mainly caused by the geometry and not by non-symmetric layup or offset in the loads. This local bending behaviour is found to be a linear phenomenon. In principle, it would also be possible to have non-linear localized bending behaviour. However, this requires much larger changes in the

geometry than is represented for the actual blade. In the SSP 34m blade there is a significant geometry change in the cap curvature in the transition area (6-8m), see Figure 38. This transition area is where the thin aerofoil increases in height in order to "connect' to the root section.

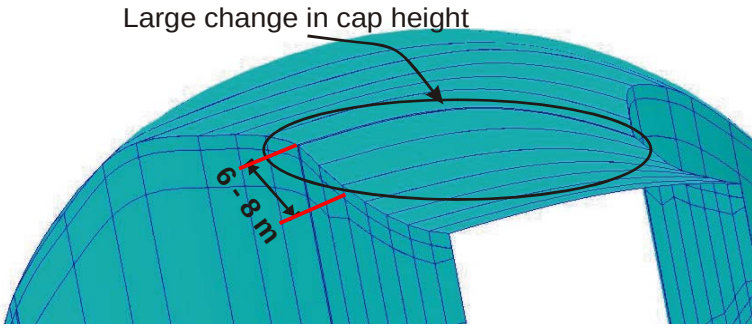

Figure 38. CAD-model (or FE-model) shows a large geometric change in profile height in the transition area (6-8m).

Cap deformations were measured in different positions during the first two full-scale tests using mechanical displacement sensors. Figure 39 shows results from the first full-scale test are shown.

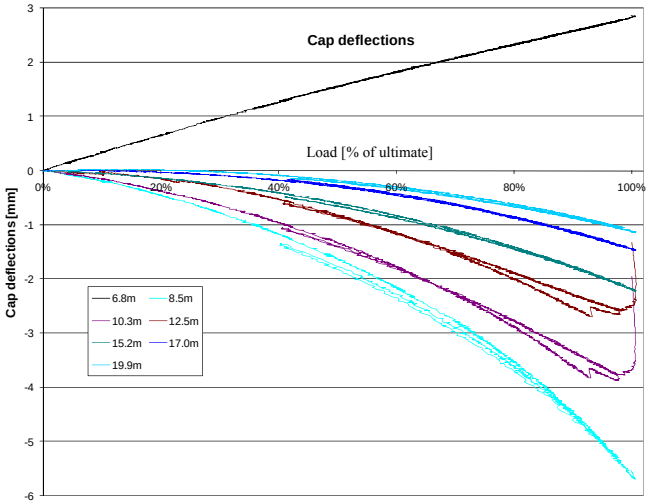

Figure 39. Measured cap deflections in seven sections from full-scale test 1.

Figure 39 shows outward cap deflection at the 6.8m section (black curve), which is different from the other six sections, which do not have this large geometry change, shown in Figure 38. From 8.5m to 19.9m the caps have inward non-linear deformation due to ovalisation caused by the Brazier effect. Of course, the Brazier effect is also represented in section 6.8m since there is longitudinal curvature, but the linear outward behaviour, caused by jump in section hight, is dominating. In the box girder area (8.5m-19.9m) there is also a linear contribution to the local bending deflection, but it cannot be seen easily in the cap deformation, in Figure 39. 'Back to back' strain measurements must be studied in order to observe this behaviour. An example from the first full-scale test is presented in Figure 40. In this test no buckling was observed, so all the local bending is caused by one of the reasons shown in Figure 37.

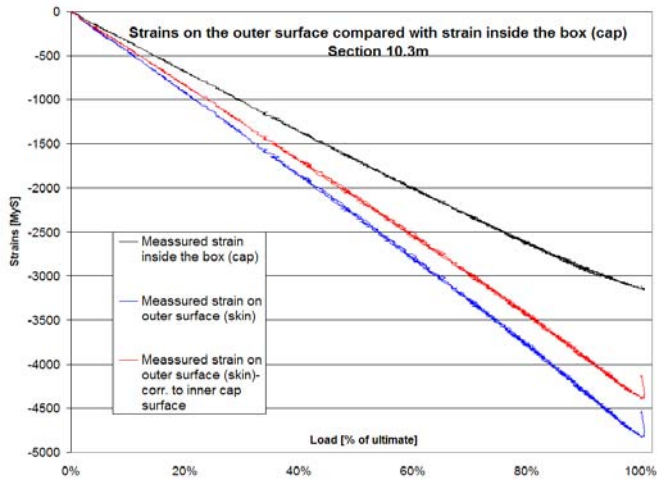

Figure 40. 'Back to back' strain measurements in 10.3m section from the first full-scale test. The red curve is without correction for global bending, while the blue curve includes this correction**.**

The increasing difference between the blue and the black curves indicate that caps bend locally. However, before a final conclusion can be drawn, a correction of the contribution from the global bending needs to be made. The overall bending of the box girder results in compression and tension in the two caps, when the blade is loaded in flapwise direction. The distance from the neutral axis determines how large the strain values are, see Figure 41.

The strain gauge positioned inside the box girder (blue curve in figure 40), has a lower value than the strain gauge on the outer surface (black curve). This is caused by the difference in distance to the neutral axis. This is illustrated in Figure 41. The contribution from the global bending must be removed, so that the outer and inner strain values can be compared without influence of the global bending. This 'correction' is made by taking the blue curve results and multiplying them with a factor to compensate for the different distances to the neutral axis. The factor for the 10m section is approximately 0.93 (435mm/470mm) and is plotted with a red colour in Figure 40. The difference between the red and the black line results is caused by cap panel local bending.

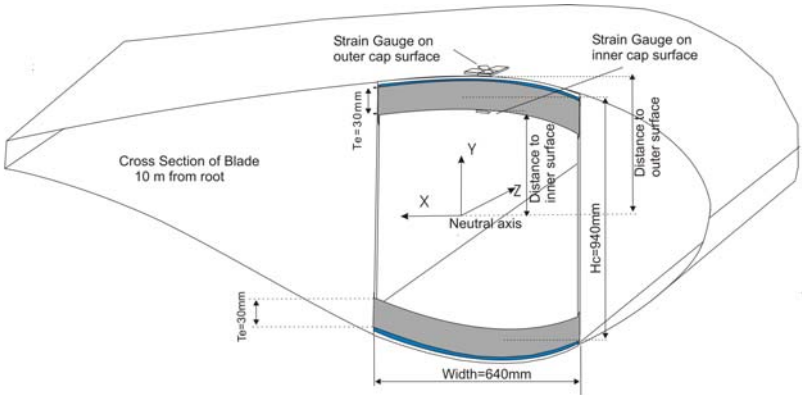

Figure 41. Sketch shows the different distances to neutral axis in 10m section. The distance from the neutral axis to the outer surface is 470mm and the distance to the inner surface.

For other sections the correction is larger, see e.g. the 17m section, where the factor is 0.84 due to lower profile height and thicker laminate in this section is 435mm.

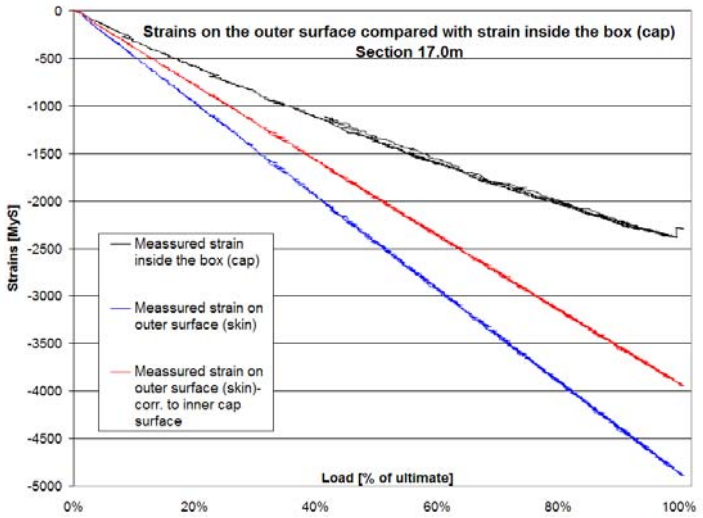

Figure 42. 'Back to back' strain gauge measurements in 17m section. The red curve is measured strain on outer surface without correction for global bending, and the blue curve shows where the global bending contribution is omitted.

In Figure 42, the 'back to back' results are plotted (black and blue curves), but also an extra curve (red curve) is added to show the strain on outer surface with the global bending.

From Figure 42 it can be concluded that this section also bends locally. It is expected that this happens due to changes in the tapering of the box girder, which is also a geometric effect similar to a 'geometry jump' shown in Figure 37a. This needs to be studied in detail before a final conclusion can be drawn. This phenomena has been addressed in this PhD-project, and a FE- and theoretical study has been started together with Dr Paul Weaver and Dr Luca Chechinni from the University of Bristol, but the work is not finished at the time of writing. One thing which will be studied in the future is the influence of changes in tapering on the buckling capacity. If the effect has a significant influence on the buckling strength, the obvious improvement would be to design the geometry with a smoother tapering, in order to minimize local bending. For the SSP34m blade it is obvious that the transition zone should be extended to a larger area so this sudden change in profile height is avoided, but other areas might also be optimized to avoid localised bending behaviour.

6 Failure mechanism in a blade box design

Four important failure mechanisms have been either observed during the full-scale tests or in the numerical FE-Study. These mechanisms are:

Section 6.1: Skin peeling – Debonding of the aerofoil from the box girder
Section 6.2: Interlaminar shear failure in the cap caused by Brazier loads
Section 6.3: Web failure
Section 6.4: Transverse shear distortion of the cross section

6.1 Skin peeling – Debonding of the aerofoil from the box girder

The SSP 34m blade analyzed in this PhD-work has a load-carrying box girder attached to the outer skin (aerofoil), see Figure 43. The connection between the outer skin and the box girder is an adhesive joint of approximately 5mm in thickness. This adhesive joint is sensitive to peeling stresses, which was observed in the first full-scale test, see Figure 43a.

Fig. 43a

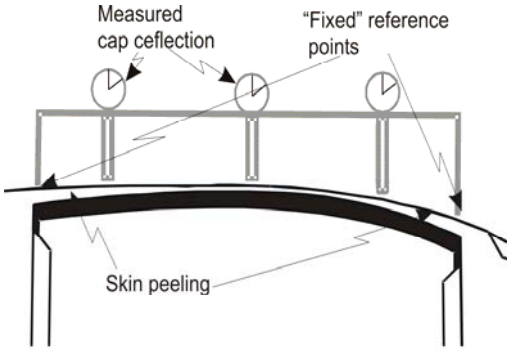

Fig. 43b

Figure 43. Skin peeling from cap observed in the first full-scale test a) Photo of skin peeled of the box girder b) Sketch of measure equipment and reference frame to cap deflection measurement equipment.

A study of measured cap deflections showed that the skin peeling starts at 92% load, see Figure 44. The jump in measured deformation has not occurred due to sudden chordwise bending of the cap. Instead, it was caused by the skin debonding from the cap, during which it assumes more of the initial curvature. The reference frame for measuring cap deflection is attached to the outer skin rather than directly to the box girder corner illustrated in Figure 43b. In Figure 44 another skin peeling jump can be observed at 97% load.

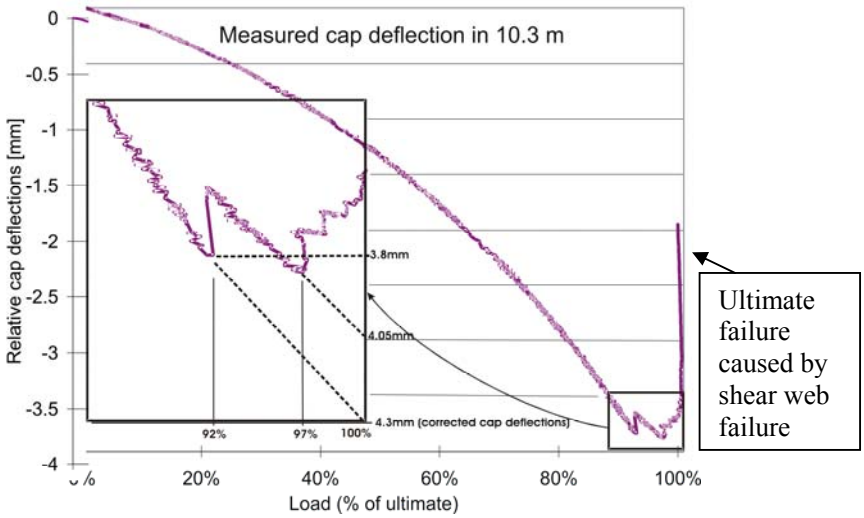

Figure 44. Measured skin peeling from the first full-scale test. The dotted lines show "corrected' cap values.

The actual maximum cap deformation of 4.3mm was obtained by extrapolation, see dashed line in Figure 44. This value would be observed if measurements were taken directly on the box girder or if the debonding had not occurred. Failure of the wind turbine blade can also be observed in Figure 44 at 100% load, just before failure. This behaviour is caused by the shear webs' failure, see explanation in Section 6.3.

6.2 Interlaminar shear failure in the cap caused by Brazier loads

Interlaminar shear failure is a mechanism that occurs between the layers in the load-carrying cap laminate, see Figure 45. The failure is caused by interlaminar shear stresses. The interlaminar shear failure can be developed by the crushing pressure causing biaxial stress distributions, interlaminar and peeling stresses due to the curved structure being flattened out, see Figure 45a. Brazier forces, explained in Section 5.1, cause the out-of-plane deformation of the cap. The cap deflections are increased by the lay-up, since the fibres are mainly placed in the longitudinal direction of the blade. The lack of fibres in the transverse direction causes the cap to be relatively flexible in the lateral direction, see Figure 45a.

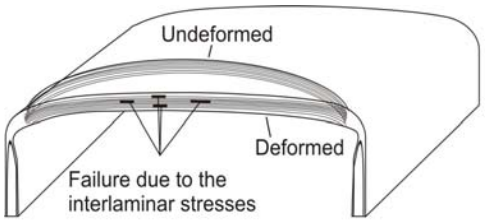

Fig. 45a

Fig. 45b

Fig. 45c

Figure 45. Interlaminar shear failure of the load-carrying cap. a) Sketch of cap deformation and failure between layers b) Photo of a cap with delamination c) Photo of a cap with a manufacturing defect.

Layered composite materials do not have large resistance against peeling (mode I) and interlaminar stresses (mode II), which may lead to failure, see Figure 45b. Furthermore, it is common that manufacturing defects inside the laminate further reduces the limit for the peeling stresses, see Figure 45c. To further investigate the interlaminar failure observed in the tests of cap specimens from an SSP 34m blade were cut out and tested in 3 and 4-point bending tests. These tests were performed at Imperial College – Department of Mechanical Engineering by PhD-student Amit Puri and Dr John Dear, see Figure 46 and ref. [70], [72].

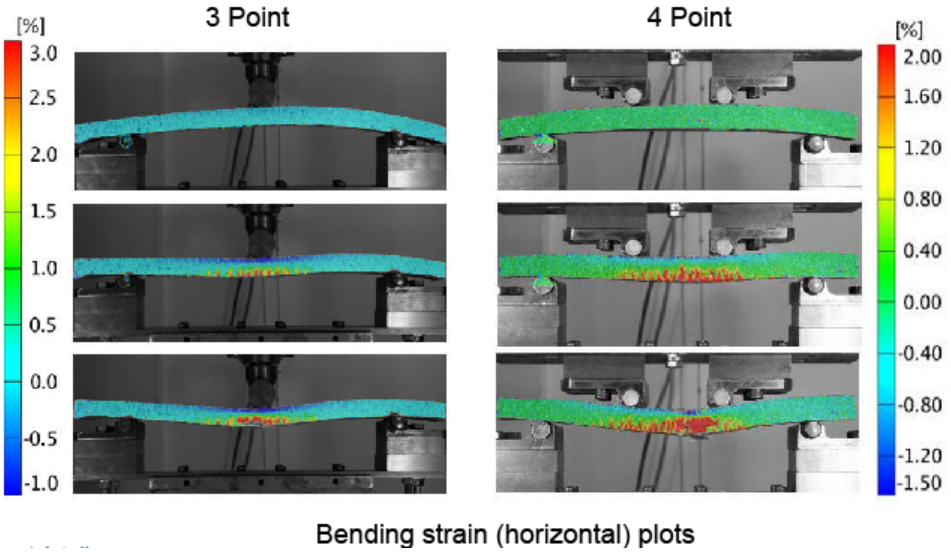

Fig. 46a Fig. 46b

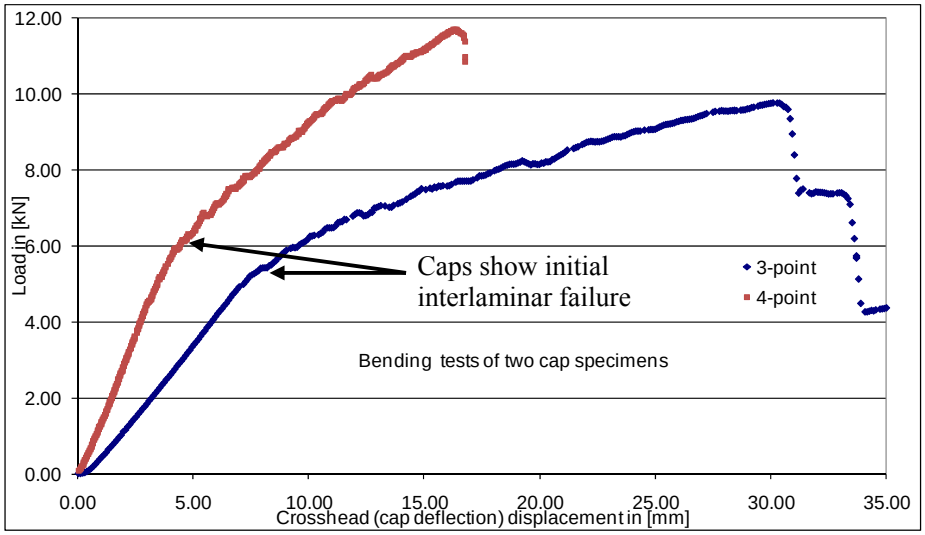

Fig. 46c

Figure 46. 3 and 4-point bending tests of two cap specimens. The bending tests were performed at Imperial College – Department of Mechanical Engineering, see ref. [70], [72]. Subfigures a) and b) The overlaid contour plots shows the strains along axis of the test specimen (referring to the transverse strains in the box girder) caused by the bending loads c) The bending tests lead to initial interlaminar failure after 8mm and 4mm deflections in the 3 and 4-point bending tests. Figures from ref. [70].

The two bending tests (3- and 4 point) showed that deflections at 4mm and 8mm, devolop interlaminar crack growth (change in stiffness), respectively, see Figure 46c.

From the first full-scale test the cap deflections were in the range of 1-6mm, so lateral bending stiffness may be too small to avoid interlaminar failure, see Figure 47.

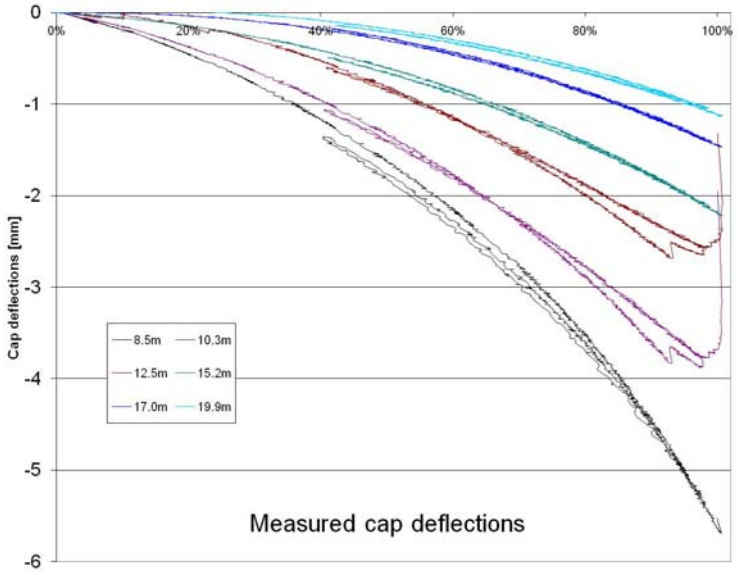

Figure 47. Cap deflections of the centreline in different sections in the first full-scale test.

6.3 Web failure

Web failures have been observed as the main reason for collapse in the first two full-scale tests, see Figure 48. Later in this section, explanation and results from the first two full-scale tests are presented. The third 'blade' (box girder no. 2), also seems to fail in the shear webs. Results and conclusions from this test (test 5) are presented in Section 7.1.

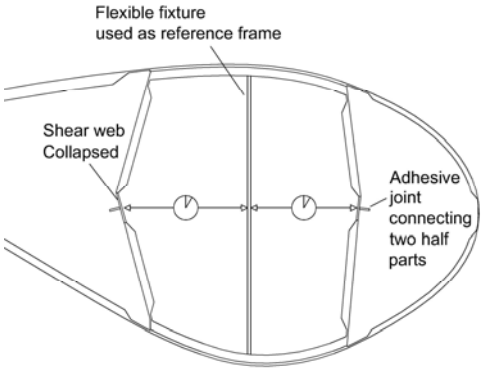

Fig. 48a

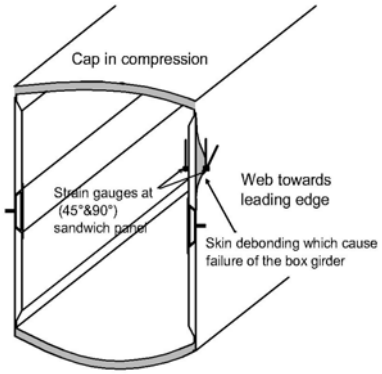

Fig. 48b

Figure 48. Sketch of two different web failure modes observed in the first two full-scale tests. a) Shear webs collapse at the first full-scale test which had no additional reinforcement where the two half parts were connected b) Skin debonding failure of the sandwich shear webs which was observed in the second full-scale test with reinforced webs.

In Figure 48a, the collapse of the original SSP-blade design and in Figure 48b, the web failure with reinforced shear webs are shown. The original SSP 34m blade, which had no additional reinforcement, had no problems to pass the required certification loads, see ref. [88]. The reinforcement was performed in this PhD-project, in order to understand other types of failure modes in wind turbine blades. Obviously, this is individual for each blade manufacturer and strongly depends on the blade design. The web failure mechanism and results from the first two full-scale tests are presented further.

Web failure - Results from the first full-scale test

In Figure 49a, the measured web deflections are shown. It is clearly visible here that the web towards the trailing edge collapsed just before ultimate failure, since a dramatic change in web deformation is observed. The FE-model predicted the same failure, see Figure 49b.

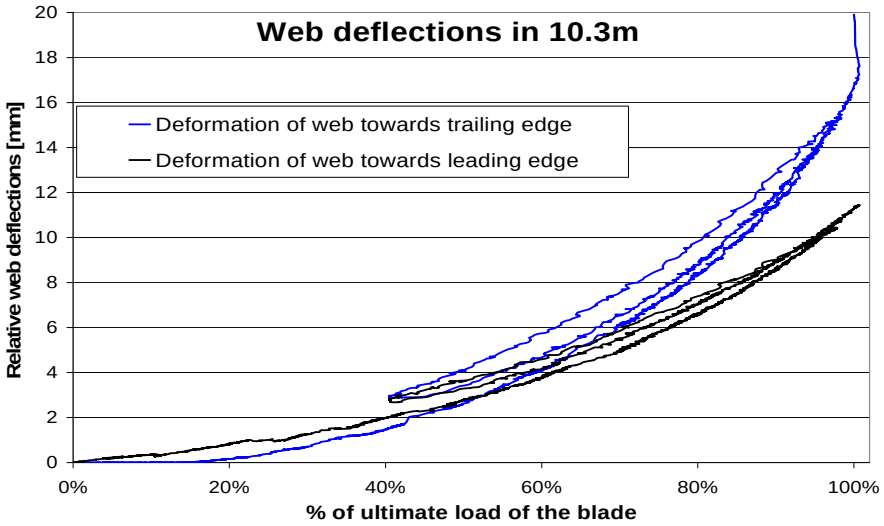

Fig. 49a

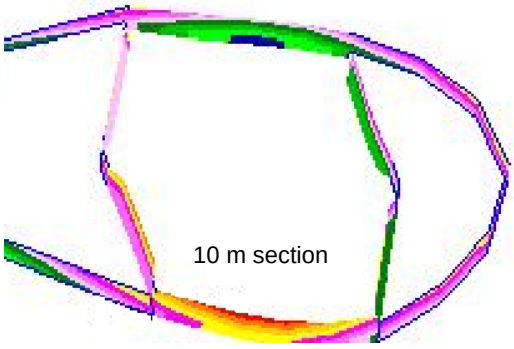

Fig. 49b

Fig. 49c

Figure 49. Collapse of the shear web in the first full-scale test a) Measured web deflections at 10.3m b) A non-linear FE-prestudy indicated that the shear web connection between the two half parts would be a weak point c) Photo of the shear towards trailing edge after the blade was failed also indicated that the shear web had caused ultimate failure of the blade.

The photo of the shear web, given in Figure 49c, is taken after the blade collapses, and shows the identified shear web failure. However, it could also be a failure occurring after other failures had happened, so study of failure modes must include measurement during the test like the shown in Figure 49a and explained earlier.

Web failure - Results from the second full-scale test

Figure 50a presents a frozen frame picture of the first, and critical, failure mode of the box girder full-scale test. In white circel(light green colour) initial face debonding of the outer skin on the shear web's sandwich section are shown, leading to ultimate collapse of the box girder.

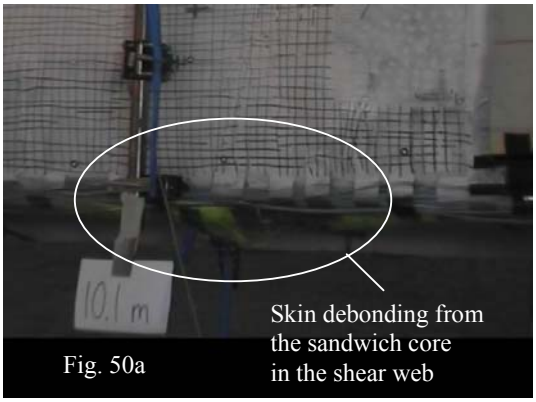

Fig. 50a

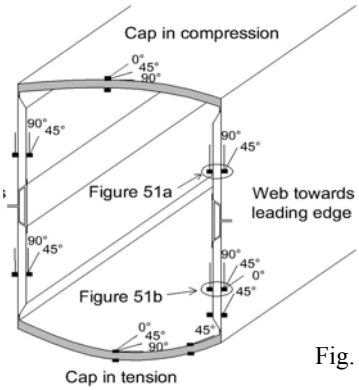

Fig. 50b

Figure 50. Skin debonding of the sandwich web towards leading edge in the second full-scale test a) Still picture which shows that the outer skin debond from the sandwich core b) Strain gauge locations at the 10m span position. The sketch is rotated by 90º with respect to the photo.

During the full-scale test strain has been measured in different locations; figure 50b shows measurement locations in 10m. The 'back to back' strain measurements are presented in Figure 51.

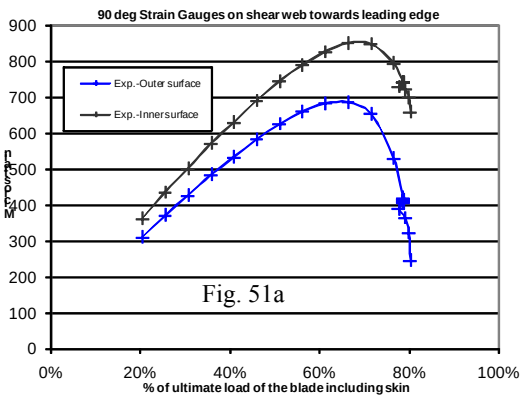

Fig. 51a

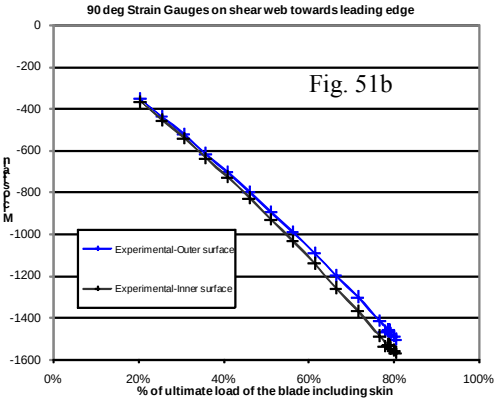

Fig. 51b

Figure 51. Strain gauge measurements (back to back) in the second full-scale test a) Upper web part (compression) b) Lower web part (tension).

The 0^0 (longitudinal) strains in the box girder caused by global bending, leads to associated strains in the 90^0 direction due to the Poisson's ratio effect; positive in the shear webs of the upper (longitudinal compressive) half part of the box girder and negative in the lower (longitudinal tensile) as shown in Figure 51. Normally, the

transverse deformation is small in axially loaded 0º laminates, but for ±45º laminates the Poisson's ratio is large, typically for the materials in question [12.]. In the FE-model of the box girder described in following section the ±45º laminates are modelled as 0º laminates with an axial Poisson's ratio of 0.6. The theoretical Poisson's strain in the 90º direction ($\varepsilon_{Poisson}$) is given by:

$$\varepsilon_{Poisson} = \nu \cdot \varepsilon_{axial} \qquad (3)$$

where ν is the axial Poisson's ratio, and ε_{axial} is the 0^0 strain in the longitudinal direction related to global bending.

The combination of compressive strains due to the Brazier crushing forces and the axial tension, results in higher absolute circumferential strains on the tensile side of the blade than on the compressive side. The drop in the strain-load curves at 70-80% load in the full-scale test in the upper (longitudinal compressive) side of the web is caused by buckling of the cap. Figure 52 shows the location of the observed buckling deformations.

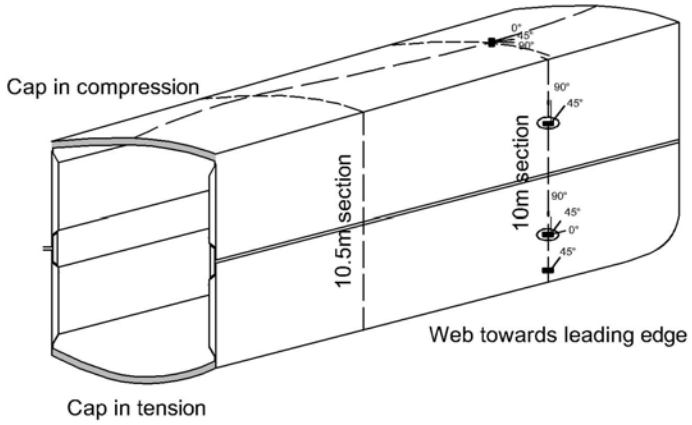

Figure 52. Position of the cap buckling pattern.

Once buckling of the box girder initiates, the inward buckling wave and the associated reaction in the shear webs at the 10m section introduces compressive strains at the compressive side of the shear web, subseqquently producing the sudden drop in strains demonstrated in Figure 51a at 70% load.

Results from FE-model

Figure 53 shows 90^0 strains at two locations in the compressive and tensile side of the web placed symmetrically around the neutral axis of the girder at 10m from the root. The two locations are identical to the locations where strain gauges were placed in the test. Both linear and non-linear strains are found in the upper part and lower part, see Figure 53.

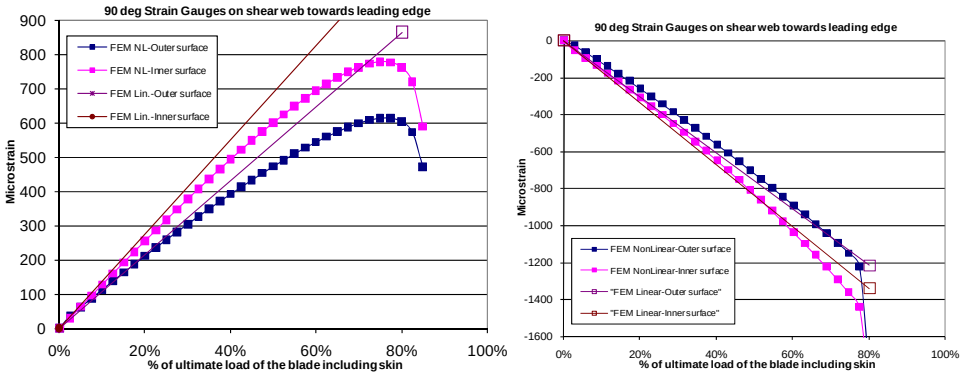

Fig. 53a Fig. 53b

Figure 53. Linear and non-linear FE-results a) Upper web part b) Lower web part.

The difference between the linear and the non-linear FE-results is, at least in part, caused by the Brazier effect. The crushing pressure, attempting to flatten the cross-section, introduces compressive strains into the shear webs. However, this crushing pressure varies with the square of the applied load resulting in the noted deviation from linear responses. Other non-linear phenomena, such as changes in geometry and loading configuration (which follows the geometry in the non-linear analysis), will also contribute to the observed nonlinearities.

Buckling produces the sudden drop in strains at 80% load, similar to the test. In Figure 54 part of the model is shown and the buckling is visualized by plotting the transverse (x-direction) strains.

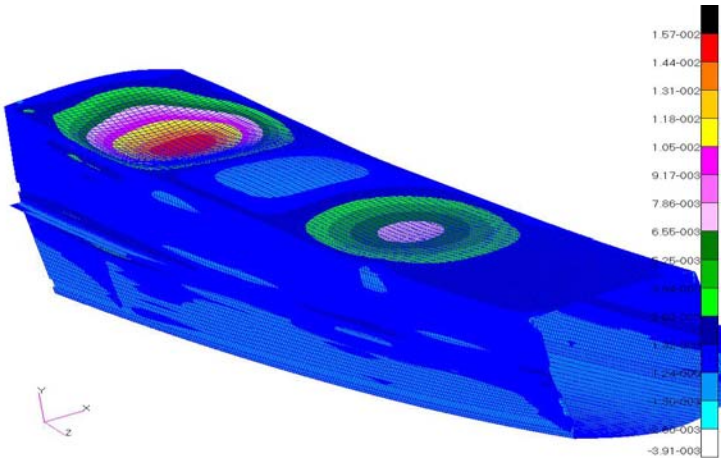

Figure 54. Section of finite element model from 9.5m to 13.2m from the root. Strain in global x-axis (transverse) is presented.

6.4 Transverse shear distortion of the cross section

Transverse shear distortion of a wind turbine blade cross-section is an important failure mechanism, see Figure 55.

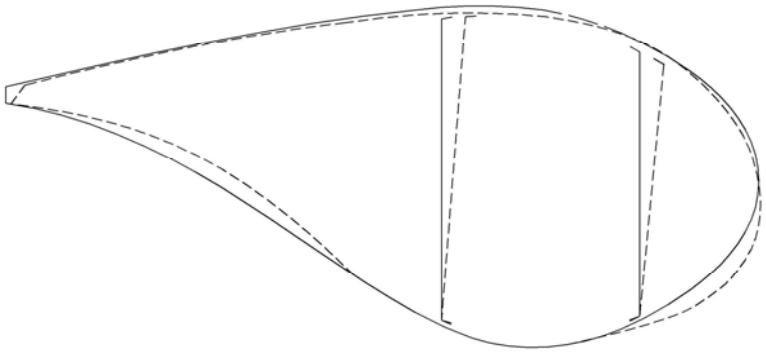

Figure 55. A sketch of a distorted wind turbine profile

In the literature considering wind turbines no invetigations have been found relating to this failure mechanism. In other industries, such as aeronautic (wings to aeroplanes and blades for helicopters) and bridges, it is a well-known mechanism which must be taken into account in the design process, see e.g. ref. [22], [62], [63], [87]. In the literature, a twisted rectangular section is often presented, see Figure 56.

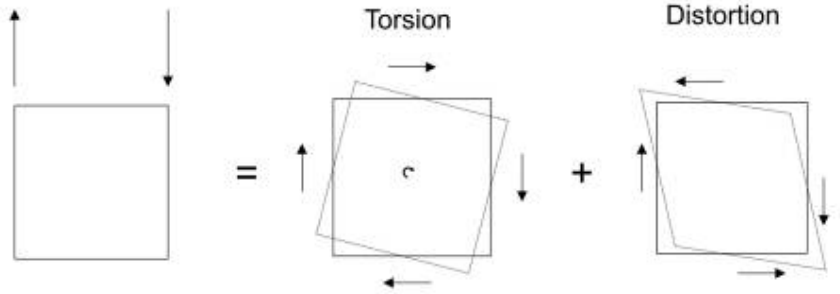

Figure 56. A sketch from ref. [87] shows the two distributions (torsion and distortion) when a box girder is twisted.

For some reason nobody, to the Authors knowledge, in the wind energy area has paid much attention to this failure mechanism. However, it is obvious that a thin walled structure without any internal reinforcement will try to distort the profile in the transverse direction. This is even more prominent when the blade is non-symmetric, both in geometry and in lay-up, since the blade will try to twist. Furthermore, the lay-up is highly orthotropic with the majority of fibres in the longitudinal directions, so the circumferential stiffness is small.

The combined flap- and edgewise load direction, which is a more realistic load case as mentioned in Section 1.3, may also be partly the reason why this failure mechanism

has not had much attention before. Larger blades are expected to be more critical for this failure mode since it is almost impossible to increase the corner stiffness in order to account for the increase in transverse shear forces.

Furthermore, if future wind turbine blades are lighter due to optimization, the longitudinal curvature will increase, which will raise the crushing pressure and this could be critical for a distorted blade section, see Figure 57.

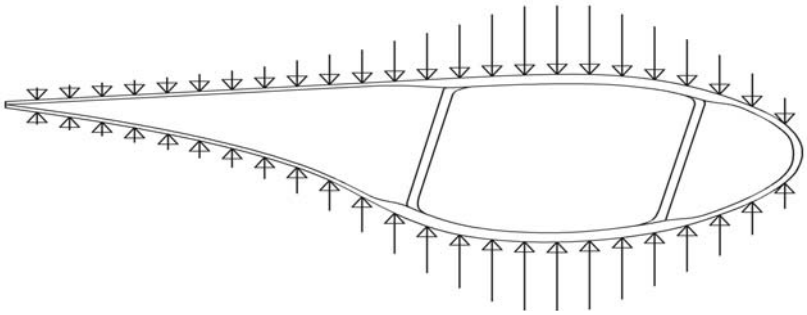

Figure 57. Crushing pressure from the longitudinal bending (Brazier loads) at a distorted profile.

In Figure 57, the blade section is distorted and collapse of the entire blade is critical, due to the crushing pressure from the Brazier loads.

A FE-prestudy of the box girder showed that transverse shear distortion was likely, so the box girders were supported in transverse direction in test 2-5 as explained in Section 2.3. Of course, a box girder does not have the representative transverse shear distortion stiffness of a full wind turbine blade section. FE-studies and experimental investigations need to be performed for the actual blade before it can be concluded whether this failure mechanism is critical or not. FE-studies of a SSP 34m blade have indicated that it is critical, especially in combined loading conditions, see Figure 58.

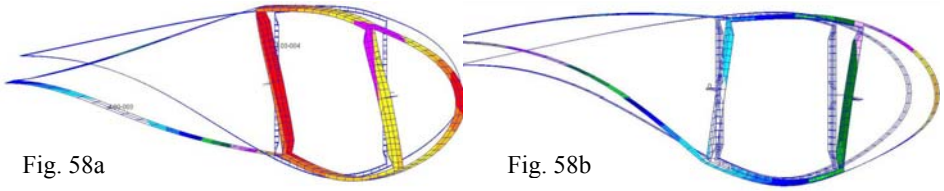

Fig. 58a Fig. 58b

Figure 58. FE-plots of a distorted section in two different load cases with combined flap- and edgewise loads a) Combined flap- and edgewise loads towards leading edge b) Combined flap- and edgewise loads towards trailing edge. Both figures are shown with an non-deformed and deformed shape. The deformation is shown without the global deflections to illustrate the distortion of the profile more clearly.

The distorted cross sections in Figure 58 are loaded in a combined flap- and edgewise direction, one where the gravity is towards the trailing edge (a) and one where it is towards the leading edge (b), explained in section 4.2. Reinforcement has been introduced to solve the distortion problem, is presented in section 7.5.

7 Design reinforcements

As part of the PhD-work, six independent reinforcements have been suggested. The rib reinforcement introduced in section 7.1 is not new and no patent application has been made. For the five remaining reinforcements four patent applications (one application includes two reinforcements) have been submitted at the end of 2006 or the beginning of 2007.

In this chapter only the basic principals are described. More figures and other configurations can be found in the patent applications, see appendix B. The focus will be put on results obtained in the different Proof of Concept phases.

The six reinforcements are presented in the following sub sections:

Section 7.1: Rib/Bulkhead reinforcement
Section 7.2: Invention "Cap reinforcement" (patent A)
Section 7.3: Invention "Web coupling reinforcement" (patent B)
Section 7.4: Invention "Floor reinforcement" (patent B)
Section 7.5: Invention "Shear cross reinforcement" (patent C)
Section 7.6: Invention "U-box girder design" (patent D)

7.1 Rib/Bulkhead reinforcement

Inspired by the aeronautical industry (e.g. ref. [21], [64]), transverse ribs in wings are presented, see Figure 59a.

Fig. 59a

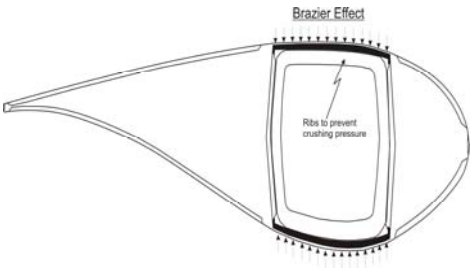

Fig. 59b

Figure 59. Rib reinforcement a) Ribs used in aircraft today [21] b) Rib reinforcement in a wind turbine blade.

In the aeronautic industry where ribs are very common the manufacturing processes are different which is part of the reason why ribs are not used in the wind turbine industry today, see Section 1.2. Another explanation is that the focus has not been on structural strength to the same extend as for the aeronautical industry. The main reason to insert ribs is to prevent ovalisation, see ref. [62], [63], [64].

Ribs do also have a positive effect relating to the flattening problem of the cap, see Section 6.2. The transverse shear distortion, explained in Section 6.4, is also expected to be solved in regions where ribs are inserted. Insertion of ribs does not prevent buckling effectively, since the buckling waves can buckle between the ribs. FE-studies performed before the test showed that ribs spaced with 1m increase the buckling capacity with approximate 10-20%. Thus, if a large increase in loads is to be applied or the cap thickness is to be reduced, other solutions must be found to avoid buckling.

In the following section 'proof of concept' results from full-scale test 5 (with ribs), are presented.

Proof of Concept for rib reinforcement

Ribs were inserted after test 4 was performed, but only in region (0-17m) where it was possible to enter the section. Luckily it was possible to insert ribs in the region where the 'blade+box girder' had failed earlier, see Figure 60.

Fig. 60a Fig. 60b

Figure 60. Full-scale test with ribs a) Photo of a rib/bulkhead inserted at 10.2m b) Ultimate collapse of the box girder with transverse ribs. The failure happened at 11.5m between two ribs.

The box girder with ribs, failed at 104% load, which is an increase in the ultimate load by 30% compared with the first box girder test (test 2) without ribs. The increase in ultimate load is dramatic taking into consideration that only few ribs were inserted and no other reinforcements were performed. Detailed studies of what was the first dominating failure mechanism have not been performed, since the major purpose was to see the effect on the ultimate load and not so much to study failure mechanism with ribs inserted. It is likely that the failure was either buckling or shear failure in the shear web. If the shear webs and the buckling strength have been improved then the ultimate load is expected to be considerably higher, since the general strain level is very low compared with maximum 'allowable' strain level, see explanation in Section 1.4. The failure could also be caused by damage found on the shear web during the first trial test, see Figure 61a.

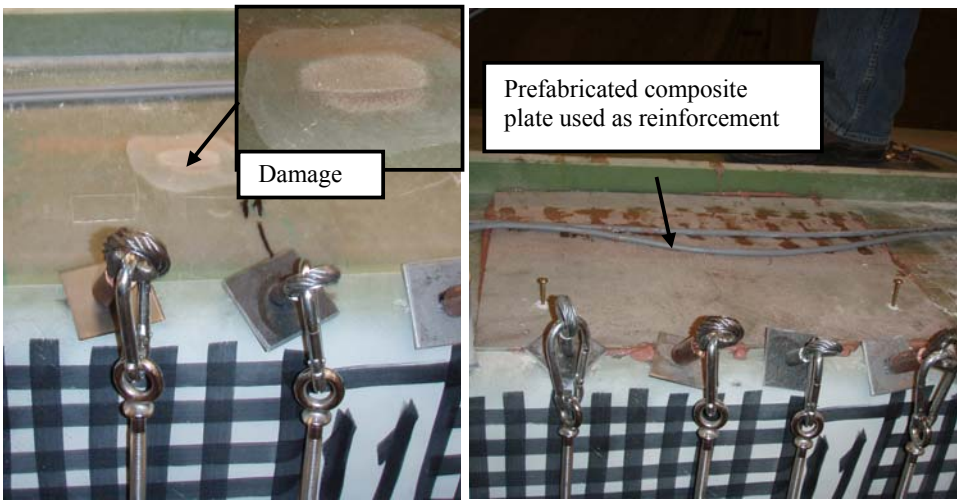

Fig. 61a Fig. 61b

Figure 61. Damage was found on the shear web in a critical area a) Photo of the damage on the shear web in 11.1m b) The damage was reinforced by a prefabricated composite plate glued to the shear web.

The damage happened during the instrumentation of measurement equipment when a hole in the outer skin on the sandwich shear web was made. The position of the damage was unfortunate since the blade was expected to be critical in that area and a reinforcement was made, see Figure 61b. Even though the blade was reinforced, it failed where the reinforcement was placed, see Figure 62.

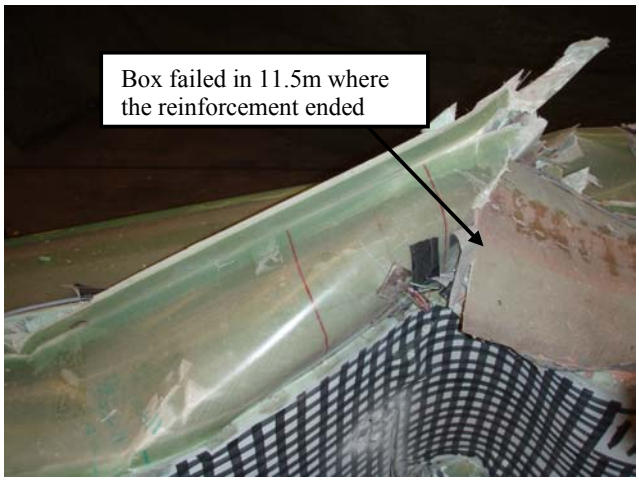

Figure 62. The box girder failed in the region where the damage was found.

From the photo in Figure 62 it looks like the failure happened in the area where the reinforcement ended, which is a typical situation when reinforcement is implemented. This could be localized bending caused by an 'asymmetric' layup as shown in Figure 38c.

7.2 Invention: 'Cap reinforcement' (Patent A)

The first invention presented is a reinforcement of the cap, which prevents a curved (aerodynamic shape) cap from flattening out, see Figure 63.

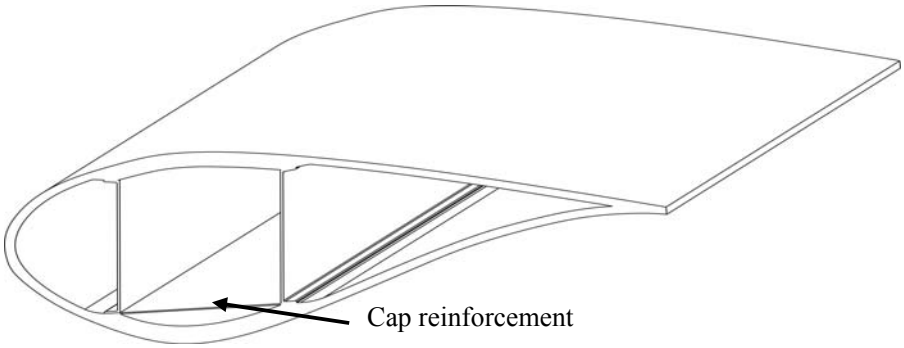

Figure 63. Sketch of the cap reinforcement which prevents the curved cap from flattening out due to the corners being restrained from sideward deformations

The restriction of the out of plane deformation of the cap is due to the corners being restrained from sideward deformations, thus increasing the flexural stiffness of the cap. The reinforcement is expected to be thin in comparison to the cap thickness, since the reinforcement should carry only tension. Increased flexural stiffness of the cap prevents three elastic phenomena from happening to the same extend as without reinforcement. These responses, described in Chapter 5, are ovalisation (flattening of the cap), buckling and localized bending.

The cap reinforcement can be made of any material, such as wires, fibres, dry fibre mats etc. an the reinforcement needs only to carry tension. In Figure 64a, a dry fibre mat is presented and a pultruded profile is shown in Figure 64b. Pultruded profiles, which have not yet been seen in wind turbine blade design, may be an interesting alternative.

Fig. 64a Fig. 64b Fig. 64c

Figure 64. Different embodiments of the cap reinforcement a) Dry fibre mat b) Pultruded profile c) Wire or pin solution

Also wires or pins can be used, as showed in Figure 64c. A special wire solution, shown in Figure 65, was used in the full-scale test, since it was the simplest solution to implement in an existing box girder. Of course this solution could never be used in practice, but in a 'proof of concept' test it is satisfactory, see the following 'proof of concept' section.

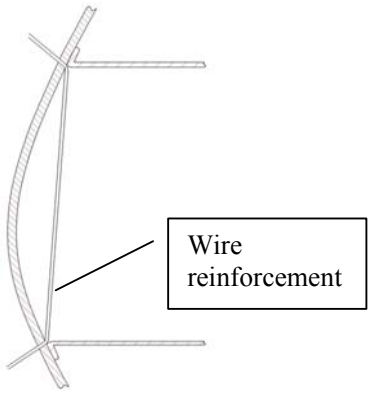

Figure 65. Sketch of the wire reinforcement solution used in the full-scale test. The sketch is rotated 90º , so it is comparable to the full-scale test presented in the next section.

Proof of Concept for invention/patent A

A proof of concept test was performed for the cap reinforcement. The work includes numerical and experimental work, but here only the experimental results are presented. As described in Chapter 2, two full-scale tests were performed for box girder 2 in order to validate the cap reinforcements. Test 3 was conducted without wires and test 4 was with wires, see Figure 66.

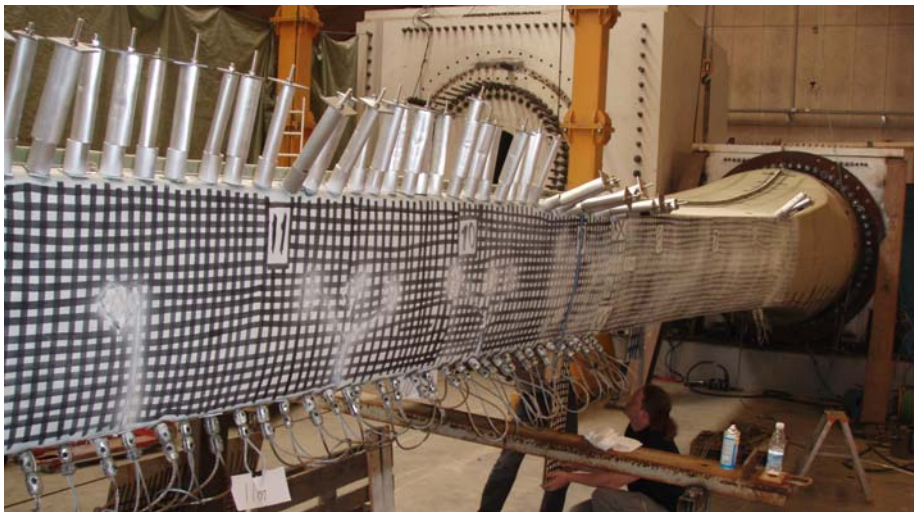

Figure 66. Full-scale test of a box girder with wire reinforcement (test 4) as part of a 'proof of concept' for the cap reinforcement invention.

Based on a FE-study two areas were found critical to buckling and cap reinforcement (wires) was placed in these two regions. One critical region was the 5m section, where three wires were placed to prevent buckling, see Figure 67.

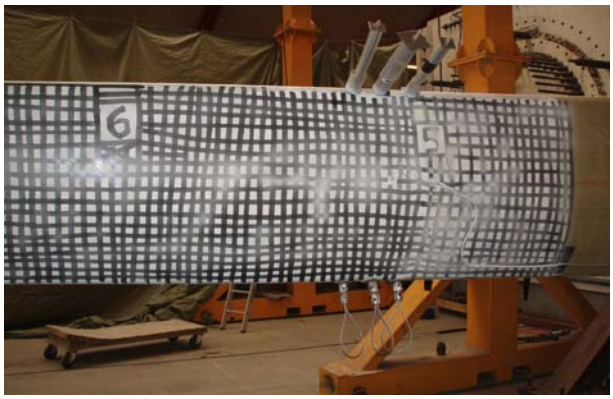

Fig. 67a

Fig. 67b

Figure 67. Wire reinforcement in 5m region a) Photo outside the box girder which shows the wires in 5m b) Photo inside the box girder.

In Figure 68 wires in 10-12m section are presented and the big difference in the transverse curvatures of these two regions (5m and 10-12m) can also be observed, see Figure 67b and Figure 68b.

Fig. 68a

Fig. 68b

Figure 68. Wire reinforcement in 8.5-12m region (only 10-12m shown a) Photo outside the box girder which shows the wires in 10-12m b) Photo inside the box girder.

FE-studies which were performed before the full-scale test showed that the reinforcement should have an effect also in regions with small transverse curvatures. The same results were observed in the full-scale test using the DIC system, see Figure 69a. The graphs in Figure 69a are a comparison between the two full-scale tests (test 3+4) where the effect of the wires are demonstrated. In Figure 69a, the deformed centrelines from the two tests of the cap along the blade are plotted. The blue line is from test 4 (with wires) and the red from test 3 (without wires).

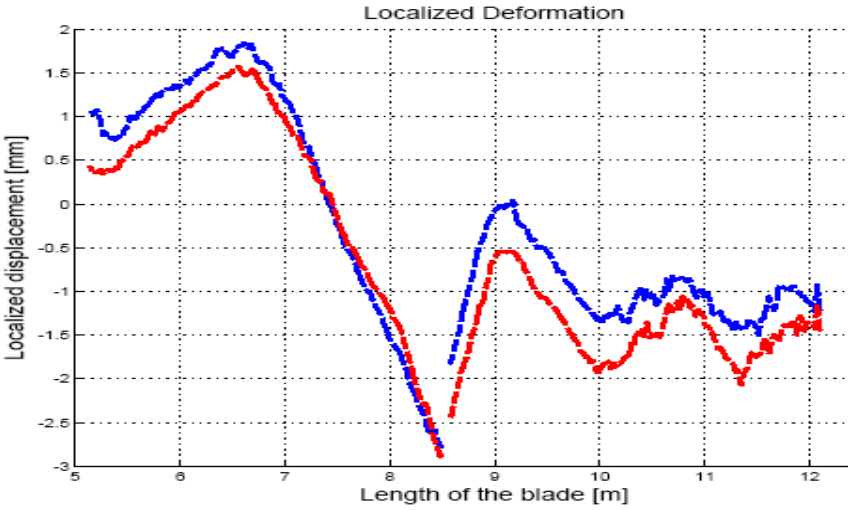

Fig. 69a

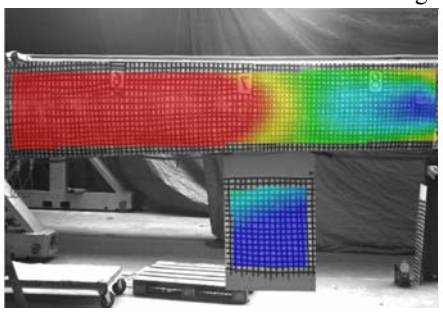

Fig. 69b

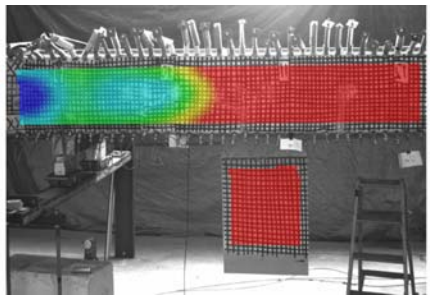

Fig. 69c

Figure 69. Cap deformations measured using Aramis DIC system. a) Two curves show the cap deformations of the centreline. Red line is from test 3 (without wires) and blue line is from test 4 (with wires) b) and c) Photos with an overlaid contour plot from the DIC system. The photos are mirrored so they fit the graph above in the length direction. Details can be found in ref. [37].

In the two regions where wires were placed, the out of plane deformation of the cap is reduced by 10-30%. In the region 6.5-8.5m, there were no wires and no significant differences are observed comparing the two tests. In the region 5.2-6.5m there is a difference even though there are no wires. This is due to the wires in 5-5.2m region which affects this, due to the large reinforcement effect caused by the large transverse cap curvature. As expected it is mainly the buckling waves which bend inwards that have been reduced. For example sections 10m and 11.5m have reduced their deformations with around 30%, while sections 10.8m and 11.8m only have reductions around 10%, see Figure 69a.

Not only have the out of plane deformations changed due to the cap reinforcement, the measured strain has also been reduced. In Figure 70, the measured strains in the transverse direction are plotted, for section 10.8m and 11.5m.

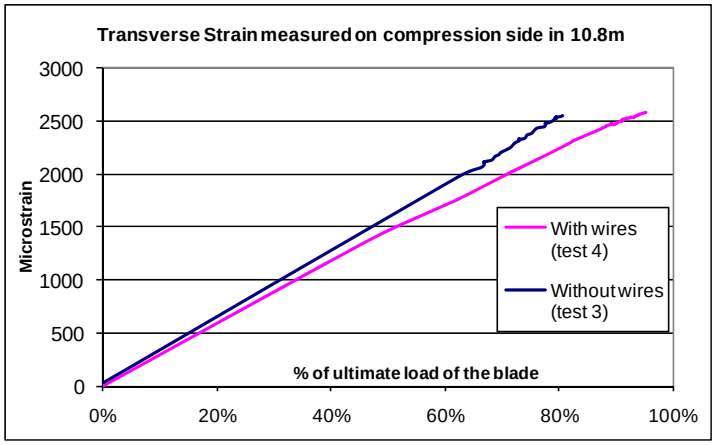

Fig. 70a

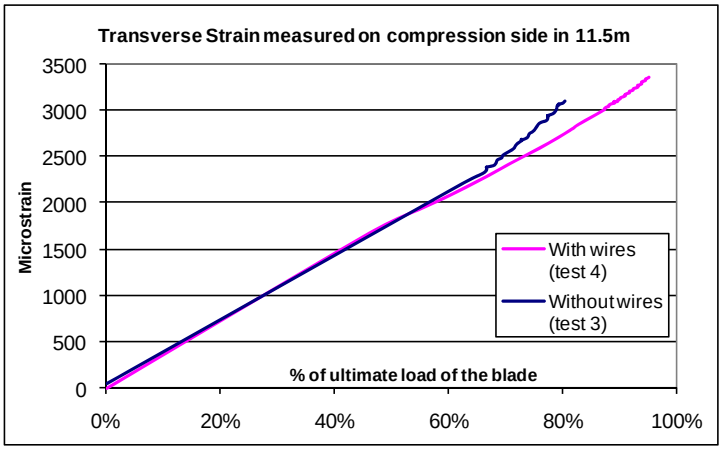

Fig. 70b

Figure 70. Transverse strain measurements with and without cap reinforcement. Measurements for section 10.8m and 11.5m are showed.

In Figure 70a, a difference in the linear strain response is observed, while in Figure 70b a non-linear behaviour in the specimen without wires can be observed after 70% loading. The non-linearity is caused by buckling of the cap, which can also be seen in the measured out of plane measurement from Figure 69a. The test with cap reinforcements (test 4) did not show any tendency to buckling even though the box girder was loaded up to 95%. If these observations can be generalized then it can be concluded that the buckling capacity has been increased with at least 35% and maybe more if the box girder had been loaded further. However the Author could not take the risk that the blade would fail since the final destructive test should be made with rib reinforcements, namely test 5 presented earlier.

7.3 Invention 'Web coupling reinforcement' (Patent B)

The ovalisation has been observed in both non-liner FE-calculations and in the full-scale tests, see Figure 71b. In particular, the web failure in the first full-scale may have been avoided if the two shear webs were coupled to each other, see Figure 71a.

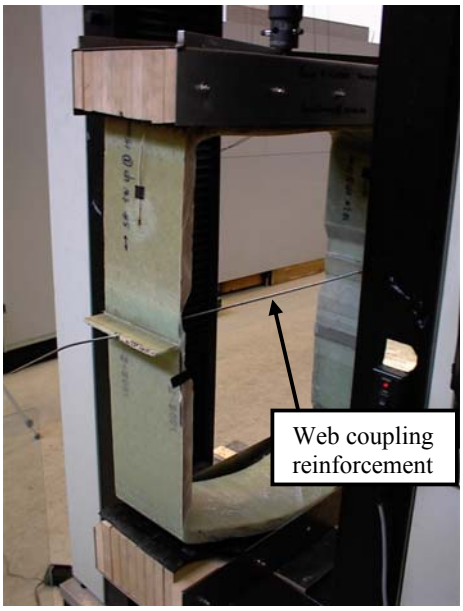

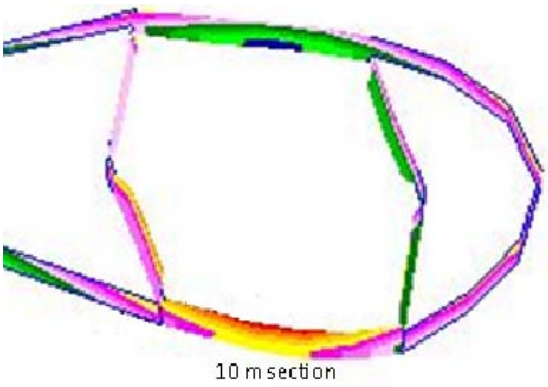

Fig. 71a Fig. 71b

Figure 71. Web coupling reinforcement a) Cross sectional tests proofed that coupling the two shear webs results in higher crushing loads b) Non-linear FE-studies showed that ovalisation would be dominating in the first full-scale test, since no additional reinforcement was implemented in the connection between the two box girder half parts.

To verify the web coupling reinforcement, cross sections of the blade were experimentally tested, see Figure 71a. A crushing load was applied to the structure to induce cross-sectional flattening. This force mimics the Brazier crushing forces. Two sections were tested and the test without web coupling reinforcement failed at a load similar to the crushing pressure which the first full-scale test has failed, see ref. [43]. The test specimen with a web coupling reinforcement, see Figure 71a, failed at load approximately two times higher than for the test without a web coupling reinforcement. Plans for the 'proof of concept' in a full-scale test are described at the end of the next section.

7.4 Invention: 'Floor reinforcement' (Patent B)

Patent B contains another invention which solves problem types other than the ovalisation problem. The floor invention is a flat 'horizontal' panel which connects different points in wind turbine blades, see Figure 72. The web coupling and the floor inventions are put in the same patent application, since there is an overlap in the area between the shear webs. The mechanisms and the problems the reinforcements solve are different, however, and they are therefore placed in separate chapters of this thesis.

In Figure 72 two configurations of the floor are shown, but in the patent application, several other embodiments are shown, see appendix B.

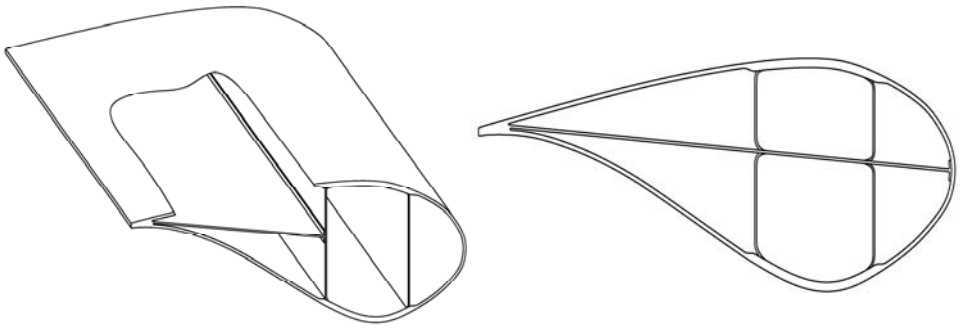

Fig 72a Fig. 72b

Figure 72. Floor reinforcement a) 3D-sketch of a floor inserted in the trailing edge region b) 2D-sketch of a blade section with a floor from leading edge to trailing edge. The webs are divided into two parts. The two half part solution is invented by SSP-Technology, see ref. [83], which connect the two half parts are connected with adhesivejoints in the same region as illustrated on the drawing.

Transfer loads to the root section

One of the main reasons for inserting a floor root section (e.g 2m-15m) is to transfer shear loads from the trailing edge to the main structure in the root section and/or the shear webs when the blade is loaded in the edgewise direction, see Figure 73.

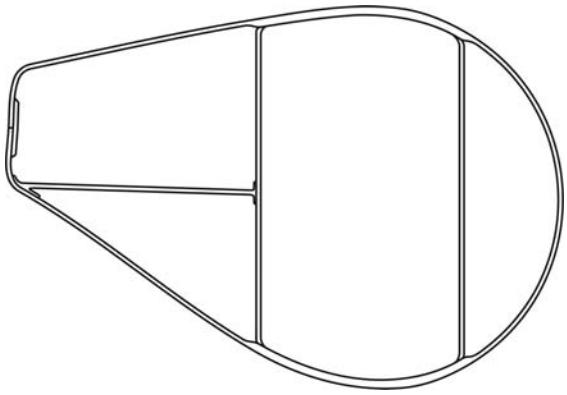

Figure 73. Floor reinforcement in the 'root' section. 3m section shown, but the floor should at least have an extension to 6m where the span of the chord is biggest. For larger blades the floor should have a still larger extent.

Fatigue problem in the trailing edge connection

Another purpose of inserting floors is to minimize deformation of the aerofoil. This is needed for several reasons e.g. trailing edge fatigue problems and aerodynamic efficiency. The aerodynamic efficiency will not be discussed here, only the fatigue problem will be addressed in this thesis, and a brief explanation can be found in the patent application, see appendix B. Today forces are carried by the double curved airfoils, which leads to out of plane deformation, see Figure 74a. Out of plane deformations cause peeling stresses in the trailing edge, and failures in the trailing edge are often seen, see Figure 74b.

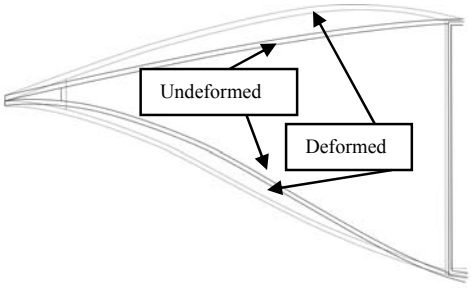

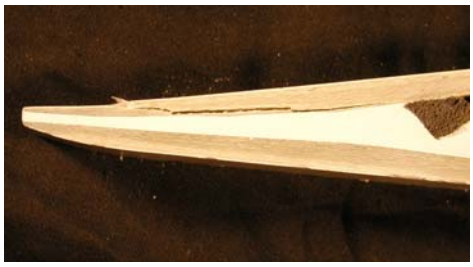

Fig. 74a Fig. 74b

Figure 74. Trailing edge failure a) Sketch of the trailing edge shells with 'out of plane' deformations b) Fatigue failure in the trailing edge.

When a plane floor is inserted, the trailing edge shells keep their original shapes and redistribution of the forces is avoided, see force distributions in Figure 75a and b. This is due to the fact that buckling of the trailing edge shells has been prevented, see Figure 75c.

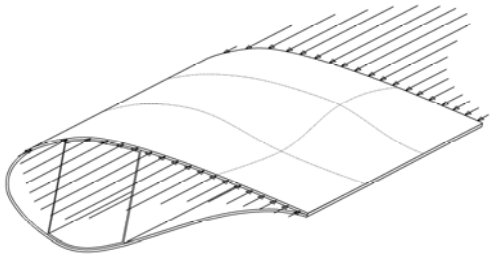

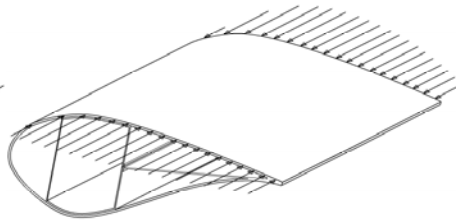

Fig. 75a Fig. 75b

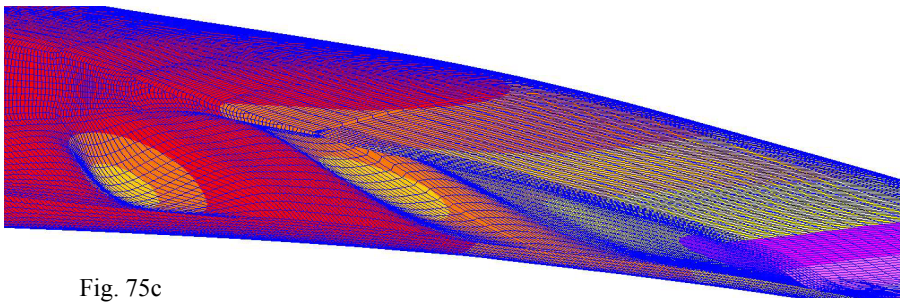

Fig. 75c

Figure 75. Buckling of the trailing edge shell. a) Sketch without floor where the trailing edge panel has out of plane deformations, which lead to redistribution of the forces b) Sketch with floor minimizing 'out of plane' deformations of the trailing edge shells and no redistribution of the forces is illustrated c) FE-model without floor shows out of plane deformation of the trailing edge shells.

The floor panel also help preventing overall buckling of the trailing edge, see Figure 76.

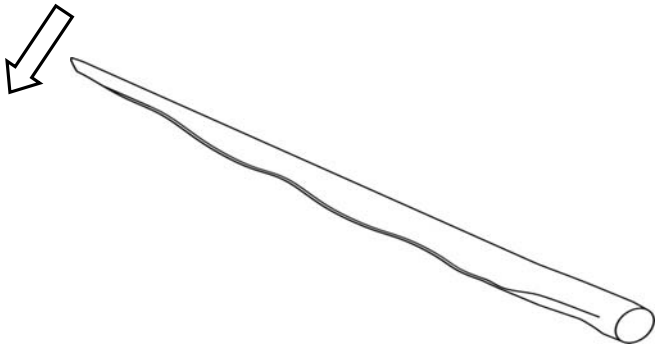

Figure 76. Buckling of the trailing edge.

The floor reinforcement also prevent 'out of plane' deformation of the shear webs and ovalisation is also minimized, see Figure 77.

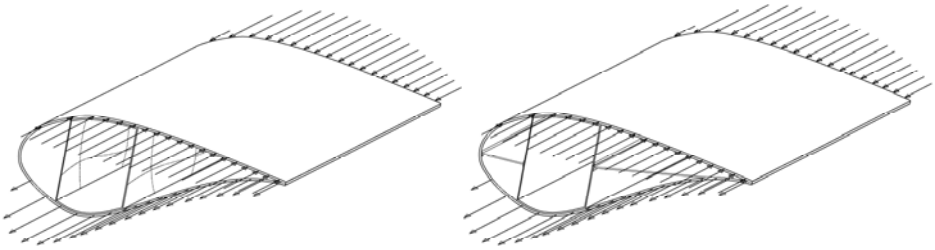

Fig. 77a Fig. 77b

Figure 77. Out of plane deformations of the shear webs a) Sketch of shear webs which are buckled or deformed due to the Brazier forces (ovalisation) b) Sketch with floors inserted prevent buckling of the shear webs and ovalisation.

Another 'unexpected' positive influence of the floors seems to be a positive effect on the transverse shear distribution, see Figure 78.

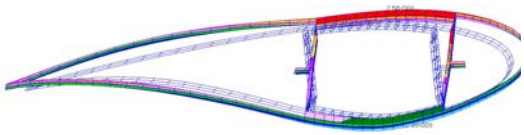

Fig. 78a

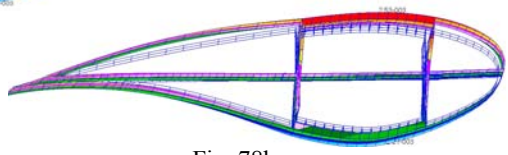

Fig. 78b

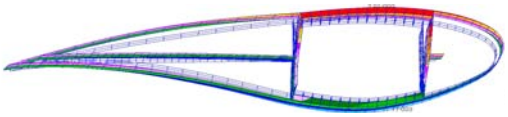

Fig. 78c

Figure 78. Blade with a transverse shear distorted profile a) Distorted blade profile without floor b) 'Full' floor from leading to trailing edge reduce transverse shear distortion, significantly c) Floor in the trailing edge region, only, also reduce the transverse shear distortion.

Another and more efficient solution to the transverse distortion problem is presented in Section 7.5.

7.5 Invention: 'Shear cross reinforcement' (Patent C)

In Figure 79 a cross-reinforcement in the box girder or between two shear webs are shown. The cross prevents from transverse shear distortion. The transverse shear distortion failure mode has been explained in Section 5.4.

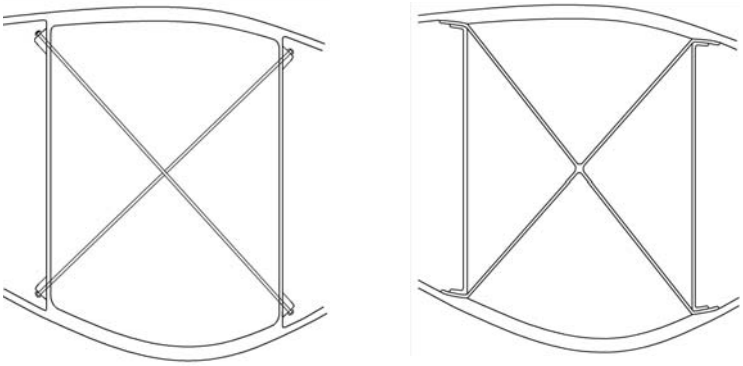

Fig. 79a Fig. 79b

Figure 79. Cross to avoid transverse shear distortion collapse a) Wire or pin solution b) Dry fibremat solution.

In Figure 79a, a wire (or pin) solution is shown and the wires (or pin) should be positioned each 2-5 metres, depending on the design, loads etc. Alternatively, a dry fibre mat solution could be used, see Figure 79b. From a structural point of view, there are no reasons to impregnate the fibre mats since only tension loads have to be carried. The dry fibre mat solution will have different embodiments, see Figure 80. Two fibre mat solutions are shown and the best choice depends on the manufacturing techniques.

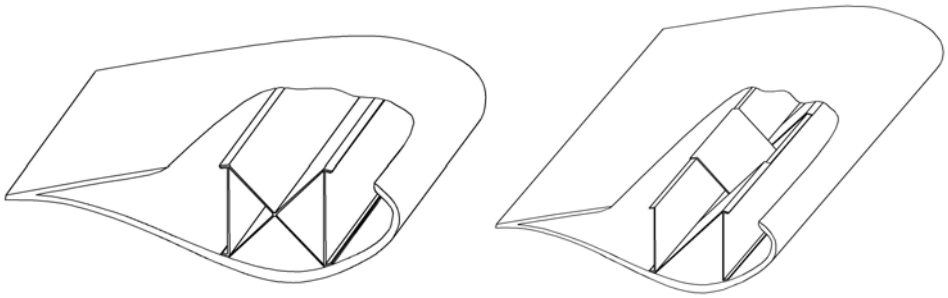

Fig. 80a Fig. 80b

Figure 80. 3D sketches of two dry fibre mat solutions a) Full shear cross b) The shear reinforcement alternates in the length direction.

In Figure 81, a FE-study of the SSP-blade has been performed with combined flap- and edgewise loading, as described in section 4.2.

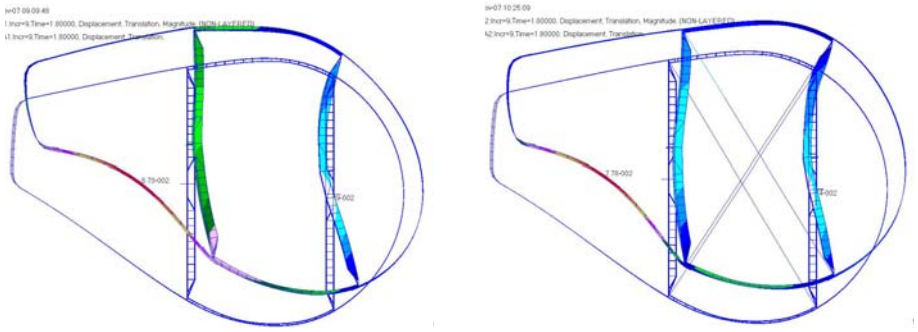

Fig. 81a Fig. 81b

Figure 81. FE-calculations show transverse shear distortion with combined loading as described in section 4.2. 4m section shown with deformed and non-deformed shape a) Without cross reinforcement b) With cross reinforcement.

7.6 Invention: 'U-design' (Patent D)

This invention differs significantly from the other 4, since it is mainly a production friendly design rather than a design preventing a structural failure mechanism. However, the production friendly design also takes the structural aspects into consideration. The main idea with the invention is to create favourable manufacturing conditions for the upper cap part, which often are the critical part, since it is in compression. This has been 'solved' by having an upper part (cap cover) without taking the shear webs into consideration. The shear webs are integrated in the lower cap as a U-design, see Figure 82.

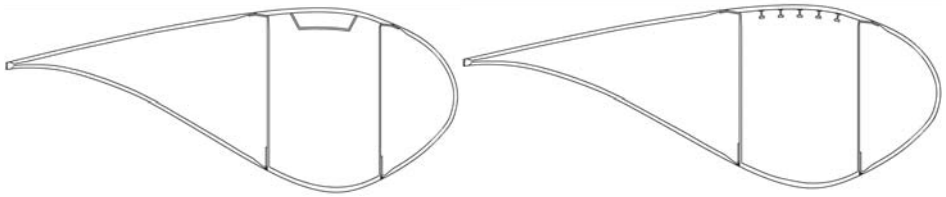

Fig. 82a Fig. 82b

Figure 82. Sketch of a wind turbine section with U-design concept a) Cap cover design with a tophat integrated in the load carrying cap which is in compression (upper part) b) Cap cover design with I-stiffeners integrated in the cap cover part.

The production friendly design of the cap enables the manufacturer to ingrate stiffeners and to produce the cap with a high quality. The stiffeners could be a tophat design (Figure 82a) or I-stiffeners (Figure 82b). Especially the I-stiffeners would be impossible in traditional (aero) manufacturing, since the parts are too big to be put into an autoclave, which is needed to ensure that the stiffeners have satisfactory connection to the load carrying cap. Today autoclaves exist which are 40m long. However, the height and the width of such autoclaves are too small to have other than a cap part inside the autoclave. The large autoclaves are nowadays used to manufacture masts for sail boats. However, even though the blade manufacturers would consider making their own autoclaves, the price will increase considerably. Even if the compression camper is kept to a minimum it will be very costly to integrate this manufacturing technique into wind turbine blade industry. There has not been any real cost

estimation of this, but it is likely that the extra cost will be saved elsewhere in the blade structure, which could still be manufactured with traditional manufacturing techniques used in the wind turbine industry.

The U-design solution also has other important advantage e.g. the shells in the leading edge can be manufactured in one part (see Figure 83a) and for the inner third of the blade the trailing edge shells can also be manufactured in one part, see Figure 83b.

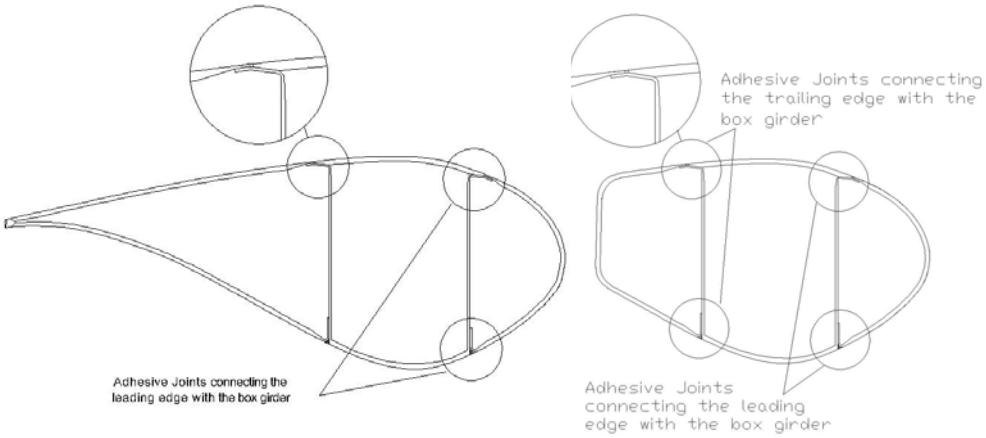

Fig. 83a Fig. 83b

Figure 83. Adhesive joints connecting the upper and lower shells are moved to the box girder section where the stress state distribution is more favourable a) Aerofoil section of the outer 2/3 of the blade where 'only' the adhesive joint in the leading edge part has been moved b) Aerofoil section of the inner third of the blade where both the adhesive joints in the leading edge and trailing edge part have been moved to the box girder section.

The main reason to move the adhesive joints, as shown in Figure 83, is that the stress state distribution is less critical in the box section area since the peeling stresses are considerably lower here. Furthermore, the fatigue stress levels are also lower here than in the leading and trailing edge regions due to the edgewise loading distribution.

The last advantage with the U-design profile, which will be mentioned here, is two alternative manufacturing techniques to manufacture the cap part this desing opens up for. In Figure 84 a cap cover part is shown with the cap reinforcement (see Section 7.2) integrated in the manufacturing process. This could be done either as a winding process, see Figure 84a, or a pultruded manufacturing process, see profile in Figure 84b.

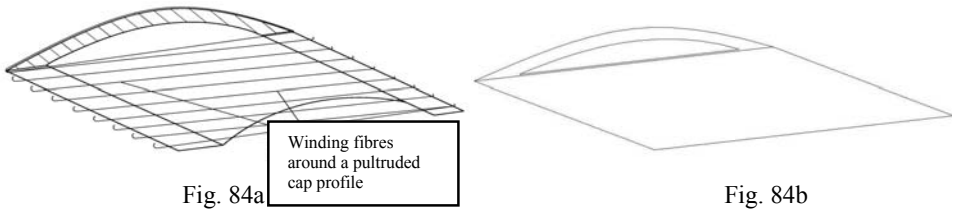

Fig. 84a Fig. 84b

Figure 84. Cap cover part with cap reinforcement integrated in the manufacturing process a) Winding manufacturing process integrated in the cap cover part b) Pultruded manufacturing process integrated in the cap cover part.

Winding manufacturing technique is today used by some manufacturers, e.g. Vestas who uses the technique to connect the load carrying box girder to the root section, but no one has used it in the cap cover part, as shown in Figure 84a. The winded fibres will be in tension when the cap tries to flatten out (ovalisation explained in Section 5.1) or if it tries to buckle downwards either due to buckling or localised bending, explained in Section 5.2 and 5.3, respectively. The pultruded cap profile, shown in Figure 84b, is also based on a manufacturing technique which is new to the wind turbine blade industry. Mainly because the profile does not have a constant geometry due to twisting and changing aerodynamic profile in the length direction. An extruded cap-profile (and maybe also the U-profile) with the major part of the fibres in the longitudinal direction is expected to be flexible enough to twist the cap profile, so it follows the correct twisting in the blade. The changing in the aerodynamic shape is more difficult to change, but the geometric changes are very small, so it may be necessary to accept that there are no geometric changes in the aerofoil in the cap area part of the blade. Alternatively, the pultruded cap profile can be manufactured without cap reinforcement (which decreases the flexural stiffness considerably), and then the winding process can be integrated afterwards. Further work has to been done to find the optimal solution, and on this basis find out whether it is an economically attractive solution.

7.7 Future blade design – Use of combined reinforcements

The ideal scenario would be obtained if a blade could be totally redesigned and new manufacturing methods could be considered as add-on to the existing manufacturing methods. However tests on exiting blade design also could have relevance, if some of the suggested reinforcements were used. For example, a box girder test with both ribs and cap reinforcement (wires) would be a good combination, since wires prevent buckling, ribs carry the crushing pressure and avoid the blade to collapse in transverse shear distortion. To obtain edgewise fatigue loads a floor should be inserted in the trailing edge region or the U-profile solution should be considered where the adhesive joint in trailing (and leading) edge is moved to the box section area. In Figure 85, a blade design is shown where four out of the suggested six reinforcements are used. The web coupling reinforcement is not needed in the regions where there are floors inserted in both the trailing and leading edge. The rib reinforcements are not integrated since it is difficult to implement in a manufacturing process. The floor between the shear web and the leading edge could be omitted, if experiences shows that there are no fatigue problems in this adhesive joint on the leading edge. The floor in the leading edge region could be omitted, since no adhesive joints are expected to be critical due to the adhesive joint being moved to the U-box section area.

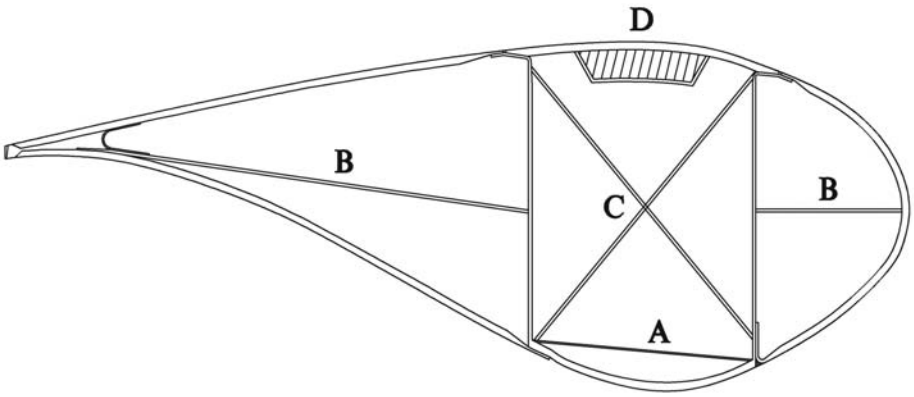

Figure 85. Blade design with use of 4 reinforcements.

The extent of reinforcements along the blade must depend on more FE-studies with combined loading on the actual design. The choice of reinforcement depends on many parameters such as manufacturing process, design, materials and the size of the blade etc. Further, a comprehensive experimental test program is needed because introducing reinforcements can cause other non-expected problems. One problem could be that a fatigue problem could arise at the connection of the reinforcement to the blade structure.

8 Summary of ultimate loads obtained in the full-scale tests

In this chapter the ultimate loads obtained in the full-scale tests are compared and discussed. In tests 3 and 4 (with and without wire reinforcement), the blade was not tested to failure, but the effect of the wire reinforcement was found, see Section 7.2.
All percentage values in Table 2 refer to the first full-scale test, where the entire blade was tested. The load assumptions are described in Section 2.2, and the percentage refers to the root moment in the first full-scale test. The moment and the shear force distributions were higher for tests 2-5 than for test 1. This makes the comparison between test 1 and the shortened box girder tests (test 2-5) conservative.

The second full-scale test (the first box girder test) carried 20% less load than the first full-scale test of the entire blade (test 1). This was expected since the buckling capacity was reduced without the aerofoil included in the test. The reason why the blade (test 1) did not carry the estimated 30-40% higher load, as predicted in the FE-studies, is expected to be the weak shear web connections in the first full-scale test, see Section 6.3.

Full-scale test	Blade/Box girder	Reinforcement type	Ultimate load in percentage
Test 1	Blade 1	No reinforcements	100%
Test 2	Box girder 1	Web + Tophat reinforcements	80%
Test 3	Box girder 2	Web reinforcement	(80%)
Test 4	Box girder 2	Web + Cap reinforcements	(95%)
Test 5	Box girder 2	Web + Rib reinforcements	104%

Table 2. List of full-scale tests where the last column is the maximum obtained load. The two percentage values in paragraphs are when the girder was not tested to failure. All percentage values refer to the root moment in the first full-scale test.

One of the main conclusions which can be drawn when the failure loads are compared from test 2 vs. test 5, is that inserting ribs results in a failure load increase of 30%. If the damage on the shear web, described in Section 7.1, could have been avoided then the differences may have been larger. Taking into account that the box girder was also critical to buckling, the result was expected and satisfactory. Test 4 (with cap reinforcement) was expected to carry higher loads than test 5, since buckling is critical for the box girder design. Further, the ribs do not prevent buckling to the same extent as the cap reinforcement does. Even though there was no sign of failure in test 4, the test was stopped at 95% load, since the box girder was supposed to be used for validating the reinforcement and collapse would have been a disaster. The aim of test 4 was just to compare the effect of cap reinforcement (wires) compared with the non-reinforced (without wires) test 3. This comparison is given in Section 7.2 and will not be repeated here.

9 Conclusions and future work

9.1 Conclusions and discussions

On the basis of the static load cases considered here it is concluded that wind turbine blades could be much lighter. In principle the blades' weight could be reduced by a factor 4 or 5. In practice, this is not expected to be possible, but a realistic weight reduction by 20-50% is also very attractive. Some of the difficulties, which could arise include that the blade would be too flexible in the flapwise direction due to the problem of tip clearance between the tower and blade tip. In order to increase the distance between the blade tip and the tower during operation, the rotor can be coned, blades can be pre-bended or the rotor plane can be tilted. A tilt angle of about 5° between the rotor axis and the horizontal plane is common, but a bigger angle could also be considered. In the past, on some wind turbines the rotor plane was placed in the wake behind the tower, it was called a 'back runner'. If the blades not are allowed to be as flexible as the strength optimization allow the 'remaining' strength capacity will result in extra reliability, which is also an important issue for the wind turbine manufacturers.

Three elastic structural responses and four failure mechanisms are expected to be critical for most current and future wind turbine blades. The elastic structural responses are buckling, localized bending and the Brazier effect. The four failure mechanisms are skin peeling, interlaminar shear failure, web failure and transverse shear distortion. Some of the elastic structural responses and failure modes are expected to be even more critical in future blades designs. E.g. if the cap laminates get thinner then the tip deflection and the longitudinal curvature increase. The increase in the longitudinal curvature effects in substantially larger crushing pressure (increase with squared to the curvature), which makes the failure modes related to the Brazier load (interlaminar failure in cap and failure in the webs) more critical.
Both buckling and interlaminar failure are expected to be critical if the cap thickness is reduced. The crushing pressure was found to be the main reason why the first test blade failed, but that was mainly due to a special single skin connection in the webs of the SSP blade design. This 'weakness' was reinforced in the following tests and the Brazier loads were not the only reason for the next two collapses. The failures were also partly caused by buckling, which resulted in skin debonding in the sandwich shear webs. The buckling problem is automatically solved for the SSP 34m blade when the aerofoil is included, and it is doubtful that the webs would have failed without the contribution from the buckling. The interlaminar shear failure mechanism has not been measured in the full-scale tests but in other experimental tests (3-and 4-point bending) and the level of measured deformations on the cap indicate that this failure mechanism could be critical for current wind turbine blades. The transverse shear distortion failure mechanism is dominating in non-liner FE-studies with combined loading, but in the full-scale test this failure type was restrained since only flapwise load was applied.

In the first full-scale test only a few local displacement sensors were included, in addition to the strain gauges required by the certification test. Without these cap and web measurements it would not have been possible to conclude that the blade first showed skin peeling and afterwards collapse of the shear web towards the trailing edge. In the second full-scale test it was easier to conclude which failure mechanisms were involved, since a large number of strain gauges and displacement sensors were located in the area where the box girder failed. Furthermore, camera was used which clearly showed that the sandwich skin debonded and therefore the collapse was inevitable. A more detailed study of the failure using all the measurements, including the DIC system, showed that the caps prebuckled before the web failed. The study also revealed that this small scale buckling contributed to the strain distribution in the shear webs which led to the skin debonding from the sandwich core, causing unstable buckling and the box girder collapsing. Without the large number of strain gauges, displacement sensors and the DIC measurement it would have been difficult to identify the failure modes. Studying failures after the blade has collapsed is extremely difficult. Therefore it is recommended that intensive FE-studies and a large number of measurement equipment are used to detect the failure. It is especially important to measure deformations on the local scale, which often shows non-linear behaviour, while the global deformations can be used to validate the FE-model. In this thesis this calibration approach has shown to be valuable and it is strongly recommended. It is also important that more advanced test equipment is used in the future full-scale tests if the first critical failure mechanisms are to be addressed.

The precision of predicting ultimate failure from the FE-analysis depends on failure mode critical for the individual test. Nonetheless, in general, the elastic mechanisms can be predicted with a sufficient accuracy, using detailed non-linear FE-models. The accuracy has been especially satisfactory when the FE-model was calibrated to experimental results obtained earlier, such as the box corner stiffness. This was done after the first test and hereafter the predictions were more reliable for the following tests. Non-elastic damage related failures, such as interlaminar failure or the sandwich skin debonding from the sandwich core, could never be predicted by this type of FE-analysis. This will require use of other element types such as cohesive interface elements. These types of elements are very useful for smaller sections but not for large structures, such as wind turbine blades. Today, the inputs to these elements are very comprehensive, since mixed mode laws have to be found experimentally. Numerical FE-studies with realistic load combinations are applied showing that transverse shear collapse is a realistic failure mode, especially if the non-linear effects are taken into account. This type of failure could be the reason why the blades fail at a low strain value.

Six different types of structural reinforcements preventing undesired structural elastic mechanisms are found to be validated for current and future wind turbine blades. The functionality of two of the suggested structural reinforcements was demonstrated in full-scale tests and the rest trough FE-studies. The extent of the needed reinforcement depends on the blade design, manufacturing process, materials, etc., but some of the failure mechanisms are more or less generic and are expected to be relevant for almost

all blade designs. Another important issue, which will decide how large an extent these reinforcements will have in future wind turbine blades, is how realistic the design and certification process will be in the future. If some of the 'observations' found in this PhD-thesis regarding the limitations in the load application and the need for more complex loading, are not changed in the future design process, then some of the addressed problems may not appear in full-scale test but 'only' in the real life. When a blade fail in the real life then it is often extremely difficult to decide which failure mechanism cause the collapse and it may also take several years before an extreme load combination occur, so it is strongly recommended that the full-scale tests of the blades are as realistic as possible.

Proofs of concept based on experimental observations have been performed for the web coupling reinforcement, as well as rib and cap reinforcement. They all gave results predicted by the FE-studies. The cap reinforcement was validated by two full-scale tests, when the box girder was tested with and without wires representing the cap reinforcement. The full-scale tests showed that the cap reinforcement is very promising, even in areas where the transverse curvature is small. The cap reinforcement is expected to be placed in all areas where buckling and/or interlaminar failure is a problem. Thus, if no alternative solutions are used, this reinforcement is expected to be used in large regions of the blade. An alternative solution for the buckling problem is the invention of the U-shape profile with a cap with a tophat or I-stiffeners. If the cap cover part is winded with fibres, then both interlaminar failures due to flattening and buckling problems are expected to be solved. The rib reinforcement was tested in the second box girder (test 5) and it failed at 104% load, which is an increase in the ultimate load at 30% compared to the first box girder test (test 2). The increase in ultimate load is dramatic considering that only six ribs are inserted. Detailed studies of what was the first dominating failure mechanism has not been done since the major purpose was to see the effect on the ultimate load. It is probable that the failure was either buckling or the shear web failure. In such a case the rib solution would have even more significant effect if the box girder was designed against these high loads. The failure could also be caused by an unwelcome weakness (damage) found on the shear web. From a structural point of view inserting ribs is found to be a good solution to prevent different failure mechanisms. The major problem with ribs is the manufacturing process, especially in regions where it is impossible to insert the ribs after the blade has been cured.

9.2 Future work

In beginning of 2009 a full-scale test of another SSP 34m blade is planned. The full-scale test is prepared in Risø DTU's new test facilities, see Figure 86.

Figure 86. Risø DTU's new research blade test facility. The blade shown is a shortened (25m) 34m SSP-blade.

The main idea is to make a 'Proof of Concept' of the floor and web coupling invention. The deformations will be measured by the DIC system and a large number of mechanical deformation sensors inside and outside the blade are planned, see Figure 87.

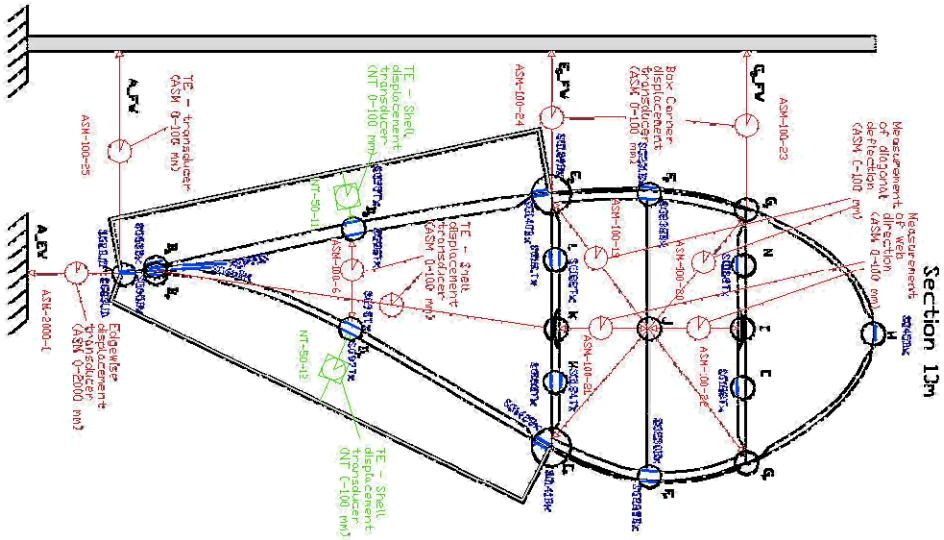

Figure 87. Sketch of measuring equipment planned for the forthcoming full-scale test at Risø DTU.

In the first full-scale test the focus will be on a test without any of the suggested reinforcements in order to get a good reference for comparison with the next full-scale

tests with reinforcements. The second test will be with a flat sandwich panel (floor reinforcement) inserted in the trailing edge. It is expected that the floor panel will have a positive effect on the deformations of the trailing edge panels and out of plane deformations of the shear web as well. After the second test the sandwich panel will be removed and the web coupling invention will be tested. This is simply done by inserting a pin between the two shear webs.

The full-scale test can also be used for proof of concept of the transverse shear distortion (Patent C), but it is expected that the loads have to be much higher than for the other (floor and web coupling) proof of concept tests, to make the effect of the shear cross visible.
The U-profile invention with a cap cover part in high quality opens up for new manufacturing methods. The cost of including these expensive manufacturing techniques should be investigated and be compared with the savings.
The three latest inventions, see ref. [34][35][36], are all related to the field presented in this thesis. 'Proof of concept' of these new inventions will be performed in 2009 and 2010.

10 References

[1] Berggreen, C., Branner, K., Jensen, J. F., Schultz, J. P. "*Application and Analysis of Sandwich Elements in the Primary Structure of Large Wind Turbine Blades*". Journal of Sandwich Structures and Materials (in press).

[2] Berggreen, C., Tsouvalis, N., Hayman, B., Branner, K. *"Buckling Strength of Thick Composite Panels in Wind Turbine Blades – Part I: Effect of Geometrical Imperfections"*. 4th International conference on composites testing and model identification, 20-22, Dayton, Ohio, USA. (submitted). (October 2008).

[3] Berring. P., Branner, K., Berggreen, C., Knudsen, H. W. "*Torsional Performance of wind Turbine Blades – Part I: Experimental Investigation*". (2007).

[4] Branner K. *"Modelling Failure in Cross-Section of Wind Turbine Blade"*. Risø National Laboratory, NAFEMS-Seminar. Denmark (June 2006).

[5] Branner, K., Berring, P., Berggreen, C. "*Buckling Strength of Thick Composite Panels in Wind Turbine Blades – Part II: Effect of Delamination"*. 4th International Conference on Composites.

[6] Branner, K., Berring, P.H., Berggreen, C., Knudsen, H. W. "*Torsional Performance of wind Turbine Blades – Part II: Numerical Validation*". (2007).

[7] Branner, K., Jensen, F.M., Berring, P., Puri, A., Morris, A., Dear, J. "*Effect of sandwich core properties on ultimate strength of a wind turbine blade*". 8th edition. International Conference on sandwich Structures. (April 2008).

[8] Brazier, L.G. Late of the Royal Aircraft Establishment. *"On the flexure of thin cylindrical shells and other 'thin' sections"*. Reports and Memoranda no1081 (M.49), pp (1– 30) (1926).

[9] Brazier, L.G. Late (1926), The Royal Aircraft Establishment. *"The flexure of thin cylindrical shells and other 'thin' sections"*. Reports and Memoranda no1081 (M.49).

[10] Brøndsted, P., Lilholt, H., Lystrup, Aa. *"Composite materials for wind power turbine blades"*. Materials Research Department, Risø National Laboratory (April 4, 2005).

[11] BTM Consultaps ApS. *"International Wind Energy Development – World Market Update 2006"*. Ringkøbning, Denmark. (2007).

[12] Cecchini L. S. Weaver P. M. *"The Brazier effect in multi-bay aerofoil sections"*. University of Bristol – UK.

[13] Cecchini L. S. *"The non-linear flexural response of thin-walled beams"*. PhD-Thesis. University of Bristol – UK. (2006).

[14] De Goeij, W.C., van Tooren, M.J.L., Beukers, A. *"Implementation of bending-torsion coupling in the design of a wind-turbine rotor-blade"*. Netherlands. (1999).

[15] Dear, J., Puri, A., Fergusson, A., Morris, A., Dear, I., Branner, K., Jensen, F.M. *"Digital image correlation based failure examination of sandwich structures for wind turbine blades"*. International conference on sandwich Structures. (April 2008).

[16] *DNV-OS-J102*

[17] DNV/Risø publication, *"Guidelines for Design of wind Turbines"* 3rd edition. Denmark. (2008).

[18] Geiger, T. *"Buck Blade"*. Report about buckling tests. (1998).

[19] Griffin, D. *"Evaluation of Design Concepts for Adaptive Wind Turbine Blades"*. USA. (August 2002).

[20] Hahn, F., Kensche, C.W., Paynter, R.J.H., Dutton, A.G., Kildegaard, C Kosgaard, J. *"Design, fatigue Test and NDE of a Sectional Wind Turbine Rotor Blade"*. Journal of Thermoplastic Composite Materials (May 2002).

[21] Hallett, S. *"Analysis of light Aircraft Structures"*. Lecture notes, University of Bristol – UK.

[22] Horne, M. R., Holloway, B.G.R., Richmond, B. Sriskandan, K. *"Structural Action in Steel Box Girders"*. (April 1977).

[23] Högberg, J. L., Sørensen, B. F., Stigh, U. *"Constitutive behaviour of mixed mode loaded adhesive layer"*. International Journal of Solids and Structures. (2007).

[24] International Electrotechnical Commission. *"IEC 61400-1: Wind turbine generator systems-Part 1: Safety Requirements"*. 2nd edition, International standard 1400-1, (1999).

[25] International Electrotechnical Commission. *"IEC 61400-23 TS. Wind turbine generator systems - Part 23. Full-scale structural testing of rotor blades for WTGSs"*. 1st edition, International standard.

[26] Jackson, J.K., Zuteck, M.D., Van Dam, C.P., Standish K. J. Berry, D. *"Innovative Design Approaches for Large Wind Turbine Blades"*. (November 2004).

[27] Jensen, C. *"Defects in FRP Panels and their influence on Compressive Strength"*. Master's Thesis. Technical University of Denmark and Risø National Laboratory. (February 2006).

[28] Jensen, F. M. *"Bending behaviour of a wind-turbine blade under full-scale testing"*. Keynotepresentation. NAFEMS-UK Seminar in UK, November. 5 pages abstract (2006).

[29] Jensen, F. M. *"Reinforced aerodynamic profile – Cap reinforcement"*. PCT/DK2007/000547. (Dec. 2006).

[30] Jensen, F.M. *"Reinforced blade for wind turbine - floor"*. PCT/DK2008/000017. (Jan. 2007).

[31] Jensen, F. M. Nielsen, P. H. *"Reinforced blade for wind turbine cross"*. PCT/DK2008/000032. (Jan. 2007).

[32] Jensen, F. M. *"Wind turbine blade – U – profile"*. PCT/DK2008/000040. (Jan. 2007).

[33] Jensen, F. M. *"Compression Strength of a Fibre Composite Main Spar in a Wind Turbine Blade"*. Risø-R-1393(EN). (June 2003).

[34] Jensen, F. M, Nielsen, P. H. *"080624 P12737 DK Coupling of trailing edge panels (patent E)"*

[35] Jensen, F. M *"080701 P12735 DK Soft Floor (patent B2)"*

[36] Jensen, F. M *"080623 P12736 DK Angled Girders (patent C2)"*

[37] Jensen, F. M., Branner, K., Nielsen, P. H., Berring, P., Antvorskov, T. S., Nielsen, M., Lund, B., Jensen, C., Reffs, J. H., Nielsen, R. F., Jensen, P. H., McGugan, M., Borum, K., Hansen, R. S., Skamris, C., Sørensen, F., Nielsen, R. S., Laursen, J. H., Klein, M., Morris, A., Gwayne, A., Stang, H., Wedel-Heinen, J., Dear, J. P., Puri, A., Fergusson, A. "*Full-scale Test of a SSP34m box girder 1 – Data Report*". Risø-R-RIS88(EN). (March 2008).

[38] Jensen, F.M. , Branner, K., Nielsen., P. H, Berring, P., Antvorskov, T. S., Nielsen, M., Reffs, J.H., Jensen, P.H, McGugan, M., Skamris, C., Sørensen, F., Nielsen, R.S., Laursen, J.H., Klein, M., Morris, A., Stang, H., Wedel-Heinen, J., Dear, J.P., Puri, A., Fergusson, A. "*Full-scale Test of a SSP34m box girder 2 – Data Report*". Risø-R-1622(EN) in progress. (April 2008).

[39] Jensen, F. M., Falzon, B.G., Ankersen, J., Stang, H. *"Structural testing and numerical simulation of a 34m. composite wind turbine blade"*. Composite Structures 76. 52-61 (August 2005).

[40] Jensen, F. M., Falzon, B.G., Ankersen, J., Stang, H. *"Structural testing and numerical simulation of a 34m. composite wind turbine blade"*. ICCM15-paper. Conference in Durban. (June 2005).

[41] Jensen, F. M., Morris, A. *"Full-scale testing and finite element simulation of a 34 metre long wind turbine blade"*. NAFEMS World Congress – Vancouver. (April 2007).

[42] Jensen, F. M., Weaver, P. M., Cecchini, L. S., Stang, H. *" On aspects of non-linear bending behaviour of a wind-turbine blade under full-scale testing"*. Abstract for COMPTEST2006 Conference in Porto. (April 2006).

[43] Jensen, F. M., Weaver, P. M., Cecchini, L. S., Stang, H., Nielsen, R. F. "*The Brazier effect in Wind-Turbine Blades and its Influence on Design*". (Submitted "Strain – An international Journal for Experimental Mechanics, June 2008).

[44] Joncas, S., Jan de Ruiter, M., van Keulen, F. Delf. *"Preliminary Design of Large Wind Turbine Blades Using Layout Optmization Techniques"*. University of Technology, Delf, the Netherlands.

[45] Jørgensen, E.R., Borum, K.K., McGugan, M., Thomsen, C.L., Jensen, F.M., Debel, C.P. "*Full-scale Testing of Wind Turbine Blade to Failure – Flapwise Loading*". Risø-R-1392(EN). (2004).

[46] Karihaloo, B.L., Stang, H. *"Buckling-driven delamination growth in composite laminates: Guideline for assessing the threat posed by interlaminar matrix delamination".* Composites Science and Technology. (2006).

[47] Kedward K. T. *"Non-linear collapse of thin-walled compsite cylinders subject to flexural loading"*. Proceedings of the international conference on composite materials. (1978).

[48] Kong, C.D., Bang, J.H., Jeong, J.C., Kang, M.H., Jeong, S.H., Yoo. J.Y. *"Structural Design of Medium Scale Composite Wind Turbine Blade".*

[49] Kong, C.D., Sugiyama, Y., Lee, J., Soutis, C. *"Full-scale Structural Experimental Investigation of an E-Glass/Epoxy Composite Wind Turbine Blade"*. (October 2002).

[50] Korsgaard, J., Jacobsen, T.K. *"Integrated testing in reliable design of large wind turbine blades"*. LM Glassfiber A/S, Denmark.

[51] Kühlmeier, L. *"Buckling of wind turbine rotor blades. Analysis, design and experimental validation"*. PhD-Thesis. Special Report No. 58 (November 2007).

[52] Kühlmeier, L., Thomsen, O.T., Lund, E. *"Large scale buckling experiment and validation of predictive capabilities".* Vestas Wind Systems Denmark. Aalborg University.

[53] Laird, D.L., Montoya, F.C., Malcolm, D.J. *"Finite Element Modeling of Wind Turbine Blades"*. (2005).

[54] Lindenburg, C. *"Buck Blade. Buckling Load Design Methods for Rotor Blades*". (May 1999).

[55] Lindenburg, C., Geiger, T., Joosse, P.A., Weisser, B. *"Buck Blade Finite Element Buckling Analysis of Wind Turbine Blades".*

[56] Locke, J., Hidalgo, I.C. *"The Implementation of Braided Composite Materials in the Design of a Bend-Twist Coupled Blade"*. (August 2002).

[57] Locke, J., Valencia, U. *"Design Studies for Twist-Coupled Wind Turbine Blades"*. (June 2004).

[58] Lund, E.; Stegmann, J. *"On Structural Optimization of Composite Shell Structures Using a Discrete Constitutive Parameterization"*. Wind Energy, Vol. 8. (2005).

[59] Ma W. "*Optics measurement and numerical simulation of a wind turbine blade*". Master Project. Technical University of Denmark - Risø National Laboratory. (July 2007).

[60] McGugan, M., Bech, T., Sørensen, B.F., Jørgensen, E., Kristensen, O.J.D. *"Improving the Structural Testing of Wind Turbine Blades by Monitoring Acoustic Emission"*. Proceedings of the 4th International Workshop on Structural Health Monitoring. Stanford University. USA. (September 2003).

[61] Moslemian, R., Berggreen, C., Branner, K., Carlsson, L.A."*On the Effect of Curvature in Debonded Sandwich Panels Subjected to Compressive Loading"*. 8th international conference on sandwich structures, 6-8, University of Porto, Portugal (May 2008).

[62] Niu M. Chun-Yu. "*Composite Airframe Structures"* Hong Kong. (1992).

[63] Niu M. Chun-Yu *"Airframe Structural Design: Pratical Design Information"*. Hong Kong. (1 Jan 1999).

[64] Oliveira A., Krog L. *"Implementation of FEA in a Minimum Weight Design Process of Aerostructures"*. New Tech. Centre (HD), Airbus. United Kingdom.

[65] Overgaard, L., Lund, E. *"Damage Analysis of a Wind Turbine Blade"*. In: Proc. of the ECCOMAS thematic Conference on Mechanical Response of Composites, Portugal. (September 2007).

[66] Overgaard, L., Lund, E. *"Interdisciplinary Damage and Stability Analysis of a Wind Turbine Blade"*. In: Proc. of the 16th International Conference on Composite Materials, Japan. (July 2007).

[67] Overgaard, L., Lund, E. "*Structural Instability Phenomena in Wind Turbine Blades*". 2nd PhD Seminar on Wind Energy in Europe, Risoe National Laboratory, Denmark. (October 2006).

[68] Overgaard, L., Lund E. *"Structural Design Sensitivity Analysis and Optimization of Vestas V52 Wind Turbine Blade"*. In: Proc. of the 6th World Congress on Structural and Multidisplinary Optimization. (June 2005).

[69] Paulsen F., Welo T. *"A design method for prediction of dimensions of rectangular hollow sections formed in stretch bending"*. Journal of Material Processing Technology, 128. (2002).

[70] Puri, A., *"Researching methods for monitoring strain in wind turbine blades as part of an operation and maintenance programme"*, PhD-Thesis (in progress) Imperial College London – Department of Mechanical Engineering.

[71] Puri A., Dear J.P., Morris A., Jensen M. F. *"Analysis of Wind Turbine Material using Digital Image Correlation"*. EWEC Conference. (2008).

[72] Puri, A., Fergusson, A., Dear, J., Morris, A., Jensen, F.M. "*Digital image correlation and finite element analysis of wind turbine blade structural components"*. 2007 European Offshore Wind Energy Association conference. Germany. (December 2007).

[73] Putnam, P.C. *"Power From the Wind"*. (1948). ISBN: 0.442-26650-2

[74] Rand O. "In-plane warping effects in thin-walled boxed beams". AIAA Journal, 38, Nr. 43, 131-152. (2000).

[75] Rijswijk, K. v. *"Thermoplastic Composite Wind Turbine Blades"*. PhD-Thesis, Delft University of Technology, Netherlands. (April 2007).

[76] Rijswijk K. v., Joncas S., Malek O.J.A, Bersee H.E.N, Beukers A. *"Vacuum infused thermoplastic composites for wind turbines blades"*. 27th Risø International Symposium on Material Scince: Polymer Composite Materials for Wind Turbine Power: Roskilde, Denmark. (May 2006).

[77] Stensgaard H., Sørensen J.D. *"Stochastic models for strength of wind turbine blades using tests"*. H. Aalborg University, Denmark and Risø National Laboratory. EWEC (2008).

[78] Sørensen B.F. *"Improved design of large wind turbine blade of fibre composites based on studies of scale effects (Phase 1) – Summary Report"*. Risø-R- 1390(EN). (2004).

[79] Sørensen, B.F., Branner, K., Stang, H., Jensen, H.M., Lund, E., Jacobsen, T.K., Halling, K.H. *"Improved design of large wind turbine blades of fibre composites (Phase2) – Summary Report* Risø-R-1526 (EN). (2005).

[80] Sørensen, B. F., Gamstedt, E. K., Østergaard, R. C., Goutianos, S. *"Micromechanical model of cross-over fibre bridging - prediction of mixed mode bridging laws"*. Mechanics of Materials, in press. (2007).

[81] Sørensen, B. F., Jacobsen, T.K. "*Delamination of fibre composites: Determination of mixed mode cohesive laws"*. (Journal of the Mechanics and Physics of Solids).

[82] Sørensen, B.F., Lading, L., Sendrup, P., McGugan, M., Debel, C.P., Kristensen, O.J.D, Larsen, G.C., Hansen, A.M., Rheinländer, J., Rusborg, J., Vestergaard, J.D.*"Fundamentals for remote structural health monitoring of wind turbine blades - a preproject"*. Risø-R-1336(EN). (2002).

[83] Sørensen, F., Schytt-Nielsen, R. *"A blade for a wind turbine and a method of assembling laminated profiles for a blade"*. PCT W003/08572 A1.

[84] T. von-Kármán Zeit. *"Ueber die formänderung dünnwanger rohre, insbesondere federnder ausgleichrohre"* Des vereines Deutscher Ingenieure. (1911).

[85] Tadich J.K., Wedel-Heinen. *"Full-scale Testing of Blades. Now, and For the Future"* J. EWEC. (May 2007).

[86] Tadich J.K., Wedel-Heinen, J., Petersen, P. *"New guidance for the development of wind turbine blades"*. Det Norske Veritas – Global Wind Energy conference, Copenhagen, Denmark. (2005).

[87] The Steel Construction Institute. *"Design Guide for Composite Box Girder Bridges"*. 2nd edition.

[88] Thomsen, C.L., Eisenberg, Y. *"Blade test SSP34#2 Edgewise and Flapwise Final Static test"*. Risø-I-2083(EN).

[89] Thomsen C. L., Jørgensen E. R., Borum K. K., McGugan M., Debel C. P., Sørensen B., Jensen F. M. *"V52 Statisk Styrke"*. Risø-I-Report. (April 2003).

[90] Tvindskolerne. 1977. Lad 100 møller blomstre. 6 ed. *Forlaget Skipper Klement.Special-Trykkeriet A/S. Viborg, Denmark* (In Danish).

[91] Østergaard, Rasmus C. *"Interface fracture in composite materials and structures"*. PhD-Thesis, Technical University of Denmark, Department of Mechanical Engineering. DCAMM Special report No. S102. (November 2007).

[92] Jensen, F.M. *"WO 2008-071195 Reinforced aerodynamic profile" (cap reinforcement- patent A)*

[93] . Jensen, F.M. *"WO 2008-086805 Reinforced blade for wind turbine (floor-patent B)"*

[94] Jensen, F.M., Nielsen, P.H. *"WO 2008-089765 Reinforced blade for wind turbine (shear cross- patent C)"*

[95] Jensen, F.M. *"WO 2008-092451 Wind turbine blade(U-profile-patent D)"*

Appendix A – Key papers

Appendix A1 – “The brazier effect in wind-turbine blades and its influence on design”. Find M. Jensen, Paul M. Weaver, Luca S. Cecchini, Henrik Stang, Rune F. Nielsen

THE BRAZIER EFFECT IN WIND-TURBINE BLADES AND ITS INFLUENCE ON DESIGN

F.M. Jensen[1], P.M. Weaver[2], L.S. Cecchini[3], H. Stang[4], R.F. Nielsen[1]

[1]Department of Wind Energy – Risoe National Laboratory for Sustainable Energy, Technical University of Denmark, – Roskilde, Denmark

[2]Department of Aerospace Engineering – University of Bristol – Bristol, UK

[3]DeepSea Engineering & Management Ltd

[4]Department of Civil Engineering-Technical University of Denmark – Lyngby, Denmark

KEYWORDS

Brazier effect, crushing pressure, full-scale testing, wind turbine blades, non-linear finite element, ultimate failure, post buckling.

SUMMARY

Critical failure was observed in the shear web of a wind turbine blade during full scale testing. This failure occurred just before ultimate failure and was partly caused by buckling and linear and non-linear cross-sectional strain.

The current paper demonstrates how a combined experimental and theoretical approach can be applied in the analysis of the shear webs in the reinforced wind turbine blade. Only elastic behaviour is analyzed and attention is primarily addressed to the Brazier effect. The complex, geometrically non-linear, elastic stress-strain behaviour of the shear webs and the cap in compression are analyzed.

The crushing pressure from the Brazier effect which contributes to the non-linear distortion of the profile is studied using different approaches based on experimental, numerical and analytical work.

Brazier pressure may have a significant impact on the design of new blades and An optimized box girder has been studied to show the importance of including Brazier pressure in the design process for future wind turbine blades.

LIST OF SYMBOLS

C: Bending curvature of beam

E: Young's modulus

h: Box girder's depth

I: Second moment of area

l : Segment length

M: Bending moment

P_{crush} : Crushing pressure acting on each shear web, per unit length of the blade

R: Bending radius of the box girder

w : Local width of the box girder

Z: Distance to the neutral axis

δ: Local deflection

ε: Local strain

ν : Poisson's ratio

ψ_{braz} : Brazier crushing force

$1/a_{11}$ In-plane laminate stiffness in 1-direction

1. INTRODUCTION

The size of wind turbine blades is expected to increase considerably in the future as initiatives to increase the contribution to energy production from renewable energy sources accelerate. In order to achieve this a better understanding of the structural behaviour of composite turbine blades is required. The detailed structural behaviour must be investigated beyond the elastic range, including identification of failure modes leading to ultimate collapse. Such failure modes typically include combinations of large, geometrically nonlinear deformations such as buckling and wrinkling and material non-linear effects such as fibre failure, matrix cracking, skin debonding and delamination.

So far wind turbine blades have typically been optimized through a combination of testing and simplified analytical and numerical methods. However, numerical simulation tools are gaining wider acceptance as they become more sophisticated in their predictive capability, thus offering a route to significantly lower developmental costs.

An important geometrically non-linear effect, which so far has been somewhat overlooked in failure analysis of wind turbine blades, is the so-called Brazier effect. Since von-Karman [13.], it has been recognised that thin-walled, hollow structures, under bending, suffer a flattening of the cross-section. This flattening is manifested as an ovalisation in circular sections and as “suck in” for squared tubes, see Figure 2.

The flattening effect is caused by internal forces and appears when large deformations occur. When large deformations of e.g. a box girder cross section subjected to a bending moment are taken into account, the forces in the flanges can be resolved in transversal and longitudinal components, see Figure 3. The

transversal components are responsible for the flattening effect. These internal force components are referred to as the crushing pressure in the following.

The distortion reduces the section's second moment of area, and thus its bending stiffness. Brazier [10.]-[12.], however, was the first to realise that such a reduction in the second moment of area would lead to a non-linear bending response, and eventual structural collapse. From Brazier's analysis it follows that the crushing pressure increases with the square of the curvature of the section, and thus (before large cross-sectional deformations occur) with the square of the bending moment. Since Brazier's pioneering work, the analysis of this non-linear response has progressed into the investigation of composite structures[14.], non-circular cross-sections (e.g.[15.]]) and aerofoil sections.

Recently a series of tests have been carried out at Risø DTU in Denmark in an attempt to optimize a 34 m blade design from SSP-Technology A/S in a combined experimental and theoretical approach. First, a full scale 34m blade was tested to failure in flap-wise loading, see Figure 1a. and [3.]. Ovalization of the load carrying box girder was measured in the full-scale test, see Figure 1b and simulated in non-linear FE-calculations. The nonlinear Brazier effect was characterized by a crushing pressure which caused the ovalization. To capture this effect, non-linear FE-analyses at different scales were employed. A global non-linear FE-model of the entire blade was prepared and the boundaries of a more detailed sub-model were extracted. The FE-model was calibrated based on full-scale test measurements. Local displacement measurements helped identify the location of failure initiation which lead to catastrophic failure. Comparisons between measurements and FE-simulations showed that delamination of the outer skin was the initial failure

mechanism followed by delamination buckling which then led to collapse as shown in the sketch in Figure 4a.

Based on experiences from the first full-scale test a new reinforced blade was manufactured and the weak point at the shear webs was reinforced, see Figure 4b.

A new full-scale test was performed, shown in Figure 5.

This time only the load carrying box girder was tested. The set-up for the new full-scale test is presented in [4.] and [5.]. In [4.] buckling of the cap was identified as a potential failure mode. Consequently, a 'tophat' reinforcement was introduced in the root section. The complete records of the test of the reinforced box girder can be found in [5].

The current paper demonstrates how a combined experimental and theoretical approach can be applied in the analysis of the shear webs in the reinforced wind turbine blade box girder. Only elastic behaviour is analyzed and attention is primarily addressed to the Brazier effect. The complex, geometrically non-linear, elastic stress-strain behaviour of the shear webs and the cap in compression are analyzed. The crushing pressure from the Brazier effect which contributes to the non-linear distortion of the profile is studied using different approaches based on experimental, numerical and analytical work.

To verify the strength of the web reinforcements shown in Figure 4b, cross sections of the box girder were tested by applying a crushing load. This experimental work described in [6.] is further elaborated on in this paper.

Finally a substantial discussion on the importance of taking the Brazier effect into account in future wind turbine blade designs is presented along with the final conclusions.

2. EXPERIMENTAL WORK

Full scale tests have recently been conducted at Risø DTU with a 34 m wind turbine blade [3.] manufactured by SSP Technology A/S. Based on experiences from this full-scale test a new reinforced blade was manufactured and the weak points at the shear webs was reinforced, see Figure 4b. Further a so-called tophat reinforcement was introduced to avoid buckling of the cap [4.]. To verify the web reinforcements, before the full-scale test of the reinforced box girder, transverse sections of the unreinforced, original and the new reinforced box girder were tested, see Figure 6 and [6].

2.1 Verification of the web reinforcement subjected to a crushing pressure

A load perpendicular to the box girder axis in the flap-wise direction was applied to 100 and 200 mm sections of the unreinforced and the reinforced box girder respectively to induce cross-sectional flattening. This load mimics the Brazier crushing pressure. In the unreinforced 2D section test the single skin and the adhesive connection of the two half parts buckled, see Figure 6a. For the test of the reinforced section, the failure also happened in the shear web, but this time in the sandwich area, see Figure 6b.

The applied load was approx. 9kN for the specimen without web reinforcement and approx. 18kN with web reinforcement. The test specimens without reinforcement had a depth of 200mm and the reinforced specimens a depth of 100mm, thus

consequently, the reinforcement approximately increased the strength by a factor 4. Based on this observation and the expected crushing pressure in the full-scale test it was concluded that the reinforcement had sufficient strength to ensure that the failure would not occur due to crushing pressure in the adhesive joint. The observed failure mechanisms in the reinforced sections were similar to those observed in other transverse section tests, see ref. [7.].

2.2 Failure observed in the shear web in the reinforced girder

As mentioned, the full-scale test involved only the reinforced load carrying box girder.

Figure 7a shows a frozen frame picture from a video recording of the first failure mode of the box girder full-scale test at 10.1m from the root. It shows initial face debonding of the outer skin on the shear web's sandwich section, leading to ultimate collapse of the box girder. Figure 7b shows a sketch illustrating the failure and the strain gauges attached in that area.

During the full-scale test, strain was measured in different locations using strain gauges.

Figure 8a shows the position of all strain gauges located in a section 10m from the root. Figure 8b shows the position of the 'back to back' strain gauges (i.e. strain gauges on either side of the girder wall at the same position) analysed in the following. These strain gauges are measuring the strain perpendicular to the girder axis and are denoted 90^0 strain gauges in the following. The readings from the 90^0 gauges in measuring points placed symmetrically around the neutral axis in the longitudinal compressive and tensile side of the web are presented in Figure 9.

The longitudinal compressive and tensile strains are due to global bending of the box girder. In Figure 9a the 90^0 strains in the longitudinal compression side of the web on the inner and outer side are shown. These strains are positive (tensile) and increase with increasing load until 70% of the ultimate load is reached after which the strains decrease. Strains on the inner surface are consistently larger than the strains on the outer surface. The 90^0 strains on the longitudinal tensile side of the web – on the other hand – are negative (compressive) as shown in Figure 9b. These strains decrease with increasing load without any sudden change, however the strain-load response is slightly non-linear. Strains on the inner surface are slightly larger numerically than strains on the outer surface.

The 0^0 (longitudinal) strains in the box girder caused by global bending, leads to associated strains in the 90^0 direction due to the Poisson's ratio effect; positive in the shear webs of the upper (longitudinal compressive) half part of the box girder and negative in the lower (longitudinal tensile) as shown in Figure 9. Normally, the transverse deformation is small in axially loaded 0º laminates, but for ±45º laminates the Poisson's ratio is large, typically for the materials in question [12.]. In the FE-model of the box girder described in following section the ±45º laminates are modelled as 0º laminates with an axial Poisson's ratio of 0.6. The theoretical Poisson's strain in the 90^o direction ($\varepsilon_{Poisson}$) is given by:

$$\varepsilon_{Poisson} = \nu \cdot \varepsilon_{axial} , \qquad [1]$$

where ν is the axial Poisson's ratio, and ε_{axial} is the 0^0 strain in the longitudinal direction related to global bending.

From Brazier [10.], the crushing pressure acting locally on the cross-section (per unit length) is given by:

$$\psi_{braz} = \frac{1}{a_{11}} \varepsilon_{axial} C = \frac{1}{a_{11}} ZC^2 \qquad [2]$$

where C denotes the longitudinal curvature of the cross-section, Z the distance to the neutral axis, ε_{axial} the local 0^0 strain and $1/a_{11}$ is the laminate's axial, in-plane stiffness (for isotropic materials it is the Young's modulus multiplied by the wall thickness). As a result the crushing pressure increases with the square of the curvature of the section, and thus (before large cross-sectional deformations occur) with the square of the bending moment:

$$\psi_{braz} = \frac{1}{a_{11}} \frac{ZM^2}{(EI)^2} \qquad [3]$$

It is hypothesised – and substantiated in the following – that it is the combination of compressive strains from the Brazier crushing pressure and strains due to global bending that result in numerically higher 90^0 strains in points on the tensile side of the blade, than those measured in similar points on the compressive side, as seen in Figure 9a and Figure 9b.

The drop in the strain-load curves at 70% load in the full-scale test in the upper (longitudinal compressive) side of the web is caused by buckling of the cap. Figure 10 shows the location of the observed buckling deformations. Once buckling of the box girder initiates, the inward buckling wave and the associated reaction in the shear webs at the 10m section introduces compressive strains at the compressive side of the shear web, subsequently producing the sudden drop in strains

demonstrated in Figure 9a. Further the local bending of the web introduces the difference in the back to back strains.

It is interesting to note that the failure observed in shear web in the box girder was similar to the failure observed in the reinforced section test, see Figure 7a, b and Figure 6.

3. NUMERICAL STUDY OF THE BOX GIRDER

3.1 FE-model

A large finite element model of the load carrying box girder, containing both shell and solid elements, was created to analyze the elastic, geometrically non-linear structural behaviour, see Figure 11.

The caps are thick laminates, with most of the fibres in the longitudinal direction to limit tip deflection. More details about the lay-up can be found in appendix A. The caps are modelled with 4-noded layered shell elements using a thick shell formulation (taking shear deformation into account). The elements are located at the mid-thickness of the caps and shell offsets are therefore not needed.

The shear webs are sandwich structures, which main purpose is to transfer the flapwise shear forces. The webs are modelled with a combination of shell and solid elements. The thin skins on either side of the webs consisted mainly of biax lamina and are modelled with 4-noded layered shell elements placed in the mid-thickness of the material. The core material in the shear webs are modelled with one 8-noded orthotropic solid brick elements though the thickness. Furthermore, the

reinforcement of the webs (see Figure 4b) consists of adhesive and is modelled with 8-noded solid brick elements.

A relatively coarse mesh density is applied at the first 6 meter and the last 5 meter of the box girder to minimize the degrees of freedom. From 6 to 21 meter the FE-model consists of a mesh with 128 elements circumferentially and an element aspect ratio no bigger than 2. The entire model has 150000 nodes. The analyses are done through a computer cluster with up to 240 nodes (one processor machines). In this particular case, 12 nodes are used and it takes approximate 1 hour with 40 load steps to complete the analysis

3.2 Results from FE-model

Figure 12 shows 90^0 strains at two locations in the compressive and tensile side of the web placed symmetrically around the neutral axis of the girder at 10 m from the root. The two locations are identical to the locations where strain gauges were placed in the test. Both linear and geometrically non-linear calculations are presented.

The difference between the linear and the non-linear results is, at least in part, caused by the Brazier effect. The crushing pressure, attempting to flatten the cross-section, introduces compressive strains into the shear webs. However, this crushing pressure varies with the square of the applied load, resulting in the noted deviation from linear responses. Other non-linear phenomena, such as changes in geometry and loading configuration (which follows the geometry in the non-linear analysis), will also contribute to the observed nonlinearities.

Buckling is producing the sudden drop in strains at 70% load, quite similar to the measured behaviour, see section 5 for further discussion. In Figure 13 part of the model is shown and the buckling is be visualized by plotting the 0^0 strains in the cap.

4. SIMPLIFIED SEMI-ANALYTICAL MODEL

A simplified semi-analytical modelling is undertaken to help better understand the underlying physics of the blade response. Two aspects of the response are modelled below, the Poisson's strains, and the Brazier crushing pressure (section 2.2). In order to calculate the crushing pressure at a given applied load it was necessary to calculate the induced curvature in the blade and in order to provide a direct

comparison of the experimental and FEA results with the simplified analysis for both Poisson's strains and Brazier pressure, the curvature was calculated from the FE analysis and used consistently in the simplified analysis.

4.1 Theoretical Poisson's strain

The theoretical Poisson's strain is given by

$$\varepsilon_{Poisson} = \nu \cdot \varepsilon_{axial} = \nu \cdot Z \cdot C \qquad [4]$$

where ν is the Poisson's ratio, Z the distance of the strain gauge from the neutral axis, and C the local curvature. Local curvature, for a given applied load, is calculated from the FE analysis and is assumed to vary linearly with increasing load for the purposes of this model.

4.2 Theoretical crushing load

Assuming that the box-section is a rectangular, symmetric cross-section, and that the bending load is primarily supported by the box girder, Eqn. 2 can be used to calculate the crushing force acting on each shear web, per unit length of the blade, see ref. [12].

$$P_{crush} = \frac{1}{a_{11\_Cap}} \frac{h}{2} \frac{w}{2} C^2 \qquad [5]$$

where w is the local width of the box girder, and h is the box girder's depth. $1/a_{11\_Cap}$ is the laminate's axial, in-plane stiffness of the load carrying cap. More details about the lay-up of the cap can be found in appendix A.

4.3 Calculated longitudinal curvature

It follows from the above that the crushing pressure calculation requires the local, instantaneous curvature of the blade. This, unfortunately was not measured directly in the experiment. However, for small deformations the longitudinal curvature (C) 10m from the root can be found by extracting 3 node deformations δ_1, δ_2, δ_3, in three sections of the FE-model, 9m, 10m and 11m from the root, respectively, see Figure 14. The curvature can be approximated by

$$C = \frac{\delta_3 - 2\delta_2 + \delta_1}{l^2} \qquad [6]$$

where l is the segment length (1m in this case). This gives a local curvature, at 80% load, of 0.009m^{-1}. For the purposes of the subsequent comparison, this was assumed to scale linearly with load.

4.4 Calculated experimental and FE crushing load

No experimental data directly measuring the crushing pressure was recorded, and unfortunately it was not possible to locate strain gauges at the neutral axis on the web. As a result, the readings from the strain gauges (located away from the Neutral Axis) include strain due to Poisson's ratio effects (resulting from the global bending of the box girder).

Since the 10m strain gauges were located approximately symmetrically around the neutral axis, the Poisson's ratio effects can be approximately eliminated by averaging the upper and lower strain gauge readings. Further, since the skins of the sandwich panel are thin compared to the sandwich depth (and the core has a low

Young's Modulus), the total force (per unit span length) carried by the sandwich panel can be calculated by

$$P_{crush} = \varepsilon_{inner} \frac{1}{a_{11\_inner}} + \varepsilon_{outer} \frac{1}{a_{11\_outer}} \quad [7]$$

where ε is the strain in the inner and outer skins of the sandwich panel and where $1/a_{11}$ is the laminate's axial, in-plane stiffness in inner and outer skin of the sandwich panel.

In the FEA it is possible to identify the cross-sectional strain at the neutral axis, but since the layup and reinforcement complicate calculation of cross-sectional stiffness, the same approach was used to calculate the FEA crushing force as for the experimental data.

5. COMPARISON OF RESULTS

5.1 Strain

Figure 15a compares the 90^o experimental and numerical strains (from linear and non-linear FEA) on both faces of the sandwich web, with the theoretical Poisson's strains (Eqn. 4). The non-linear FE-model has good agreement with the measured results, except that the post buckling behaviour starts at 80% of the ultimate failure load, rather than the measured 70%.

The theoretical Poisson's strain in the compressive part of the web match the Linear FEA results perfectly – as expected, implying that these strains are indeed due to the Poisson's strains. However, the strains in the lower part (tensile), do not match;

which may be explained by the asymmetry of the profile, see e.g. Figure 11. The simple linear model for the theoretical Poisson's strain predicts symmetric strain values (approximate 1000μS in the absolute strain at 80% of the failure load) on the compressive and tensile parts of the webs.

The Poisson's ratio causes the linear increase in 90^{o} strains initially observed in both Figure 15a and Figure 15b. However, as the load increases, the strains become non-linear with respect to applied load and it is noted that both graphs deflect towards compressive strains. As already mentioned in section 2.2 it is hypothesised that these non-linearities in the strain response are caused by the Brazier crushing forces, as explored below.

5. 2 Crushing Pressure

With the equations predicting the theoretical crushing force per unit length (Eqn. 5 and 6) established, these can be compared to those calculated from the experimental and finite element analysis (Eqn. 7).

The resulting crushing forces at the 10m section are plotted in Figure 16 above. It should be noted that the experimental and FEA shear web lay-ups do not quite coincide at this 10m location. This has been accounted for in the calculation of crushing force via eqn. [4]. It does not (significantly) change the total crushing force, as the pressure is principally generated by the box girder and not the web.

Figure 16 shows a good correlation between the theoretical, experimental and FEA crushing pressures acting on the shear web, indicating that the crushing pressure is indeed primarily caused by the Brazier effect. The deviation of experimental results from the theoretical ones at high deformations is to be expected, both due to the

breakdown of the validity of the simplifying assumptions of the theoretical model, and due to local buckling.

6. DISCUSSION

To illustrate the importance of Brazier loads in future blade design, FE studies on an improved, load carrying box girder have been performed. In ref. [17.] cap laminates from SSP-Technology A/S, have been tested indicating a large safety margin for this particular element with strain capacities 4-5 times the strain level typically observed in full-scale tests, see ref. [3.]. If we assume buckling and other critical failure mechanisms could be eliminated the cap thickness could be reduced dramatically. In [18.],[19.],[20.],[21.],[22.],[23.],[24.] and [25.], different failure mechanisms have been studied and reinforcement arrangements have been suggested. In this study no specific reinforcement arrangements are suggested, however a FE-study of an optimized box girder is carried out. To avoid buckling a sandwich core material has been implemented in the compression cap, as suggested in [8.]. The FE-model do not take any material non-linearities into account thus the investigation is only intended to study the effect of the Brazier forces assuming that it is possible to reduce the thicknesses of the cap.

The thickness of the tension cap is reduced to 1/3 of the original thickness (approx. 10mm), see Figure 17b. From the two deformation plots in Figure 18 (plotted with a deformation scale factor of 2) it is clear that the deformation of the tension cap in the optimized non-symmetric box section is greater than in the symmetric box section. The deformation of the centre of the tension cap is plotted for the two

designs and it can be concluded that the local deformation of the tension cap is approximately ten times greater. This has two explanations. First of all the longitudinal curvature is increased by a factor of two (due to the reduced bending stiffness) which increases the "crushing pressure" by a factor 4 (crushing pressure scales with the square of the curvature). The second, and dominant, reason is the reduction of the skin's cross-sectional bending stiffness to approximately 3.6% (based purely on relative thicknesses). The change in deflection is not, however, in any significant way due to the change in composition of the lay-up, see Figure 20.

In Figure 19a, showing cap deformations and 90^0 strain, a similar pattern is observed in the response of both the optimised and original box girder design. The position of the transverse strain gauges in the original box design can be seen in Figure 19b. From Figure 19a it can also be observed that the non-linear FE-model accurately predicts both cap deflection and transverse strain.

One of the problems with thinner cap thickness and increasing crushing pressure is that when the cap deflects there is a risk of interlaminar failure; since there are both mode I (opening) and mode II (shear) interlaminar stresses. Testing of the actual cap (3 and 4 point bending) have recently been performed and here the allowable deflection before interlaminar failure is found to be approximately 4-8mm while the tested cap deflections are in the range of 1-6mm. Tests and results are presented in [9.].

Similar considerations must be accounted for when designing with carbon laminates, since these allow for a reduction in the wall thickness compared to glass fibre.

7. CONCLUSIONS

In the particular blade design investigated here it seems that the first, critical failure was skin debonding in the shear webs towards the leading edge in the upper, compressive region of the shear web. This failure appears to be caused by a complex stress state with contributions from global bending, the Brazier pressure and the downward reaction from the buckling wave. The global bending which causes the upper part to be in longitudinal compression, leads to associated positive strains in the 90^0 direction due to the Poisson's ratio effect which are subsequently reduced by the Brazier crushing pressure. Immediately after the skin was debonded from the sandwich web, the box girder collapsed,.

The Poissons effect cause linear tension (90º direction) in the upper part of the shear webs. This is caused by the longitudinal compression and tension due to the global bending. The Brazier effect and post buckling resulted in a non-linear elastic behaviour in the shear webs. Non-linear finite element analysis was used and predicted both the Brazier behaviour and the buckling behaviour with reasonable accuracy.

The through section crushing forces, as extracted from both the full scale test and the FEA were compared to simple theoretical models, and showed good correlation. To the author's best knowledge this is the first direct measurement of Brazier crushing forces carried as membrane stresses in the shear webs; and certainly the first experimental verification of the Brazier effect in wind-turbine blades. The accuracy of the simple mathematical models, allows their use in the design of future blades to ensure the capacity of the system to resist crushing forces. Hopefully this

will, in the long-term, maximize the load capacity of wind-turbine blades, and allow for their further optimization.

When future wind turbine blades are optimized further, larger longitudinal curvature will increase the Brazier crushing pressure. If the tension cap is optimized against strength and not tip deflection, thinner laminates could be used on the tension side. This will result in considerably higher cap deformation on the tension cap, which will cause higher interlaminar stresses, and may be critical. To illustrate this issue an optimized blade was designed. Sandwich core material has been implemented in the cap in compression, to prevent buckling and the thickness of the tension cap is reduced to 1/3. This has resulted in 10 times larger deformation in the tension cap.

FUTURE WORK

In order to validate the numerical FE-studies of the further optimized box girder design full scale tests are needed..

ACKNOWLEDGEMENTS

The invaluable help and assistance from the blade manufacturer, SSP-Technology AS, who has delivered the blade and the box girder, is acknowledged.

APPENDIX A – Layup for the box girder

MSC-Patran and the laminate modeller module have been used for pre- and post processing. MSC-Marc has been used as non-linear FE-solver.

The caps mainly consist of unidirectional (UD)-glass, see Figure 20. The effective Young's modulus of the cap is estimated to be 32GPa (per the rule of mixtures). Young's modulus of the UD laminate is approx. 40GP (in the fibre direction), and approx. 13GPa for a ±45, biaxial laminate. The web is comprised of a sandwich panel, with a 22mm core of PVC-foam with a Young's modulus at 48MPa.

REFERENCES

[1.] Erik R. Jørgensen, Kaj K. Borum, Malcolm McGugan, Christian L. Thomsen, Find M. Jensen, Christian P. Debel *"Full Scale Testing of Wind Turbine Blade to Failure – Flapwise Loading"* Risø-R-1392(EN) (2004)

[2.] Find M. Jensen *"Compression Strength of a Fibre Composite Main Spar in a Wind Turbine Blade"* Risø-R-1393(EN) (June 2003)

[3.] Find M. Jensen, B.G. Falzon, J. Ankersen, H. Stang *"Structural testing and numerical simulation of a 34m. composite wind turbine blade"* Composite Structures 76 (2006).

[4.] Find M. Jensen, Andy Morris *"Full-scale testing and finite element simulation of a 34 metre long wind turbine blade"*. NAFEMS World Congress (April 2007).

[5.] Find M. Jensen, Kim Branner, Per H. Nielsen, Peter Berring, Troels S. Antvorskov; Brian Lund; Christian Jensen, Joan H. Reffs, Rune F. Nielsen; Peter H. Jensen, Malcolm McGugan, Kaj Borum, Rene S. Hansen, Carsten Skamris, Flemming Sørensen, Rune Schytt Nielsen, Jeppe H. Laursen, Marcus Klein, Andy Morris, Andy Gwayne, Henrik Stang, Jakob Wedel-Heinen, John P. Dear, Amit Puri, Alex Fergusson *"Full-scale Test of a SSP34m box girder 1 – Data Report"*. Risø-R-RIS88(EN) (January 2008).

[6.] Rune F. Nielsen *"Experimental and numerical analysis of a wind turbine blade cross section - Under lateral load conditions"*. Student Report (special course) - Technical University of Denmark and Risø National Laboratory. (December 2006).

[7.] Kim Branner *"Modelling Failure in Cross-Section of Wind Turbine Blade"*. Risø National Laboratory, NAFEMS-Seminar. Denmark (June 2006).

[8.] C. Berggreen, K. Branner, J. F. Jensen, J. Schultz *"Application and Analysis of Sandwich Elements in the Primary Structure of Large Wind Turbine Blades*, J. P. Journal of Sandwich Structures and Materials, Vol. 9 (November 2007).

[9.] Amit Puri, Alexander Fergusson, John Dear, Andrew Morris, Find M. Jensen "*Digital image correlation and finite element analysis of wind turbine blade structural components*" 2007 European Offshore Wind Energy Association conference. Germany.

[10.] L.G. Brazier *"On the flexure of thin cylindrical shells and other 'thin' sections"* Late of the Royal Aircraft Establishment. Reports and Memoranda no1081 (M.49), pp (1– 30) (1926).

[11.] Luca S. Cecchini, Paul M. Weaver *"The Brazier effect in multi-bay aerofoil sections"*, University of Bristol – UK.

[12.] Luca S. Cecchini *"The non-linear flexural response of thin-walled beams"*. PhD thesis. (2006), University of Bristol – UK.

[13.] T. von-Kármán Zeit*"Ueber die formänderung dünnwanger rohre, insbesondere federnder ausgleichrohre"*. Des vereines deutscher ingenieure (1911)

[14.] K.T. Kedward *"Non-linear collapse of thin-walled compsite cylinders subject to flexural loading"*. Proceedings of the international conference on composite materials (1978)

[15.] O. Rand *"In-plane warping effects in thin-walled boxed beams"*. AIAA Journal, 38, Nr. 43, 131-152 (2000)

[16.] Frode Paulsen, Torgeir Welo *"A design method for prediction of dimensions of rectangular hollow sections formed in stretch bending"*. Journal of Material Processing Technology, 128, (2002)

[17.] Christian Jensen "*Defects in FRP Panels and their influence on Compressive Strength*". Master's thesis. Technical University of Denmark and Risø National Laboratory. (February 2006)

[18.] Find M. Jensen "*Ultimate strength of a large wind turbine blade*". PhD Thesis. Risø National Laboratory for Sustainable Energy, Technical University of Denmark. (Submitted May 2008)

[19.] Find M. Jensen *"WO 2008-071195 Reinforced aerodynamic profile"(cap reinforcement- patent A)*

[20.] Find M. Jensen *"WO 2008-086805 Reinforced blade for wind turbine (floor- patent B)"*

[21.] Find M. Jensen, Per H. Nielsen *"WO 2008-089765 Reinforced blade for wind turbine (shear cross- patent C)"*

[22.] Find M. Jensen *"WO 2008-092451 Wind turbine blade(U-profile-patent D)"*

[23.] Find M. Jensen, Per H. Nielsen *"080624 P12737 DK Coupling of trailing edge panels (patent E)"*

[24.] Find M. Jensen*"080701 P12735 DK Soft Floor (patent B2)"*

[25.] Find M. Jensen *"080623 P12736 DK Angled Girders (patent C2)"*

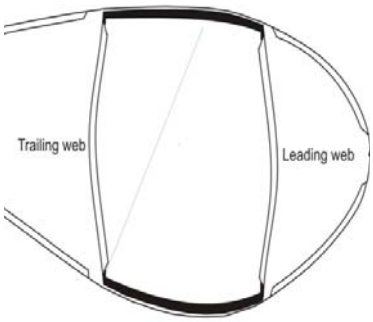

Fig. 1b

Figure 1: Full-scale test of a 34m blade from SSP-Technology A/S 1a) Photo from ref. [3.] 1b) Wind turbine blade subject to bending, leading to ovalization of the profile

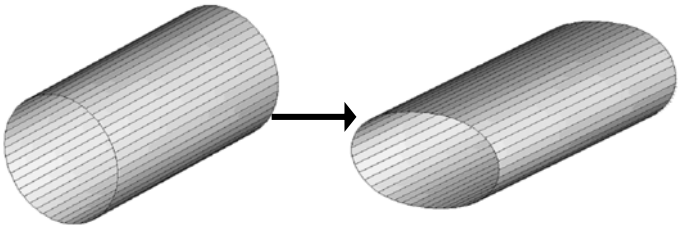

Fig. 2a

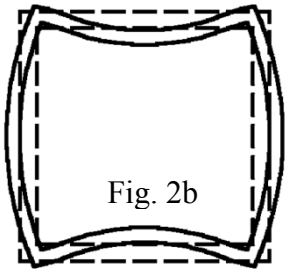

Fig. 2b

Figure 2: Inward crushing forces on a thin walled structure subject to bending, leading to flattening of the cross-section. a) Ovalisation of a circular section - figure from [12.]
b) "Suck in" of a squared tupe - figure from [16.].

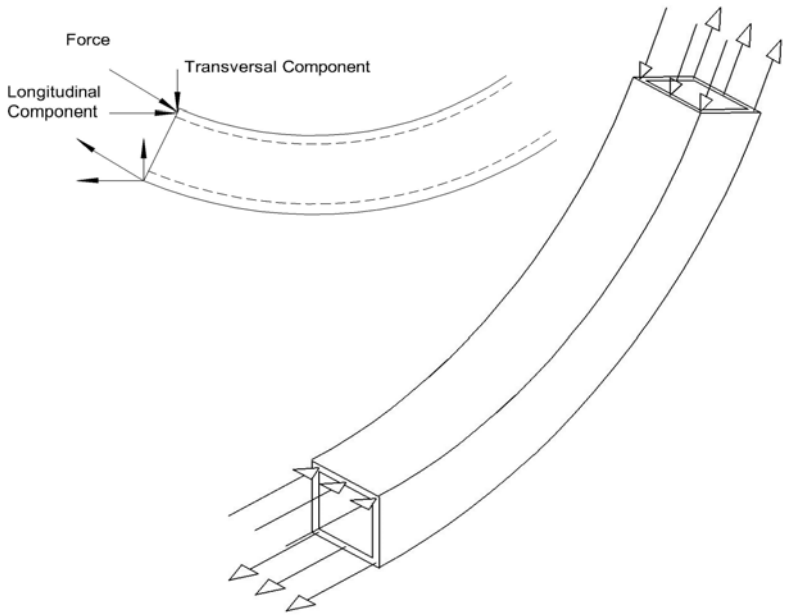

Figure 3: Inward crushing forces on a thin walled structure subject to bending, leading to flattening of the cross-section

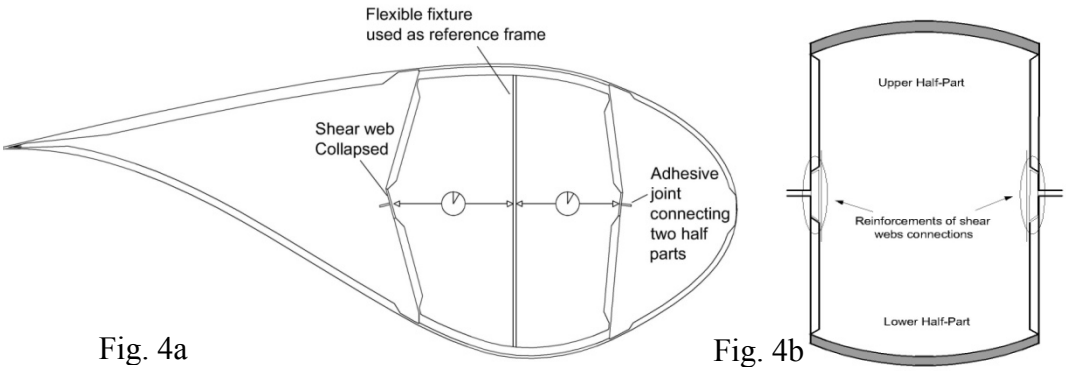

Fig. 4a Fig. 4b

Figure 4: Cross sections of an unreinforced wind turbine blade and a reinforced box girder both from SSP-Technology A/S a)Web failure of SSP34m blade b) Reinforced shear webs in a new full-scale test of a SSP34m load carrying box girder

Figure 5: Full-scale test of 34m (shortened to 25m) load carrying box girder from SSP-Technology A/S, see ref. [4.] and [5.].

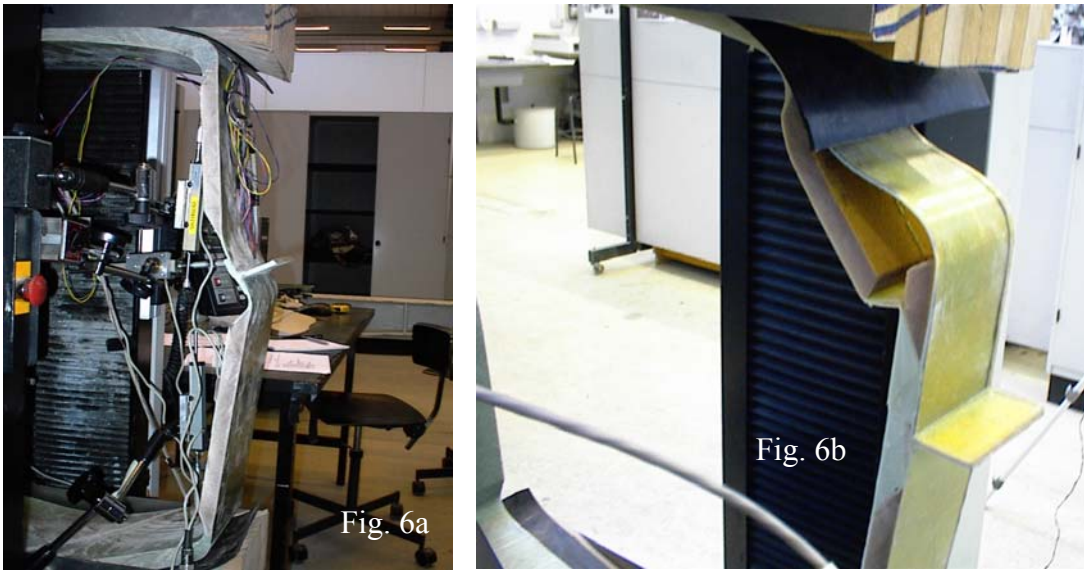

Figure 6: 2D-section experiments of original box girder (6a) and reinforced box girder (6b)

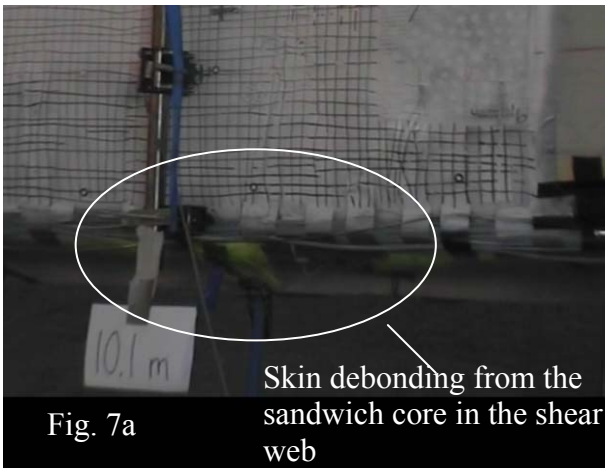

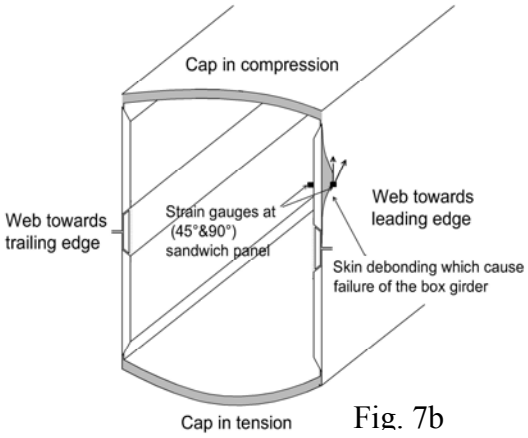

Figure 7: Failure observed at the shear web in the "new" box girder test a) Frozen frame picture showed skin debonding of the sandwich web towards leading edge b) Sketch which illustrate the failure and the strain gauges attached in that area.

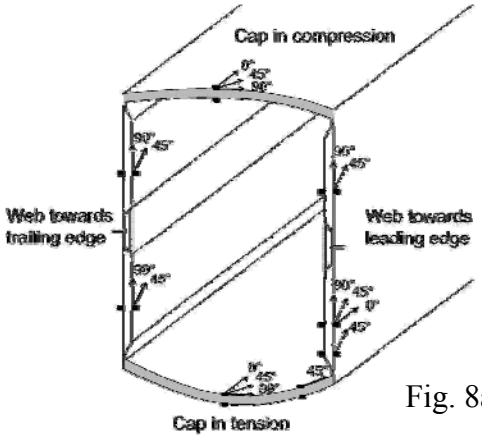

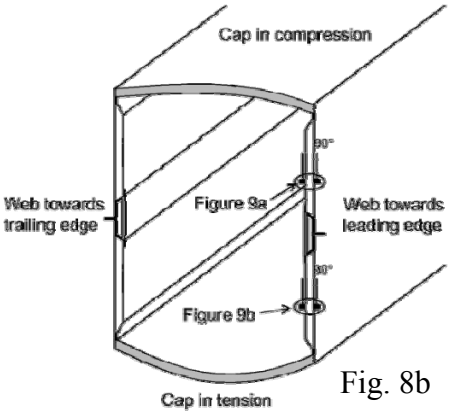

Figure 8: a) Strain gauge locations at the 10m span position b) Position of strain gauges which results presented in Figure 9.

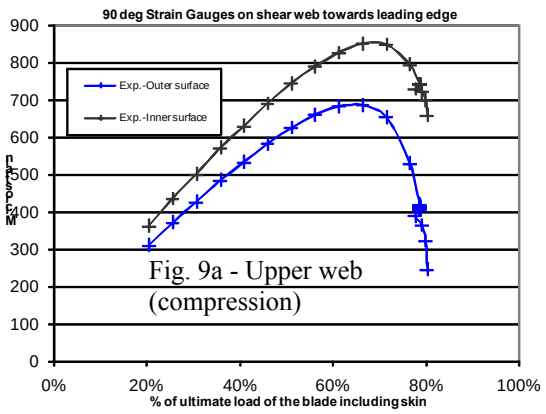

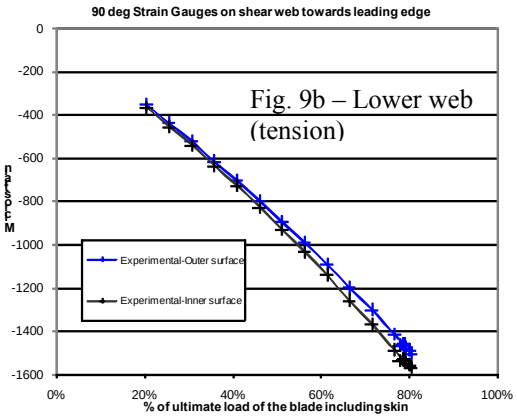

Figure 9: Experimental strain gauge measurements (back to back) a) Upper web part b) Lower web part. The load scales refer to a previous full-scale test (see ref. [3.]) where the aerofoil was included.

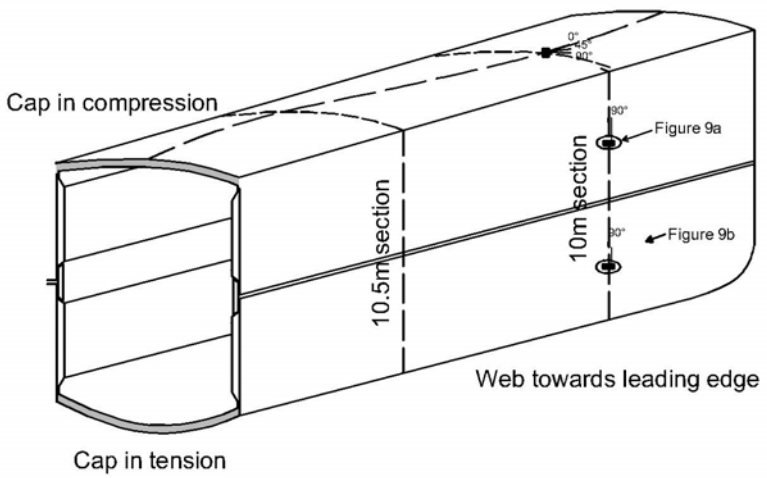

Figure 10: Position of the cap buckling pattern

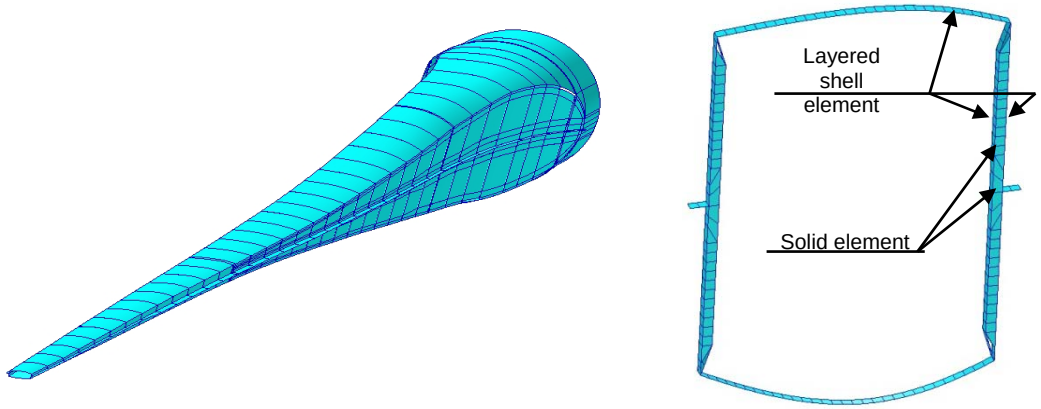

Figure 11: FE-model a) Entire model of the shortened (25m) box girder. No elements are shown, only geometry b) Section of finite element model

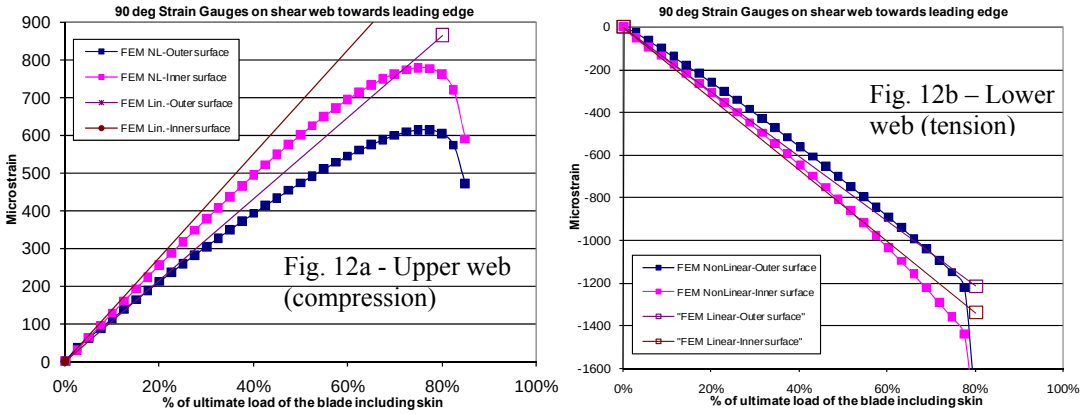

Figure 12: Linear and non-linear FE-results a) Upper web part b) Lower web part. The load scales refer to a previous full-scale test (see ref. [3.]) where the aerofoil was included.

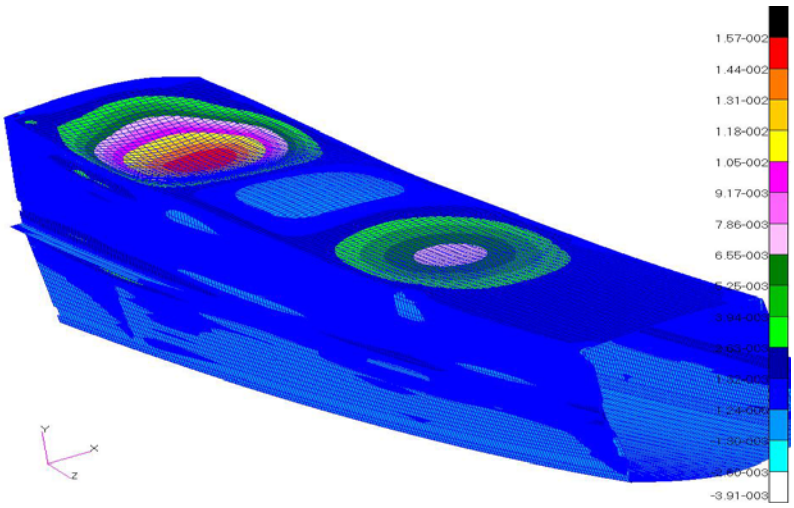

Figure 13: Section of finite element model from 9.5m to 13.2m from root. Strain in global x-axis (transverse) is shown.

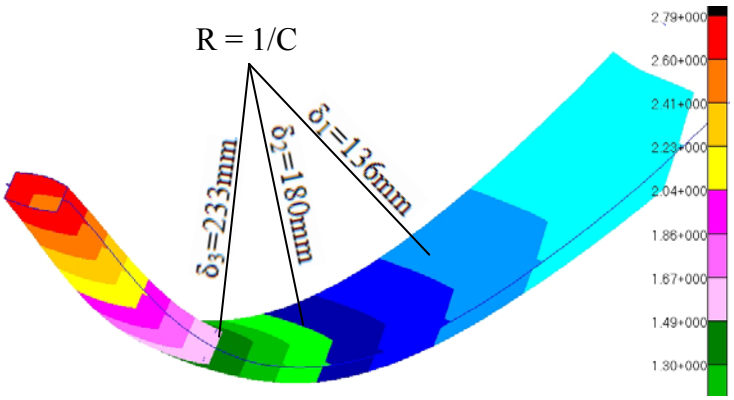

	Long. position	Blade deflection
δ_1	9.0m	136mm
δ_2	10.0m	180mm
δ_3	11.0m	233mm

Figure 14: Longitudinal curvature extracted from the FE-model (at 80% load)

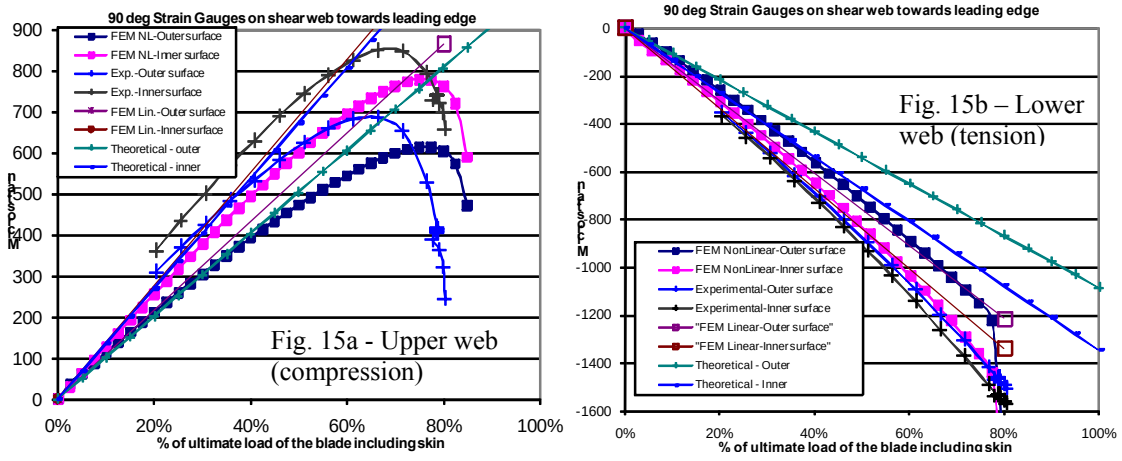

Figure 15: Comparison of experimental, numerical and theoretical results a) Upper web part b) Lower web part.

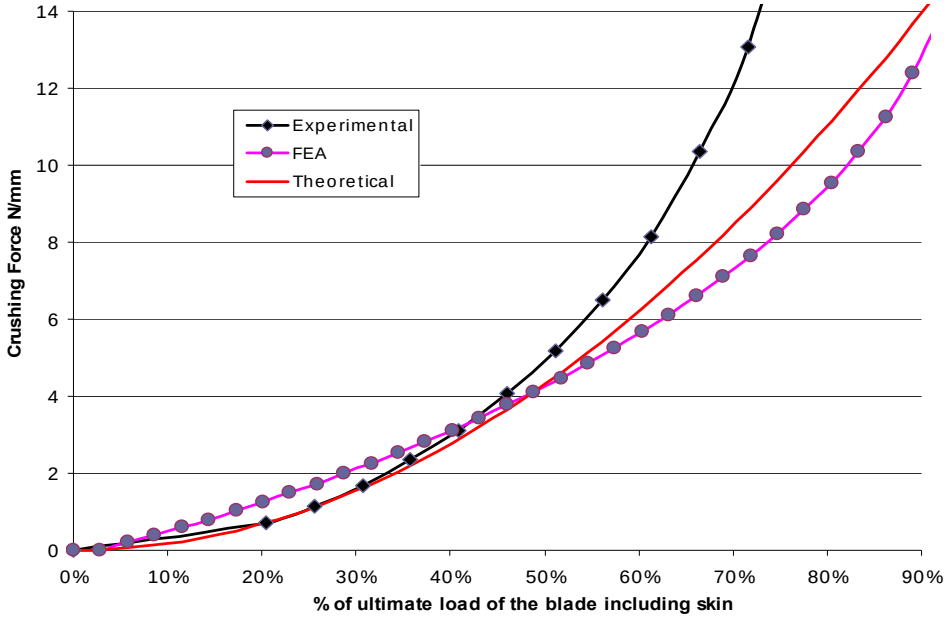

Figure 16: Comparison of theoretical FEA and experimentally measured crushing force carried in the leading web

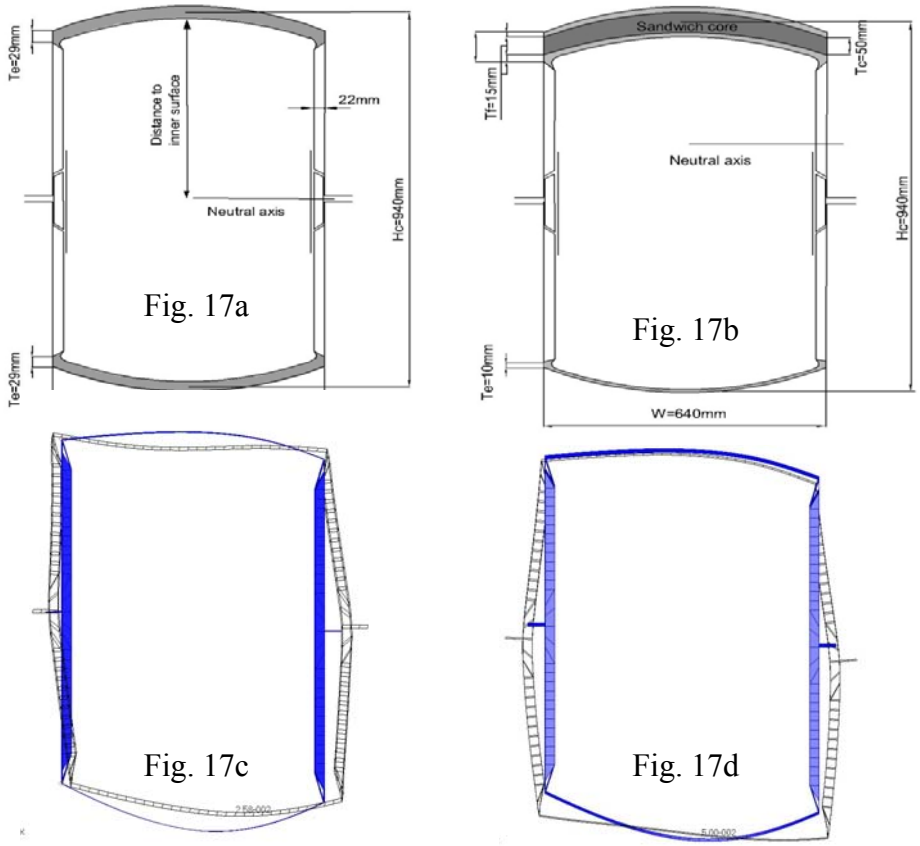

Figure 17: Sketches and deformation plots of an optimized (non-symmetric) box section and an original (symmetric) design. Figure a+c show the original box girder design and figure b+d the optimized design. The two deformation plots (c+d) are showed with a deformation scale at 2. The solid colour are the undeformed.

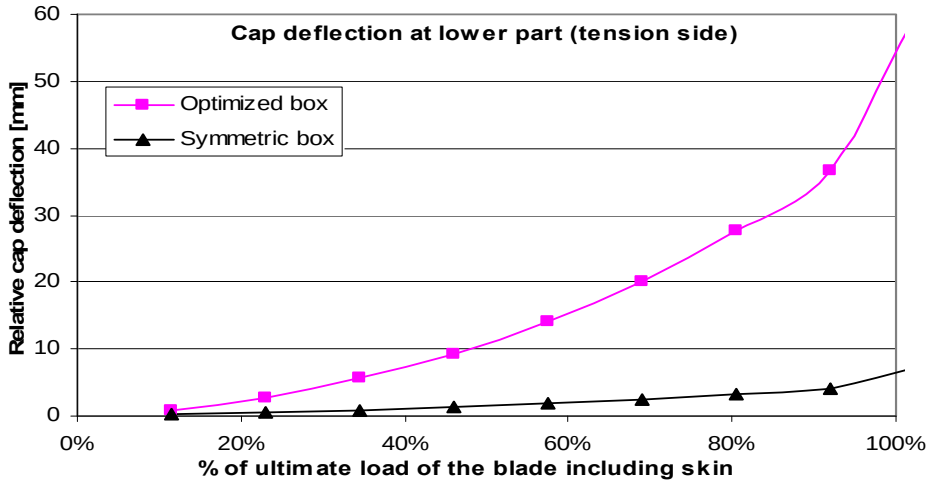

Figure 18: Cap deformations of an optimized (non-symmetric) box section and original (symmetric) box girder – Cap in tension is shown

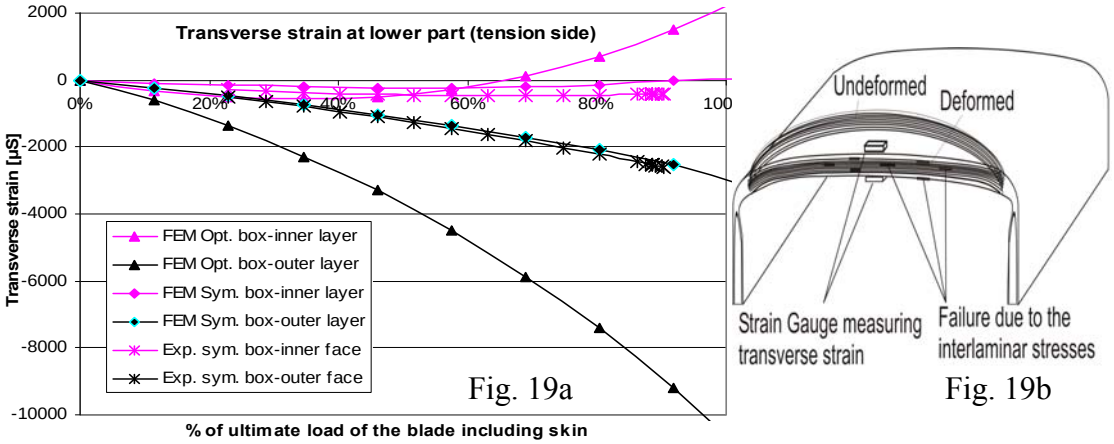

Figure 19: Cap deformations and transverse strain gauges(17b) of an optimized (non-symmetric) box section and original (symmetric) box girder – Cap in tension is shown

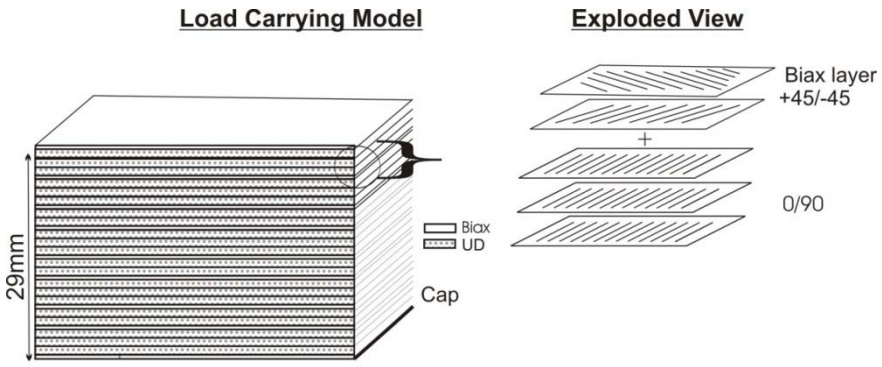

Figure 20: Layup of the load carrying cap

Appendix A2 – “Full-scale testing and finite element simulation of a 34 metre long wind turbine blade”. Find M. Jensen, Andy Morris

FULL-SCALE TESTING AND FINITE ELEMENT SIMULATION OF A 34 METRE LONG WIND TURBINE BLADE

Find M. Jensen[1], Andy Morris[2]

KEYWORDS

Full-Scale testing, wind turbine blades, non-linear finite element, ultimate failure, post buckling, laser shearography.

SUMMARY

The load carrying structure (box girder) of a 34 m composite wind-turbine blade was tested to failure under flap-wise loading. A top-hat reinforcement in the root section and extra supports has resulted in a successful test, with a realistic ultimate failure. Critical failure was observed in the shear webs just before ultimate failure.

Non-linear strain behaviour was observed in the shear webs at a lower load level and non-linear finite element analysis has been used to simulate the structural elastic response.

Furthermore, stable post buckling has been measured in the load carrying laminate by use of non-contact full field strain measurement techniques. The buckling pattern is also identified in the non-linear finite element analysis at the same location and load level.

Laser shearography inspection of the box girder has shown the potential of this technique as a means of quantifying the extent of delaminated areas within a composite structure.

[1] Department of Wind Energy, Risoe National Laboratory, Technical University of Denmark Roskilde, Denmark. E-mail find.moelholt.jensen@risoe.dk

[2] Technical Head Integrity, E.ON UK, Power Technology, Ratcliffe-on-Soar, Nottingham, NG11 0EE UK. E-mail andy.p.morris@eon-uk.com

FULL-SCALE TESTING AND FINITE ELEMENT SIMULATION OF A 34 METRE LONG WIND TURBINE BLADE

INTRODUCTION

A failure of a wind turbine blade is of concern to both turbine manufacturers and end user generators such as E.ON UK. A failure would pose an immediate commercial loss and may also have safety implications, depending on the location of the wind turbine. It is clear that routine maintenance and inspection programmes play an important role in ensuring that wind turbines are operated safely and profitably.

The size of wind turbine blades are expected to increase considerably in the future as initiatives to increase the contribution of renewable energy sources accelerate; hence this will demand a better understanding of the structural behaviour of composite turbine blades. The detailed structural behaviour must be investigated beyond the elastic range, which may include the identification of failure modes that lead to ultimate collapse. Wind turbine blades have typically been optimized by experimental tests and simplified analytical methods. However, numerical simulation tools are gaining wider acceptance as they become more sophisticated in their predictive capability as well as offering a route to significantly lower developmental costs.

Based on experiences from a previous full-scale test, see figure 1 and ref. [1], a new full-scale test was setup, however for the purposes of this test only the load carrying structure was tested, see figure 3.

Figure 1: Full-Scale Test – Entire Structure

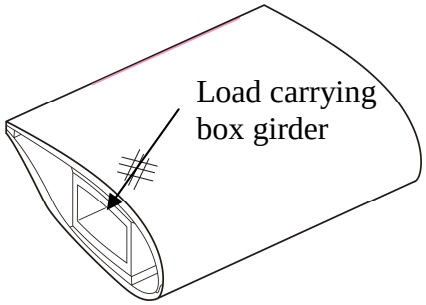

Figure 2: Blade with a load carrying main spar

Figure 3: Full-Scale Test – Load Carrying box girder

FULL-SCALE TESTING AND FINITE ELEMENT SIMULATION OF A 34 METRE LONG WIND TURBINE BLADE

One of the objectives of the full-scale test was to assess whether future wind turbine blades could be designed with less laminate in the load carrying caps, and still be able to carry the loads, even after stable post buckling has been observed using non-contact full field strain measurement techniques.

The finite element method (FEM) [2] was used to determine if any non-relevant failure modes, caused by the assumption of not including the aerofoil, would occur during the test. As a result of this study a top-hat reinforcement and extra supports have been incorporated in the box girder test to ensure that realistic deformation and failure modes are obtained. The shear webs were shown to be the weak point when the blade was tested without the outer skin (aerofoil).

Only idealised loads can be imposed in a full-scale test and in this paper the critical flap-wise load case is evaluated.

This paper is focused on improving understanding of the local structural behaviour and the ultimate strength aspects of the design. The assessment of remaining service life (defect acceptance and growth) is a different aspect, which will be covered in future work.

NEW TEST SETUP OF THE LOAD CARRYING BOX GIRDER

A full-scale 34 m wind-turbine blade, manufactured by SSP-Technology A/S, was tested to failure under flap-wise loading as shown in figure 1. The results from this work are presented elsewhere [1].

Based on experiences from this full-scale test, which included the aerofoil section, a new full-scale test was prepared. However, this time only the load carrying box girder was tested, as illustrated in figure 3.

Besides savings in experimental costs there are several advantages associated with not including the aerofoil section in the full-scale test. For example, it allows measurement equipment to be mounted on the outer faces of the box girder, which enables a more valid assessment of the FE model response. It should be noted that the aerofoil section only carries a small part of the total load. The load carrying box girder carries approximate 90% of the flapwise bending load but reduces the buckling capacity by 30-40% in the area close to the root section where the span of the blade is much larger than for the outer two-thirds of the blade length. In this area buckling is normally not critical; however when the aerofoil is removed previous FE analyses has shown that this area can be sensitive to buckling failure, see figure 4a. This failure mode is unrealistic and unwanted since it would never occur on a production blade that includes the aerofoil. Consequently a top-hat girder section has been added to the box girder under test to compensate for the removal of the aerofoil; hence

the unrealistic failure mode has been eliminated, as illustrated in the stress contour plots, figure 4b+c.

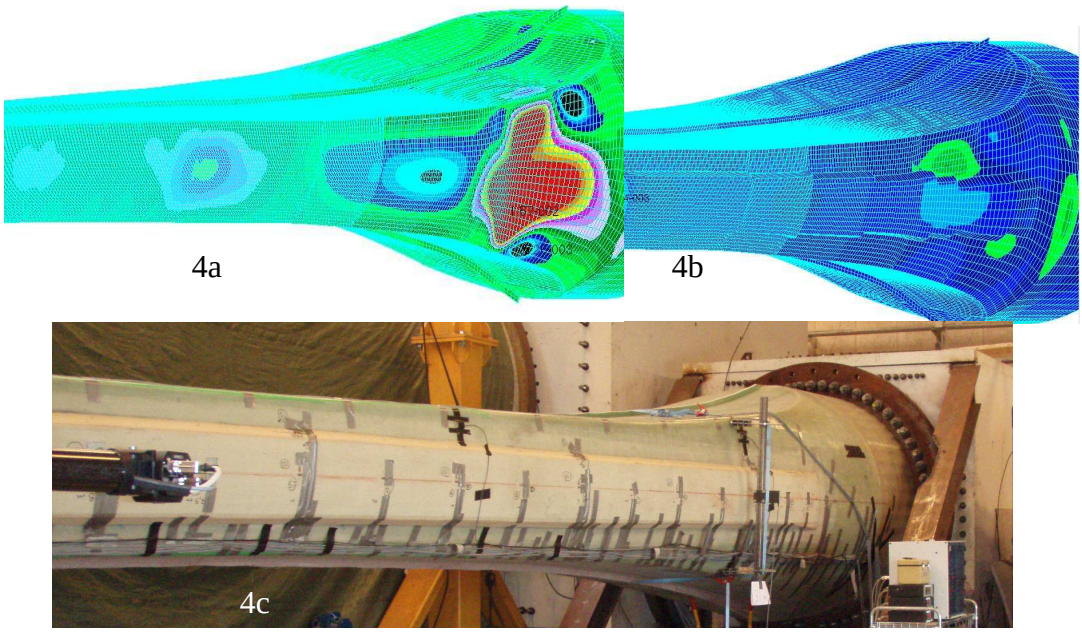

Figure 4: Top-hat girder eliminates unrealistic failure modes

Another important unwanted and unrealistic failure mode is transverse shear distortion of the box profile see figure 5a.

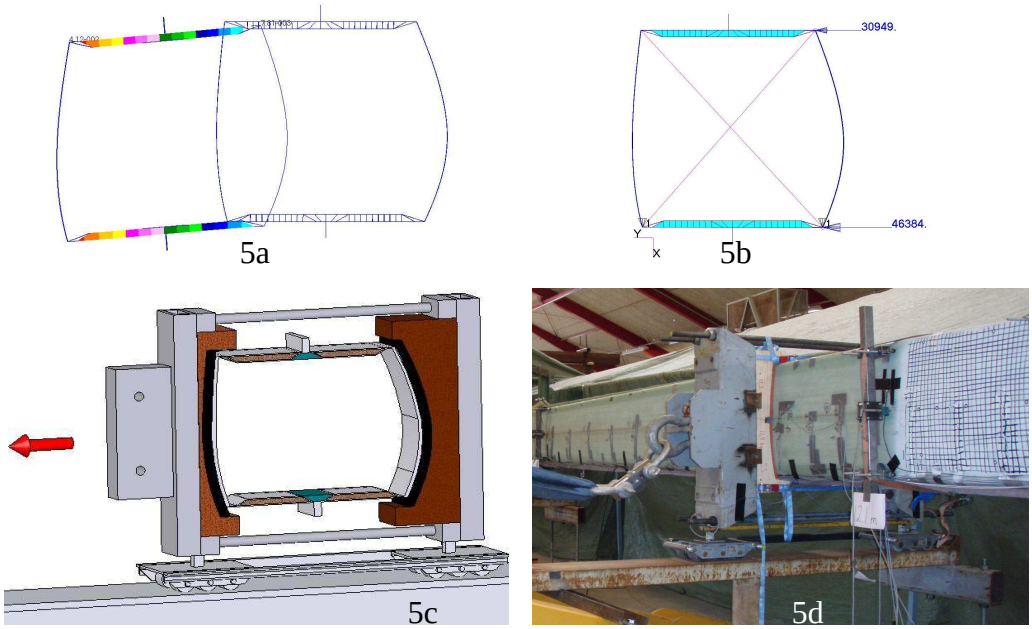

Figure 5: Transverse shear distortion eliminated by supporting the corners in transverse movement (perpendicular to the load direction)

If the loading is transmitted through the shear centre then torsion of the box girder section would theoretically be eliminated, however since there are only three loading points and the box girder geometry is twisted, it is not possible to eliminate torsion in practice. The box girder section will twist due to these torsional loads; this tendency is exacerbated by the relatively low bending stiffness at the box girder corners. Furthermore, the crushing pressure (Brazier loads) from the longitudinal bending curvature will try to collapse the profile. Normally, the aerofoil section restrains this behaviour; however for this test extra supports must be implemented to counter these effects, as illustrated in figures 5c-d. In the FE-model rebars, figure 5b, are used to distribute support to the upper corners; thereby simulating the effects of the stiff clamps and distributing the reaction forces to all four corners in the full-scale test. Three of these supports at 9m, 13.2m and 19m positions along the box girder has eliminated this transverse distortion, and this has ensured that a realistic failure mode is achieved from the full-scale test, see figure 8 and description later in this paper.

STRUCTURAL BEHAVIOUR OBSERVED DURING THE TEST

During the full-scale test strain and local deflections has been measured; figure 6 shows typical measurement locations.

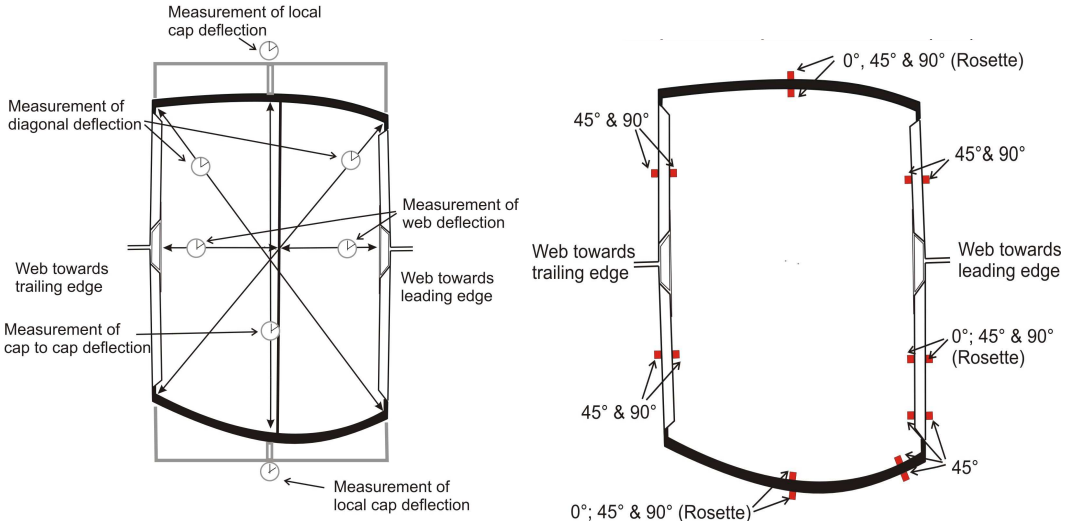

Figure 6: Strain gauges and displacement sensors in the failed section at 10m position

Figure 7b show the measured strains (back to back) on the upper web part towards leading edge, which lead to a non-linear behaviour plotted in figure 8a. The FE-model shows the same non-linear behaviour, even though there is a difference in the strain level. Since the FE-model does not include any plasticity

or damage modelling capability, it can be concluded that it is due to poor elastic behaviour. The non-linear elastic behaviour can be explained by two counter acting phenomena; Anticlastic effect and the Brazier effect and post buckling of the cap. The Anticlastic effect causes positive strain in the shear webs of the upper half part of the box girder. Normally, the "transverse" expansion is small in isotropic materials and 0º laminates, but for ±45º laminates in 0º compression the expansion caused by the shear modulus is high. In the FE-model the ±45º laminates are assumed to be 0º laminates with a high poissons ratio, estimated to be 0.6. This value is often seen in the literature, but the actual value for the laminate must be found by experimental test. The Elastic modulus in the 0º direction can either be compensated for by using a transformation in classical laminate theory or by use of materials properties found from experimental test, where the ±45º laminate is tested in the 0º direction. From figure 7a+b it can be seen that the linear anticlastic effect dominates with only a small nonlinear contribution from the crushing pressure at low load. The change in stiffness at 70-80% load is caused by post buckling in the cap, which contributes an extra "crushing pressure" for the actual cross section where the buckling wave has its minimum. If buckling would not occur then the Brazier effect would be more dominant at high load, because of the increase in the longitudinal curvature squared.

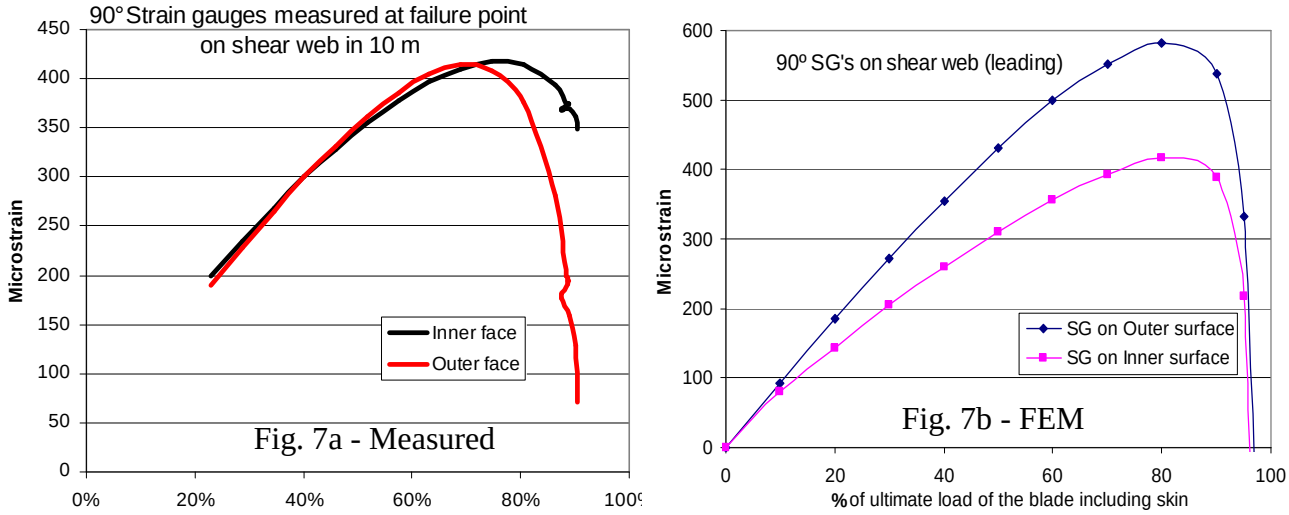

Figure 7: Back to back strain gauges in 10m. The load scales refer to the first full-scale test where the aerofoil was included.

FULL-SCALE TESTING AND FINITE ELEMENT SIMULATION OF A 34 METRE LONG WIND TURBINE BLADE

FAILURE OBSERVED IN THE SHEAR WEBS DURING THE TEST

During the full-scale test a camera was used to capture the first and critical failure mode, which was debonding of the outer face skin on the sandwich shear webs, see figure 8.

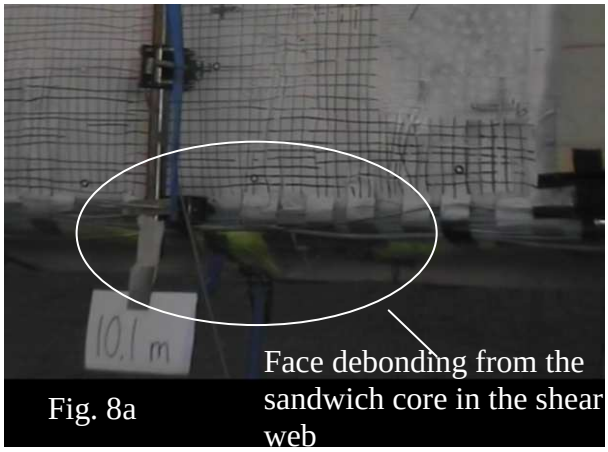

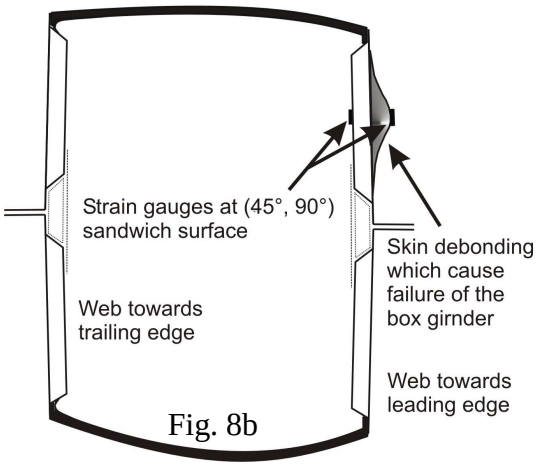

Figure 8: Skin debonding of the sandwich webs in 10m

A brief movie clip of the failure is shown in the presentation that clearly shows initial face debonding, leading to ultimate collapse of the box girder.

The failed region is in an area where there is no top-hat reinforcement, additional transverse supports or loading has been applied. Consequently the failure is expected to be at the weak point on this specific blade. Other blades may have stronger (or weaker) webs but the analyses and tests have shown that in all cases it is important to include the crushing pressure, which can only be accounted for in the FE analysis by including non-linear geometric analysis. It is worthwhile to note that even when non-linear effects are included in the FE analysis it is difficult to simulate this type of failure. This is because surface wrinkling theory, debonding and strain based failure criteria cannot predict the failure very accurately.

The use of cohesive interface element could be one way to simulate this type of failure. However, the analyst would have to have some insight regarding likely failure locations, since it is not possible to add cohesive interface elements at all likely locations in such large laminate structures. The analysis of the response of sub-component tests and FE submodels could be one way to reduce the errors associated with solving these problems; these are techniques often used in other industries such as aeronautics.

FULL-SCALE TESTING AND FINITE ELEMENT SIMULATION OF A 34 METRE LONG WIND TURBINE BLADE

BUCKLING OBSERVED USING AN OPTICAL MEASURING SYSTEM

Besides face skin debonding, localised bending and stable post buckling was observed during the experiment and in the FE study. The out of plane deformation was measured during the test using the ARAMIS optical system [3]. The system uses a pair of cameras to track the motion of a prescribed pattern or grid on the surface of the box girder. Subsequent image processing, using digital image correlation techniques provide surface strain contour plots as illustrated in figure 9a.

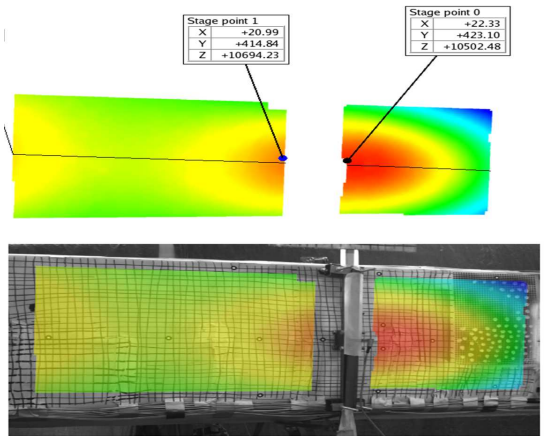

Fig. 9a: ARAMIS measurement

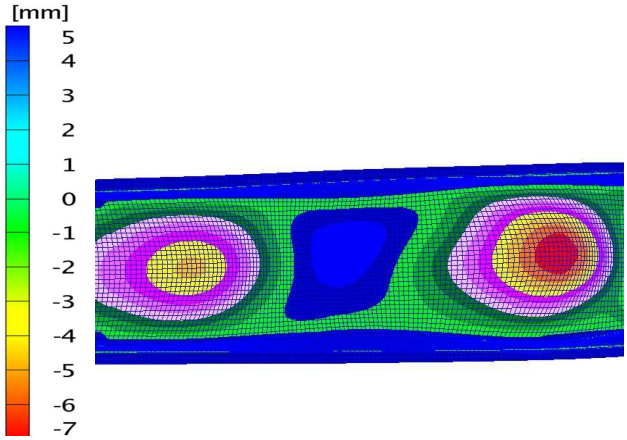

Fig. 9b: Non-linear FE-model

Normally, the out of plane bending stiffness of the load carrying cap is 30-40% higher, when the outer skin (aerofoil) is included. Removing the outer skin has a significant influence on the local bending stiffness, while the overall stiffness of the blade is only reduced by around 8-10%. One of the objectives of the full-scale test was to assess whether future wind turbine blades could be designed with less laminate in the load carrying caps, and still be able to carry the loads, even after stable post buckling has been observed.

The buckling first became unstable when the skin debonded from the webs, which resulted in collapse of the blade, see figure 10.

Figure 10. Ultimate failure: Buckling collapse after the shear webs was failed

From this experiment the preliminary indications are that no cracks or delaminations have developed and it seems to be possible to load the blade in the post buckling range as long as it is a relatively infrequent occurrence, such as a 50-year wind event. More tests must be performed to verify that larger defects are not critical. Different sizes of defects have been studied in [4], but two-dimensional testing with biaxial loading is not addressed. Ideally an end user generating company would find great benefit from the continuous capture of meaningful information on the structural health of the turbine blade. This information would as a minimum alert the generator to changes in characteristic response, and at best provides quantitative information on the structural health of the turbine blade.

NON-DESTRUCTIVE TESTING

A laser shearography inspection of a nominated region of the box girder was also undertaken prior to and during various stages of the load test. This technique enables sub-surface anomalies, introduced during manufacturing, to be detected and sized, see figure 11.

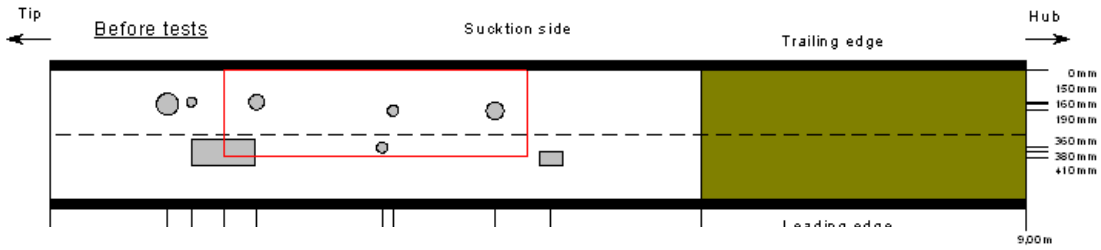

Figure 11. Production defects detected at the cap before testing

Two laser speckle systems, Vacuum Hood and Strainmapper [5] were assessed during pre-test; this confirmed that the Vacuum Hood system gave the best results. Both systems use lasers to illuminate the target area to be inspected with a diffuse speckle pattern. The speckles are formed by the interference of the laser light waves as they are reflected from the surface of the component in its static state. A load to slightly deform the component (mechanical or thermal) is applied and the speckle pattern changes. The initial static image is overlaid on to the loaded image and any interference fringes, which represent changes in strain distribution, are caused by the presence of defects. The main difference between the two systems is that one uses a vacuum to apply the load and the other uses a heating element to create transient heat. The main test load was removed at convenient intervals to allow the vacuum hood system to be used to scan selected regions of the box girder.

A number of minor anomalies were detected within the spar section prior to testing, and at some locations propagation under load was detected. A range of additional post-test examinations of sections of the spar were undertaken to aid the correlation between test and simulation, which will be described in a future paper.

CONCLUSIONS

A new test setup has been tested successfully. A few additional boundary constraints and the inclusion of a top-hat reinforcement in the root section has been shown to effectively move the ultimate failure point to a realistic location along the blade. From camera still images and strain gauges measurement it can be concluded that first critical failure mode occurs on the webs, possibly due to the crushing pressure. Buckling was also observed, but that was also expected since the outer skin contributes 30-40% of the local out of plane bending stiffness but is still not the weakest important “location” in the actual wind turbine blade. When future wind turbine blades are optimized further, buckling is expected to be the dominating failure.

Anticlastic effect, Brazier effect and post buckling resulted in a non-linear elastic behaviour in the shear webs, which also was “captured” in the non-linear finite element analysis.

Laser shearography inspection of the box girder has shown the potential of this technique as a means of quantifying the extent of delaminated areas within a composite structure. Additional system calibration is required to improve the effectiveness of the system, however it is potentially a useful technique to apply, on a sample basis, to blades in the manufacturers workshop prior to site installation. The use of non-contact full field strain measurement techniques, such as ARAMIS has great potential for future test work and will help to further enhance understanding of blade failure modes.

FUTURE WORK

The FE modelling and testing described here has illustrated some of the challenges facing the development of improved high performance wind turbine blades. Clearly, refinements to the modelling of the progression of ‘damage’ during a blade test will be considered in future work. However, any improvements in the application of advanced FE modelling methods will be complemented by the use of novel/emerging test methods such as ARAMIS and laser shearography. Improvements in these test and modelling techniques will eventually provide data that could be used to validate structural health monitoring systems. This would be of great benefit to generating companies due to the potential to increase availability and improve maintenance scheduling. The author’s are actively pursing developments in these areas.

ADKNOWLEDGEMENTS

The blade manufacture SSP-Technology AS who has delivered the box girder and Blaest Test center who has let us use their test facilities for free.

The company GOM/Zebicon for measuring deformations during the tests using the ARAMIS system.

The authors would also like to acknowledge the services provided by Andy Gwynne from Laser Optical Engineering for the use of the laser shearography system, which to our knowledge is the first use of this type of test technique on a full-scale blade test.

REFERENCES

[1] Find M. Jensen, B.G. Falzon, J. Ankersen, H. Stang "Structural testing and numerical simulation of a 34m composite wind turbine blade" Composite Structures 76 (2006) 52-61

[2] MSC-Patran and MSC-Marc www.mscsoftware.com

[3] Aramis System, Zebicon a/s www.zebicon.dk and GOM Optical Measuring System www.gom.com

[4] B. L. Karihaloo, H. Stang "Buckling-driven delamination growth in composite laminates: Guideline for assessing the threat posed by interlaminar matrix delamination" Composites Science and Technology, 2006

[5] Laser Shearography Systems, Laser Optical Engineering Ltd, www.laseroptical.co.uk

Appendix A3 – “Structural testing and numerical simulation of a 34m. composite wind turbine blade”. Find M. Jensen, Brian G. Falzon, Jesper Ankersen, Henrik Stang

Available online at www.sciencedirect.com
ScienceDirect
Composite Structures 76 (2006) 52–61
COMPOSITE STRUCTURES
www.elsevier.com/locate/compstruct

Structural testing and numerical simulation of a 34 m composite wind turbine blade

F.M. Jensen [a,*], B.G. Falzon [b], J. Ankersen [b], H. Stang [c]

[a] Department of Wind Energy, Risoe National Laboratory, P.O. Box 49, Roskilde, Denmark
[b] Department of Aeronautics, Imperial College London, South Kensington Campus, London SW7 2AZ, UK
[c] Department of Civil Engineering, Technical University of Denmark, Lyngby, Denmark

Available online 12 July 2006

Abstract

A full-scale 34 m composite wind turbine blade was tested to failure under flap-wise loading. Local displacement measurement equipment was developed and displacements were recorded throughout the loading history.

Ovalization of the load carrying box girder was measured in the full-scale test and simulated in non-linear FE-calculations. The non-linear Brazier effect is characterized by a crushing pressure which causes the ovalization. To capture this effect, non-linear FE-analyses at different scales were employed. A global non-linear FE-model of the entire blade was prepared and the boundaries to a more detailed sub-model were extracted. The FE-model was calibrated based on full-scale test measurements.

Local displacement measurements helped identify the location of failure initiation which lead to catastrophic failure. Comparisons between measurements and FE-simulations showed that delamination of the outer skin was the initial failure mechanism followed by delamination buckling which then led to collapse.

Keywords: Structural testing; Wind turbine blades; Non-linear finite element analysis; Sub-modelling; Failure mechanism; Brazier effect; Anticlastic effect

1. Introduction

The size of wind turbine blades are expected to increase considerably in the future, demanding a better understanding of the structural behaviour on a different scale. Detailed structural behaviour must be investigated beyond the elastic range. This may include the identification of failure modes which lead to ultimate collapse. Wind turbine blades have typically been optimized by experimental tests and simplified analytical methods. However, numerical simulation tools are gaining wider acceptance as they become more sophisticated in their predictive capability as well as offering a route to significantly lower developmental costs.

2. Numerical methods

The finite element method (FEM) has traditionally been used in the development of wind turbine blades mainly to investigate the global behaviour in terms of, for example, eigenfrequencies, tip deflections, and global stress/strain levels. This type of FE-simulation usually predicts the global stiffness and stresses with a good accuracy. Local deformations and stresses are often more difficult to predict and little has been published in this area. One reason is that the highly localised deformations and stresses can be non-linear, while the global response appears linear for relatively small deflections. Another factor is that a relatively simple shell model can be used for representing the global behaviour, while a computationally more expensive 3D-solid model may be necessary to predict this localised behaviour.

Even with a highly detailed 3D solid model it would rarely be possible to predict deformations or stresses accurately without calibration of the FE-model. This

* Corresponding author.
E-mail address: find.moelholt.jensen@risoe.dk (F.M. Jensen).

0263-8223/$ - see front matter © 2006 Elsevier Ltd. All rights reserved.
doi:10.1016/j.compstruct.2006.06.008

calibration is necessary due to large manufacturing tolerances. Features such as box girder corners and adhesive joints often differ from specifications. Geometric imperfections are often seen and can cause unexpected behaviour, especially relating to the strength predictions but also the local deformations can be affected. In this paper, box girder corners were not modelled in detail using solids. Instead, the rotational stiffness of the corners was calibrated with deflections measured in the full-scale test.

A big advantage of using FEM is that, once the model is set up and calibrated, complex load cases representing actual wind conditions can be analyzed. Only idealised loads can be imposed in a full-scale test and in this paper the critical flap-wise load case is evaluated.

3. Full-scale test of 34 m SSP-blade

A full-scale 34 m wind turbine blade, manufactured by SSP-Technology A/S, was tested to failure under flap-wise loading as shown in Fig. 1. The blade had passed all static and dynamic (correspond to 20 years life time) tests required by the classification bodies. The SSP-blade is made of glass-epoxy pre-preg material and is designed with a load carrying box girder, see Fig. 2.

Earlier experience from another full-scale test [1] and FE-simulations [2] has shown that the cap deflect non-linearly. The conclusion from these investigations is that the load carrying box girder ovalizes when the blade bends flap-wise. New equipment has been developed to record the web deflection resulting from ovalization, see Fig. 3.

Each web sensor can independently measure in- and outward web deflection which occurs when the box girder ovalizes or is subjected to other types of deformation. In the 8 m segment near the root, effects due to change in geometry interact with conventional ovalization effects resulting in a counterintuitive non-linear response. Mechanisms which explain these deformations and the relevance of including these effects are presented.

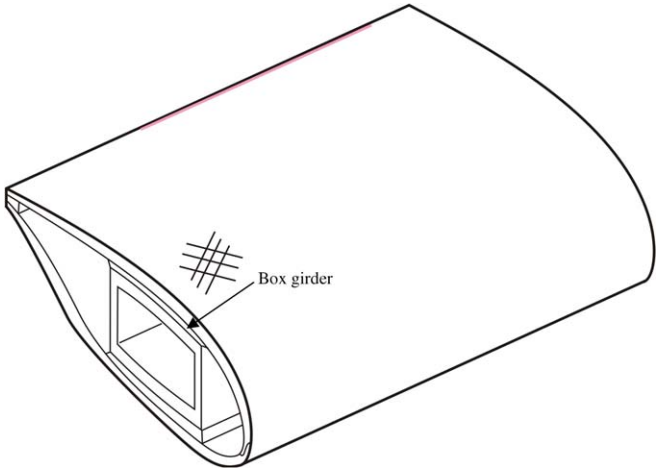

Fig. 2. Blade with a load carrying main spar.

A combination of measurements and FE-simulation has shown that delamination of the outer skin was the initial failure mechanism followed by delamination buckling which led to collapse.

4. Sub-modelling techniques

A local model, using shell and brick elements, was developed for a span-wise segment of the blade. The 0–13 m segment is found to be the most critical part and final failure also occurred in this section. The boundary conditions used in this sub-model were based on the displacement field taken from the global FE-model. Normally, the linear displacement field is used in sub-modelling techniques, but in this case this technique cannot be used, since non-linear effects dominate. The explanation as to why the use of a

Fig. 1. Full-scale test – flap-wise loading.

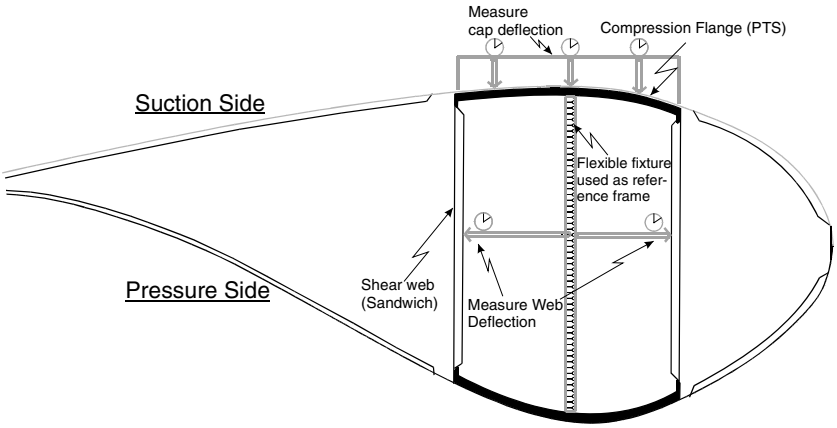

Fig. 3. Local displacement equipment in a blade section.

non-linear displacement field is required, even at moderate non-linearity, is given in this paper.

5. Experimental results

Deflections at the centre of the upper spar cap have been measured at seven different sections. In the section 10.3 m from the root, three chord-wise locations were measured, as shown in Fig. 3.

New equipment for deflection measurement was developed for use inside the box girder. The equipment is shown in Fig. 3 and measures local web deflections with a fixed reference frame in the centre of the box girder. The central reference frame is telescopic to allow for change in section height during ovalization of the box girder.

6. Non-linear geometric deformations

Different deformation patterns were observed during the full-scale test. The blade showed three distinct deformation patterns dependent on the span-wise location (all measured from the root):

- Root segment (0–4 m)
- Transition segment (4–8 m) from root to box girder segment
- Box girder segment (8–34 m)

The first two segments will only be treated very briefly in this paper, but are included to illustrate the complexity of local deformations. Deformations in the root segment also influence the boundary conditions on the box girder segment, which starts 8 m from the root. It should be noted that the box girder actually runs along the full length of the blade but behaves differently in the three segments describe in the following.

6.1. Root segment (0–4 m)

Part of the web deformations are due to the gravity load, which causes the webs to show a non-symmetric behaviour before loading. This behaviour is specific to the SSP-blade, and is due to the change in box girder section geometry along the root segment.

A sketch of the non-symmetric web deflection is shown in Fig. 4a and measurements are shown in Fig. 4b. The measurements exclude deflections due to pre-load (gravity load) because the measuring gauges were reset prior to loading of the blade. The unusual behaviour of the webs is not discussed further here but is most likely related to the constraints imposed by the stiff root connection to the hub. In the current context, it is merely of interest to be able to apply the correct boundary conditions on the segments further away from the root.

6.2. Transition segment (4–8 m)

A large change in cap curvature, and therefore cap height, takes place in the transition segment, see Fig. 5a.

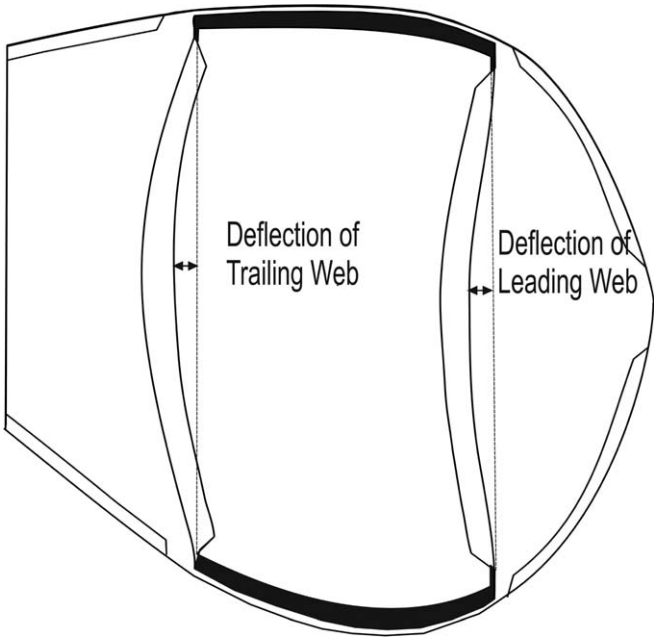

Fig. 4a. Sketch of non-symmetric.

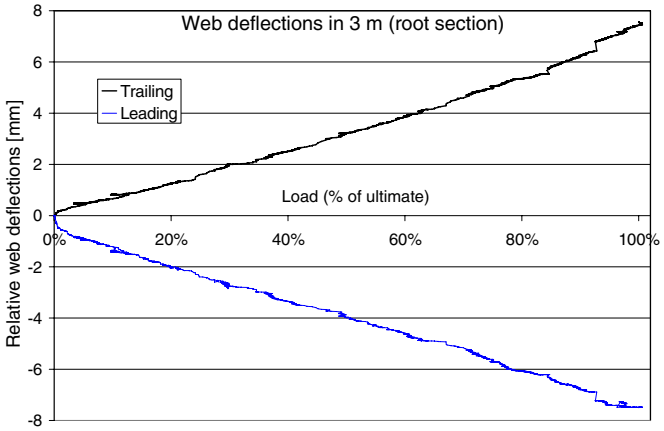

Fig. 4b. Relative web deflections versus load.

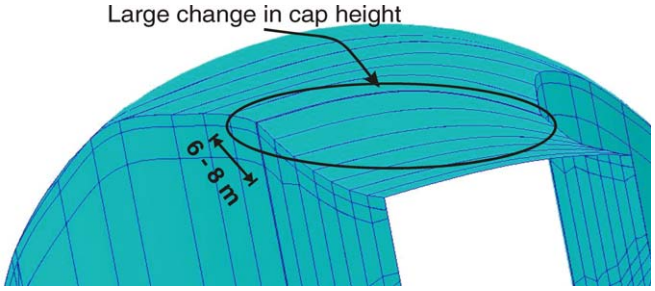

Fig. 5a. Changes in profile height.

Outward cap deformations were measured during the full-scale test as shown in Fig. 5b. These outward deflections were seen on the compression side of the blade and are linked to the rapid change in cap profile in this segment.

Box girder segment (8–34 m). In this segment the expected ovalization caused by flap-wise bending was observed. This non-linear deformation or "flattening" of the cross section is also known as the Brazier effect [1] and is most pronounced for long thin hollow beams

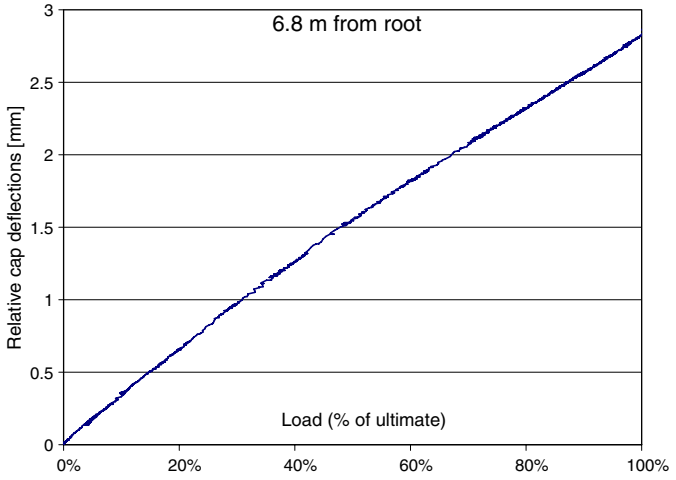

Fig. 5b. Outward cap deformation – measured.

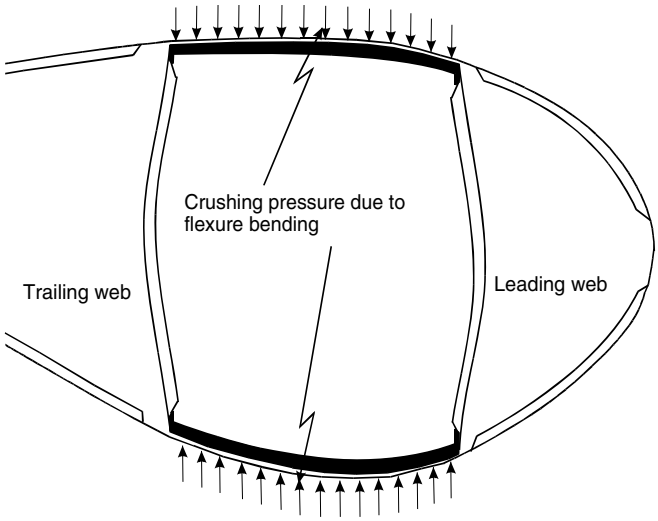

Fig. 6. Crushing pressure from the Brazier effect.

subjected to bending. The crushing pressure caused by the Brazier effect has a large effect on the web deflections and local deformation sensors have measured up to 20 mm displacement at the trailing web and 11 mm for leading web (Fig. 6).

Outer skin debonding from the box girder, see Fig. 7a, was observed after collapse, but it was not clear at which load this failure mode had occurred. A study of measured cap deflections has shown that the skin peeling starts at 92% of the ultimate load, see Fig. 7c. The jump in measured displacement is not due to sudden chord-wise bending of the cap, instead it was caused by the skin debonding from the cap where the skin assumes more of the initial curvature. The reference frame for measuring cap deflection is attached to the outer skin rather than directly to the box girder corner. Fig. 7b illustrates this observation. In Fig. 7c another skin peeling jump can be observed at 97% of ultimate load.

The actual maximum cap deformation of 4.3 mm was obtained by extrapolation, see Fig. 7c. This is the value that would have been observed if measurements were taken directly on the box girder or had debonding not occurred.

The skin debonding is expected to have a major influence on the final collapse. Buckling capacity of the blade is reduced dramatically once the outer skin and box girder separate. This buckling behaviour can be observed in Fig. 7c at 100% load, just before failure.

7. Final failure – buckling assumption

7.1. Cap and web deformations

The cap centerline deflections were measured at four span-wise positions (8.5 m, 10.3 m, 12.5 m and 15.2 m) in the box girder segment from 8 to 15 m. A 8–15 m segment of the blade is shown in Fig. 8a with the upper cap centreline indicated. The measured cap deflections are plotted in Fig. 8b. Unfortunately no measurement was taken at

Fig. 7a. Skin peeling from cap.

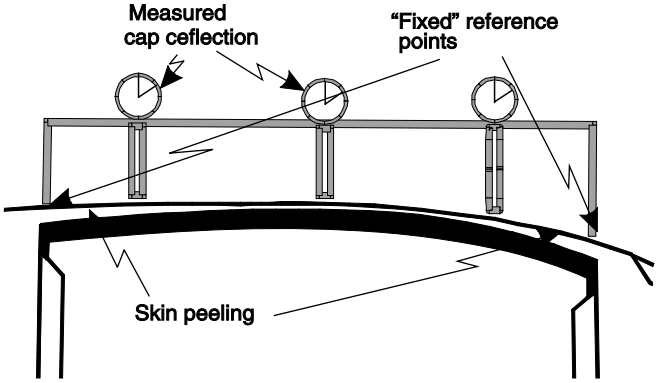

Fig. 7b. Reference points not fixed after skin peeling.

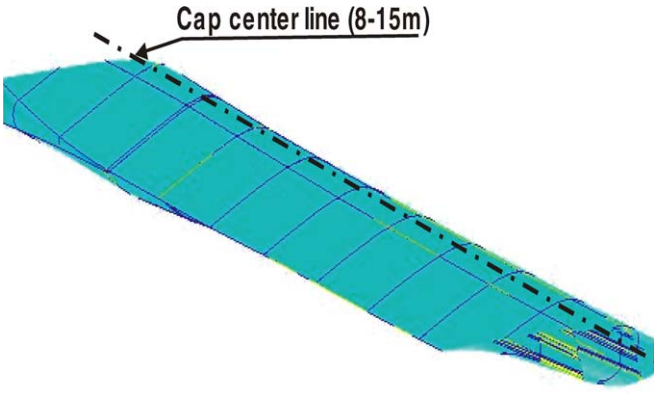

Fig. 8a. Cap centreline.

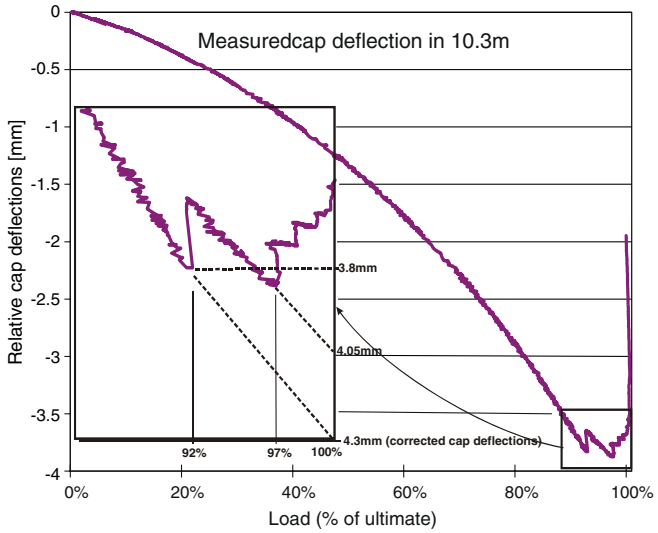

Fig. 7c. Measurements that show skin peeling and corrected cap values.

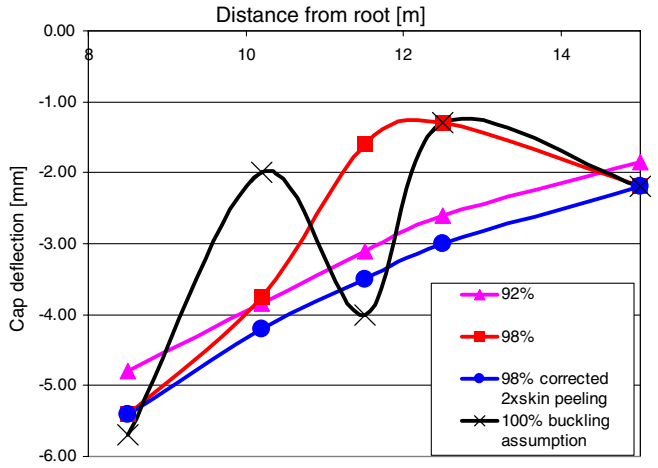

Fig. 8b. Cap deformation at different load levels.

Fig. 9. Buckling collapse.

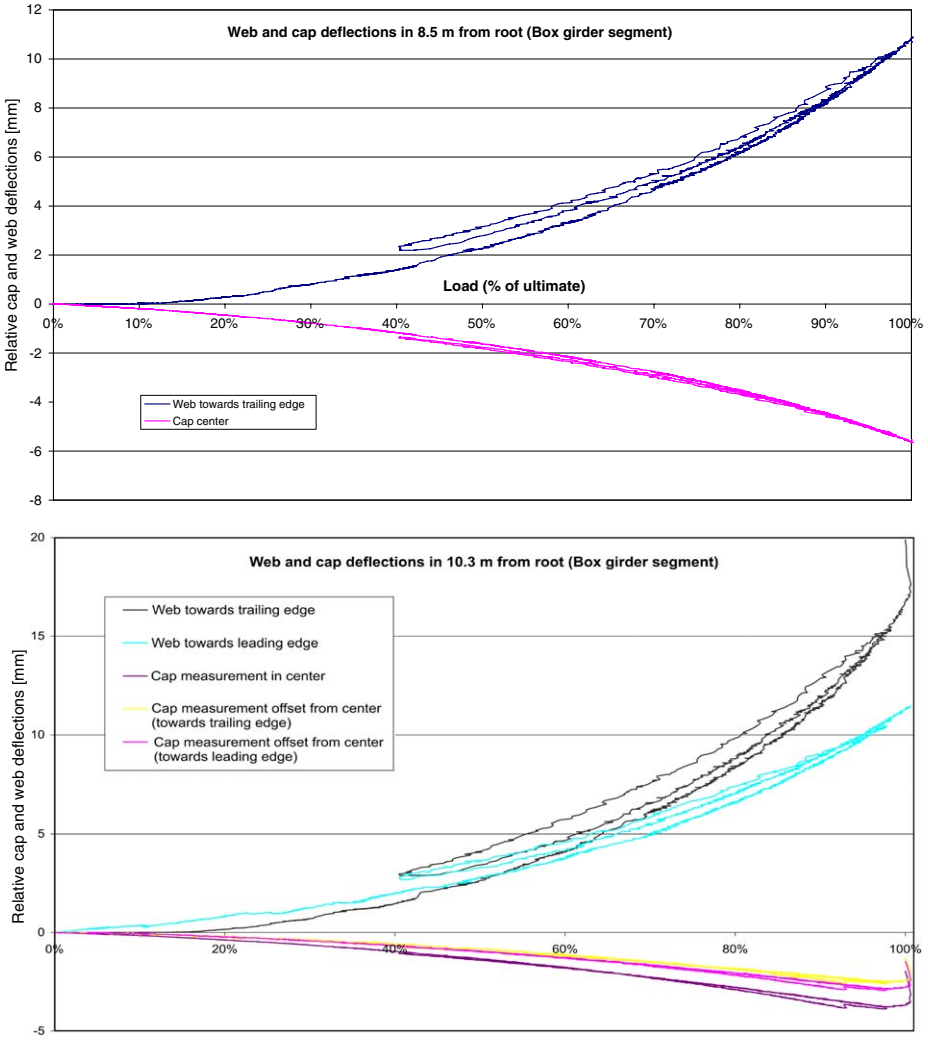

Fig. 10. Measured web and cap deflections at 8.5 m (top) and 10.3 m (bottom).

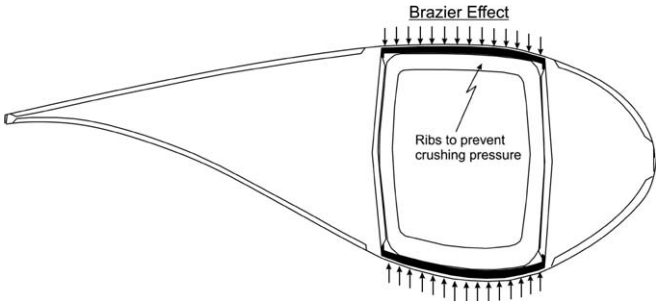

Fig. 11. Rib/bulkhead to prevent crushing pressure.

11.5 m where the final failure occurred, so cap deformation at this section is assumed. If the deformation is corrected from the skin peeling mentioned above, the cap in the longitudinal direction behaves in a smooth manner until 98% load is reached. Above this load, most likely the cap starts to buckle as shown in Fig. 8b (dark line – 100% load). This assumption is based on two observations; pictures of the blade after collapse (as in Fig. 13) and the cap measurement in 10.3 m, 12.5 m and 15.2 m which fit into this buckling pattern, see Fig. 8b.

The buckling assumption does not take the clamp at 13.2 m into account, see Fig. 9. This approximation may affect the buckling pattern since the cap is not able to buckle outwards at this location while inwards deformation is unconstrained. The inwards displacement actually looks smooth and fits into the deformation pattern up to the ultimate buckling load, see the blue (●) and pink (▲) line in Fig. 8b.[1]

The skin peeling assumption and the final buckling behaviour assumption can be confirmed by checking other measurements (strain gauges and web deflection sensors) in this segment of the wind turbine blade. Unfortunately, web sensors were only placed at 8.5 m and 10.3 m and no web measurements were taken at 12.5 m and 15.2 m.

Measurements from both sections at 8.5 m and 10.3 m support the skin peeling assumption and the buckling assumption. At 92% load where skin peeling starts, there is no sign of sudden displacement jumps in the webs at either of the sections. Displacement jumps in the cap are seen at 10.3 m but not at 8.5 m. This ties in with what one would expect from skin peeling occurring at 11.5 m, i.e. only cap deflection is affected at the nearest measuring station. The web towards the trailing edge shows a moderate increase in deflection at the 8.5 m station and a much more pronounce increase at the 10.3 m station as the load approaches ultimate. This does to some degree also confirm that buckling occurs further outboard of the 10.3 m station. Alternatively, the web may have failed locally leading to buckling in the cap. Wing structures used in the aeronautical industry (helicopter blades and fixed aircraft wings) are usually designed with the trailing edge web stronger than the web towards the leading edge. Perhaps this should also be considered in the design of wind turbine blades. Another obvious difference between wind turbines blades and aircraft wings is the lack of internal ribs/bulkheads in the wind turbine blades. This should also be considered eventhough these ribs/bulkheads may add complexity to the manufacturing process. An example of how a web/bulkhead could be incorporated in the existing blade design is shown in Fig. 10 (Fig. 11).

[1] For interpretation of colour in Figs. 1, 4, 5, 7–10, and 12–15, the reader is referred to the web version of this article.

8. Finite element results

In this section results from the numerical modelling (FEM) will be presented. The main focus will be on the 8–13 m section, where the collapse occurred.

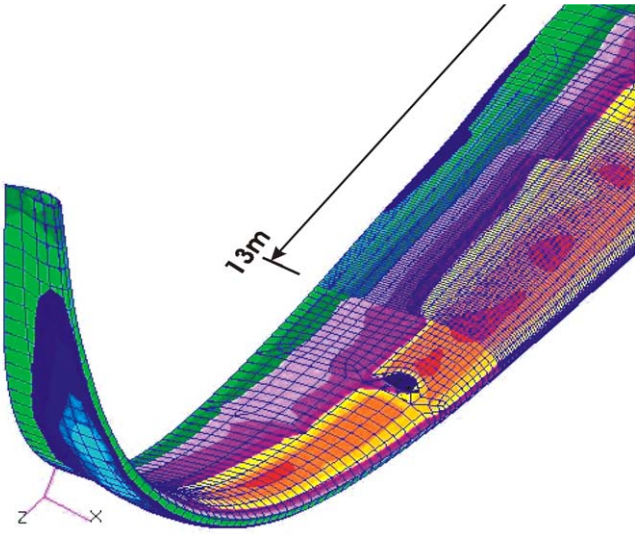

Fig. 12a. Global 34 m FE-model.

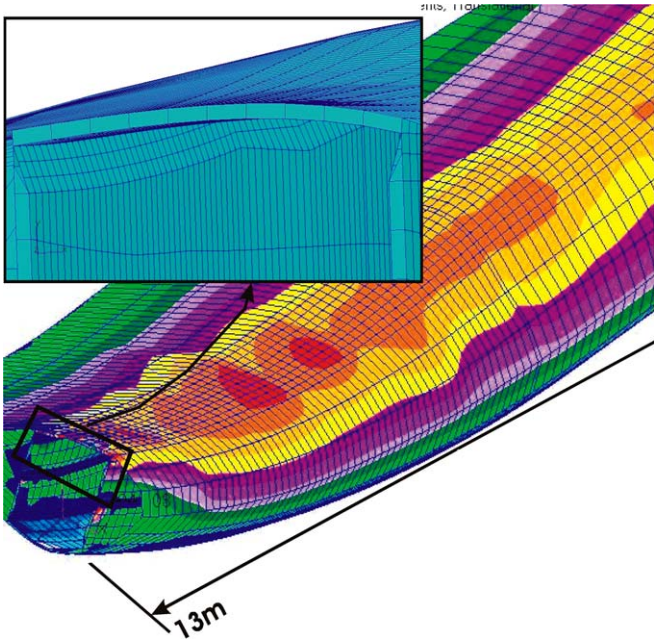

Fig. 12b. 0–13 m sub-model.

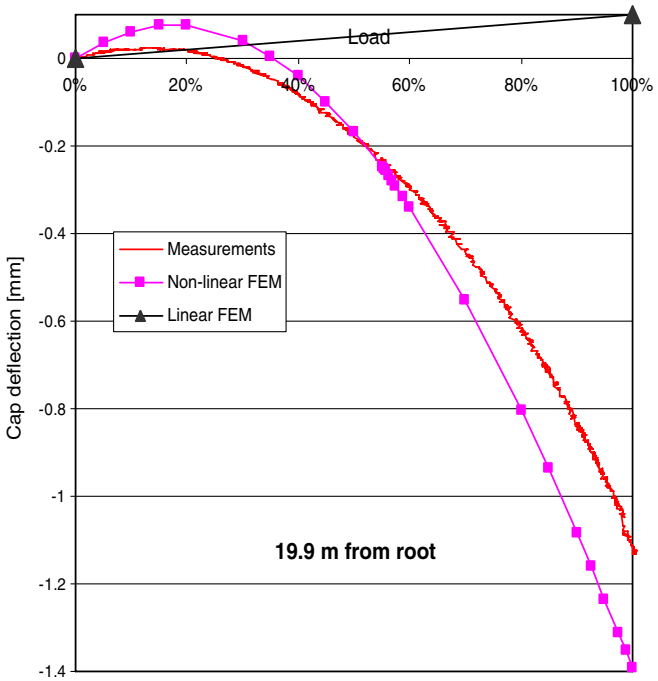

Fig. 13. Non-linear response in global model.

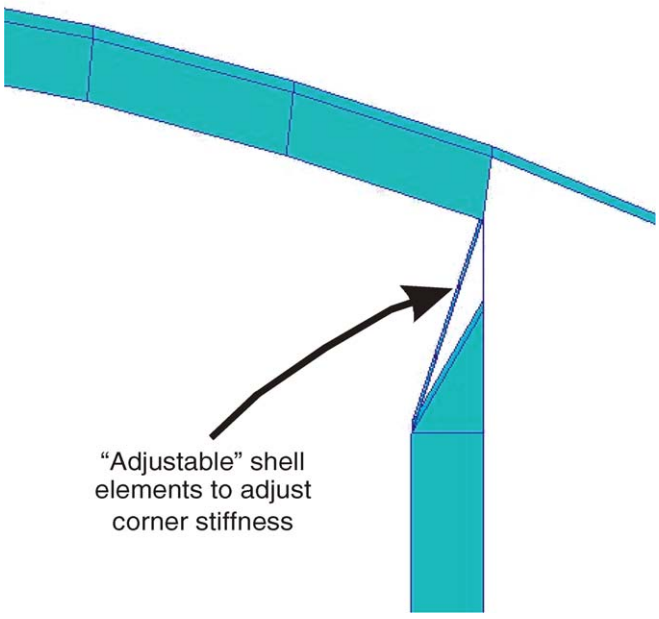

Fig. 14b. Box corner used for calibration.

8.1. 0–13 m sub-model

Capturing the correct deformation pattern required a more detailed sub-model of the 0–13 m section. The detailed sub-model includes solid elements in the webs and spar caps, see Fig. 12b.

The main purpose of a global FE-model of the whole blade is to provide representative boundaries for the 0–13 m sub-model. Non-linear analysis is clearly necessary here due to the large deflections seen in the blade at higher loads. More interestingly, a combination of the anticlastic effect [3], which is a linear phenomenon, and the non-linear Brazier effect [4,5] seem to counteract one another at certain locations along the blade. At small loads the anticlastic

Fig. 14a. Section through a box corner.

effect can cause outward cap deflection which then changes to inward deflection at higher loads as the Brazier effect (ovalization) takes over. This observation is illustrated in Figs. 12a and 12b. Linear analysis would simply not capture deflections due to the Brazier effect (Fig. 13).

9. Calibration of corner stiffness in the FE-model

Working with large wind turbine blades, made of fibre composites, a large margin of production tolerances must be accepted. SSP-Technology A/S uses a relative high quality production method (pre-preg without autoclave). Imperfections, such as voids, are most pronounced in areas where pre-preg layers terminate such as the corner of a box girder (Figs. 14a and 14b).

In principle all variations could be identified by cutting the blade into small pieces, measure the local stiffness, and then make a detailed FE-model which includes all these variations. In practise this is prohibitively expensive and a simpler approach was applied. Box girder corners in the FE-model were only represented with a coarse mesh of layered shell elements, which of course do not give the true picture of the corner stiffness. However, the modulus of an "adjustable" element was tuned to obtain the best fit with the actual deflections measured in the full-scale test.

10. Comparison of experimental test and numerical modelling

Comparing experimentally measured cap deflections with FE predictions, the agreement is found to be acceptable following calibration of the corner stiffness, see Fig. 15a. The web deflections, however, are not satisfactory above 80% load, see Fig. 15b. It was not possible to obtain better results by further adjustment of the corner stiffness and other improvements must be considered in the future work. It appears that a geometrical softening mechanism

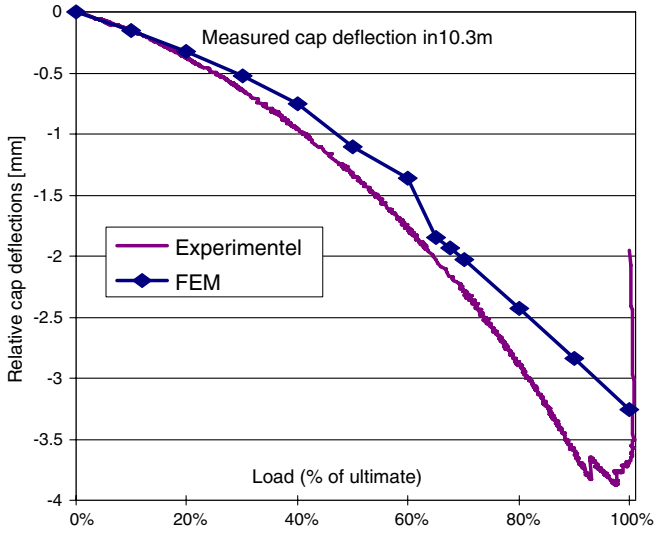

Fig. 15a. Comparison of cap deflections.

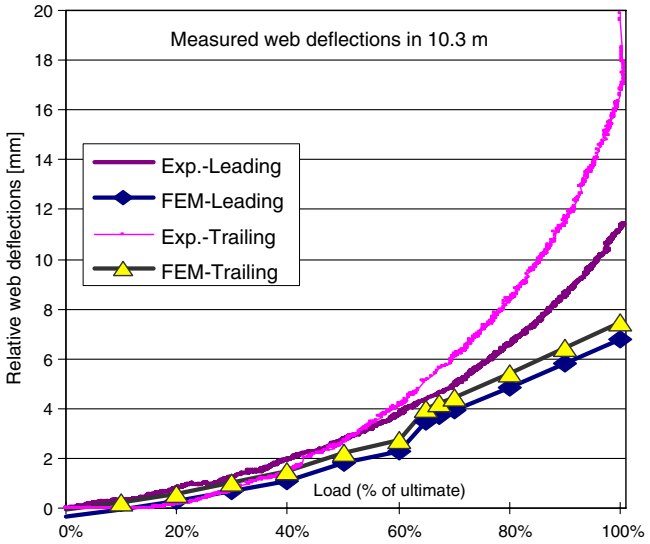

Fig. 15b. Comparison of web deflections.

or material non-linearity exists in the actual blade. This is not accounted for in the FE-model hence good correlation is seen at lower loads while the FE-model is over-stiff at higher loads approaching ultimate strength. Also, a kink is evident on the FE deflection curves at 60% load which is hardly noticeable on the curves obtained from the test. If certain features in the FE-model are too stiff it is conceivable that localized post buckling or snap-through has a more pronounced effect on the lateral deflections of the box girder. It should be mentioned that the overall flap-wise blade deflection shows exact agreement between test and FE-model. This is also the case for natural vibration modes, which are not included in this paper.

If the accuracy of the local FE-results are to be improved, manufacturing imperfections must be included in the FE-model. For the blade in question, the section at 10.3 m turned out to have a relatively large geometric imperfection in the load carrying cap which one would expect to influence local deformation behaviour.

11. Conclusion

Non-linear finite element analyses of a 34 m wind turbine blade with a load carrying box girder and loaded in flap-wise bending have revealed a variety of behaviour along the span. The Brazier effect dominates outwards of the 8 m section. This non-linear effect was also found to dominate at the 13 m section where the boundary conditions from the global FE-model were applied to a local FE-model. This ties in with the requirement for a non-linear global FE-model.

Simulation of local behaviour relied on calibration of the FE-model, mainly due to the variations in production. Especially corners in the box girder show large variations, hence the sub-model did not include fine details, but was calibrated against measured local deformations from the full-scale test.

Measurements supported by FE-results also show that debonding of the outer skin was the initial failure mechanism followed by delamination buckling which led to collapse. When the skin debond reaches a certain size the buckling strength of the load carrying laminate becomes critical and final collapse occurred.

12. Future work

The skin debonding failure, observed in the full-scale test, will be investigated further using computational methods. It is intended to use fracture mechanics based cohesive interface elements in a finite element model. These elements are capable of predicting both initiation and propagation of a delamination.

Extensive delamination was observed in the failed blade and this failure mode was due to interlaminar tensile stress caused by straightening of the curved caps. This deformation is a result of the crushing pressure from the Brazier effect. This failure mode will be studied in more detail also by the use of cohesive elements in a finite element model.

Finally, in this paper only the displacement measurements are presented but strain measurements were also recorded throughout the loading history and will be compared with the FE-results.

References

[1] Jørgensen ER, Borum KK, McGugan M, Thomsen CL, Jensen FM, Debel CP. Full scale testing of wind turbine blade to failure – flapwise loading. Risø-R-1392(EN) ISBN 87-550-3184-6; ISBN 87-550-3185-4 (Internet) ISSN 0105-2840.

[2] Jensen FM. Compression strength of a fibre composite main spar in a wind turbine blade. Risø-R-1391(EN) ISBN 87-550-3184-6; ISBN 87-550-3185-4 (Internet) ISSN 0105-2840.

[3] Swanson SR. Anticlastic effects and the transition from narrow to wide behaviour in orthotropic beams. Comp Struct 2001;53:449–55.

[4] Brazier LG. The flexure of thin cylindrical shells and other 'thin' sections, Late of the Royal Aircraft Establishment. Reports and Memoranda, No. 1081 (M.49), 1926, p. 1–30.

[5] Cecchini LS, Weaver PM. The Brazier effect in multi-bay aerofoil sections, University of Bristol, UK.

Appendix B - Patents

Appendix B1 - “WO 2008-071195 Reinforced aerodynamic profile”(cap reinforcement- patent A). Find M. Jensen

(12) INTERNATIONAL APPLICATION PUBLISHED UNDER THE PATENT COOPERATION TREATY (PCT)

(19) World Intellectual Property Organization
International Bureau

(43) International Publication Date
19 June 2008 (19.06.2008)

PCT

(10) International Publication Number
WO 2008/071195 A2

(51) International Patent Classification: Not classified

(21) International Application Number:
PCT/DK2007/000547

(22) International Filing Date:
14 December 2007 (14.12.2007)

(25) Filing Language: English

(26) Publication Language: English

(30) Priority Data:
PA2006 01651 15 December 2006 (15.12.2006) DK

(71) Applicant *(for all designated States except US)*: **TECHNICAL UNIVERSITY OF DENMARK** [DK/DK]; Anker Engelundsvej 1, DTU-bygning 101A, DK-2800 Kgs. Lyngby (DK).

(72) Inventor; and

(75) Inventor/Applicant *(for US only)*: **Find Mølholt** [DK/DK]; Emilsgave 8, DK-4130 Viby Sjælland (DK).

(74) Agent: **ALBIHNS A/S**; H. C. Andersens Boulevard 49, DK-1553 Copenhagen V (DK).

(81) Designated States *(unless otherwise indicated, for every kind of national protection available)*: AE, AG, AL, AM, AT, AU, AZ, BA, BB, BG, BH, BR, BW, BY, BZ, CA, CH, CN, CO, CR, CU, CZ, DE, DK, DM, DO, DZ, EC, EE, EG, ES, FI, GB, GD, GE, GH, GM, GT, HN, HR, HU, ID, IL, IN, IS, JP, KE, KG, KM, KN, KP, KR, KZ, LA, LC, LK, LR, LS, LT, LU, LY, MA, MD, ME, MG, MK, MN, MW, MX, MY, MZ, NA, NG, NI, NO, NZ, OM, PG, PH, PL, PT, RO, RS, RU, SC, SD, SE, SG, SK, SL, SM, SV, SY, TJ, TM, TN, TR, TT, TZ, UA, UG, US, UZ, VC, VN, ZA, ZM, ZW.

(84) Designated States *(unless otherwise indicated, for every kind of regional protection available)*: ARIPO (BW, GH, GM, KE, LS, MW, MZ, NA, SD, SL, SZ, TZ, UG, ZM, ZW), Eurasian (AM, AZ, BY, KG, KZ, MD, RU, TJ, TM), European (AT, BE, BG, CH, CY, CZ, DE, DK, EE, ES, FI, FR, GB, GR, HU, IE, IS, IT, LT, LU, LV, MC, MT, NL, PL, PT, RO, SE, SI, SK, TR), OAPI (BF, BJ, CF, CG, CI, CM, GA, GN, GQ, GW, ML, MR, NE, SN, TD, TG).

Published:
— *without international search report and to be republished upon receipt of that report*

(54) **Title:** REINFORCED AERODYNAMIC PROFILE

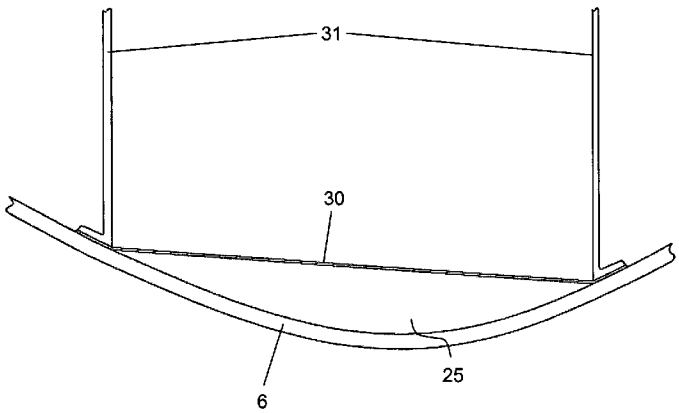

(57) **Abstract:** The present invention relates to the prevention of deformations in an aerodynamic profile caused by lack of resistance to the bending moment forces that are created when such a profile is loaded in operation. More specifically, the invention relates to a reinforcing element inside an aerodynamic profile and a method for the construction thereof. The profile is intended for, but not limited to, use as a wind turbine blade, an aerofoil device or as a wing profile used in the aeronautical industry.

WO 2008/071195 A2

REINFORCED AERODYNAMIC PROFILE

The present invention relates to the prevention of deformations in an aerodynamic profile caused by lack of resistance to the bending moment forces that are created when such a profile is loaded in operation. More specifically, the invention relates to a reinforcing element inside an aerodynamic profile and a method for the construction thereof. The profile is intended for, but not limited to, use as a wind turbine blade, an aerofoil device or as a wing profile used in the aeronautical industry.

The invention described in this application takes as its starting point blades or wings for wind turbines, but it should be understood that the invention is not in any way intended as being limited to aerodynamic profiles for this particular purpose, as the invention may be equally relevant to any other type of aerodynamic profile or use thereof.

A wind turbine blade normally consists of an aerodynamic shell and an internal girder such as a beam or a spar, the girder can be a single beam, but often two girders are used, and along with the shell the girders can be said to form a box profile. The top and bottom of the box profile are often referred to as the caps. The caps typically follow the aerodynamic shape (or curvature) of the profile, and therefore themselves have a transverse curvature. The aerodynamic shell is typically a laminate of fibreglass and/or other materials.

The section(s) of the aerodynamic shell where the internal girders are placed is/are usually reinforced in some way and is/are consequently often quite thick. The other part(s) or section(s) of the aerodynamic shell is typically only a thin skin or a laminate such as a sandwich construction with thin skins and a core material. A blade is typically provided by gluing or bonding or otherwise connecting parts to each other.

In operation, the blade is primarily loaded in the flapwise direction by aerodynamic and inertia forces. By flapwise direction is meant a direction substantially perpendicular to a transverse axis through a cross-section of the broad side of the blade. Alternatively, the flapwise direction may be construed as the direction (or the opposite direction) in which the aerodynamic lift acts on the profile. The flapwise direction is illustrated by way of example as indicated by arrow A in Fig. 1a. The forces induce a bending moment on the blade and this in turn causes an ovalization, or flattening, (Figs. 1a and 1b) of the box profile and can also lead to buckling failure of the blade. When the blade is loaded in the flapwise direction, the material in one of the caps is loaded in compression. When this compression load is exceeding a certain limit, which is dependent on the thickness, the curvature, the materials and the orientation of the materials of the cap, the cap is pushed

out of its original shape, and a buckling pattern is forming. If the flapwise load, and thereby the compression load increases further, the blade may suddenly collapse.

In the currently available blades, the caps are typically heavily reinforced to provide the necessary moment of inertia to take up the load from the bending moment. Failure of a blade is determined by several individual factors. However, one very important factor is the resistance of the caps against buckling. If or when buckling occurs, the curvature of the profile's cross-section may e.g. transform as shown in Figs. 2a and 2b.

The ovalization caused by the crushing pressure from the bending moment causes a multiaxial stress condition in the typically laminated material of the shell and this increases the stresses in the cap, see Fig. 3. This may lead to the formation of interlaminar cracks (delamination and skin debonding) – for further explanation reference is made to the article "Structural testing and numerical simulation of a 34 m composite wind turbine blade" by F. M. Jensen et.al. published by Elsevier in Composite Structures 76 (2006) 52-61) in the material and consequently weaken the construction a little more each time it is loaded. The interlaminar cracks will also decrease the buckling resistance of the caps consequently building an increased risk of buckling failure of the blade.

If the transformation of the curvature of the profile's cross-section is prevented and the multiaxial stress condition of the laminated material is reduced or eliminated, the buckling resistance of the caps and thereby the ultimate strength of the entire profile, is increased significantly.

It is therefore an object of the present invention to provide an aerodynamic profile with improved resistance against buckling failure of the profile.

It is also an object of the present invention to provide an aerodynamic profile with improved resistance against formation of interlaminar cracks in the facing.

It is another object of the present invention to provide an aerodynamic profile with reduced weight.

It is yet another object of the present invention to provide an aerodynamic profile with improved overall strength and overall stiffness.

It is a further object of the present invention to provide a reinforced cap part for an aerodynamic profile.

It is yet another object of the present invention to provide an aerodynamic profile that can be produced at a reduced manufacturing cost compared to the existing solutions.

It is a further object to provide an aerodynamic profile capable of working under severe aerodynamic loads and to optimise the aerodynamic performance, e.g. energy output of the profile.

It is yet another object to provide a method for constructing a reinforced aerodynamic profile.

It is still another object to provide a method for constructing a reinforced cap part for an aerodynamic profile.

It is further an object of the present invention to provide alternatives to the prior art.

In particular, it may be seen as an object of the present invention to provide an aerodynamic profile that solves the above mentioned problems of the prior art by providing the aerodynamic profile with a reinforcing element e.g. such as described by way of the examples of the following disclosure.

According to a first aspect of the invention, the above-mentioned and other objects are fulfilled by provision of an aerodynamic profile comprising a facing having an outer surface with a substantially transverse curvature, and at least one straight reinforcing element for increasing the strength of the facing against flapwise forces by inhibiting an increase of the mutual distance in the edgewise direction between two points of the facing where the at least one internal reinforcing element is attached to the facing, the at least one reinforcing element having a thickness that is less than twice the maximum thickness of the facing.

The aerodynamic profile may for example constitute a wind turbine blade in a vertical axis wind turbine, such as a Darrieus wind turbine, a wind star turbine, etc., or a wind turbine blade in a horizontal axis wind turbine, such as common modern wind turbines usually three-bladed, sometimes two-bladed or even one-bladed (and counterbalanced), etc. The aerodynamic profile may also constitute an aerofoil device or a wing profile used in the aeronautical industry, such as a helicopter wing, an airplane wing, etc.

The aerodynamic profile may be applicable not only to wind, but also to a variety of water flows, including free-flow (rivers, creeks), tidal flow, oceanic currents, wave motion, ocean wave surface currents, etc.

The facing or shell of the aerodynamic profile may preferably, but not exclusively, comprise a composite or laminated material. The material may preferably, but not exclusively, comprise fibreglass and/or carbon fibres and/or other durable and flexible materials typically with a high strength/weight ratio. This may further comprise at least in part light weight metals or alloys. The facing may typically be a laminate or sandwich-construction.

The at least one internal reinforcing element is connected with at least two connections to an inner surface of the aerodynamic profile with a substantially transverse curvature between the two connections. Preferably, in the context of this application a reinforcing element is distinct from a traditional girder being a structural load-carrying element. A force in the flapwise direction applied to the facing between the two connections and urging the facing towards the inner volume of the facing also urges the two connections away from each other. However, the reinforcing element keeps the two connections in substantially mutually fixed positions and thus prevents the distance between the connections from increasing thereby strengthening the facing against forces in the flapwise direction. Thus, the reinforcing element desirably has a high tensional strength while the reinforcing element need not be capable of resisting compression forces. Preferably, the reinforcing element has a straight shape, such as the shape of a rod or a stretched wire or a planar member. If the shape of the reinforcing element is not straight, the shape of the reinforcing element could be straightened when subjected to stretching forces leading to movement of its end points and obviously, this is not desired.

Since the reinforcing element is required to have a high tensional strength only, i.e. the reinforcing element need not carry other loads; the reinforcing element is preferably thin so that its weight and cost are kept at a minimum. The thickness of the reinforcing element is preferably less than twice the maximum thickness of the facing, more preferred less than 1.5 times the maximum thickness of the facing, even more preferred less than the maximum thickness of the facing, still more preferred less than 0.75 times the maximum thickness of the facing, most preferred less than 0.5 times the maximum thickness of the facing.

The connections on the inner surface of the profile may in principle be positioned anywhere on the inner surface but it should be observed that the chosen positioning causes the reinforcing element to be able to provide a reasonable and useful reinforcing effect in the profile. The connection of a reinforcing element to connecting points on the inner surface of the profile prevents the negative effects of buckling and ovalization as described above. The connections may comprise any suitable kind of joint such as welded, glued, melted, fused or other simple mechanical connections. The reinforcing element itself may comprise

the connections or it may comprise additional connections or connection parts adapted to engage or cooperate with the connections on the inner surface of the profile. The additional connections or connection parts must be sufficiently rigid to maintain their shape when subjected to tension in order to properly cooperate with the reinforcing element to prevent the connections on the facings from being displaced away from each other. In embodiments, the reinforcing element is connected to an inner surface of the facing of the profile. Preferably, the inner surface of the facing is shaped in a manner corresponding to the outer surface thereof, i.e. having a substantially transverse curvature. The reinforcing element may therefore preferably be so positioned on the inner surface of the facing that there will be a certain space (or distance) between the reinforcing element and the inner surface of the profile.

The reinforcing element secures and keeps the transverse curvature of the profile substantially unchanged when the aerodynamic profile is loaded by forces in the flapwise direction. This in turn causes the overall strength of the aerodynamic profile to increase significantly since the resistance against buckling is increased. With the reinforcing element according to the invention, the dimensions of the material(s) used for the profile's facing may further be drastically reduced compared to currently available solutions and thus facilitates lower dynamic loads on the other parts of the system, improved handling and transportation characteristics of the profile and of course also a reduction of material costs.

In an embodiment of the invention the aerodynamic profile further comprise(s) shoring means in longitudinal direction along at least a part of the aerodynamic profile. The shoring means is/are provided to strengthen and/or reinforce the profile in its longitudinal direction.

In an embodiment of the invention the shoring means is/are embedded in or form(s) part of the facing of the profile. Embedded shoring means may preferably, but not exclusively, comprise one or more layers or tapes of a suitable fibre material. In an embodiment one or more fibre tapes will be placed between the layers of the above described laminate type construction.

For example, at least one girder may be provided to primarily strengthen and reinforce the aerodynamic profile in its longitudinal direction and may also be referred to as a web. In this application, the girder or web should be construed as any kind of elongate constructional element capable of taking up loads, such as a beam or a spar e.g. shaped as an I-profile or an U-profile preferably made from fibre reinforced plastics or other suitable material. The web may substantially extend through the length of the blade.

However, it may also be preferred to provide the aerodynamic profile with two or more separated webs in the longitudinal direction of the aerodynamic profile, especially for facilitating handling or transporting purposes. In principle, any number of webs may be applied, however for the sake of simplicity and for keeping the overall weight of the blade as low as possible a number of one or two webs is preferred.

In this manner, an aerodynamic profile according to the invention may be produced by prefabrication of a minimum number of individual elements and then subsequently assembled to form the total aerodynamic profile. Other variations of applying shoring means in the facing of the profile may be used such as embedded metal- or fibre-wires or textiles.

Other embodiments of the invention may comprise shoring means in substantially transverse, diagonal or any other suitable directions, or combinations thereof, of the aerodynamic profile.

In an embodiment of the invention the shoring means comprise at least one internal girder connected to at least a part of the inner surface of the facing of the aerodynamic profile.

In embodiments of the invention, the connection(s) between the internal girder and the inner surface of the facing may be placed at any suitable position on the parts. Preferably, but not exclusively, the connections may be adapted in one or more points, along one or more lines or in any kind of spatial configuration. Furthermore, the connections may comprise any suitable kind of mechanical joint such as a welded, glued, melted, fused or other simple mechanical connection.

In another embodiment according to the present invention the at least one internal girder comprises a box girder or a box beam. The box girder or box beam may be adapted to accommodate different kinds of equipment on the inner sides thereof. Examples of equipment are measuring instrumentation, control mechanisms and/or systems and servo motors for powering mechanisms on or within the aerodynamic profile. The sides of the box girder may vary in thickness in its longitudinal and/or transverse direction(s) and the shape and/or the perimeter length of the cross-section of the girder may also vary along its longitudinal extent.

Obviously, the different kinds of equipment mentioned above may also be associated with any of the other embodiments of the present invention.

In an embodiment the box girder or box beam is of a substantially polygonal cross-section. The cross-section of the box girder or box beam may have any polygonal shape such as substantially rectangular, triangular, circular, oval, elliptical etc. but is preferably rectangular or substantially square.

In other embodiments the at least one reinforcing element is connected to the inner surface of the facing and/or to the shoring means with at least two connections. The reinforcing element may preferably be connected with connections positioned on those parts of the inner surface of the aerodynamic profile that form the caps. The connection of a reinforcing element to connections on the caps, i.e. two connecting points on the inner surface of the profile, prevents the negative effects of buckling and ovalization of the caps. The connections may comprise any suitable kind of joint such as welded, glued, melted, fused or other simple mechanical connections. The reinforcing element itself may comprise the connections or it may comprise additional connections or connection parts adapted to engage or cooperate with the connections on the caps. Apart from being connected to the inner surface of the facing the reinforcing element may also be connected to the shoring means.

In embodiments in which the shoring means comprise two or more internal girders or a box girder the reinforcing element may be connected solely to the shoring means.

In particular embodiments of the invention at least one of the at least two connections between the reinforcing element and the inner surface of the facing and/or the shoring means is continuous along at least one or more parts of said facing and/or said shoring means.

In an embodiment of the invention the at least one reinforcing element is a bar or a rod-like element. The element may be solid or hollow or any suitable combination thereof. Alternatively, the element may comprise wire, rope, cord, thread or fibres. They may be applied individually or may be applied as a number of individual elements together forming a "thicker" element. Particularly, the element may comprise fibres of very high stiffness and strength such as, but not limited to, aramid fibres.

In yet another embodiment of the invention the at least one reinforcing element is a plate. The plate element may be solid or hollow or any suitable combination thereof. The plate material may comprise any of metal, metal alloy, wood, plywood, veneer, glass fibre, carbon fibre and other suitable materials such as e.g. one or more composite materials. The element may further be provided as netting or a web comprising one or more of wire, rope, cord, thread or fibres. The plate element may alternatively comprise a textile or a

fabric material. The fabric material may be manufactured from materials such as, but not limited to carbon fibres or aramid fibres thus providing a high strength and a low weight. If suitable, glass fibres may also be used.

The mentioned materials may also be combined to any construction. Thus, in another embodiment the at least one reinforcing element is a laminate or a sandwich construction.

In another embodiment of the invention the plate or laminate comprises one or more cut-outs. The cut-outs may be made in any suitable kind of pattern. The cut-outs may be provided in order to provide a plate or laminate with a thickness that is strong enough to withstand handling during construction without having to protect the profile too much. Furthermore, the cut-outs may provide passage for any additional wiring or other equipment there through and also reduce the overall weight.

In yet another embodiment the reinforcing element and the shoring means are fixedly interconnected. The interconnection may comprise any suitable kind of joint such as welded, glued, melted or fused connections as previously described.

In a further embodiment the reinforcing element and the shoring means are releasable interconnected. The releasable interconnection may comprise any suitable kind of joint such as a snap-fit, press-fit, groove-and-tongue connection or other simple mechanical connection. A releasable interconnection may be used to provide an aerodynamic profile with an increased degree of flexibility.

In a particular embodiment the reinforcing element is connected to the inner surface of the aerodynamic profile in at least two connections points so that at least one space is defined between the reinforcing element and the inner surface. The two connection points may be on a cap part of the profile that may preferably have an outer surface corresponding to the surface of the facing of the aerodynamic profile. The outer surface of the cap part may be substantially flat/even or have a substantially transverse curvature.

In further embodiments the at least one space between the reinforcing element and the inner surface of the profile is at least partly filled with a filler material. The filler material may comprise one or more substances. The substances may have different physical, chemical or mechanical properties and may be mixed so as to provide one or more specific characteristics such as insulating power, stiffness, low weight, high or low conductivity etc. Preferably, however, the filler material may be a foamed material characterised by e.g. low weight and convenient working properties for forming a suitable surface that is easily further processed e.g. by further laminating with fibres or fibre tapes. Particularly, the

foamed material may comprise a PVC or PVC-based material particularly capable of absorbing pressure forces. Particularly, the foamed material may be provided as a prefabricated and/or pre-shaped element with a first (outer) surface substantially corresponding to the curvature of profile along the inner surface thereof, and a second (inner) surface being substantially plane or flat. The second surface of the pre-shaped foamed element may then form an even and aligned basis for the reinforcing element, particularly, but not exclusively, if the reinforcing element is a plate or laminate. The provision of a pre-shaped foamed element can be especially advantageous since the foamed element then may act as a mould or form for the positioning and/or connection of the reinforcing element and/or for the overall construction of the relevant part. This means that the need for a custom-made mould, e.g. of glass fibre for constructing the relevant part can be eliminated, thus reducing manufacturing costs of the relevant part.

The filler material may also or instead comprise a fluid or gaseous material being e.g. injected, sprayed or blow moulded into the space. The fluid or gaseous material may be of a kind that hardens when e.g. exposed to air. In embodiments comprising a fluid or gaseous filler material relevant means may be provided in connection with e.g. the reinforcing element for retaining such material.

In yet another embodiment the cap part may preferably be a separate cap part. The separate cap part may be manufactured in an individual manufacturing process and then provided for connection to the other part(s) of the profile when these are ready for assembly. The outer surface of the separate cap part is substantially aligned with the facing such that the outer surface of the profile has a smooth and substantially unbroken surface when they are connected.

The separate cap part may be a single piece corresponding to substantially the whole length of the profile or it may comprise smaller/shorter sections facilitating easier handling and assembling.

The providing of a reinforcing element according to the invention may preferably be integrated in the manufacturing process of the profile. However, a subsequent fitting may also be possible if the assembling conditions allow so.

Particularly, if the reinforcing element is provided on a separate cap part, a subsequent fitting of the cap part comprising the reinforcing element with the facing and/or the shoring means in a separate assembling procedure, is applicable. This may not only save production time, but also allow for an improved control of the material characteristics of the separate cap and provide the possibility of pre-stressing the reinforcing element to a

desired level. Furthermore, the aerodynamic profile may be manufactured in sections and assembled on site if suitable. It will also be possible to renew or replace cap parts on existing aerodynamic profiles.

In yet another embodiment the reinforcing element(s) or the materials of the reinforcing element is/are arranged in such manner that during flapwise loading of the profile, the reinforcing element is implementing shear forces in the surface of the profile. The shear forces will twist the aerodynamic profile, and thereby couple bending and torsion of the profile. This effect may preferably, but not exclusively, be achieved by arranging the reinforcing elements at an angle of less than 90° in relation to the longitudinal axis of the profile. If a plate of fibre reinforced materials or a textile is used the fibre directions must be less than 90°, but more than 0° in relation to the longitudinal axis of the profile.

The coupling of the bending and the torsion can be used to change the angle of attack of the profile during wind gust or similar extreme aerodynamic conditions. The unloading of the profile will decrease the maximal stresses in the profile and thereby decrease the weight.

The coupling of the bending and the torsion may also optimize the power output from the profile.

In further embodiments the reinforcing element(s) is/are equipped with or consist(s) of electrical installations, such as piezoelectric installations, that may be activated by means of voltage, current, electric or magnetic field, whereby the length of the reinforcing element changes and/or stresses are imposed on the element. By this it is possible to change the curvature of the profile's surface and thereby change the aerodynamic properties of the profile. With these installations it is possible to optimize the performance of the aerodynamic profile.

With respect to each one of the above mentioned embodiments of the invention the aerodynamic profile may further comprise means for associating the profile with a relevant structure. If the aerodynamic profile is a wind turbine blade such means may e.g. be fittings or connections for connecting the blade to the hub or the main axle of the turbine.

The aerodynamic profile according to the invention may further comprise other internal or external equipment suitable for use in the relevant structure they become a part of.

The aerodynamic profile according to the invention may also advantageously be part of a load-bearing construction such as a tower for carrying a wind turbine.

In another aspect of the present invention, it may be seen as an object to provide a method for facilitating easy assembling/construction of an aerodynamic profile comprising a reinforcing element. Particularly, it may be seen as an object to provide an assembling of reduced complexity of an aerodynamic profile with one or more reinforcing elements on an inner surface thereof.

According to a second aspect of the invention, the above-mentioned and other objects are fulfilled by provision of a method for manufacturing a reinforced aerodynamic profile comprising the steps of

- providing at least a part of a facing of the profile, and
- providing shoring means in connection with said facing, and
- providing at least one reinforcing element connected in at least two connection points to an inner surface of the profile, and optionally
- providing a filler material in a space between said reinforcing element and said inner surface of the profile.

According to the second aspect of the invention at least a part of a facing of an aerodynamic profile is constructed and connected to shoring means. The construction may preferably comprise building up layers of one or more types of fibre materials fibre material. The type of shoring means and connection(s) between such means and the facing may be one or more of those described in connection with the first aspect of the invention. The same applies for the provided at least one reinforcing element and its connections to the inner surface of the profile. The reinforcing element may be connected in at least two connection points on one side of the inner surface of the profile, e.g. two points on one side of an inner surface of at least a part of a facing of the profile. The facing part may especially be the cap part of the profile.

Particularly, but not exclusively, the reinforcing element may connect two points on the inner surface of a cap part of the profile. The inner surface of the cap part may preferably have a curvature following the transverse curvature of the outer surface of the facing. By connecting the reinforcing element to two connection points on a curved cap part, a space (or distance) is created between the parts. According to the second aspect of the invention this space may advantageously be at least partly filled with a filler material. The filler material may preferably be a substantially solid material such as a foamed material. Such foamed material may preferably be shaped beforehand to fit in the space between the reinforcing element and the cap part as described in connection with the first aspect of the invention. It may then provide a solid basis for the at least one reinforcing element and also provide an improved stiffness of the whole cap part. The reinforcing element may also

be so positioned as to connect at least one point on the inner surface of the profile *not* being on the cap part. In such embodiments the filler material may be provided as described between the reinforcing element and the inner surface, at least for improving the strength and/or stiffness of the relevant part of the profile. The filler material may be provided in the space before the connection of the at least one reinforcing element or vice versa.

Below the invention will be described in more detail with reference to the exemplary embodiments illustrated in the drawings, wherein

Fig. 1a is a schematic view of a cross-section of an aerodynamic profile indicating the crushing pressure on the profile from the bending moment acting on the profile in operation.

Fig. 1b is a schematic view of part of the cross-section of an aerodynamic profile forming the box profile and indicating the potential deformation (ovalization) caused by the crushing pressure (deformed state shown as dotted lines).

Fig. 2a is a schematic perspective view of the box profile indicating three sectional cuts illustrated in Fig. 2b and further indicating a buckling line in the longitudinal direction of the box profile (dashed line).

Fig. 2b is a schematic cross-sectional view of the box profile showing three different cross-sections of the profile in different positions corresponding to the three sectional cuts in Fig. 2a.

Fig. 3 is a schematic view of part of a cross-section of a cap part of the profile showing in principle the multiaxial stress condition and examples of crack formation in the cap part as a result of the deformation.

Fig. 4 is an enlarged schematic sectional view of an example of a facing according to the invention.

Fig. 5a is a schematic perspective view of the aerodynamic profile indicating shoring means as an embedded part of the facing and further indicating a sectional cut E shown in detail in Fig. 5b.

Fig. 5b is a schematic cross-sectional view corresponding to sectional cut E of Fig. 5a.

Fig. 5c is a schematic perspective view of the aerodynamic profile indicating shoring means as internal girders in the form of a box profile and further indicating a sectional cut F shown in detail in Fig. 5d.

Fig. 5d is a schematic cross-sectional view corresponding to sectional cut F of Fig. 5c.

Fig. 6a is a schematic partial cross-section showing a reinforcing element connected to shoring means in the form of two internal girders.

Fig. 6b is a schematic partial cross-section showing a reinforcing element connected to or integrated with shoring means in the form of a single internal girder and to an inner surface of the profile.

Figs. 7a-7d are schematic partial cross-sections showing different types of reinforcing elements connected to one or more shoring means and/or to the inner surface of the profile.

Fig. 7e is a schematic top view of a reinforcing element in the form of a plate or a laminate provided with cut-outs distributed in a pattern.

Fig. 7f is a schematic perspective view of a reinforcing element in the form of a plate or laminate positioned in the longitudinal direction of the aerodynamic profile.

Fig. 8 is a schematic partial cross-sectional view of the box profile wherein the reinforcing element in the form a plate or laminate is integrated in the manufacturing of the aerodynamic profile.

Fig. 9 is a perspective view of a prefabricated reinforced separate cap part.

Fig. 10 is a perspective view of the separate cap part of fig. 9 assembled with facing and shoring means of the aerodynamic profile.

Fig. 11 shows a plot of test results from a comparison between the strength of an aerodynamic profile according to the present invention (A) and a prior art aerodynamic profile (B).

The figures are schematic and simplified for clarity, and they merely show details which are essential to the understanding of the invention, while other details have been left out. Throughout, the same reference numerals are used for identical or corresponding parts.

The present invention will now be described more fully hereinafter with reference to the accompanying drawings, in which exemplary embodiments of the invention are shown. The invention may, however, be embodied in different forms and should not be construed as limited to the embodiments set forth herein. Rather, these embodiments are provided so that this disclosure will be thorough and complete, and will fully convey the scope of the invention to those skilled in the art. Like reference numerals refer to like elements throughout.

Fig. 1a shows a principle cross-section of an aerodynamic profile 1 having a facing 2 with a leading edge 3 and a trailing edge 4. Also indicated are the box profile 5 and the cap parts 6 thereof. The cap parts 6 are indicated as the upper and lower sides of the box profile 5. As previously described, the profile is primarily loaded in the flapwise direction by aerodynamic and inertia forces. The flapwise direction is illustrated by arrow A in Fig. 1a. The forces induce a bending moment on the profile and create a crushing pressure indicated by arrows B. The crushing pressure is also referred to as the Brazier effect (reference is made to the article "Structural testing and numerical simulation of a 34 m composite wind turbine blade" by F. M. Jensen et.al. published by Elsevier in Composite Structures 76 (2006) 52-61).

Fig. 1b shows an enlarged sectional cross-section of the box profile 5 indicating an example of the deformation of the box profile 5 with character of an ovalization caused by the bending moment on the profile. In the figure a neutral position of the box profile 5 is indicated with full drawn line as reference 5a and a loaded or ovalized (flattened out) position is indicated by dotted line 5b. Further indicated are directions that the box profile 5 may move toward when it is loaded, referenced by arrows C.

Fig. 2a shows a schematic perspective view of at least a part of the box profile 5 with the indication of three sections, referenced as 5c, 5d and 5e and further described in Fig. 2b. Also illustrated by dotted, sine-like line L is an indication of a buckling pattern of the profile. Buckling causes the shape of the cross-section of the profile to vary (or "transform") along the profile's longitudinal direction. The possible nature of such variation of cross-sections of the profile is shown by way of examples in Fig. 2b.

Fig. 2b thus shows a schematic view of the three different positioned cross-sections 5c, 5d and 5e of the profile 5. 5d and 5e indicate cross-sections in a loaded or ovalized state at different positions along the profile 5. 5c indicates the cross-section in a neutral position at another position along the profile. The figure is intended to support the understanding of how the forces on the profile cause its cross-section to vary, thus adding to a fatiguing process of the profile.

Fig. 3 shows in part a schematic cross-section of the box profile, particularly focussed on a cap part 6. The figure indicates by way of arrows D the multiaxial stress condition that arises in the laminate surface, i.e. the facing 2, of the profile 1 as a result of the deformation (the ovalization) caused by the bending moment on the profile. Also indicated are examples of interlaminar cracks 7 in the facing 2 that are potentially created due to the multiaxial stress condition in the laminate. The layers of the laminate may debond, i.e. simply be torn apart as a result of the stress condition.

Fig. 4 shows a schematic, enlarged cross-sectional view of an example of how a facing for an aerodynamic profile may be a laminate comprising many layers of one or more specific fibre materials. In Fig. 4 layers of fibre glass are indicated by reference 8 and a layer of another material such as carbon fibres is indicated 9. Further indicated are layers 10 of a bonding material such as glue.

Fig. 5a is a schematic total perspective view of an aerodynamic profile 1 indicating the longitudinal positioning of the shoring means (by dashed line 11); here in the form of a single internal girder 21. Also indicated is sectional cut E, described in more detail for figure 5b.

Fig. 5b is an enlarged view of the sectional cut E of Fig. 5a showing the shoring means 11 in the form of a single internal girder 21. It can also be seen how the internal girder spans the opposite sides of the facing 2 of the profile.

Fig. 5c is a schematic total perspective view of an aerodynamic profile 1 indicating the longitudinal positioning of the shoring means (by dashed line 11); here in the form of a box profile 12 comprising two internal girders 21. Also indicated is sectional cut F, described in more detail for figure 5d.

Fig. 5d is an enlarged view of the sectional cut F of Fig. 5c showing the shoring means 11 in the form of two internal girders 21. It can also be seen how the two internal girders span the opposite sides of the facing 2 of the profile thereby building the box profile 12. The "top and bottom" sides of the box profile 12 build the caps or cap parts 6.

Fig. 6a shows a schematic partial view of an example of a box profile 5 of an aerodynamic profile. In addition, the figure shows a part of the profile's facing 2 with an outer surface having a substantially transverse curvature, substantially corresponding to a cap part 6. The box profile 5 in the illustrated example comprises shoring means in the form of two internal girders 21. Also indicated is a reinforcing element 20 in the form of a rod

connected to each of the two girders 21 in two connection points 22. The girders 21 are each connected to an inner surface 24 of the profile with connections 23. A space or distance 25 between the reinforcing element 20 and the inner surface 24 of the profile is also indicated.

A force in the upward flapwise direction in Fig. 6a applied to the facing between the two connections 23 will urge the facing towards the inner volume 25 of the facing and also urge the two connections 23 away from each other. However, the reinforcing element 20 keeps the two connections 23 in substantially mutually fixed positions and thus prevents the distance between the connections 23 from increasing thereby strengthening the facing against forces in the flapwise direction. The rod 20 is straight and has a high tensional strength.

Since the reinforcing element is required to have a high tensional strength only, i.e. the reinforcing element need not carry other loads; the reinforcing element is preferably thin so that its weight and cost are kept at a minimum. The thickness of the reinforcing element of the illustrated embodiment is approximately equal to the maximum thickness of cap part.

Since, the reinforcing element need not be capable of resisting compression forces, the rod 20 may be substituted by a wire.

Fig. 6b like Fig. 6a shows a schematic partial view of an example of a part of the profile's facing 2 with an outer surface having a substantially transverse curvature, substantially corresponding to a cap part 6. In this example the profile comprises shoring means in the form of a single internal girder 21. The girder 21 is connected to an inner surface 24 of the cap part 6 by connection 26. A reinforcing element 20 shown in the form of a plate or laminate is integrated with, or bonded to (not shown), the girder. The girder is further shown bonded in two connections 27 to an inner surface 24 of the profile. A space or distance 25 between the reinforcing element 20 and the inner surface 24 of the profile is also indicated. The space 25 may actually be two separate spaces split by girder 21 as indicated.

Figs. 7a-7d also show schematic partial views of examples of the shoring means at the cap part 6 of the profile's facing 2. The figures show how one or more reinforcing elements 20 can be connected to an inner surface 24 of the cap part 6 and/or to the shoring means in the form of one or more internal girders 21. In Fig. 7a the profile comprises shoring means in the form of a single internal girder 21. The girder 21 is connected to an inner surface 24 of the cap part 6 by connection 26. A reinforcing element 20 shown in the form of a rod is

connected in two connection points 27 to an inner surface 24 of the cap part 6. A space or distance 25 between the reinforcing element 20 and the inner surface 24 of the profile is also indicated. In the figure the reinforcing element 20 is not connected to the internal girder 21, however the internal girder is provided with a passage or hole (not shown) that the reinforcing element 20 extends through. In Fig. 7b is shown a single reinforcing element in the form of a textile 30 connected in two connection points on the inner surface of the cap part 6. Shoring means in the form of one or two substantially U-shaped internal girders 31 may be bonded on top of the textile (U-shaped girders 31 are only shown in part). In Fig. 7c a reinforcing element in the form of a plate 32 is laminated to the body of each of two internal girders 21 constituting the shoring means. In Fig. 7d is shown a reinforcing element in the shape of a plate 33 comprising one or more feet 34 having a surface of a certain extension for assisting in the bonding of the plate 33 to each of the two internal girders 21.

Fig. 7e is a schematic top view e.g. of the plate 33 of Fig. 7d further comprising cut-outs 35 in the plate 33 distributed in a pattern. Any kind of pattern may of course be applied to any of the reinforcing elements in the form of the described plates or laminates. The figure also indicates an outline of the two internal girders 21 of Fig. 7d.

Fig. 7f shows in perspective at least a part of an aerodynamic profile 1 comprising a reinforcing element 20 in the shape of a plate or laminate extending substantially through the length of the profile 1. The element 20 is connected with continuous connections 36 to the shoring means in the shape of two internal girders 21. As previously described the element 20 may be connected to the girders 21 at any suitable position by connections 36.

Fig. 8 shows a similar sectional cut of a profile 1 as shown in figure 7f. However, in fig. 8 the reinforcing element 20 in the shape of a plate or laminate or textile is provided as an integrated part of the inner surface 24 of the profile. A space 25 is provided between the reinforcing element and the inner surface. Two substantially U-shaped internal girders 21 are shown bonded to the surface of the reinforcing element that faces the centre of the profile 1 and/or at least also partly to the inner surface 24. The figure is partly intended to illustrate that a reinforcing element may be provided during the manufacturing of the profile's facing and may accordingly become an integrated part thereof when the facing 2 is manufactured, typically by laying down layer upon layer of fibre material in a suitable mould. Fig. 8 further indicates that the caps or cap parts 6 of the profile may constitute a thicker part of the facing 2 than the other parts. In this embodiment it will be particularly advantageous to provide a pre-shaped foamed material in the space between the reinforcing element and the inner surface of the cap part since the foamed material may then form an excellent plan/even basis for the positioning of the reinforcing element.

Fig. 9 is a perspective schematic view of a separate reinforced cap part 40 that is pre-shaped before its assembly with the facing and/or the shoring means of the profile 1. The separate cap part 40 may substantially correspond to the construction of the integrated cap part of Fig. 8. It differs from the integrated cap part of Fig. 8 in that it is an individual element that can be assembled with the facing 2 and the shoring means in a procedure apart from the structural build-up of the profile 1, such as described with respect to Fig. 8. The reinforcing element 20 is e.g. a plate, the "open" or "profile centre facing" surface of which is shown as being substantially flat or plan.

Fig. 10 is a perspective view of a profile 1 assembled with a separate cap part 40 corresponding to the cap part 40 of Fig. 9. As it may be understood from Figs. 9 and 10 the entire separate cap part 40 (or a minor part thereof) can be renewed or replaced in case of failure of the existing cap part. The existing cap part may be removed by a suitable cutting procedure and a new separate cap part 40 may then be bonded or otherwise connected to the existing profile 1. The outer surface 41 of the cap part itself may then form the surface of the profile in that particular region (not shown) or an entire, or at least a part of such, new facing 2 may be provided in order to cover the region having received a replaced cap part.

Although the present invention has been described in connection with the specified embodiments, it should not be construed as being in any way limited to the presented examples. The scope of the present invention is set out by the accompanying claim set. In the context of the claims, the terms "comprising" or "comprises" do not exclude other possible elements or steps. Also, the mentioning of references such as "a" or "an" etc. should not be construed as excluding a plurality. The use of reference signs in the claims with respect to elements indicated in the figures shall also not be construed as limiting the scope of the invention. Furthermore, individual features mentioned in different claims, may possibly be advantageously combined, and the mentioning of these features in different claims does not exclude that a combination of features is not possible and advantageous.

As a part of a research project, the inventor has measured the effect of the invention on a full-scale test-object. The test are documented in the report "Full-scale Test of a SSP34m box girder 2 – Data Report" Find M. Jensen, Kim Branner, Per H. Nielsen, Peter Berring, Troels S. Antvorskov, Joan H. Reffs, Peter H. Jensen, Malcolm McGugan, Risø-R-1622(EN) (in progress) and in the PhD-Thesis "Ultimate strength of a large wind turbine blade" Find M. Jensen, Risø National Laboratory -Technical University of Denmark (in progress).

A load carrying box girder (spar) of a 34 m wind turbine blade designed for use on a 1.5 MW wind turbine was tested. The box girder was loaded in the flapwise direction with loads that were close to the ultimate loads of the blade. The box girder was equipped with 3 different and independent measuring systems - strain gauges, position transducers and optical stereoscopic cameras - and the test was performed in a well established test facility for wind turbine blades. The test was initially performed with the box girder in its original design. After the initial test, the test-object was the modified by addition of reinforcing elements in accordance with the present invention in the form of wires fastened to each side of the cap. After the modification of the box girder, the test was repeated using the same loads and measuring systems. The results from the tests were compared and the result is shown in Fig. 11. The graphs show the deformation of the centre of the cap, and are plotted as a function of the length of the blade.

The test demonstrates that, depending on the distance from the end of the blade, the deformation of the cap is reduced 30-40% in the aerodynamic profile according to the present invention as compared to the prior art aerodynamic profile. By reducing the deformation of the cap at this level, the box girders resistance to buckling is increased significantly and this will in turn increase the ultimate strength of a complete wind turbine blade with the aerodynamic profile according to the present invention.

The reduction of the deformation of the cap will also prevent formation of interlaminar cracks in the material of the cap to a great extend, and this will increase both the reliability and the ultimate strength of the blade.

CLAIMS

1. Aerodynamic profile comprising
a facing having an outer surface with a substantially transverse curvature, and at least one straight reinforcing element for increasing the strength of the facing against flapwise forces by inhibiting an increase of the mutual distance in the edgewise direction between two points of the facing where the at least one internal reinforcing element is attached to the facing, the at least one reinforcing element having a thickness that is less than twice the maximum thickness of the facing.

2. Aerodynamic profile according to claim 1, further comprising shoring means in longitudinal direction along at least a part of the aerodynamic profile.

3. Aerodynamic profile according to claim 2, wherein said shoring means is/are embedded in or form part of said facing.

4. Aerodynamic profile according to claim 2, wherein said shoring means comprise at least one internal girder connected to at least a part of the inner surface of said facing.

5. Aerodynamic profile according to claim 4, wherein said at least one internal girder comprises a box girder or a box beam.

6. Aerodynamic profile according to any one of claims 3, 4 or 5, wherein said at least one reinforcing element is connected to the inner surface of said facing and/or to said shoring means with at least two connections.

7. Aerodynamic profile according to claim 6, wherein at least one of said connections is continuous along at least one or more parts of said facing and/or said shoring means.

8. Aerodynamic profile according to any preceding claim, wherein the at least one reinforcing element is a bar or rod-like element.

9. Aerodynamic profile according to any preceding claim, wherein the at least one reinforcing element is a plate.

10. Aerodynamic profile according to any preceding claim, wherein the at least one reinforcing element is a laminate.

11. Aerodynamic profile according to any one of claims 9 or 10, wherein said plate or laminate comprises one or more cut-outs.

12. Aerodynamic profile according to any one of the preceding claims, wherein said reinforcing element and said shoring means are fixedly interconnected.

13. Aerodynamic profile according to any one of claims 1-12, wherein said reinforcing element and said shoring means are releasable interconnected.

14. Aerodynamic profile according to any of the preceding claims, wherein said reinforcing element is connected to the inner surface of the profile in at least two connection points so that at least one space is defined between said reinforcing element and the inner surface of the profile.

15. Aerodynamic profile according to claim 14, wherein said space is at least partly filled with a filler material.

16. Aerodynamic profile according to claim 15, wherein said filler material is provided as an element of a foamed material.

17. Aerodynamic profile according to any of the preceding claims, wherein the at least one reinforcing element and a part of the surface of the profile are comprised in a separate cap part connected to the inner surface of the profile and/or to said shoring means.

18. Aerodynamic profile according to any one of the preceding claims, further comprising means for associating the profile with a relevant structure.

19. Wind turbine with two or more blades wherein the blades comprise an aerodynamic profile according to any one of claims 1-17.

20. Load-bearing construction comprising one or more aerodynamic profiles according to any one of claims 1-17.

21. A method for manufacturing a reinforced aerodynamic profile comprising the steps of

- providing at least a part of a facing of the profile, and
- providing shoring means in connection with said facing, and
- providing at least one reinforcing element connected in at least two connection points to an inner surface of the profile, and

- providing a filler material in a space between said reinforcing element and said inner surface of the profile.

22. A method according to claim 21, wherein the step of providing a filler material comprises adapting of an element of a foamed material to fit in said space.

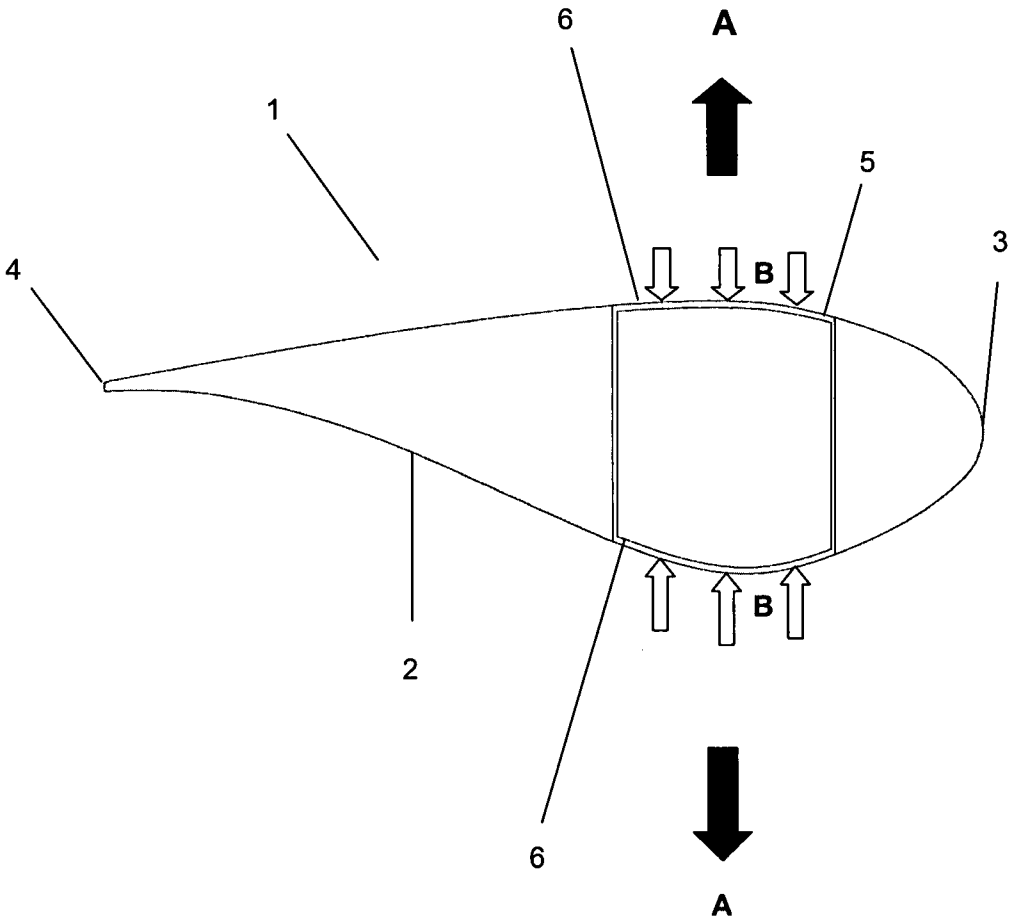

Fig. 1a

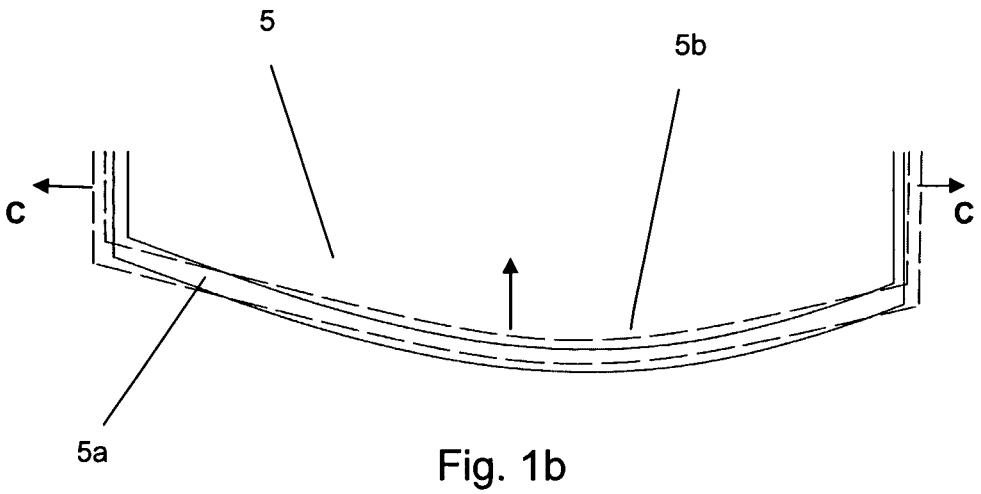

Fig. 1b

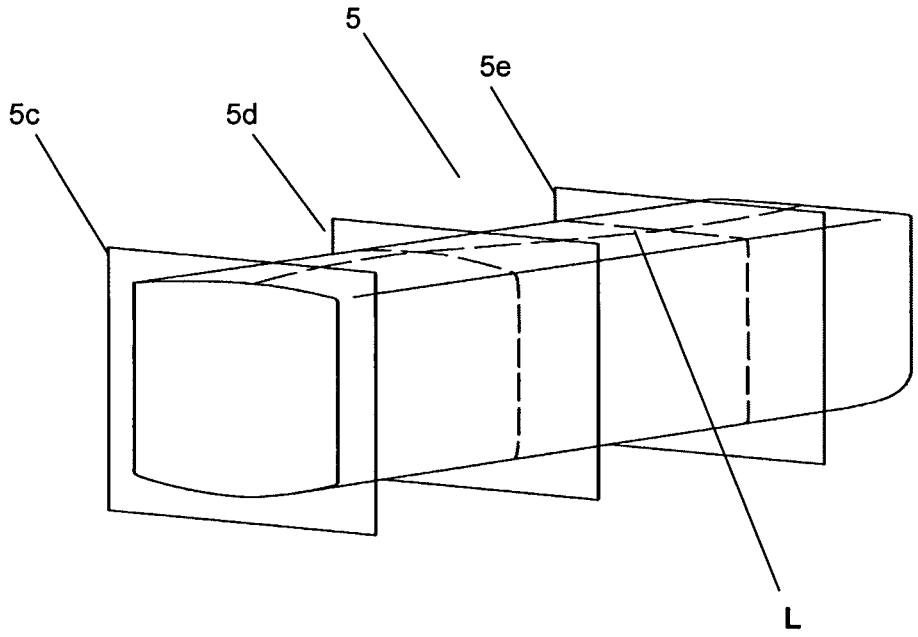

Fig. 2a

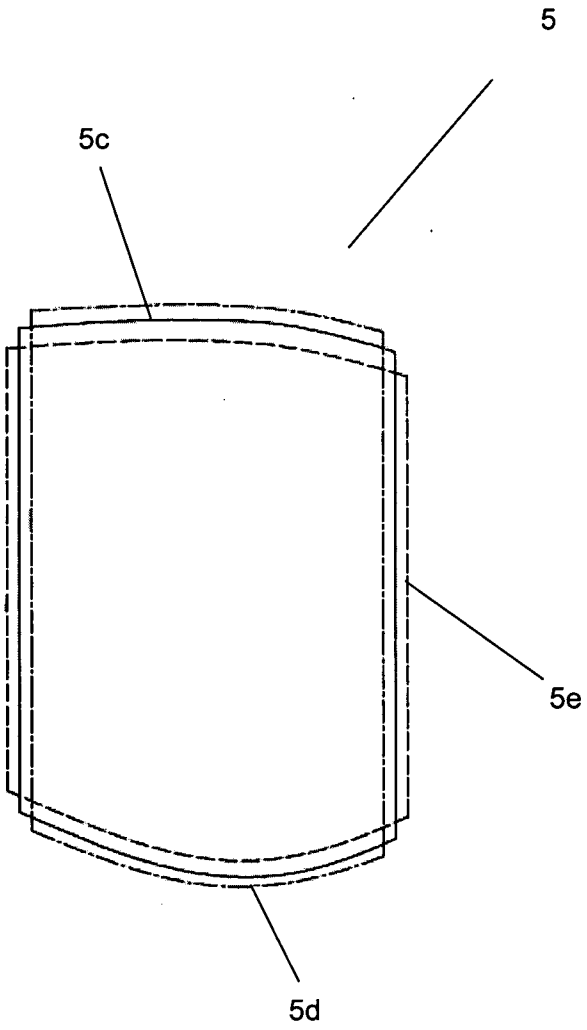

Fig. 2b

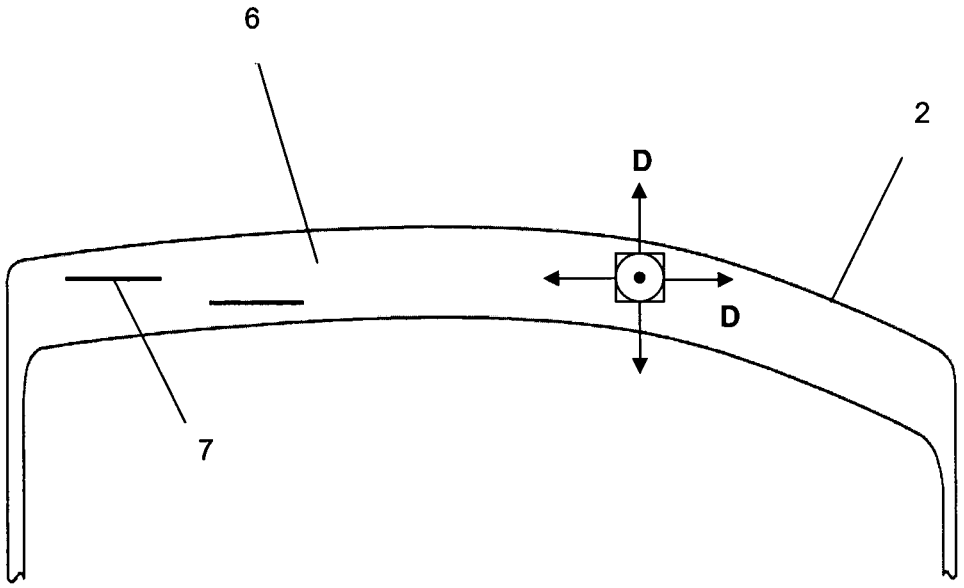

Fig. 3

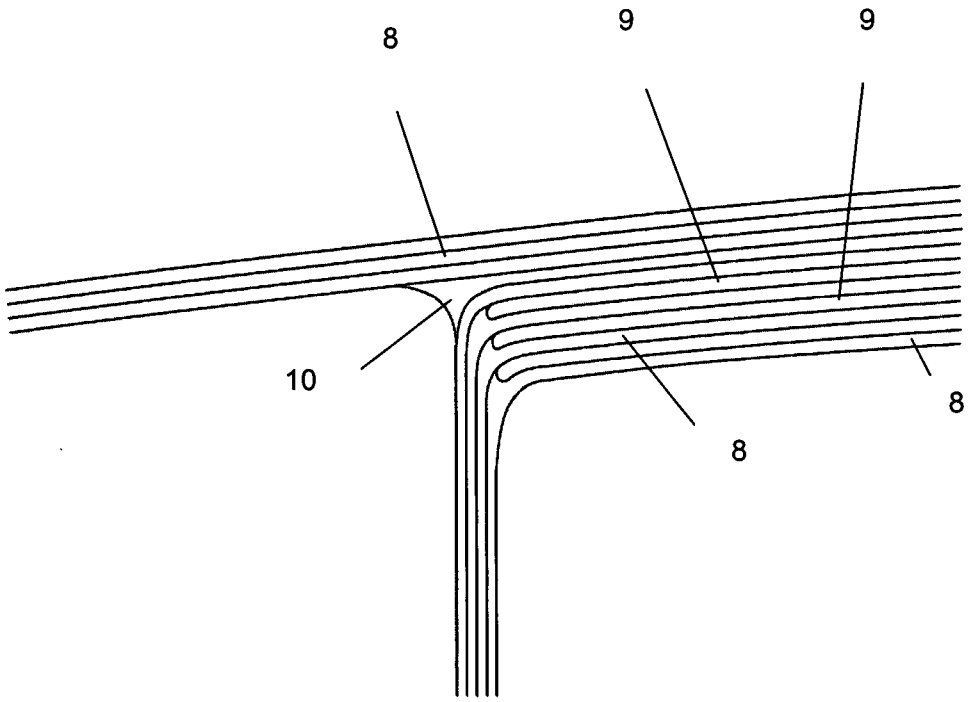

Fig. 4

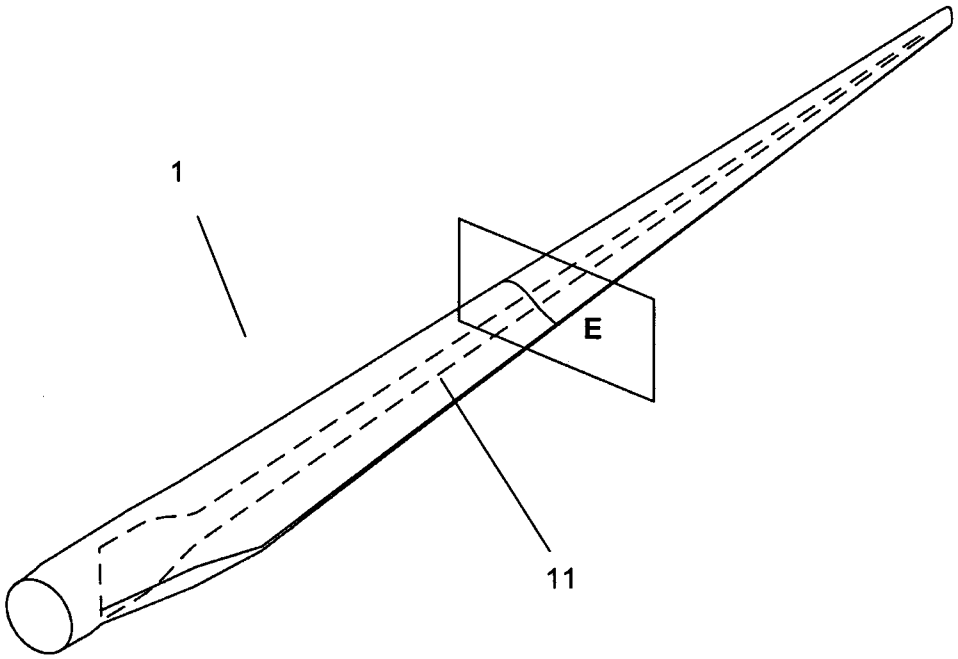

Fig. 5a

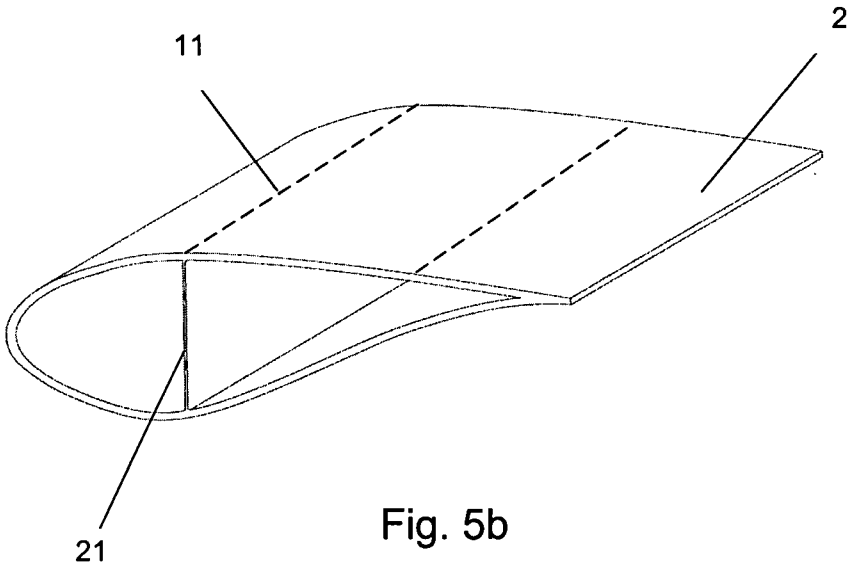

Fig. 5b

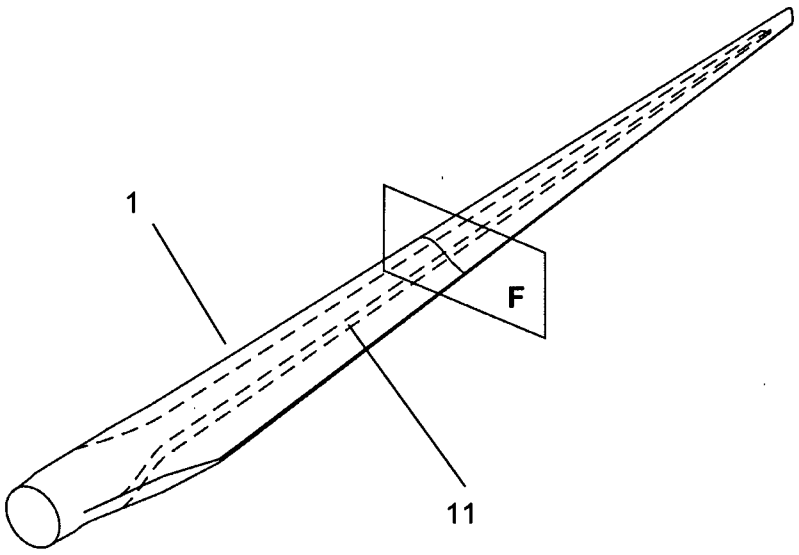

Fig. 5c

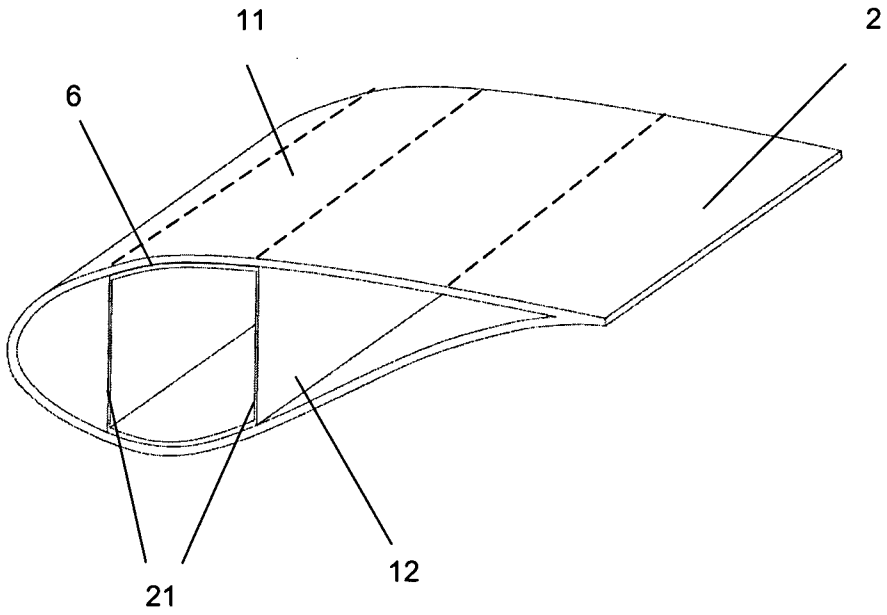

Fig. 5d

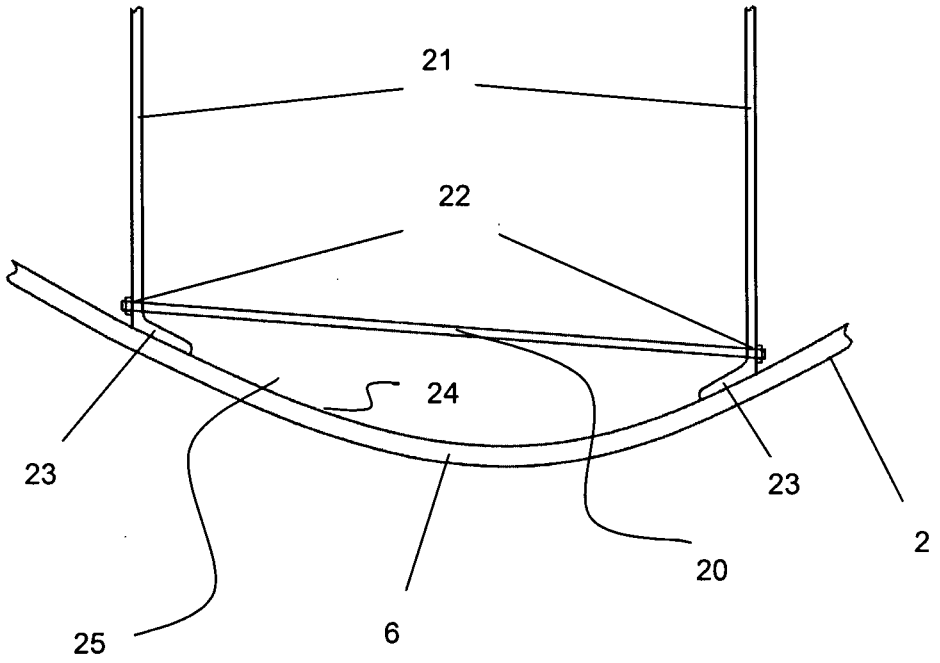

Fig. 6a

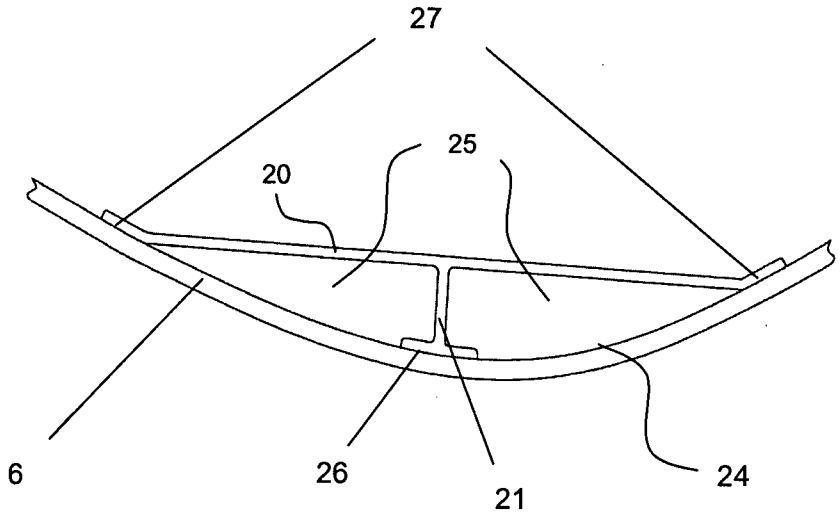

Fig. 6b

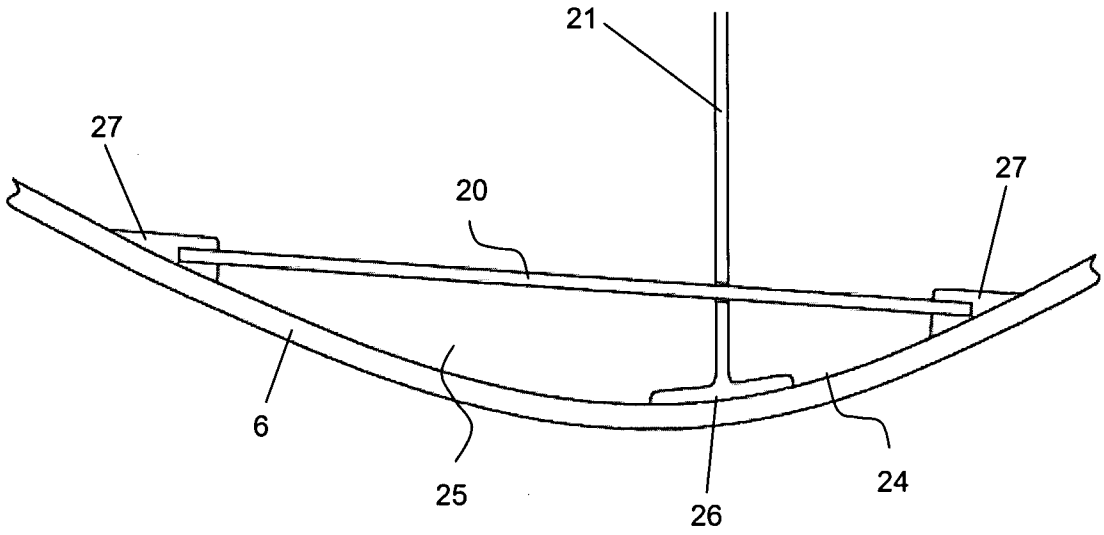

Fig. 7a

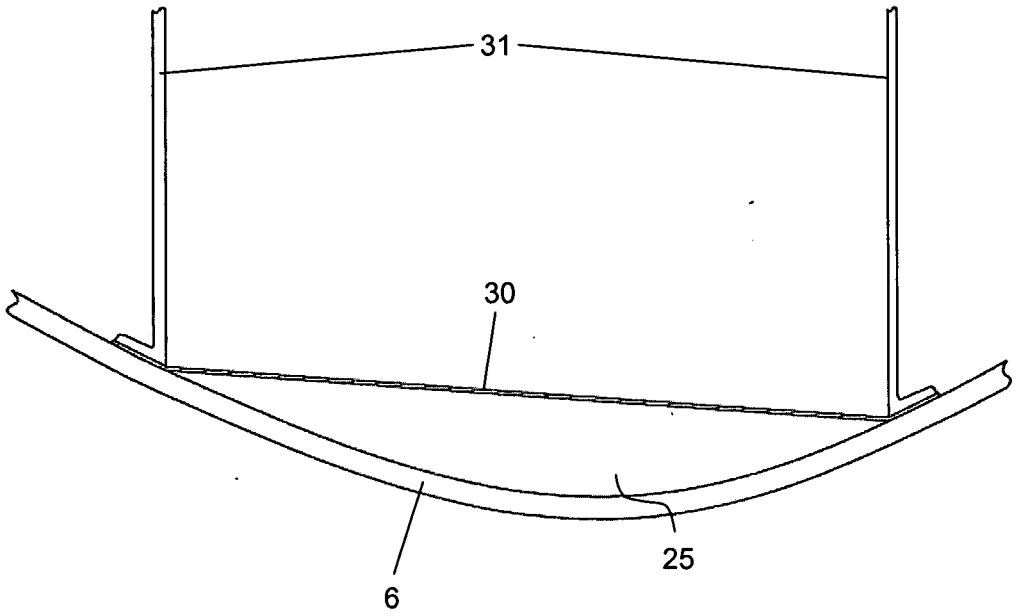

Fig. 7b

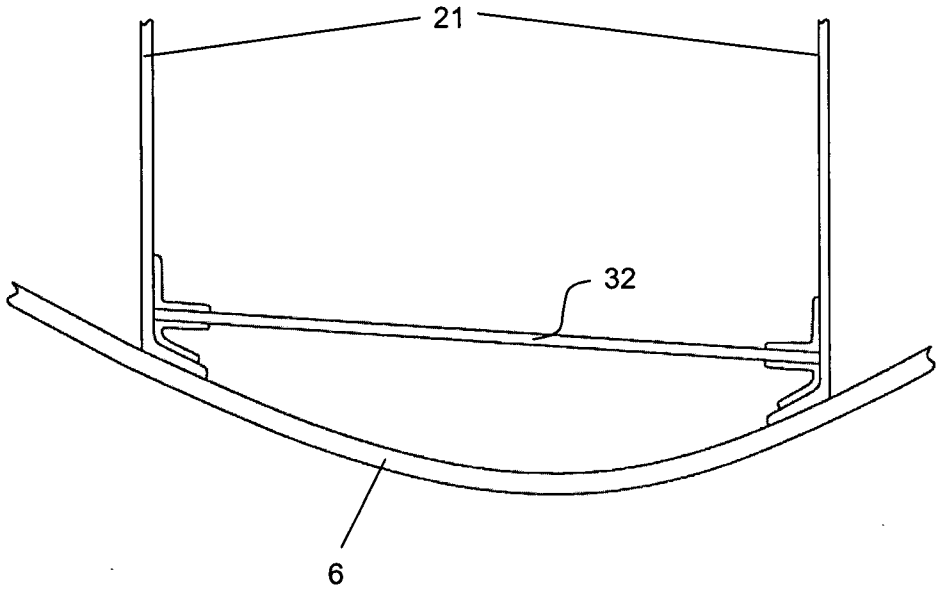

Fig. 7c

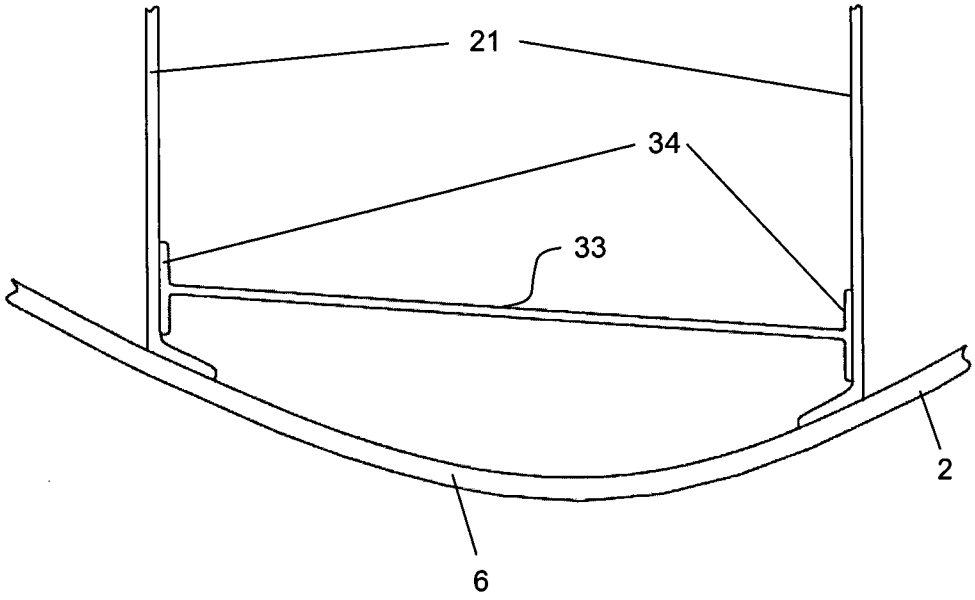

Fig. 7d

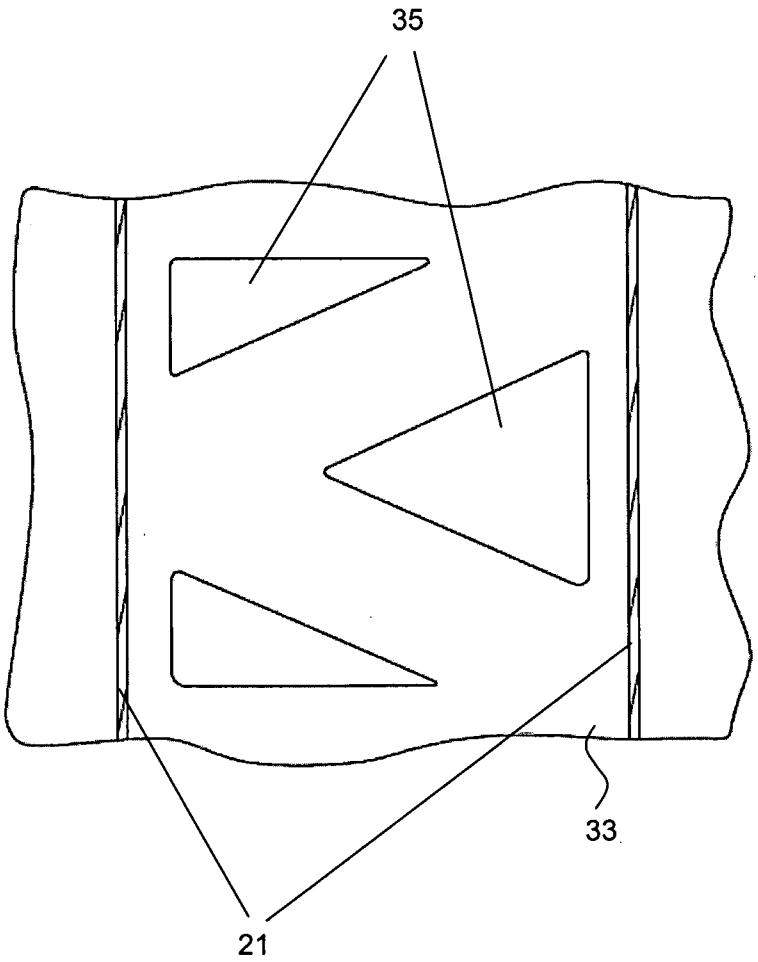

Fig. 7e

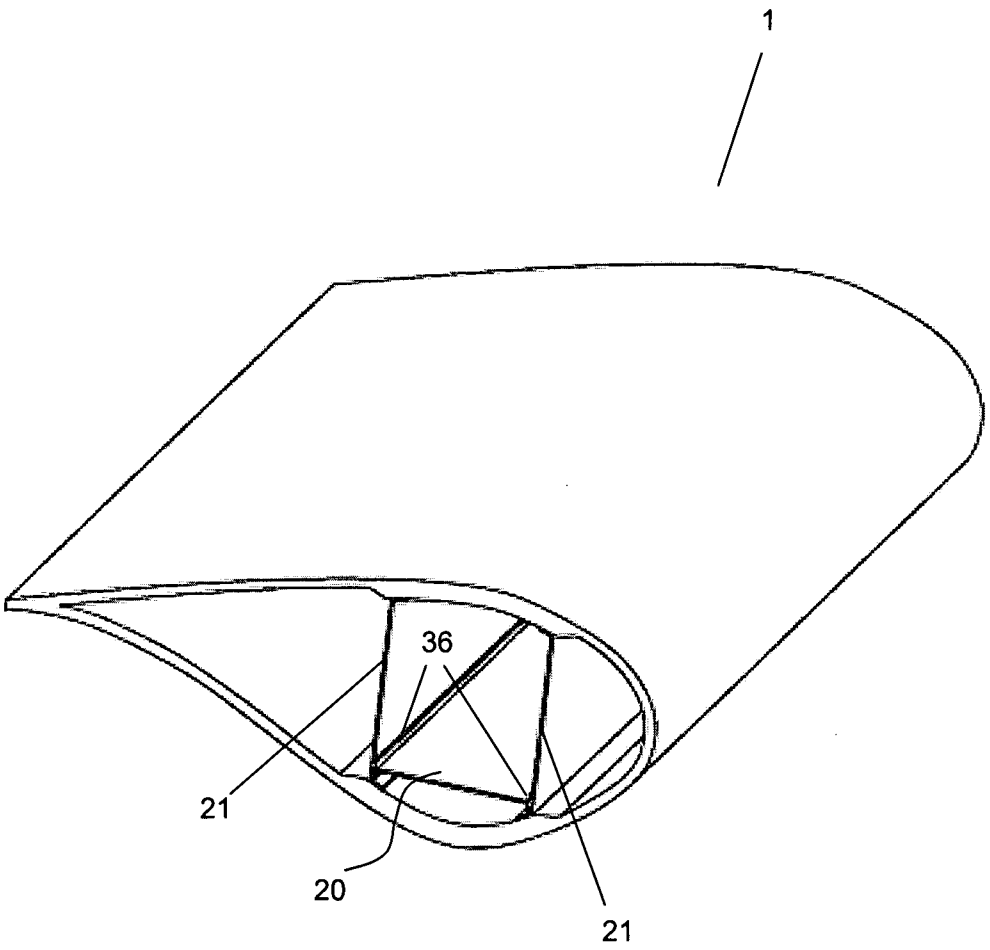

Fig. 7f

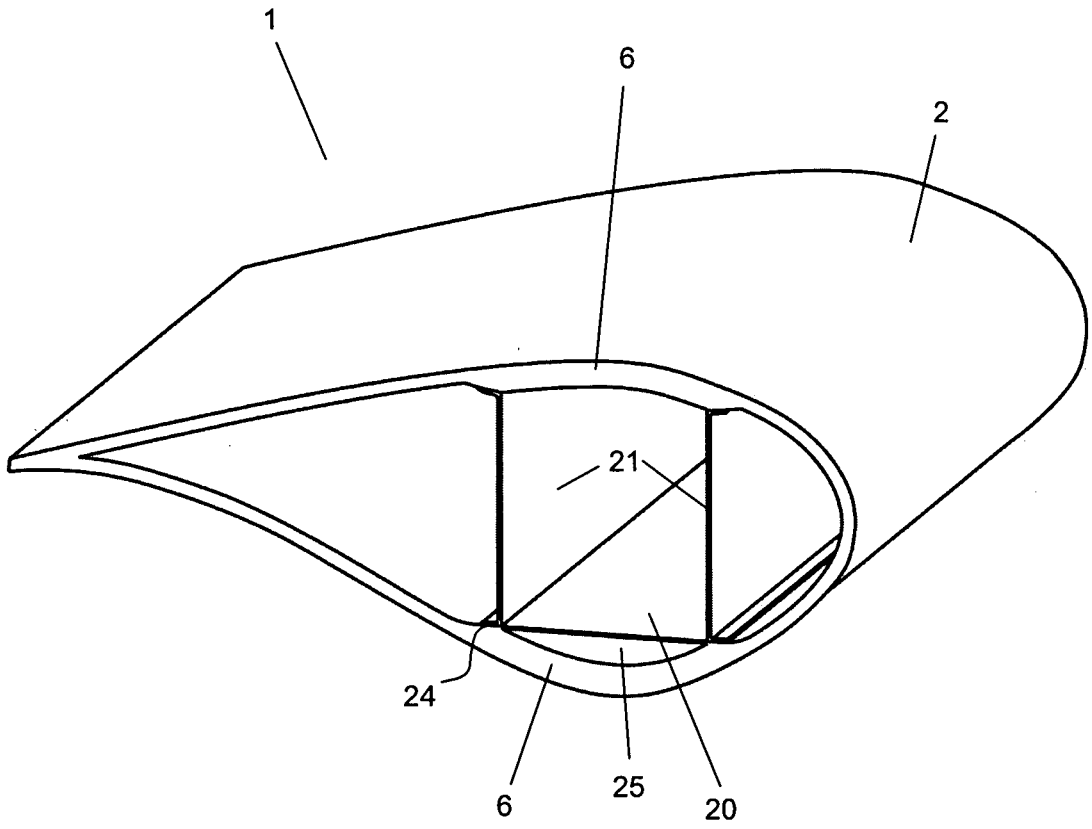

Fig. 8

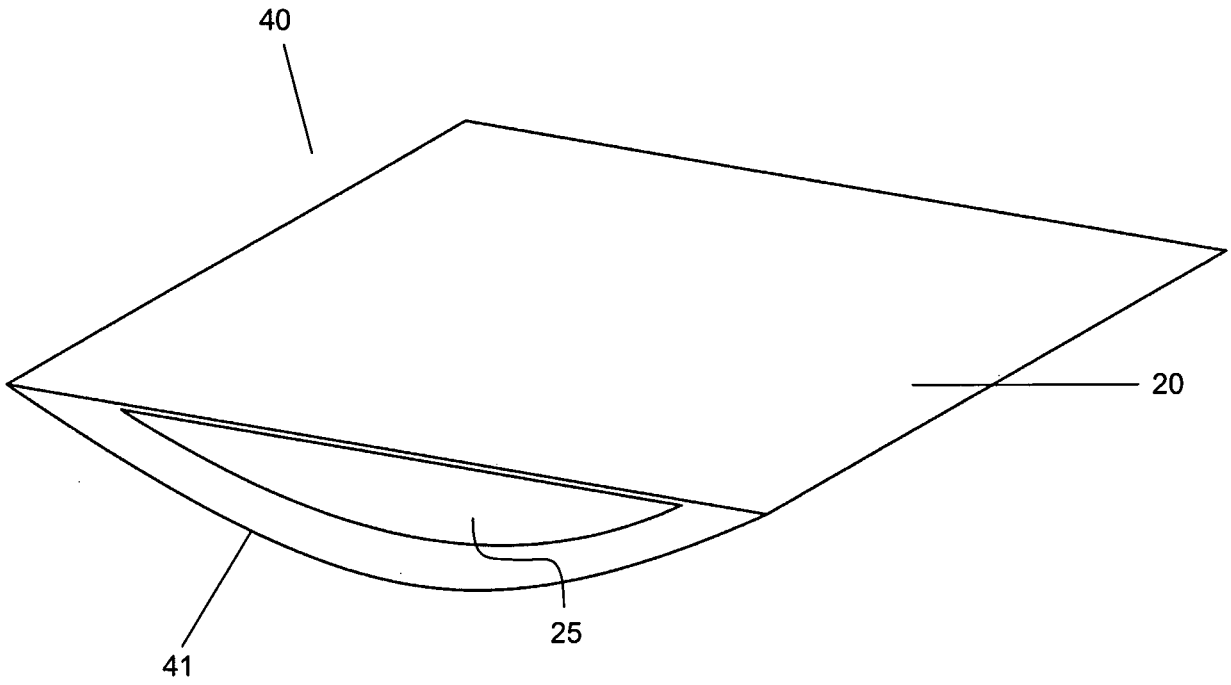

Fig. 9

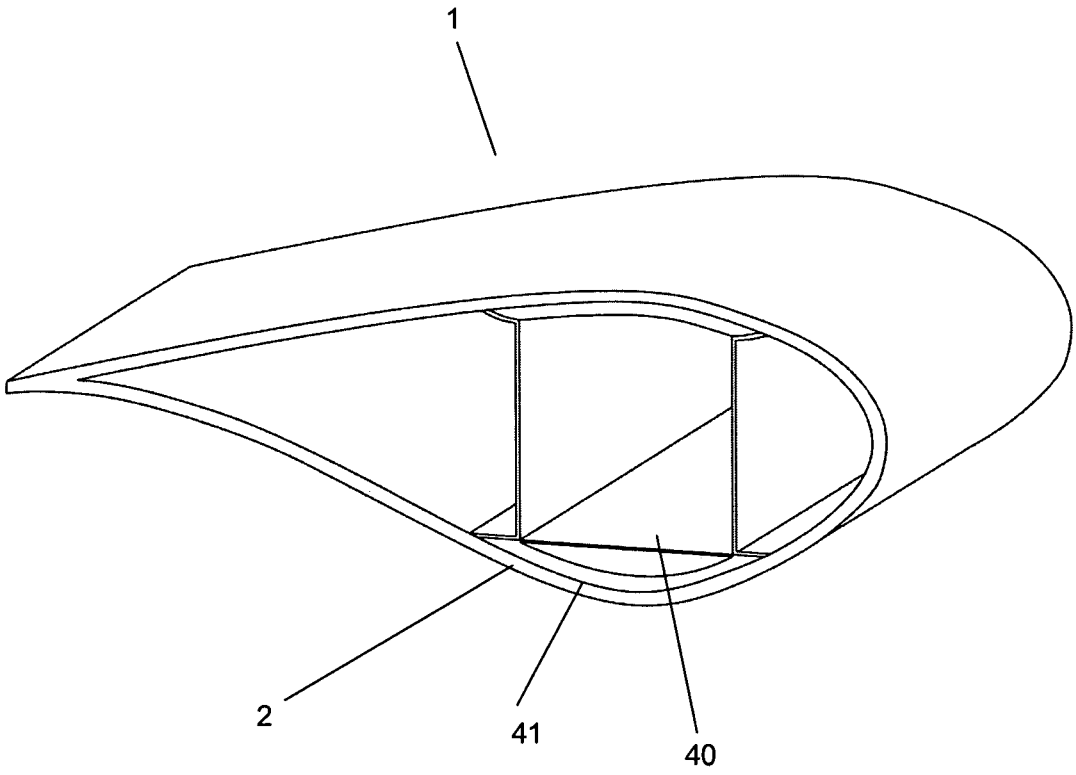

Fig. 10

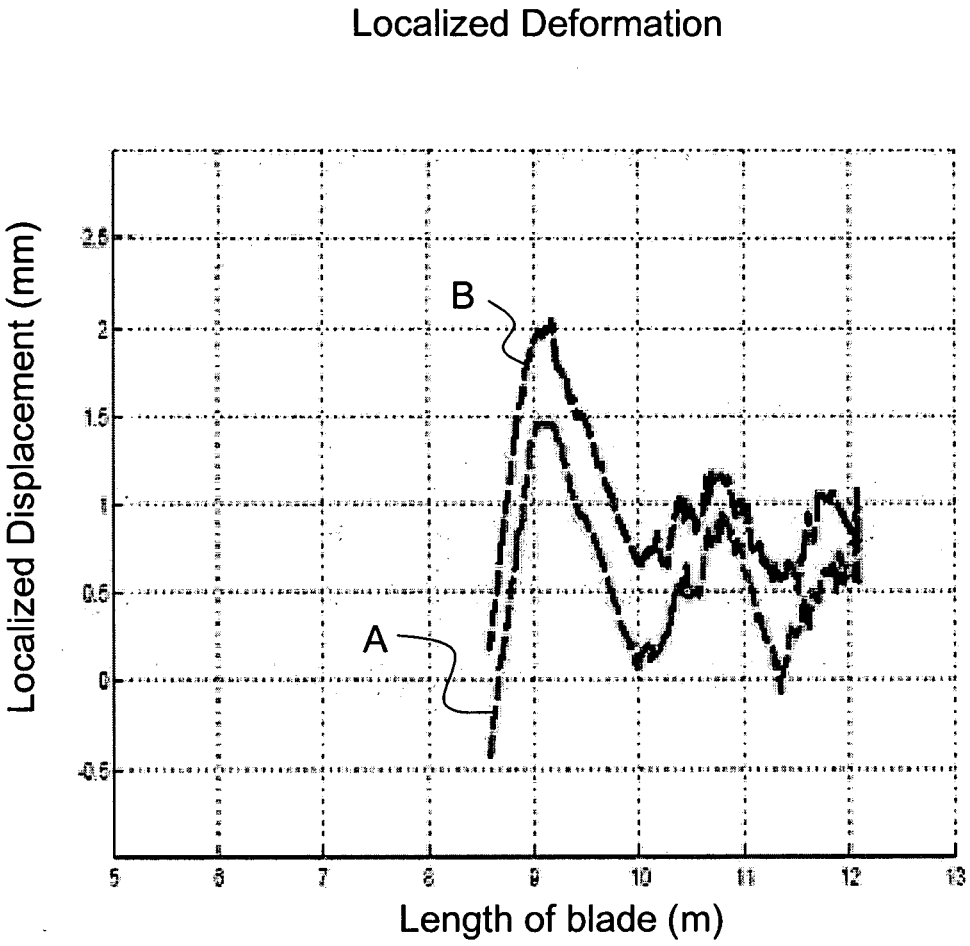
Localized Deformation
Localized Displacement (mm)
2.5
2
1.5
1
0.5
0
-0.5
B
A
5
6
7
8
9
10
11
12
13
Length of blade (m)

Fig. 11

Appendix B2 - “WO 2008-086805 Reinforced blade for wind turbine (floor- patent B)”. Find M. Jensen

(12) INTERNATIONAL APPLICATION PUBLISHED UNDER THE PATENT COOPERATION TREATY (PCT)

(19) World Intellectual Property Organization
International Bureau

(43) International Publication Date
24 July 2008 (24.07.2008)

PCT

(10) International Publication Number
WO 2008/086805 A2

(51) International Patent Classification: Not classified

(21) International Application Number:
PCT/DK2008/000017

(22) International Filing Date: 16 January 2008 (16.01.2008)

(25) Filing Language: English

(26) Publication Language: English

(30) Priority Data:
PA 2007 00065 16 January 2007 (16.01.2007) DK

(71) Applicant *(for all designated States except US)*: **DANMARKS TEKNISKE UNIVERSITET** [DK/DK]; Anker Engelundsvej 1, Bygning 101A, DK-2800 Kgs. Lyngby (DK).

(72) Inventor; and

(75) Inventor/Applicant *(for US only)*: **JENSEN, Find, Molholt** [DK/DK]; Emilsgave 8, DK-4130 Viby Sjælland (DK).

(74) Agent: **ALBIHNS A/S**; Havneholmen 29, bygn. 2, 3. sal, DK-1561 København V (DK).

(81) Designated States *(unless otherwise indicated, for every kind of national protection available)*: AE, AG, AL, AM, AO, AT, AU, AZ, BA, BB, BG, BH, BR, BW, BY, BZ, CA, CH, CN, CO, CR, CU, CZ, DE, DK, DM, DO, DZ, EC, EE, EG, ES, FI, GB, GD, GE, GH, GM, GT, HN, HR, HU, ID, IL, IN, IS, JP, KE, KG, KM, KN, KP, KR, KZ, LA, LC, LK, LR, LS, LT, LU, LY, MA, MD, ME, MG, MK, MN, MW, MX, MY, MZ, NA, NG, NI, NO, NZ, OM, PG, PH, PL, PT, RO, RS, RU, SC, SD, SE, SG, SK, SL, SM, SV, SY, TJ, TM, TN, TR, TT, TZ, UA, UG, US, UZ, VC, VN, ZA, ZM, ZW.

(84) Designated States *(unless otherwise indicated, for every kind of regional protection available)*: ARIPO (BW, GH, GM, KE, LS, MW, MZ, NA, SD, SL, SZ, TZ, UG, ZM, ZW), Eurasian (AM, AZ, BY, KG, KZ, MD, RU, TJ, TM), European (AT, BE, BG, CH, CY, CZ, DE, DK, EE, ES, FI, FR, GB, GR, HR, HU, IE, IS, IT, LT, LU, LV, MC, MT, NL, NO, PL, PT, RO, SE, SI, SK, TR), OAPI (BF, BJ, CF, CG, CI, CM, GA, GN, GQ, GW, ML, MR, NE, SN, TD, TG).

Published:
— *without international search report and to be republished upon receipt of that report*

(54) Title: REINFORCED BLADE FOR WIND TURBINE

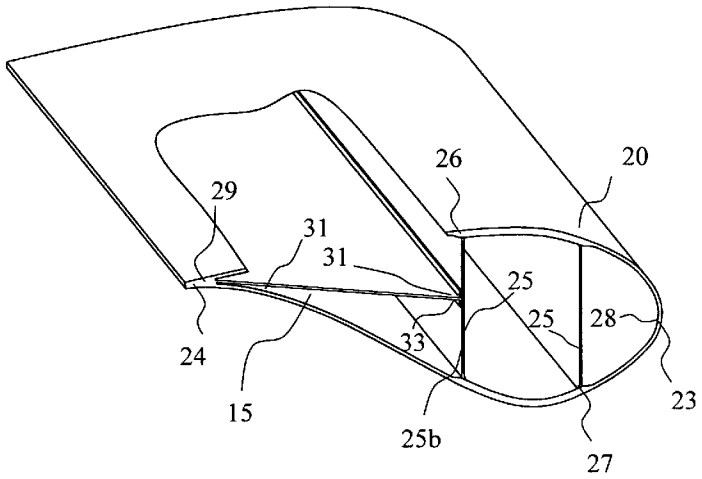

Fig. 8

(57) Abstract: The present invention relates to a reinforced blade for a wind turbine, and in particular to a wind turbine blade comprising a shell having a section with an aerodynamic profile, and at least one internal reinforcing floor connected inside the shell and extending substantially along the profile chord in order to increase the strength of the blade and to prevent or reduce deformations of the surface of the blade caused by edgewise and flapwise loading of the blade structure.

WO 2008/086805 A2

REINFORCED BLADE FOR WIND TURBINE

The present invention relates to a reinforced blade for a wind turbine, and in particular to a wind turbine blade comprising a shell having a section with an aerodynamic profile, and at least one internal reinforcing floor connected inside the shell and extending substantially along the profile chord in order to increase the strength of the blade and to prevent or reduce deformations of the surface of the blade caused by edgewise and flapwise loading of the blade structure.

A wind turbine blade normally consists of an aerodynamic shell and an internal girder such as a beam or a spar, the girder can be a single beam, but often two girders are used, and along with the shell the girders can be said to form a box profile. The aerodynamic shell typically comprises a laminate of fibre reinforced plastics, fibreglass and/or other materials.

The section(s) of the aerodynamic shell where the internal girders are placed is/are usually reinforced in some way and is/are consequently often quite thick. The other part(s) or section(s) of the aerodynamic shell is typically only a thin skin or a laminate such as a sandwich construction with thin skins and a core material. A blade is typically provided by gluing or bonding or otherwise connecting two shell parts to each other.

In operation, the blade is subject to flapwise, edgewise and torsional loads. By flapwise direction is meant a direction substantially perpendicular to a transverse axis through a cross-section of the widest side of the blade. Alternatively, the flapwise direction may be construed as the direction (or the opposite direction) in which the aerodynamic lift acts on the profile. The edgewise direction is perpendicular to the flapwise direction. The edgewise loads, even though typically smaller than the flapwise loads, can potentially cause damage to the blade, especially fatigue damage and ultimately lead to failure of the blade.

When a blade is subjected to edgewise loading the section of the shell between a trailing edge of the blade and the internal girder is deforming out of the plane of the "neutral" (or initial) plane of the surface, see Fig. 1. This deformation induces peeling stresses in the trailing edge of the blade and consequently this can lead to a fatigue failure in the adhesive joint of the trailing edge where the two shell parts are connected to each other. This may then ultimately cause the blade to break apart. Furthermore, the aerodynamic efficiency of the blade is also compromised since the designed shape of the blade profile is no longer maintained.

The edgewise loads can further cause the trailing edge of the blade to deform in a stable post buckling pattern, see Fig. 2. This is caused by bending of the blade from the leading

edge towards the trailing edge. The blade material in the leading edge is then subject to tension and the trailing edge to compression. As the trailing edge is relative thin, it cannot withstand substantial compression forces before it bends out of its neutral plane. When this happens, some of the load on the trailing edge is transferred to and distributed through part of the shell further away from the trailing edge, until equilibrium of the forces is established. Although this deformation does not immediately lead to failure, it decreases the safety margin for the general failure load of the blade and also increases the peeling and shear stresses in the trailing edge.

Furthermore, the edgewise loads can induce compression forces in a leading edge section of the blade, and therefore a sandwich construction is often provided in the leading edge to increase the resistance against buckling, i.e. preventing the section's surface from bulging out of its plane.

Subjected to flapwise loads, the section of the aerodynamic shell between the trailing edge and the internal girder is deforming out of the plane of the surface's "neutral" position in a similar way as described above for the edgewise loads. This deformation also induces shear and peeling stresses in the trailing edge of the blade. The section will deform into a state of "lowest energy level", i.e. a situation wherein as much as possible of the stress in the blade is distributed to other sections of the blade. When part of the shell deform in this manner, it is usually referred to as an "ineffective panel". The distribution of the stresses to other parts of the blade means that these parts are subjected to at higher load. This will result in a larger tip deflection of the blade. Furthermore, the deformations of the blade's surface compromise the aerodynamic efficiency of the blade, because the designed shape of the profile is no longer maintained.

Under flapwise loading, crushing pressure (see Fig. 3) occur on the box profile of the blade due to its longitudinal curvature. This effect is often referred to as ovalization (reference is made to the article "Structural testing and numerical simulation of a 34 m composite wind turbine blade" by F. M. Jensen et.al. published by Elsevier in Composite Structures 76 (2006) 52-61). The crushing pressure loads the internal girder in compression (see Fig. 4). The flapwise loads also induce in-plane shear forces in the internal girder. During the operation of the blade, transverse shear forces occur in the blade as shown on a cross-section of the blade (see Fig 5). The shear forces are generated by the flapwise and edgewise loads because the blade has asymmetric geometry and material distribution. The transverse shear forces distort the profile as shown on Fig. 5. The distortion of the profile reduces the blade's resistance to the crushing pressure and can cause a sudden collapse of the blade.

Presently, there is thus a need for a wind turbine blade in which deformations of the shell are prevented or minimised and wherein the blade structure is strengthened without increasing the overall weight. It is also desirable to provide improvements of a blade with at least one internal girder leading to increased resistance against buckling from crushing pressure and in-plane shear in order to carry the loads in the blade.

It is therefore an object of the present invention to provide a wind turbine blade with improved resistance against deformations of the shell.

It is yet another object of the present invention to provide a wind turbine blade with increased overall strength and overall stiffness.

It is another object of the present invention to provide a wind turbine blade with reduced weight.

It is also an object of the present invention to provide a wind turbine blade with improved reliability of joints between shell parts.

It is another object of the present invention to provide a wind turbine blade with an improved transferral of forces in the transition between the blade and the circular root.

It is yet another object of the present invention to provide a wind turbine blade that can be produced at a reduced manufacturing cost compared to the existing solutions.

It is still another object of the present invention to provide a wind turbine blade with an increased resistance against crushing pressure.

It is a further object to provide a wind turbine blade capable of working under severe aerodynamic loads and to optimise the aerodynamic efficiency, e.g. energy output of the blade.

It is another object to provide a wind turbine blade wherein the dynamic inertia loads the blade is applying on the other structural parts of the wind turbine construction are reduced.

It is further an object of the present invention to provide alternatives to the prior art.

In particular, it may be seen as an object of the present invention to provide a wind turbine blade that solves the above mentioned problems of the prior art by providing the blade with a reinforcing floor e.g. such as described by way of the examples in the following disclosure.

According to a first aspect of the present invention, the above-mentioned and other objects are fulfilled by a wind turbine blade comprising a shell having a section with an aerodynamic profile, and at least one internal reinforcing floor connected inside the shell for increasing the strength of the blade and having a cross section transversely to the longitudinal extension of the blade that extends substantially in a direction from the trailing edge to the leading edge of the blade.

According to a second aspect of the invention, the above-mentioned and other objects are fulfilled by a method of increasing the strength of a wind turbine blade having a shell with a section having an aerodynamic profile, wherein the method comprises the step of positioning and connecting at least one internal reinforcing floor inside the shell for extension substantially in a direction from the trailing edge to the leading edge of the blade.

The wind turbine blade may for example have a at least one internal reinforcing floor connected to an inner surface of the shell at the trailing edge of the blade and to an inner surface of the shell at the leading edge of the blade in order to prevent or reduce deformations of the surface of the blade, in particular deformations caused by edgewise loading of the blade structure.

The wind turbine blade may further have at least one internal girder, and at least one internal reinforcing floor connected to an inner surface of the shell and to the internal girder.

The connection(s) between the internal girder and the inner surface of the facing may be placed at any suitable position on the parts. Preferably, but not exclusively, the connections may be adapted in one or more points, along one or more lines or in any kind of spatial configuration. Furthermore, the connections may comprise any suitable kind of mechanical joint such as a welded, glued, melted, fused or other simple mechanical connection.

The profile chord of the blade is an imaginary surface that contains the leading edge and the trailing edge of the blade and extends therebetween. Thus, in accordance with the present invention, an internal reinforcing floor extends along, or substantially along, the profile chord of the blade. Thus, a connection between one of the at least one internal reinforcing floor and a respective one of the at least one internal girder is preferably located with a shortest distance to the shell that is larger than 0.16 times, more preferred larger than 0.33 times, the total distance between the upper part of the shell and the lower part of the shell along a transversal extension of the respective girder at the connection. For example, the connection may be located halfway or approximately halfway

between the upper part of the shell and the lower part of the shell along a transversal extension of the respective girder at the connection.

The at least one internal girder may comprise a box girder or a box beam. The sides of the box girder may vary in thickness in its longitudinal and/or transverse direction(s) and the shape and/or the perimeter length of the cross-section of the girder may also vary along its longitudinal extent.

Preferably, the box girder or box beam is of a substantially polygonal cross-section. The cross-section of the box girder or box beam may have any polygonal shape such as substantially rectangular, triangular, circular, oval, elliptical etc. but is preferably rectangular or substantially square.

The shell of the blade may preferably, but not exclusively, comprise a composite or laminated material. The material may preferably, but not exclusively, comprise fibreglass and/or carbon fibres and/or other durable and flexible materials typically with a high strength/weight ratio such as other fibre reinforced plastic materials. This may further comprise, at least in part, light-weight metals or alloys. The shell may typically be a laminate or sandwich-construction. The thickness of the shell may vary along its length and/or width.

In an embodiment of the invention, at least one girder is provided to primarily strengthen and/or reinforce the blade in its longitudinal direction and may also be referred to as a web. In this application the girder or web should be construed as any kind of elongate constructional element capable of taking up loads, such as a beam or a spar e.g. shaped as an I-profile preferably made from fibre reinforced plastics or other suitable material. The web may substantially extend through the length of the blade. However, it may also be preferred to provide the blade with two or more separated webs in the longitudinal direction of the blade, especially for facilitating handling or transporting purposes. In principle, any number of webs may be applied, however for the sake of simplicity and for keeping the overall weight of the blade as low as possible a number of one or two webs is/are preferred. Preferably, in a direction perpendicular to its longitudinal extension, each girder or web of the at least one internal girder extends from the lower part of the shell to the upper part of the shell in a substantially flapwise direction and is connected to the upper part and lower part, respectively, of the shell. Thus, in embodiments with a plurality of girders or webs, the shell interconnects the girders or webs.

The at least one internal reinforcing floor may be connected to the inner surface of the shell and to the at least one web. The connection on the inner surface of the shell and on the web may in principle be positioned anywhere thereon, but it should be observed that

the chosen positioning causes the reinforcing floor to be able to provide a reasonable and useful reinforcing effect in the blade. The connection of a reinforcing floor between connecting points on the inner surface of the shell and the web prevents or minimises the problematic deformations described above. The connections may comprise any suitable kind of joint such as welded, glued, melted, fused or other simple mechanical connections such as bolt-and-nut connections. The reinforcing floor itself may comprise the connections or it may comprise additional connections or connection parts adapted to engage or cooperate with the other connections.

In embodiments the at least one internal reinforcing floor is connected to the inner surface of the shell in or in the vicinity of a trailing edge part and/or a leading edge part of the profile. The trailing and leading edge parts are indicated and illustrated in the figures.

In an embodiment with at least one internal girder, a reinforcing floor may be provided between the trailing edge and the at least one internal girder. If more than one internal girder is provided, the reinforcing floor may be provided between the trailing edge and the internal girder or web closest to the trailing edge. A reinforcing floor may of course also or instead be provided between the leading edge and the at least one internal girder. If more than one internal girder is provided the reinforcing floor may be provided between the leading edge and the internal girder or web closest to the leading edge. Reinforcing floors may of course also be provided between both the trailing and the leading edges and the one or (respectively closest) more internal girders. The one or more internal girder(s) may also comprise one or more divided or cut webs that are connected to the reinforcing floor(s) by bonding or lamination.

In other embodiments, an extent of the trailing edge in the direction towards the leading edge may be made solid or, due to manufacturing considerations, embodiments may comprise a cavity between the lower and upper shell parts and a plate fastened between the two parts some extent from the trailing edge. The cavity may be filled with lightweight material such as foam. Thereby, it may not be possible to fasten the reinforcing floor directly to the trailing edge, but instead to a part of the shell as near the trailing edge as possible. By connecting the reinforcing floor to a part of the shell near the trailing edge, instead of directly to the trailing edge, one can still obtain the advantages discussed above.

In an embodiment a single reinforcing floor may be connected to both the trailing and leading edges and to the internal girder. The internal girder may comprise one or more divided or cut webs that are connected to the reinforcing floor by bonding or lamination. In embodiments the at least one internal girder or web is a box profile. The reinforcing floor may then be provided between the trailing and/or leading edge(s) of the blade and the

side of the box profile closest to the respective edge. The box profile may be formed by two girders or webs along with sections of the shell or it may be a total individual box profile.

In an embodiment the reinforcing floor may comprise a plate shaped element. The plate element may be solid or hollow or any suitable combination thereof. The thickness of the plate may vary along different sections of the plate or it may be substantially equally thick over its entire area. However, it is required that the plate element is able to take up in-plane compression forces in the floor and the material and the dimensions of the floor must have this capability. The material may preferably, but not exclusively, be a fibre reinforced plastic material or another material such as metal, metal alloy, wood, plywood, veneer, glass fibre, carbon fibre and other suitable materials such as e.g. one or more composite materials. The reinforced plastic material may be manufactured from materials such as, but not limited to glass fibres, carbon fibres or aramid fibres thus providing a high strength and a low weight.

The mentioned materials may also be combined to any construction. Thus, in another embodiment the at least one reinforcing element is a laminate or a sandwich construction having relatively hard/durable outer surfaces, such as a fibre reinforced plastic, and an inner core of another material, such as, but not limited to, a softer and/or lighter material such as a foamed material.

Additionally, the plate element may comprise one or more stiffeners for e.g. maintaining strength and stiffness while minimising the weight of the construction. The stiffeners may comprise any suitable shape and material such as rods or bars or lattices of a fibre reinforced plastic material or another light-weight material such as aluminium.

Furthermore, in embodiments the plate element may comprise one or more cut-outs in order to reduce weight and/or increase the stiffness of the plate element. The cut-outs may be provided in any suitable pattern.

By connecting or coupling the trailing edge with the closest web using a reinforcing floor that can withstand compression forces, the deformations in the shell between the trailing edge and the web are reduced since the greater part of the forces causing the deformations are taken up by and distributed through the reinforcing floor and the web. This will decrease the potentially damaging forces in the joint between the shell parts, as the forces are distributed towards the floor and the web.

As deformations are reduced, the shell is kept in its original shape or position to a much higher degree. The result is that the "ineffective" panels of the shell carry an increased

part of the load on the blade, and thereby decrease the load taken up by other parts of the blade. This results in an increased stiffness of the blade in the flapwise direction and thereby decreases the tip deflection. Along with this, the aerodynamic efficiency of the blade is increased since the blade profile will remain closer to its originally designed shape.

The coupling will also increase the resistance of the trailing edge against buckling due to the edgewise loads because the damaging forces are distributed to the web through the floor.

As a result, the joint between the shell parts in the trailing edge is less exposed to damaging peeling and shear forces and the weight of the blade can be reduced since a less strong construction of the blade is needed. The lower weight reduces the dynamic inertia loads originating from the operation of the blade on the other parts of the wind turbine structure. Furthermore the aerodynamic efficiency of the blade is increased.

The reinforcing floor have a substantial desirable effect on the edgewise stiffness of the blade. As presented above, it prevents the deformation of the shell, which in itself has a positive effect on the edgewise stiffness, but it will also carry some of the edgewise loads. This will take load off of other parts of the blade which means the edgewise stiffness is increased substantially. Such increased edgewise stiffness provides a higher edgewise eigenfrequency. It is an advantage to have a higher edgewise eigenfrequency because it decreases the dynamic inertia loads the blade is applying on the other structure of the wind turbine, because an increase of the eigenfrequency reduces the amplitude of the harmonic oscillations of the blade.

The floor also reduces the transverse shear force distortion of the profile of the blade, and this increases the blade's capability of taking up crushing pressure. This again helps maintaining the blade profile closer to its original shape and thus potentially increases the power output from the turbine.

By connecting or coupling the leading edge with the closest web using a reinforcing floor that can withstand compression forces, the loads on the leading edge are distributed towards the floor and the web, thereby reducing the potentially damaging forces in the joint between the shell parts. The reinforcing floor stabilises the shell in and in the vicinity of the leading edge section and increases the resistance of the shell against buckling in the leading edge section. When the buckling resistance is increased, the thickness of the laminated material used for shell can be reduced or, in embodiments where a sandwich construction is provided, the thickness of the core can be reduced. In embodiments the use of a sandwich construction in the leading edge section of the shell can be completely omitted and instead a single kind of material may be used for the leading edge. As a

result, the weight of the blade can be further reduced without compromising strength and stiffness, a more simple construction of the blade is provided and consequently the blade can be produced at a lower total price.

As a result of the flapwise load, crushing pressure and shear forces is generated in the webs. These forces can cause the web to collapse, because the web buckles out of the plane of the web. When the web buckles due to the crushing pressure, the whole side of the web bends outwards in one direction. The buckling due to shear forces in the web shows a distinct wave pattern bending outwards to one side in one part of the web and to the other side in a neighbouring part of the web. When a reinforcing floor is connected to a web (either the web towards the trailing edge or the web towards the leading edge, in case two webs are used), it supports the part of the web that tries to buckle, and this increases the resistance of the web to buckling, and therefore a thinner core is needed in the sandwich construction in the web. This will allow for a reduction of the weight of the blade, and a reduction of material costs.

In the lower part of the blade, it comprises a transition from a wide aerodynamic profile to a cylindrical root section. The root is the part of the blade that is mounted on the wind turbine axle. In this part of blade, a reinforcing floor in the trailing edge is a very efficient structure for transfer of stresses from the blade shell to the circular cylindrical root. Thereby the stresses in the trailing edge section in the part of the blade proximal to the root are significantly reduced and the risk of failure in the connection between the shell parts in the trailing edge of the blade are minimised.

Furthermore, a connection or coupling of both the trailing and the leading edges with the web will increase the torsional stiffness of the blade. This will increase the torsional eigenfrequency of the blade and in return decrease the dynamic inertia loads the blade is applying on the other structure of the wind turbine, because an increase of the torsional eigenfrequency reduces the amplitude of the harmonic oscillations of the blade.

In embodiments, the floor(s) used in the connection or coupling between the trailing and/or leading edge(s) and the web may be specially tailored so that the bending and torsion of the blade is coupled. This is used to take the load of the blade when strong wind gusts occur. This leads to lower fatigue loads on the blade and also facilitate a higher energy output of the wind turbine.

Below the invention will be described in more detail with reference to the exemplary embodiments illustrated in the drawings, wherein

Fig. 1 is a schematic view of a cross-section of a wind turbine blade indicating a deformation of the blade shell (or panel) between a trailing edge and an internal girder/web due to flapwise loads,

Fig. 2 is a schematic perspective view of a wind turbine blade indicating a deformation in a trailing edge of the blade in the form of a buckling pattern caused by an edgewise load that is also indicated,

Fig. 3 is a schematic view of a cross-section of a wind turbine blade indicating the crushing pressure on the blade from the bending moment acting on the blade in operation,

Fig. 4 is a schematic view of part of the cross-section of a wind turbine blade, in particular showing a web in the form of a box profile and indicating the potential deformation (ovalization) caused by the crushing pressure (deformed state shown as punctured lines),

Fig. 5 is a schematic perspective view of a wind turbine blade indicating deformations caused by the influence of transverse shear forces on the blade profile,

Fig. 6 is a schematic cross-sectional view of a reinforced wind turbine blade according to the invention showing the blade with two webs and a reinforcing floor extending from a trailing edge section to the closest web and connected by bonding,

Fig. 7 is a schematic cross-sectional view of a reinforced wind turbine blade according to the invention showing the blade with two webs and a reinforcing floor extending from a position in the vicinity (near) of the trailing edge to the closest web and connected by laminating,

Fig. 8 is a perspective view of the embodiment shown in Fig. 7,

Fig. 9 is a schematic cross-sectional view at the root of the embodiment also shown in Figs. 7 and 8,

Fig. 10 is a schematic cross-sectional view of a reinforced wind turbine blade according to the invention showing the blade with two webs and a reinforcing floor extending from a leading edge to the closest web,

Fig. 11 is a schematic cross-sectional view of a reinforced wind turbine blade according to the invention showing the blade with two webs and two reinforcing floors, one extending from a trailing edge and one extending from a leading edge to their respective closest web,

Fig. 12 is a schematic cross-sectional view of a reinforced wind turbine blade according to the invention showing the blade with one web and two reinforcing floors, one extending from a trailing edge and one extending from a leading edge to each side of the web,

Fig. 13 is a schematic cross-sectional view of a reinforced wind turbine blade according to the invention showing the blade with two webs which are each divided in two and a single reinforcing floor extending from a trailing edge to a leading edge of the blade,

Fig. 14 is a schematic cross-sectional view of a reinforced wind turbine blade according to the invention showing the blade with two webs and two reinforcing floors, one extending from a trailing edge and one extending from a leading edge to each of the webs,

Fig. 15 is a schematic cross-sectional view of a reinforced wind turbine blade according to the invention showing the blade with two webs and one reinforcing floor extending between the two webs,

Fig. 16 is a schematic cross-sectional view of a reinforced wind turbine blade according to the invention showing the blade with no webs and one reinforcing floor extending from a trailing edge to a leading edge,

Fig. 17 shows the deformation of a conventional wind turbine blade at a sector near the middle of the blade,

Fig. 18 shows the deformation of a wind turbine blade according to the invention at a sector near the middle of the blade,

Fig. 19 shows the deformation of a conventional wind turbine blade at a sector near the root of the blade, and

Fig. 20 shows the deformation of a wind turbine blade according to the invention at a sector near the root of the blade.

The present invention will now be described more fully hereinafter with reference to the accompanying drawings, in which exemplary embodiments of the invention are shown. The invention may, however, be embodied in different forms and should not be construed as limited to the embodiments set forth herein. Rather, these embodiments are provided so that this disclosure will be thorough and complete, and will fully convey the scope of the invention to those skilled in the art. The figures are schematic and simplified for clarity, and they merely show details which are essential to the understanding of the invention,

while other details have been left out. Throughout, the same reference numerals are used for identical or corresponding parts.

Fig. 1 shows a cross-section of a wind turbine blade 1 indicating (by punctured line) a deformation of the blade shell (or panel) 2 between a trailing edge 4 and an internal girder/web 5 due to flapwise loads originating from the aerodynamic and inertia forces on the blade in operation. The flapwise direction is illustrated by arrow A in Fig. 3. The shell 2 shown in this embodiment comprises two shell parts, designated in this example as upper part 6 and lower part 7. The upper and lower shell parts are connected by bonding in joints 8 and 9 (not indicated), preferably in or close to the leading and trailing edges 3 and 4 respectively, of the blade.

Fig. 2 shows a perspective view of a wind turbine blade 1 indicating a deformation (drawn exaggerated for the purpose of clarity) in the trailing edge 4 of the blade in the form of a buckling pattern caused by an edgewise load indicated by arrow F.

Fig. 3 shows a principle cross-section of a wind turbine blade 1 having a shell 2 with leading edge 3 and trailing edge 4. Also indicated is a box profile "composed by" two webs 5 and sections 10 and 11 of the shell 2 located between the webs. The aerodynamic and inertia forces working on a blade in operation induce a bending moment on the blade and create a crushing pressure indicated by arrows B. The crushing pressure is also referred to as the Brazier effect (reference is made to the article "Structural testing and numerical simulation of a 34 m composite wind turbine blade" by F. M. Jensen et.al. published by Elsevier in Composite Structures 76 (2006) 52-61). The flapwise direction is illustrated by arrow A.

Fig. 4 shows a schematic partial view of a cross-section of the blade 1. The blade is shown in a loaded or ovalized state, indicated by the punctured line. The figure also indicates a cross-section of the blade in a neutral or un-loaded position (fully drawn line). The figure is intended to support the understanding of how the forces on the blade cause its cross-sectional profile/shape to vary. The repeated exposure to ovalization adds to fatiguing the blade structure over time.

Fig. 5 is divided into two schematic, perspective views of a wind turbine blade 1. Fig. 5a indicates the transverse shear forces (arrows C) on the blade profile and Fig. 5b indicates in principle the resulting deformed blade profile from the influence of the transverse shear forces. The blade 1 is illustrated as being "twisted clockwise" by the transverse forces.

Fig. 6 shows a cross-section of a reinforced wind turbine blade 20 according to the invention where the blade 20 has two webs 25. Along with the shell 22, the girders form a box profile. The top and bottom of the box profile are often referred to as the caps. The

caps follow the aerodynamic curved shape of the shell 22 and therefore have a transverse curvature. The caps are reinforced. Elsewhere, the aerodynamic shell is typically only a thin skin or a laminate such as a sandwich construction with thin skins and a core material.

Further, the blade 20 has a reinforcing floor 15 extending from the trailing edge 24 to the closest of the webs 25b. In the illustrated embodiment, the blade shell 22 has an upper part 26 and a lower part 27. The parts are connected to each other by bonding with suitable bonding means in connection joints 28 and 29 in or in the vicinity (near or proximal to) of the leading edge 23 and the trailing edge 24, respectively. In the illustrated embodiment, the floor 15 is connected to the trailing edge section 24 and the web 25b by means of bonding 30, and preferably, the connection 33 of the floor 15 to the web 25b is located substantially halfway between the upper part 26 and lower part 27 of the shell 22 for maximum reinforcement of the blade 20.

Fig. 7 shows a cross-section of a reinforced wind turbine blade 20 according to the invention where the blade 20 has two webs 25 and a reinforcing floor 15 extending from a position on the inner surface of the blade shell 22 in vicinity of the trailing edge 24 and to the closest of the webs 25b. In the illustrated embodiment, the blade shell 22 has an upper part 26 and a lower part 27. The upper and lower parts 26, 27 are connected to each other by bonding with suitable bonding means in connection joints 28 and 29 in or in the vicinity (near or proximal to) of the leading edge 23 and the trailing edge 24, respectively. In this particular figure, the floor 15 is connected to a lower part 27 of the shell 22 in the vicinity of the trailing edge section 24 and to the web 25b by laminating means 31, and preferably, the connection 33 of the floor 15 to the web 25b is located substantially halfway between the upper part 26 and lower part 27 of the shell 22 for maximum reinforcement of the blade 20.

Any suitable connection means or methods between the reinforcing floor 15 and the web 25, between the reinforcing floor 15 and the inner surface of the shell 22 or between the web 25 and the inner surface of the shell 22 may of course be applied in any one of the embodiments described in this application, especially, but not exclusively, bonding, laminating and mechanical means.

Fig. 8 shows the embodiment of Fig. 7 in perspective. For all embodiments, the floor may extend along substantially the entire longitudinal extension of the blade 20 or along substantially the entire longitudinal extension of the girder or web 25 or, the floor may extend along a part of the longitudinal extension of the blade. Further, the floor may be divided into a number of sections in the longitudinal direction of the blade. The reinforcing effect of the floor tends to increase towards the root of the blade 20 and decrease towards the tip of the blade 20.

Fig. 9 shows the cross-section of the blade 20 of Figs. 7 and 8 at the root of the blade 20. It should be noted that the connection point 32 of the floor 15 to the lower part 27 of the shell 22 at the trailing edge 24 is located below the connection joint 29 of the upper part 26 of the shell 22 in a position of minimum distance from the trailing edge 24 to the connection 33 of the floor 15 to the web 25b for maximum reinforcement of the blade 20.

Fig. 10 shows a cross-section of another embodiment of a wind turbine blade 20 according to the invention comprising two webs 25 and a reinforcing floor 15 extending from the leading edge 23 to the closest of the webs 25. The section 29 of the blade shell 22 forming the leading edge 23 is thereby reinforced so that it is considerably thinner than in existing wind turbine blades, thereby reducing weight of the blade 20. Preferably, the connection 34 of the floor 15 to the web 25a is located substantially halfway between the upper part 26 and lower part 27 of the shell 22 for maximum reinforcement of the blade 20.

Fig. 11 shows a cross-section of yet another embodiment of a wind turbine blade 20 according to the invention comprising two webs 25 and two reinforcing floors 15a, 15b. A first reinforcing floor 15a is provided between the leading edge 23 and the web 25a closest thereto and a second reinforcing floor 15b is provided between the trailing edge 24 and the web 25b closest thereto. The reinforcing floor 15b may in embodiments be connected to the trailing edge section 24 in the connection joint 29 between the upper and lower shell 22 parts. In such an embodiment the three parts 26, 27 and 15b are bonded together. In other embodiments the reinforcing floor 15b is connected to either the upper par 26 or preferably the lower part 27 of the shell 22 in the vicinity (near or proximal to) of the trailing edge section 24. Preferably, the connection 34 of the floor 15a to the web 25a is located substantially halfway between the upper part 26 and lower part 27 of the shell 22 for maximum reinforcement of the blade 20; and preferably, the connection 33 of the floor 15b to the web 25b is located substantially halfway between the upper part 26 and lower part 27 of the shell 22 for maximum reinforcement of the blade 20.

Fig. 12 shows a cross-section of an embodiment in which the wind turbine blade 20 comprises a single web 25 and two reinforcing floors 15a, 15b. A first reinforcing floor 15a extends from a position on the inner surface of the shell 22 in the vicinity of the leading edge 23 to a first side of the web 25 and a second reinforcing floor 15b extends from a position on the inner surface of the shell 22 in, or in the vicinity of, the trailing edge 24 to a second side of the web 25. Preferably, the connection 34 of the floor 15a to the web 25 is located substantially halfway between the upper part 26 and lower part 27 of the shell 22 for maximum reinforcement of the blade 20; and preferably, the connection 33 of the floor 15b to the web 25 is located substantially halfway between the upper part 26 and lower part 27 of the shell 22 for maximum reinforcement of the blade 20.

Fig. 13 shows another cross-sectional view of an embodiment of a wind turbine blade 20 comprising two webs 25 and a single reinforcing floor 15 extending from a position in the vicinity of the connection joint 28 in the leading edge section 23 to a position in the vicinity of the connection joint 29 in the trailing edge section 24 of the blade 20. The webs 25 are divided in two and abut the reinforcing floor 15 on both sides thereof.

Fig. 14 shows yet another example of a cross-section of an embodiment in which the wind turbine blade 20 comprises two webs 25 divided in two (25c and 25d) and further two reinforcing floors 15a and 15b. A first reinforcing floor 15a extends from a position on the inner surface of the shell 22 in the vicinity of the leading edge 23 to the webs 25c and a second reinforcing floor 15b extends from a position on the inner surface of the shell 22 in, or in the vicinity of, the trailing edge 24 to the webs 25d. Preferably, the floors 15a, 15b extend along substantially coinciding planar surfaces.

Fig. 15 is a schematic cross-sectional view of a reinforced wind turbine blade 20 according to the invention with two webs 25a, 25b and one reinforcing floor 15 extending between the two webs 25a, 25b. Preferably, the connection 34 of the floor 15a to the web 25 is located substantially halfway between the upper part 26 and lower part 27 of the shell 22 for maximum reinforcement of the blade 20; and preferably, the connection 33 of the floor 15b to the web 25 is located substantially halfway between the upper part 26 and lower part 27 of the shell 22 for maximum reinforcement of the blade 20. The reinforcing floor 15 may also extend along a plane interconnecting the trailing edge 24 and leading edge 23 of the blade 20.

A force in the flapwise direction applied to the caps between the two webs 25 urges the caps towards the inner volume of the shell 22 and also urges the two connections 33, 34 away from each other. However, the reinforcing floor keeps the two connections 33, 34 in substantially mutually fixed positions and thus prevents the distance between the connections 33, 34 from increasing or decreasing thereby strengthening the blade 20 against forces in the flapwise direction. Thus, the reinforcing floor 15 desirably has a high stiffness.

In an embodiment wherein a flapwise force would increase the distance between the connections 33, 34, the floor 15 desirably has a high tensional strength while the reinforcing floor 15 need not be capable of resisting compression forces. Preferably, the reinforcing floor 15 has a straight shape, such as the shape of a rod or a stretched wire or a planar member. In the event that the shape of the reinforcing element is not straight, the shape of the reinforcing element could be straightened when subjected to stretching forces leading to movement of its end points and obviously, this is not desired.

The at least one reinforcing element may comprise a bar or a rod-like element. The element may be solid or hollow or any suitable combination thereof. Alternatively, the at least one reinforcing element may comprise wire, rope, cord, thread or fibres. They may be applied individually or may be applied as a number of individual elements together forming a "thicker" element. Particularly, the element may comprise fibres of very high stiffness and strength such as, but not limited to, aramid fibres.

Further, the at least one reinforcing element may comprise a plate. The plate element may be solid or hollow or any suitable combination thereof. The plate material may comprise any of metal, metal alloy, wood, plywood, veneer, glass fibre, carbon fibre and other suitable materials such as e.g. one or more composite materials. The element may further be provided as netting or a web comprising one or more of wire, rope, cord, thread or fibres. The plate element may alternatively comprise a textile or a fabric material. The fabric material may be manufactured from materials such as, but not limited to carbon fibres or aramid fibres thus providing a high strength and a low weight. If suitable, glass fibres may also be used.

The mentioned materials may also be combined to any construction. Thus, in another embodiment the at least one reinforcing element is a laminate or a sandwich construction.

In order to obtain a high resistance against flapwise forces, the reinforcing floor 15 also has a high strength against compression forces. In this case, the webs 25a, 25b and the reinforcing floor 15 cooperate to form an I-profile wherein the floor 15 forms the body of the I-profile. The formed I-profile has a high stiffness against bending forces applied in the edgewise direction of the blade 20.

An embodiment of the invention was analysed with respect to increased strength as compared to a conventional wind turbine blade using experimental substructure test performed on a part of the load carrying girder of a 34 m wind turbine blade designed for use on a 1.5 MW wind turbine.

The test is described in "Experimental and numerical analysis of a wind turbine blade cross section - Under lateral load conditions". Rune F. Nielsen. Student Report (special course) - Technical University of Denmark and Risø National Laboratory. (December 2006).

In this embodiment the invention prevents the webs of the girder to collapse from the crushing pressure induces by the aerodynamic and inertia forces working on a blade in operation.

The result showed an increase of more that 50% of the ultimate crushing pressure the web can withstand compared to a conventional box girder.

Fig. 16 shows a cross-section of still another embodiment of the invention in which the wind turbine blade 20 comprises a shell 22 without webs and with a reinforcing floor 15 extending from a position on the inner surface of the shell 22 in the vicinity of the trailing edge 24 to a position on the inner surface of the shell 22 in the vicinity of the leading edge 23. The reinforcing floor 15 has a high stiffness against bending forces applied in the edgewise direction of the blade 20. An embodiment of the invention was analysed with respect to increased strength as compared to a conventional wind turbine blade using numerical modelling of a 34 m wind turbine blade designed for use on a 1.5 MW wind turbine.

The numerical analysis included Finite Element analysis of a model containing more than 150 000 shell and 3D elements. Advanced software and algorithms were used in the analysis to account for the effect of nonlinear geometrical deformations.

The model of the blade has been verified with full-scale test of the blade ("Structural testing and numerical simulation of a 34 m composite wind turbine blade" by F. M. Jensen et.al. published by Elsevier in Composite Structures 76 (2006) 52-61). The blade was loaded in the edgewise direction with loads that were similar to the certification loads for the blade. The combined loads in both the flapwise and edgewise direction were loads that should simulate to the operational loads for the blade.

The analysis showed a significant reduction of the deformation of the trailing edge section of the shell when the blade is equipped with the invention, in both edgewise loads and a combination of flapwise and edgewise loads. Figs. 17 and 18 show the results of the analysis of a sector near the middle of the blade, and Figs. 19 and 20 show the results of the analysis of a sector near the root of the blade.

The reduction of the deformation of the shell section reduces the peeling stresses in the trailing edge of the blade and therefore improves the reliability of the adhesive joint of the trailing edge

Furthermore, the aerodynamic efficiency of the blade is also improved since the designed shape of the blade profile is maintained to a higher degree.

Furthermore the analysis showed a significant reduction of the distortion of the profile and this increase the blade's resistance to the crushing pressure and thereby increases the ultimate strength of the wind turbine blade.

Although the present invention has been described in connection with the specified embodiments it should not be construed as being in any way limited to the presented examples. The scope of the present invention is set out by the accompanying claim set. In

the context of the claims, the terms "comprising" or "comprises" do not exclude other possible elements or steps. Also, the mentioning of references such as "a" or "an" etc. should not be construed as excluding a plurality. The use of reference signs in the claims with respect to elements indicated in the figures shall also not be construed as limiting the scope of the invention. Furthermore, individual features mentioned in different claims, may possibly be advantageously combined, and the mentioning of these features in different claims does not exclude that a combination of features is not possible and advantageous.

CLAIMS

1. A wind turbine blade comprising

a shell having a section with an aerodynamic profile, and

at least one internal reinforcing floor connected inside the shell for increasing the strength of the blade and having a cross section transversely to the longitudinal extension of the blade that extends substantially in a direction from the trailing edge to the leading edge of the blade.

2. A wind turbine blade according to claim 1, wherein the at least one internal reinforcing floor is connected to an inner surface of the shell at one of the trailing edge and the leading edge of the blade.

3. A wind turbine blade according to claim 2, wherein the at least one internal reinforcing floor is connected to the inner surface of the shell at the trailing edge of the blade.

4. A wind turbine blade according to claim 3, wherein the shell has a cylindrical root section for mounting of the blade on a wind turbine shaft, and wherein the at least one internal reinforcing floor is connected to the inner surface of the shell at the trailing edge along at least a part of the transition between the shell with the aerodynamic profile and the root section.

5. A wind turbine blade according to any of the preceding claims, further comprising at least one girder, and wherein the at least one internal reinforcing floor is connected to the at least one internal girder.

6. A wind turbine blade according to claim 5, wherein a connection between one of the at least one internal reinforcing floor and a respective one of the at least one internal girder is located with a shortest distance to the shell that is larger than 0.16 times the total distance between the upper part of the shell and the lower part of the shell along a transversal extension of the respective girder comprising the connection.

7. A wind turbine blade according to claim 5 or 6, comprising a first and a second girder, and wherein one of the at least one internal reinforcing floor is connected to the first and the second girder.

8. A wind turbine blade according to any of the preceding claims, wherein the at least one internal reinforcing floor comprises a textile or a fabric material with high tensional strength without a capability of resisting compression forces.

9. A wind turbine blade according to any of the preceding claims, wherein the at least one internal reinforcing floor is a plate element.

10. A wind turbine blade according to claim 9, wherein at least a part of the plate element is of a laminated construction.

11. A wind turbine blade according to any of claims 9 or 10, wherein the plate element comprises one or more stiffeners.

12. A wind turbine blade according to any one of claims 9-11, wherein the plate element is provided with one or more cut-outs.

13. A method of increasing the strength of a wind turbine blade having a shell with a section having an aerodynamic profile, the method comprising the step of positioning and connecting at least one internal reinforcing floor inside the shell for extension substantially in a direction from the trailing edge to the leading edge of the blade.

14. A method according to claim 13, wherein the step of positioning and connecting includes connecting the at least one internal reinforcing floor to the inner surface of the shell at the trailing edge of the blade.

15. A method according to claim 14, wherein the shell further has a cylindrical root section for mounting of the blade on a wind turbine shaft, and wherein the method further comprises the step of connecting the at least one internal reinforcing floor to the inner surface of the shell at the trailing edge along at least a part of the transition between the section of the shell with the aerodynamic profile and the root section.

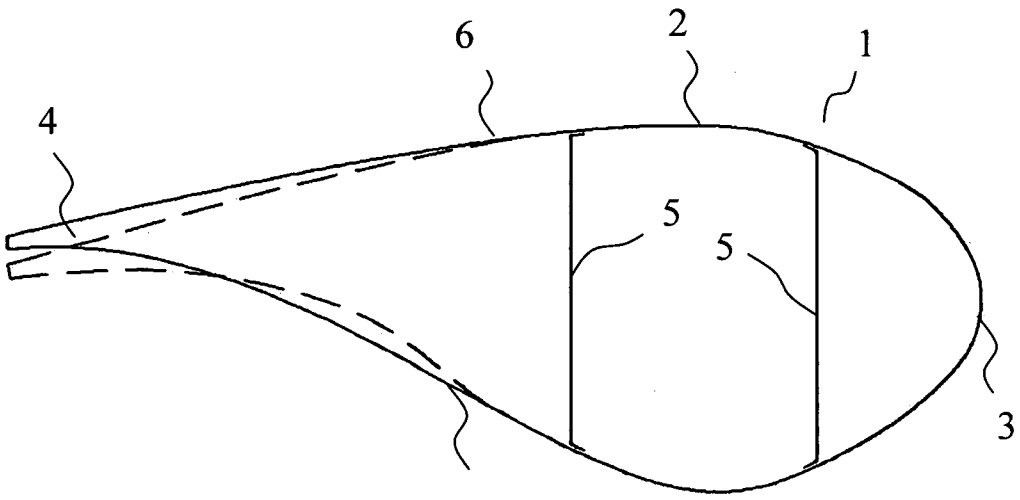

Fig. 1

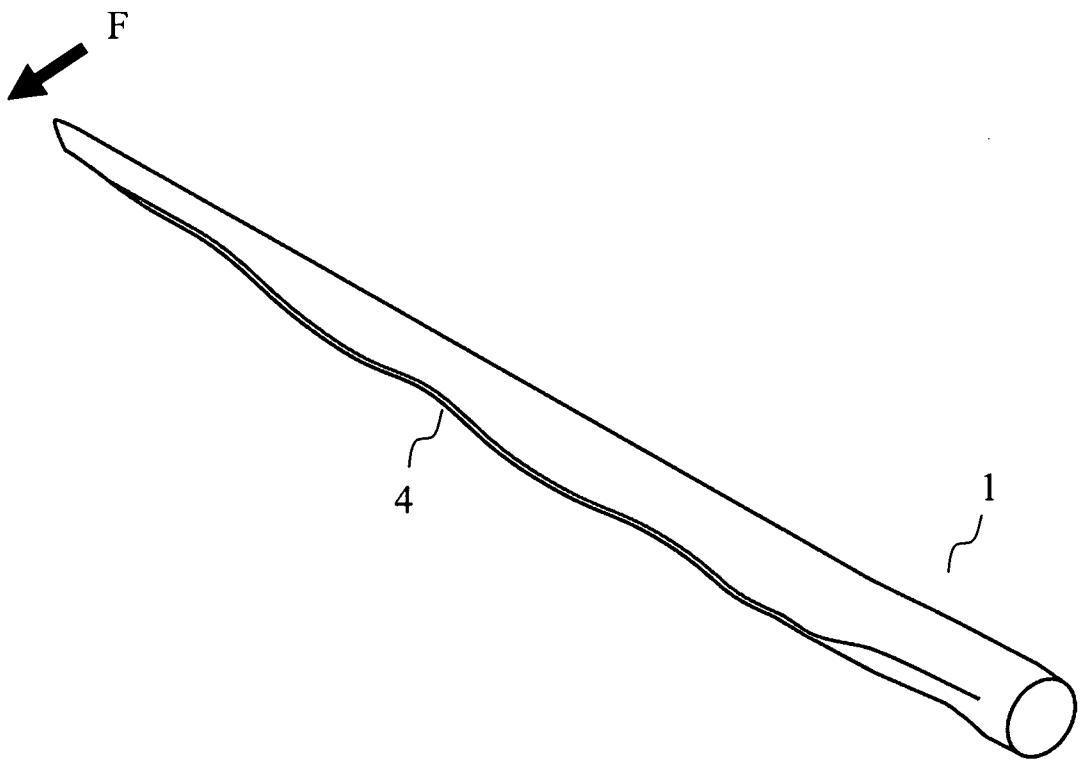

Fig. 2

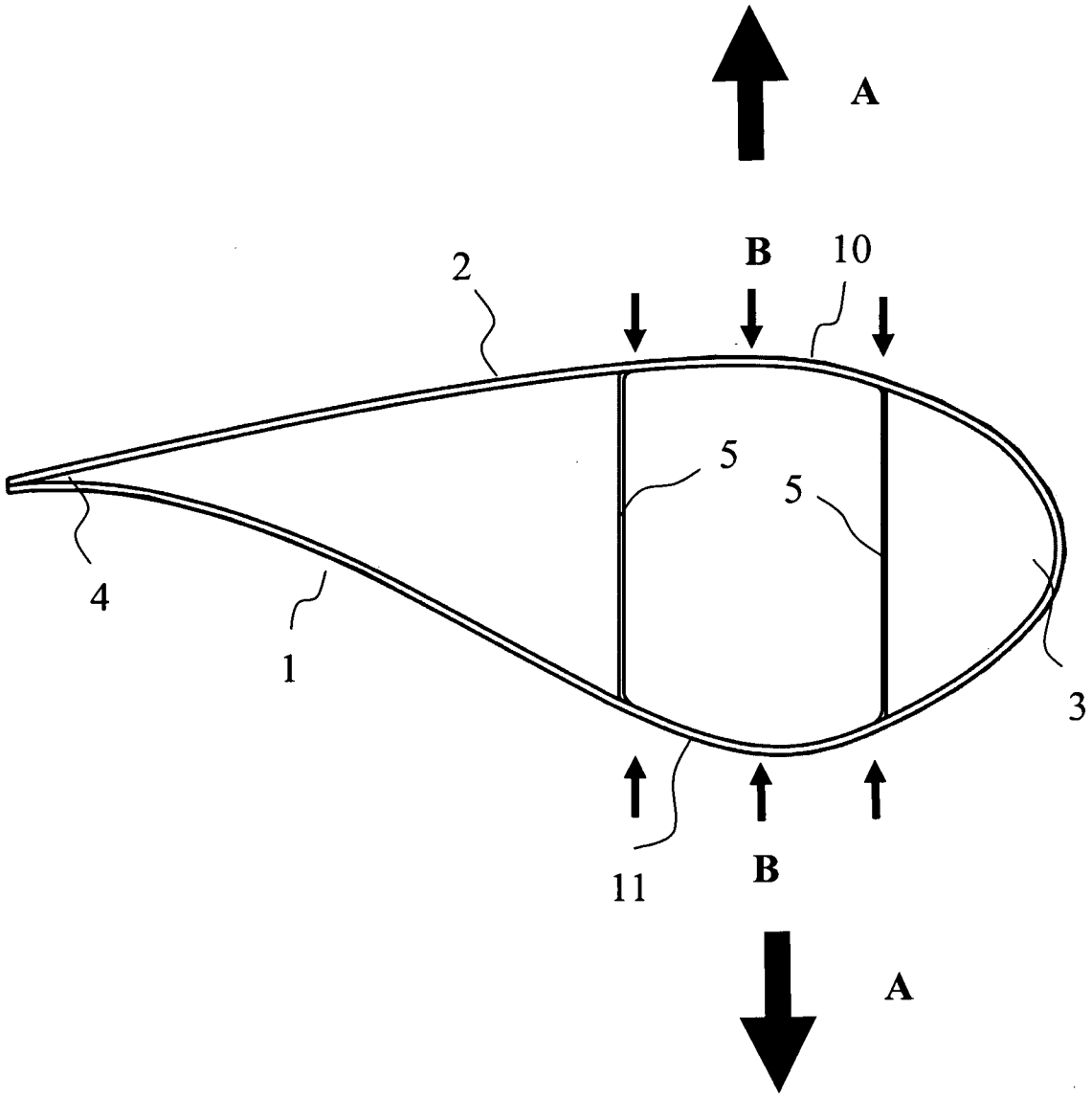

Fig. 3

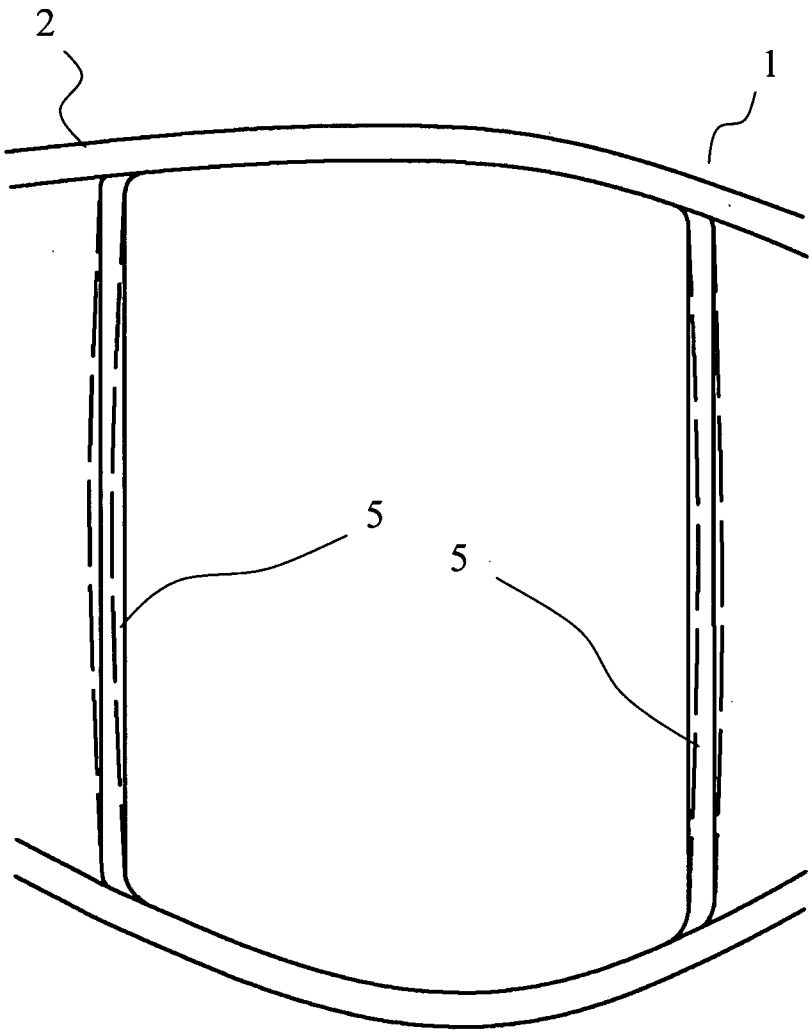

Fig. 4

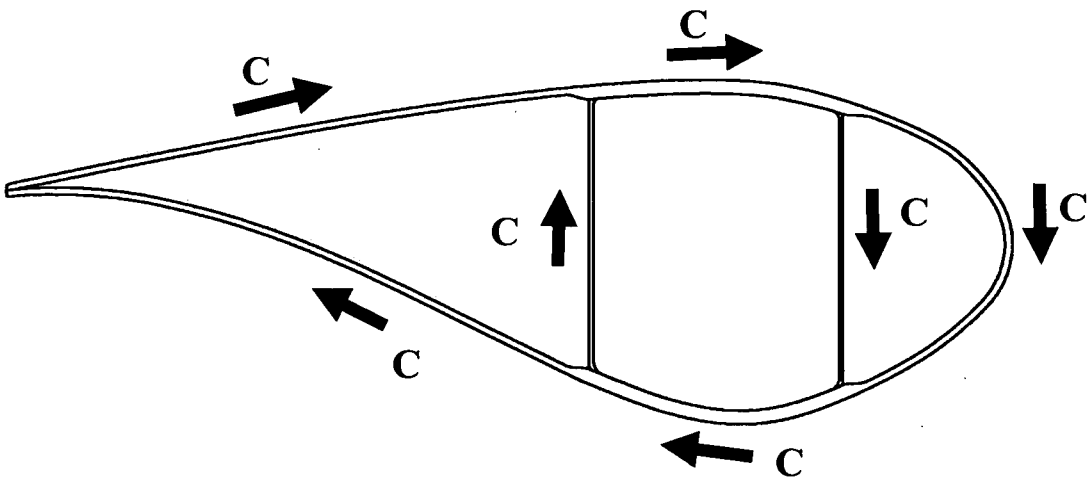

Fig. 5a

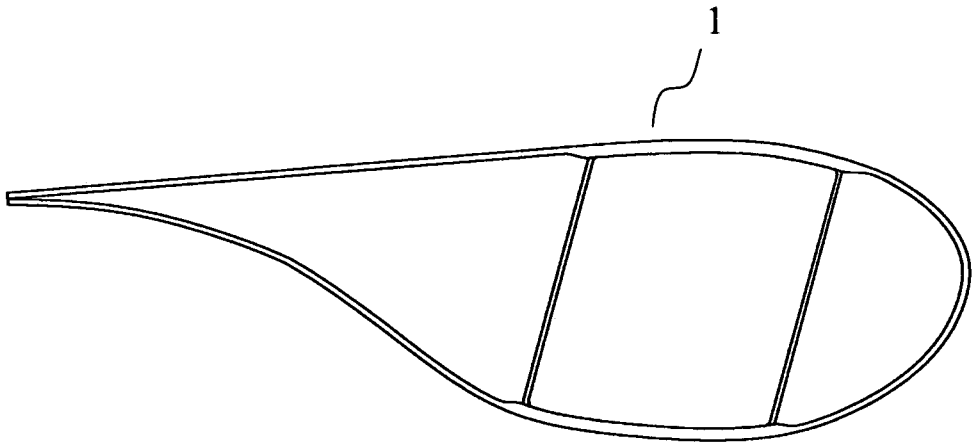

Fig. 5b

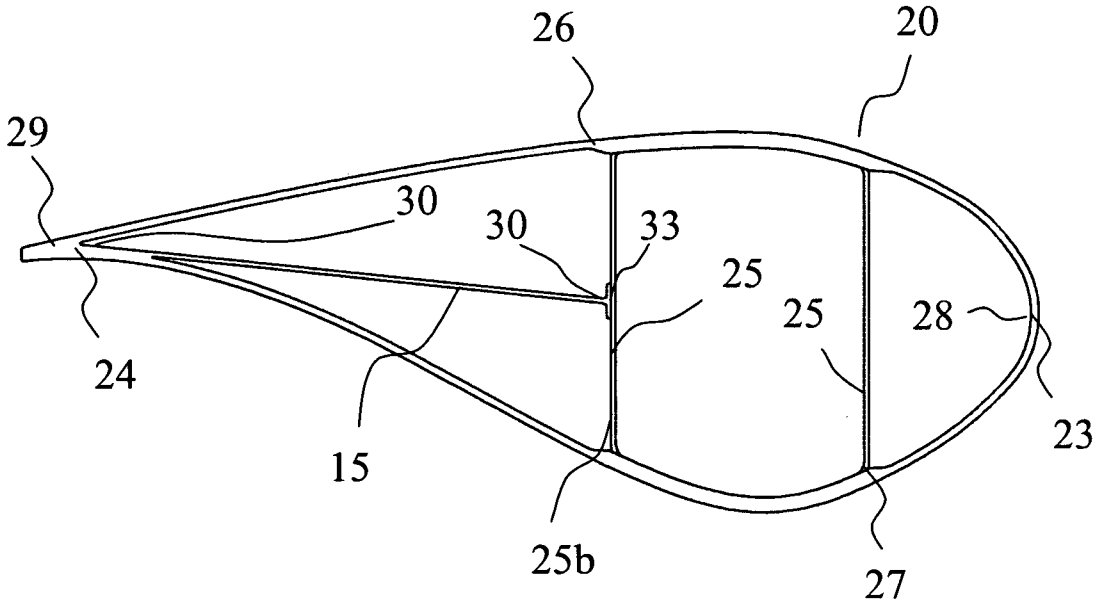

Fig. 6

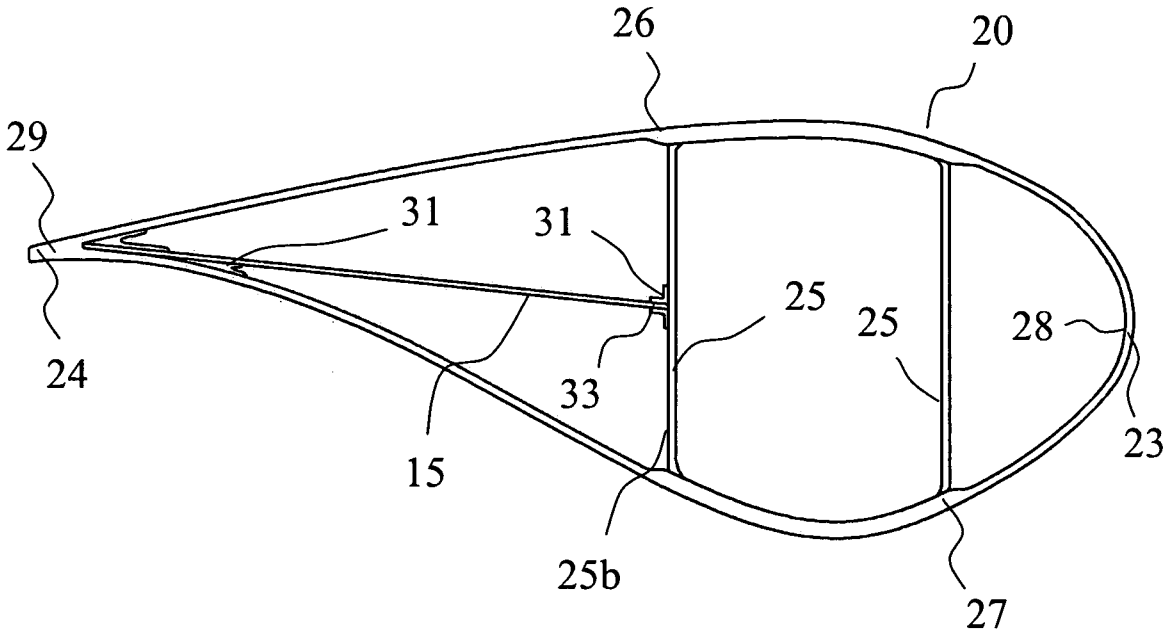

Fig. 7

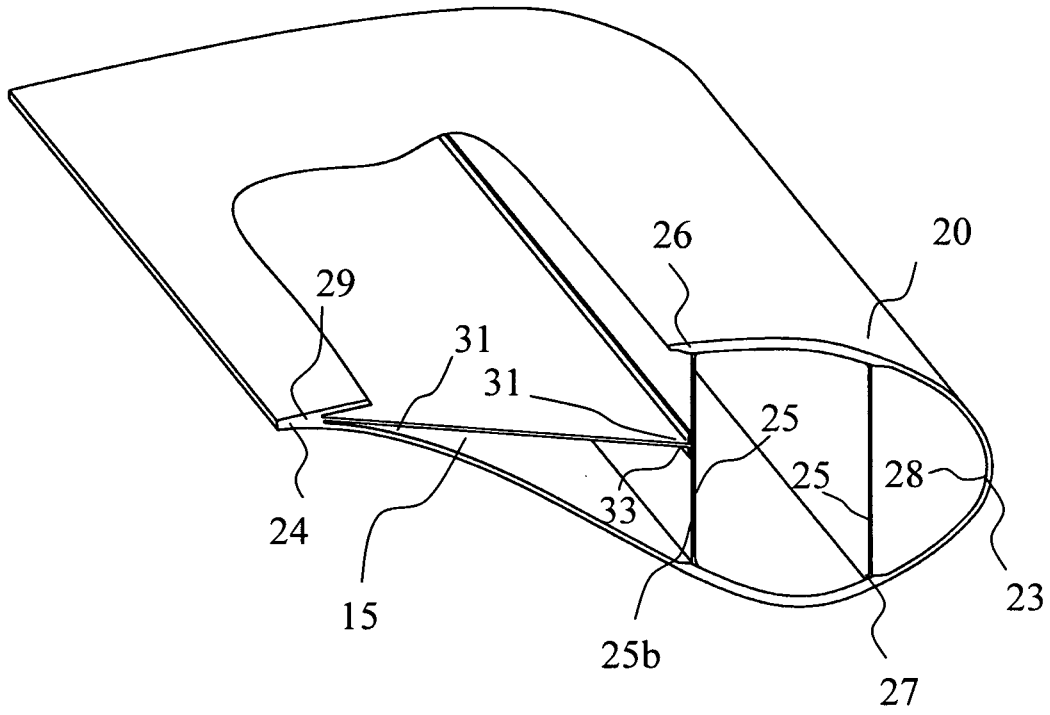

Fig. 8

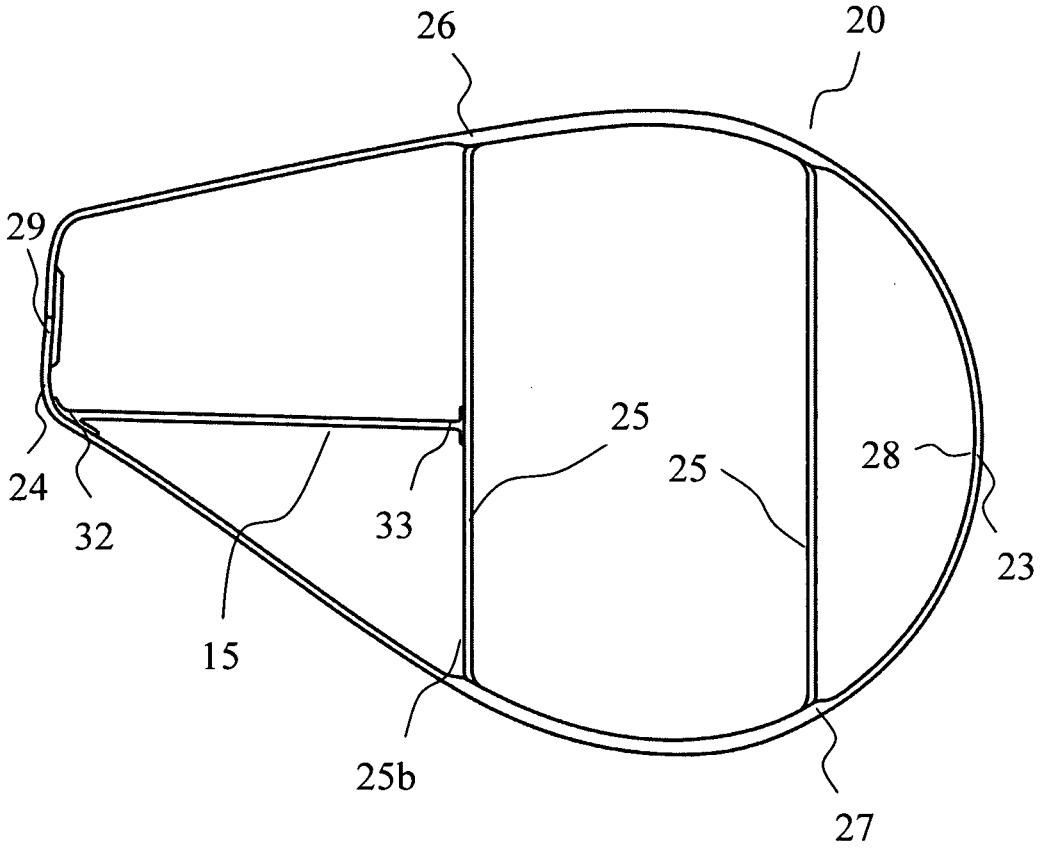

Fig. 9

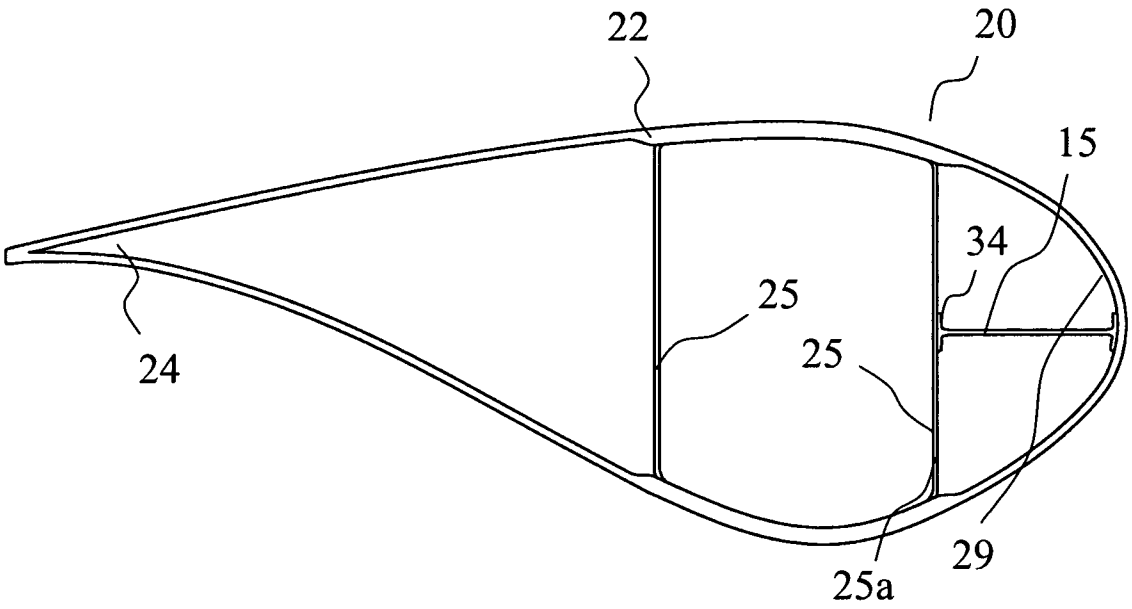

Fig. 10

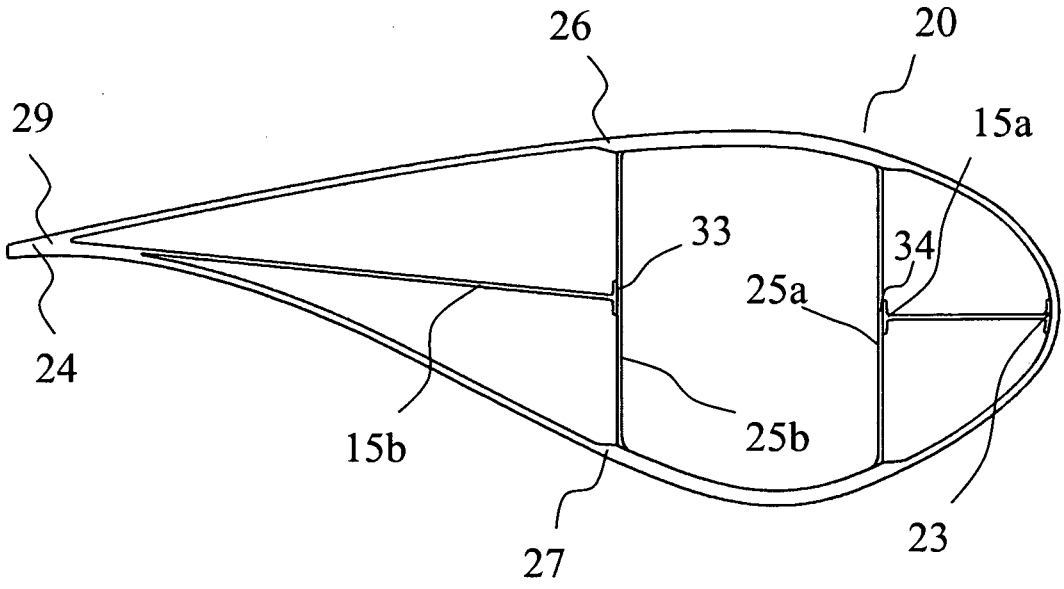

Fig. 11

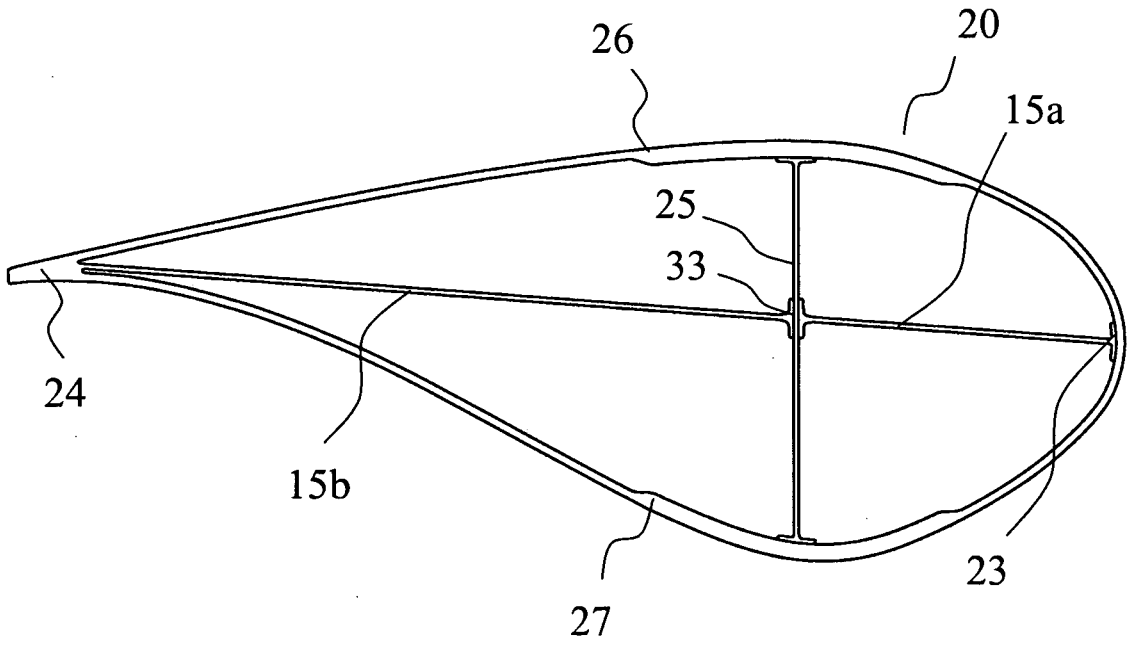

Fig. 12

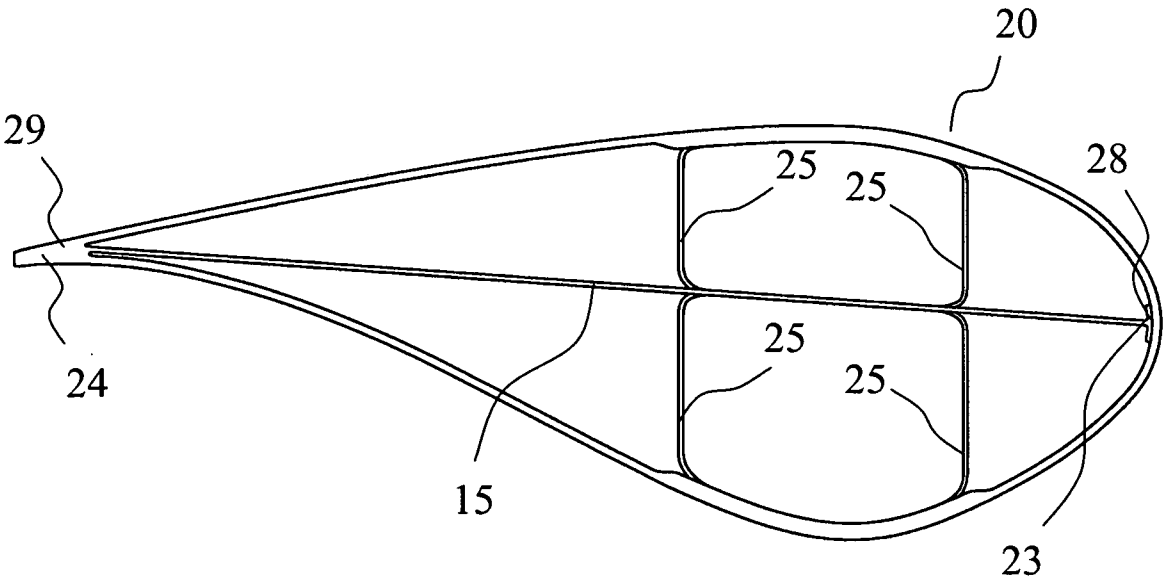

Fig. 13

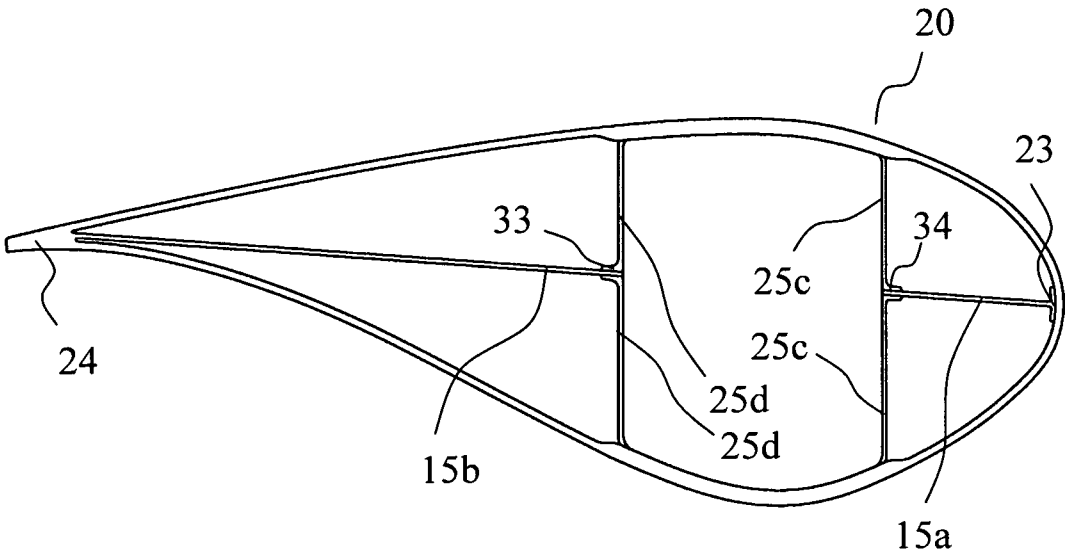

Fig. 14

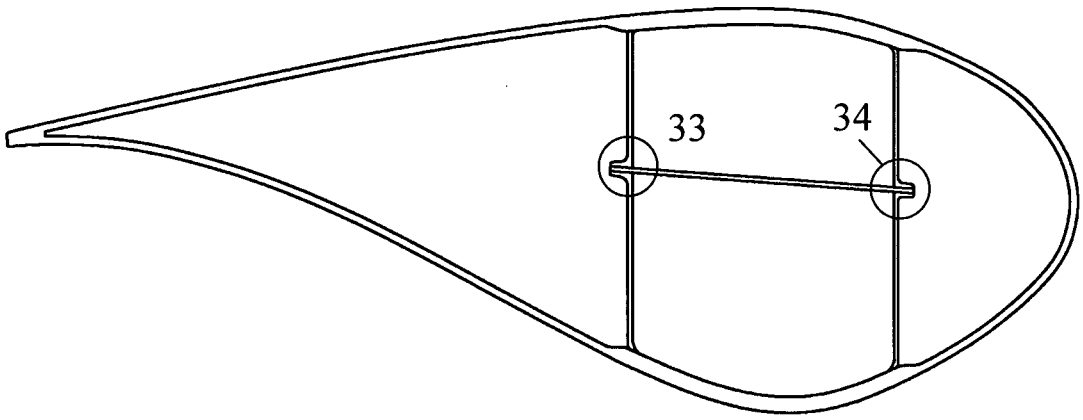

Fig. 15

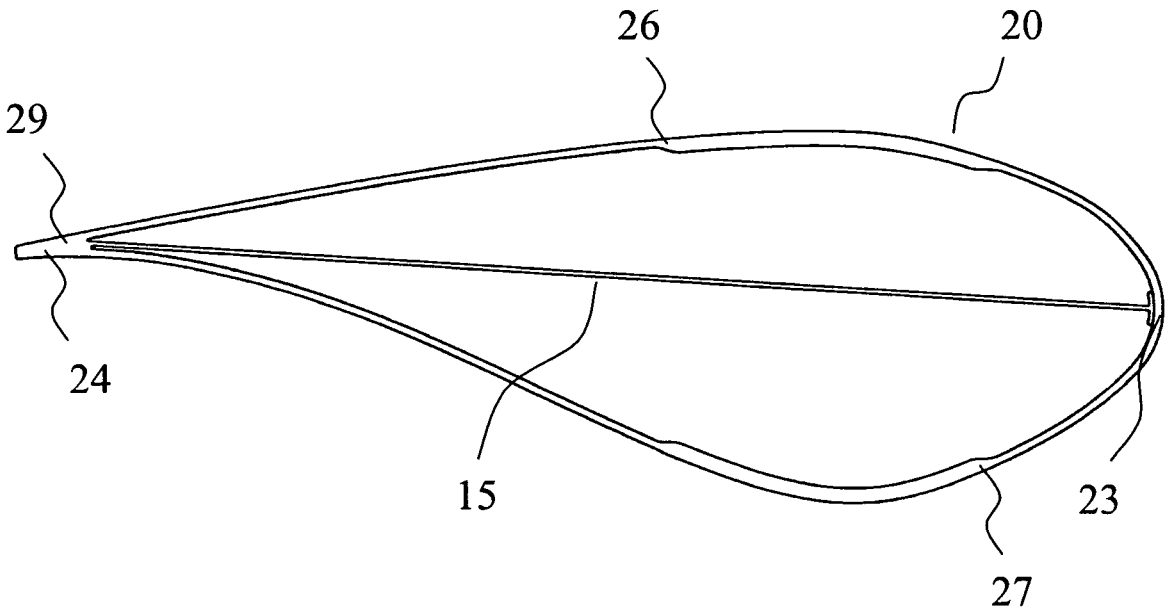

Fig. 16

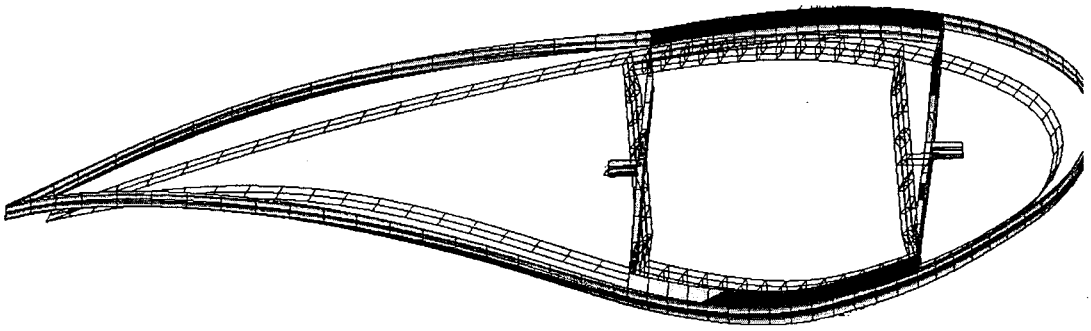

Fig. 17

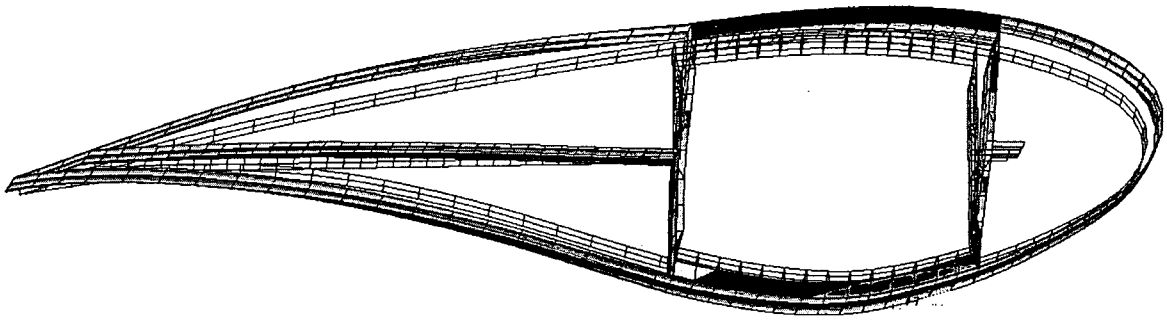

Fig. 18

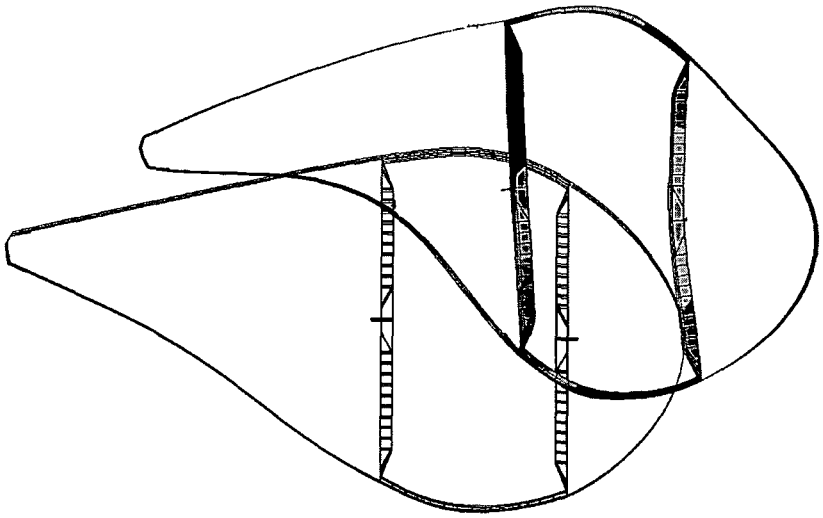

Fig. 19

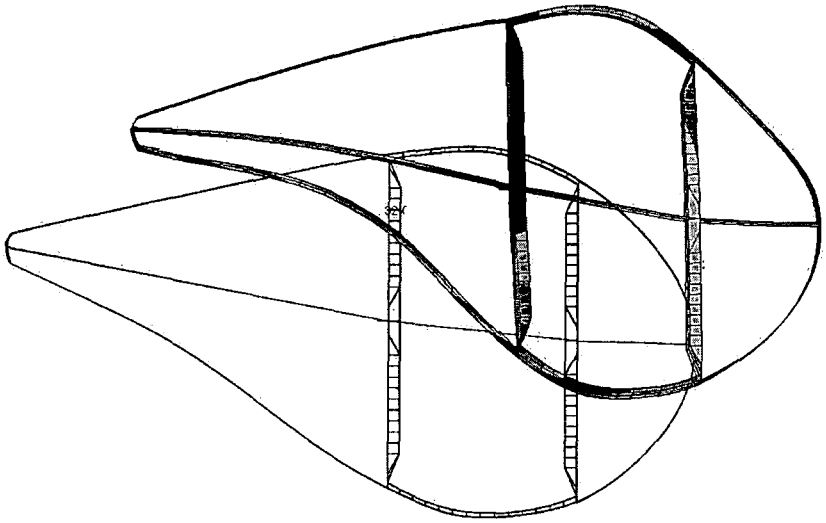

Fig. 20

Appendix B3 - “WO 2008-089765 Reinforced blade for wind turbine (shear cross- patent C)”. Find M. Jensen, Per H. Nielsen

(12) INTERNATIONAL APPLICATION PUBLISHED UNDER THE PATENT COOPERATION TREATY (PCT)

(19) World Intellectual Property Organization
International Bureau

(43) International Publication Date
31 July 2008 (31.07.2008)

PCT

(10) International Publication Number
WO 2008/089765 A2

(51) International Patent Classification:
F03D 1/06 (2006.01)

(21) International Application Number:
PCT/DK2008/000032

(22) International Filing Date: 25 January 2008 (25.01.2008)

(25) Filing Language: English

(26) Publication Language: English

(30) Priority Data:
PA 2007 00118 25 January 2007 (25.01.2007) DK

(71) Applicant *(for all designated States except US)*: **DANMARKS TEKNISKE UNIVERSITET** [DK/DK]; Anker Engelundsvej 1, Bygning 101A, DK-2800 Kgs. Lyngby (DK).

(72) Inventors; and
(75) Inventors/Applicants *(for US only)*: **JENSEN, Find, Mølholt** [DK/DK]; Emilsgave, 8, DK-4130 Viby Sjælland (DK). **NIELSEN, Per, Hørlyk** [DK/DK]; Føns Strandvej 15, DK-5580 Nr.Aaby (DK).

(74) Agent: **ALBIHNS A/S**; Havneholmen 29, bygn. 2, 3. sal, DK-1561 København V (DK).

(81) Designated States *(unless otherwise indicated, for every kind of national protection available)*: AE, AG, AL, AM, AO, AT, AU, AZ, BA, BB, BG, BH, BR, BW, BY, BZ, CA, CH, CN, CO, CR, CU, CZ, DE, DK, DM, DO, DZ, EC, EE, EG, ES, FI, GB, GD, GE, GH, GM, GT, HN, HR, HU, ID, IL, IN, IS, JP, KE, KG, KM, KN, KP, KR, KZ, LA, LC, LK, LR, LS, LT, LU, LY, MA, MD, ME, MG, MK, MN, MW, MX, MY, MZ, NA, NG, NI, NO, NZ, OM, PG, PH, PL, PT, RO, RS, RU, SC, SD, SE, SG, SK, SL, SM, SV, SY, TJ, TM, TN, TR, TT, TZ, UA, UG, US, UZ, VC, VN, ZA, ZM, ZW.

(84) Designated States *(unless otherwise indicated, for every kind of regional protection available)*: ARIPO (BW, GH, GM, KE, LS, MW, MZ, NA, SD, SL, SZ, TZ, UG, ZM, ZW), Eurasian (AM, AZ, BY, KG, KZ, MD, RU, TJ, TM), European (AT, BE, BG, CH, CY, CZ, DE, DK, EE, ES, FI, FR, GB, GR, HR, HU, IE, IS, IT, LT, LU, LV, MC, MT, NL, NO, PL, PT, RO, SE, SI, SK, TR), OAPI (BF, BJ, CF, CG, CI, CM, GA, GN, GQ, GW, ML, MR, NE, SN, TD, TG).

Published:
— *without international search report and to be republished upon receipt of that report*

(54) **Title:** REINFORCED BLADE FOR WIND TURBINE

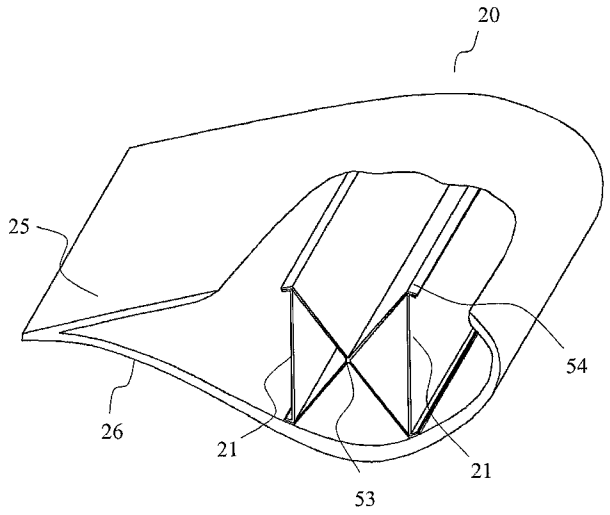

Fig. 10

(57) **Abstract:** The invention introduces a reinforcement of a box girder of a wind turbine blade. The reinforcement prevents the transverse shear distortion of the blade structure, when the blade is loaded during operation. The reinforcement connects the corners diagonally opposite inside the girder, and fixes them in relation to each other. The reinforcement increases the blade's resistance to overall collapse. The reinforcement comprises one or more individual element, such as rods or plates.

WO 2008/089765 A2

REINFORCED BLADE FOR WIND TURBINE

The present invention relates to a reinforced blade for a wind turbine, particularly to a blade having reinforcing members for reinforcing one or more structural members in the blade in order to prevent transverse shear distortion of the blade when it is loaded in operation.

Typically, a wind turbine blade has an aerodynamic shell and a girder, such as a beam or a spar. The girder can be a single beam, but often two girders are used. The two girders together with the parts of the shell extending between the two girders form a so-called box profile. The top and bottom of the box profile are often referred to as the caps. Some types of blades are designed with a spar in the form of a box profile which is manufactured separately and bonded in between prefabricated surface shells. The aerodynamic shell is typically made of a laminate of fibre reinforced plastics, fibreglass and/or other materials. Typically, the aerodynamic shell is made from two shell parts that are assembled to form the shell.

Under normal operation conditions, the wind turbine blade is subjected to loads at an angle to the flapwise direction. It is common to resolve this load on the blade into its components in the flapwise and edgewise direction. The flapwise direction is a direction substantially perpendicular to a transverse axis through a cross-section of the blade. The flapwise direction may thus be construed as the direction, or the opposite/reverse direction, in which the aerodynamic lift acts on the blade. The edgewise loads occur in a direction perpendicular to the flapwise direction. The blade is further subject to torsional loads which are mainly aerodynamic and inertia loads. These loads can subject the blade to harmonic motions or oscillations at the blade's torsional eigenfrequency; cf. Fig. 1 for an indication of the loads and the directions.

During operation of the blade, transverse shear forces are generated in the blade by the flapwise and edgewise loads. The transverse shear forces are indicated on a typical cross-section of the blade shown in Fig 2a. The transverse shear forces are induced by the flapwise and edgewise loads because of the typical asymmetric geometry and material distribution of the blade. Further, the fact that the flapwise and edgewise loads do not act through the shear centre of the blade contributes to the generation of transverse shear forces.

In a box profile, the transverse shear forces result in high in-plane bending moments in the corners of the box profile. The bending moments may be counteracted by increasing the thickness of the box profile material in the corners, but increased thickness adversely affects the weight of the blade without a justifying contribution to the strength.

In wind turbine blades where the girders are manufactured separately and bonded to the shell parts, restraints in the manufacturing process result in small material thicknesses in the section of the girder that is connected to the shell part and therefore this part of the blade has a low bending stiffness.

The low bending stiffness of the corners of the box profile combined with the high bending moments in the same area, means that the box profile is easily distorted by transverse shear forces, despite the fact that the side, top and bottom of the box profile may be relatively thick.

An example of the result of the transverse shear distortion caused by the transverse shear forces is shown in Fig. 2b. The distortion consequently changes the shape of the blade and this has an adverse effect on the blade's ultimate strength. If the transverse shear distortion exceeds a certain limit which depends on the geometry and the material distribution of the blade, the blade's resistance to crushing pressure is reduced and a sudden collapse of the blade can occur. The crushing pressure is caused by the flapwise loads and occurs in the box profile of the blade due to its longitudinal curvature. This effect is also often referred to as ovalization, c.f. Fig. 3. For a further explanation of the effects of crushing pressure, reference is made to the article "Structural testing and numerical simulation of a 34 m composite wind turbine blade" by F. M. Jensen et.al. published by Elsevier in Composite Structures 76 (2006) 52-61.

Furthermore, a deformation of the girder at the connection between the girder and the shell can lead to fatigue failure of the girder or fatigue failure in the connection between the girder and the shell or both.

Thus, there is a need for a wind turbine blade in which the structural layout of the blade profile is designed against transverse shear distortion and wherein the blade structure is generally strengthened without increasing the overall weight. It is further desirable to provide a wind turbine blade with an increased torsional stiffness.

It is therefore an object of the invention to provide a wind turbine blade that is designed against transverse shear distortion by transverse shear forces caused by flapwise and edgewise loads on the blade.

It is also an object of the present invention to provide a reinforced blade profile for a wind turbine blade.

It is a further object to provide a wind turbine blade with an increased torsional stiffness which will decrease the dynamic inertia loads of the blade on the other structural parts of the wind turbine, such as the gearbox and the tower.

It is therefore an object of the present invention to provide a wind turbine blade with improved resistance against deformations of the blade profile.

It is yet another object of the present invention to provide a wind turbine blade with increased overall strength and stiffness.

It is yet another object of the present invention to provide a wind turbine blade with increased resistance to fatigue failure.

It is yet another object of the present invention to provide a wind turbine blade, which can be produced at a reduced manufacturing cost compared to the existing solutions.

It is still another object of the invention to provide wind turbine blade capable of working under severe aerodynamic loads and to optimize the aerodynamic stability, e.g. aeroelastic stability of the blade.

It is further an object of the present invention to provide alternatives to the prior art.

According to a first aspect of the invention, the above-mentioned and other objects are fulfilled by a wind turbine blade comprising a shell, a first girder, and a reinforcing member for inhibiting transverse shear distortion of the blade, wherein the reinforcing member is a straight or linear reinforcing member with a first end and a second opposite end, and wherein the first end is connected to the first girder at a connection between the first girder and the shell at the upper part or the lower part of the shell and the second end is connected to the opposite part of the shell at a distance from the girder.

According to a second aspect of the invention, the above-mentioned and other objects are fulfilled by a wind turbine blade comprising a shell, a first girder, and a reinforcing member for inhibiting transverse shear distortion of the blade, wherein the reinforcing member is a reinforcing angle bar with a first leg abutting the first girder, and a second leg abutting the upper part or the lower part of the shell.

According to a third aspect of the invention, the above-mentioned and other objects are fulfilled by a method of inhibiting transverse shear distortion in a wind turbine blade with a shell and a first girder, the method comprising the steps of providing a straight or linear reinforcing member with a first end and a second opposite end, and connecting the first end to the first girder at a connection between the first girder and the shell at the upper part or the lower part of the shell, and connecting the second end to the opposite part of the shell at a distance from the girder.

According to a fourth aspect of the invention, the above-mentioned and other objects are fulfilled by a method of inhibiting transverse shear distortion in a wind turbine blade with a shell and a first girder wherein the first girder is connected to an upper part of the shell and a lower part of the shell, the method comprising the steps of providing a reinforcing angle bar having a first leg and a second leg; and connecting the first leg to the first girder, and connecting the second leg to the upper part or the lower part of the shell.

A wind turbine blade having a reinforcing member according to the present invention reduces the transverse shear distortion of the profile and thus increases the blade's resistance to the crushing pressure and thereby increases the ultimate strength of the wind turbine blade. Furthermore, the aerodynamic efficiency of the blade is also improved since the designed shape of the blade profile is maintained to a higher degree than for a conventional blade.

A reinforcing angle bar according to the invention reduces or eliminates the unwanted transverse shear distortion of the blade caused by transverse shear forces since the reinforcing angle bar maintains interconnected surfaces in fixed positions with relation to each other. This improves the overall strength of the blade and may also facilitate the design of a blade with lower total weight.

A straight reinforcing member keeps its end connections in substantially mutually fixed positions and thus prevents the distance between the connections from increasing thereby inhibiting transverse shear distortion and thus, strengthening the shell against transverse shear forces.

Each of the one or more reinforcing members increases the torsional stiffness of the blade. An increase of the torsional stiffness of the blade will also increase the torsional eigenfrequency of the blade and in return decrease the dynamic inertia loads of the blade on other parts of the wind turbine. Furthermore, the increase in the torsional stiffness improves the aeroelastic stability of the blade significantly.

The shell of the blade may preferably, but not exclusively, comprise a composite or laminated material. The material may comprise, alone or in any combination, fibreglass, carbon fibres, or other durable and flexible materials typically with a high strength/weight ratio, such as other fibre reinforced plastic materials that may further comprise, at least in part, light-weight metals or alloys. The shell may typically be a laminate or sandwich-construction. The thickness of the shell may vary along its length and width.

The upper part of the shell has a flat surface and during normal operation of the blade, the upper part of the shell is the suction side of the blade. The lower part of the shell has a

more curved surface and during normal operation of the blade, the lower part of the shell is the pressure side of the blade. Thus, the upper part of the shell is also denoted the suction side of the shell, and the lower part of the shell is also denoted the pressure side of the shell.

At least one girder is provided to primarily strengthen the blade along the longitudinal extension of the blade. A girder may also be referred to as a web. Throughout the present disclosure, the girder or web should be construed as any kind of elongate constructional member capable of taking up loads, such as a beam or a spar, e.g. shaped as an I-profile, preferably made from fibre reinforced plastics or other suitable material. The girder may extend along substantially the entire length of the blade.

The blade may have two or more separated girders positioned end to end along the longitudinal extension of the blade, especially for facilitating handling or transporting purposes. In principle, any number of girders may be used, however for the sake of simplicity and for keeping the overall weight of the blade as low as possible, one or two girders are preferred.

The reinforcing member may be a reinforcing angle bar further comprising a plate connected to the first and second legs and protruding therefrom for further reinforcement of the blade. The plate may for example extend centrally with relation to the first and the second leg, or the plate may for example extend at a side edge of the first and the second leg.

An angle bar may also be denoted an angle bracket or an angle plate. Throughout the present disclosure the meaning of the term angle bar includes the meaning of the terms angle bracket and angle plate.

In a wind turbine blade with an angle bar, the angle bar is positioned at the connection between the girder and the shell. The angle bar reduces the change of the angle between the girder and the shell caused by transverse shear distortion of the blade. When the change of angle between the girder and the shell is reduced, the transverse distortion is also reduced.

An angle bar according to the invention may extend along the longitudinal extension of the blade and have substantially the same length as the blade. Preferably, the angle bar is short, and preferably a plurality of angle bars is positioned spaced apart along the longitudinal extension of the blade.

The angle bar may be produced from any suitable material, preferably the angle bar is made of the same material as the shell or the girder, preferably fibre reinforced plastic.

The first leg of the angle bar abutting the girder preferably constitutes a plate or flange with a surface contour that matches the contours of the girder at the position of their interconnection. Likewise, the second leg of the angle bar abutting the shell preferably constitutes a plate or flange with a surface contour that matches the contours of the shell at the position of their interconnection. The angle bar may further have a plate connected to the first and second legs and protruding therefrom, preferably substantially perpendicular to the first and second legs, for further reinforcement of the blade. Preferably, the angle bar with the plate is manufactured in one piece.

The reinforcing member may be subjected to tensile and compressive forces when the blade is loaded. To prevent the reinforcing member from buckling when subjected to compression forces, the member can be stiffened with flanges on top of the member or stringers on the side. Further, the member may constitute a sandwich construction with a foam material with laminates on each side.

As further explained below, in an embodiment of the wind turbine blade according to the present invention, the blade is designed so that shear distortion occurs in one direction only so that a reinforcing angle bar can be positioned on the side of the girder where the angel between the girder and the shell increases so that the angle bar will be subjected to tension only whereby the risk of buckling in the angle bar is eliminated or significantly reduced.

The reinforcing angle bar may further comprise a body plate interconnecting its first and second legs whereby the first and second legs are interconnected with the girder and the shell, respectively, at some distance from the connection between the girder and the shell. Preferably, the plate extends in the longitudinal direction of the blade similarly to the legs. In its operating position in the blade, the plate may be supported by foam located in the volume defined between the girder, the shell, and the body plate to prevent buckling failure when loaded in compression. The body plate may constitute a sandwich construction or may have corrugations or stiffeners to prevent buckling failure.

The reinforcing angle bar may further comprise a third leg connected to the first leg opposite the second leg and configured for abutting the one of the upper part and lower part of the shell opposite the second leg.

In a wind turbine blade with a first and second girder, the reinforcing angle bar may be positioned between the first and the second girder.

In a wind turbine blade with a first and second girder, the reinforcing angle bar may be positioned outside the volume defined between the first and the second girder.

In a wind turbine blade with one or more straight reinforcing members according to the invention, a first end of the reinforcing member is connected to the girder in a position identical with, or near or adjacent to where the girder itself is connected to one of the two shell parts. Thus, the reinforcing member is connected to the first girder at a connection between the first girder and the shell at one of the upper part and lower part of the shell. Further, a second, opposite end of each of the straight reinforcing members may be connected to an inner surface of the other shell part. The connection on the inner surface of the shell may in principle be positioned anywhere provided that the reinforcing member exerts a reasonable and useful reinforcing effect in the blade at the selected position.

Preferably, but not exclusively, the straight reinforcing member may be connected at an angle of 15° - 75° in relation to the girder.

In a wind turbine blade with two or more girders, each of the one or more straight reinforcing members may be positioned in such a way that it connects not only an inner surface on one of the upper and lower shell parts with one girder, but also interconnects two girders. Preferably, each of the one or more reinforcing members is positioned so that it interconnects two girders and respective inner surfaces of both of the shell parts.

In an embodiment with two or more girders, each of the one or more reinforcing members may connect two girders, but may not be connected to respective inner surfaces of the upper and lower shell parts. Thereby, the assembly of the reinforced wind turbine blade may be made particularly simple or may comprise separate manufacturing or assembling steps.

The connections between reinforcing members and respective girders may comprise any suitable kind of joint such as welded, adhered, melted, bonded, fused or simple mechanical connections.

In an embodiment wherein the one or more reinforcing members are connected to an inner surface of the shell parts, such connections are preferably bonded connections.

The straight reinforcing member has a substantially straight shape, such as the shape of a rod or a stretched wire or a planar member. If the shape of the reinforcing member is not straight, the shape of the reinforcing member could be straightened when subjected to tension leading to movement of its end connections and obviously, this is not desired.

The connections on the inner surface of the profile may in principle be positioned anywhere on the inner surface but it should be observed that the chosen positioning causes the reinforcing member to be able to provide a reasonable and useful reinforcing effect in the profile. The connection of a reinforcing member to connecting points on the inner surface

of the profile prevents the negative effects of buckling and ovalization as described above. The connections may comprise any suitable kind of joint such as welded, glued, melted, fused or other simple mechanical connections. The reinforcing member itself may comprise the connections or it may comprise additional connections or connection parts adapted to engage or cooperate with the connections on the inner surface of the profile. The additional connections or connection parts must be sufficiently rigid to maintain their shape when subjected to tension in order to properly cooperate with the reinforcing member to prevent the connections on the shells from being displaced away from each other. In embodiments, the reinforcing member is connected to an inner surface of the shell of the profile. Preferably, the inner surface of the shell is shaped in a manner corresponding to the outer surface thereof, i.e. having a substantially transverse curvature. The reinforcing member may therefore preferably be so positioned on the inner surface of the shell that there will be a certain space (or distance) between the reinforcing member and the inner surface of the profile.

The reinforcing member secures and keeps the transverse curvature of the profile substantially unchanged when the aerodynamic profile is loaded by forces in the flapwise direction. With the reinforcing member according to the invention, the dimensions of the shell may be reduced compared to the prior art leading to reduced loading of other parts of the wind turbine, improved handling and transportation characteristics of the blade and reduced cost.

In an embodiment of the invention with a box profile, each of the one or more straight reinforcing members connects two diagonally opposite corners or corner regions of the box profile. A corner region is a region proximate and including the connection of the respective girder to the respective shell surface. In other words, the unwanted distortion of the blade caused by transverse shear forces may be reduced or prevented by maintaining corners, or regions near the corners, of the box profile in fixed positions with relation to each other. This improves the overall strength of the blade and may also facilitate the design of a blade with lower overall weight.

In an embodiment of the present invention, two or more straight reinforcing members are positioned end to end or in spaced relationship along a longitudinal axis of the blade in such a way that neighbouring reinforcing members alternates between diagonally opposite corners, or corner regions, in the box profile along at least a part of the longitudinal extension of the blade. Thus, a first reinforcing member extends between two diagonally opposed corners of the box profile and a second neighbouring reinforcing member extends between the opposite two diagonally opposed corners of the box profile. A third reinforcing member adjacent the second reinforcing member extends between two opposed corners along substantially the same direction as the extension of the first reinforcing member.

Throughout the present disclosure, two diagonally opposite corners connected by a reinforcing member is referred to as a set of corners.

A reinforcing member may comprise one or more elements selected from the group consisting of rods, plates, wires, ropes, tubes, textiles and fabrics. The reinforcing members may be made of any suitable material. Fibre reinforced plastic is presently preferred for rods, plates and tubes. If a rod, plate or tube type element is provided, such element may be subdivided into two or more smaller reinforcing elements over the span between the set of corners. Such smaller elements may be connected to each other or they may be connected to one or more other reinforcing members spanning the other two opposed corners of the box profile. The reinforcing members may be connected to the girders, to the inner surfaces of the shell parts, and to each other by bonding means or mechanical means.

The reinforcing member may comprise a plate possibly with one or more cut-outs, e.g. a laminated plate, such as a sandwich construction, preferably, but not exclusively, comprising a layer of a lightweight foamed material provided between two layers of a fibre reinforced plastic material.

In an embodiment of the invention, two or more straight reinforcing members are provided and arranged at a distance from the outer extremities of each other not exceeding 2xD, wherein D is the spanning distance of one of the reinforcing members, i.e. the distance between two opposing connections of the straight reinforcing member, e.g. between a set of corners in a box profile. The value of parameter D may be identical for two or more neighbouring straight reinforcing members. However, since the width of the cross-section of the wind turbine blade typically decreases towards the tip of the blade, the distance D2 of a reinforcing member located closer to the tip will be smaller than the distance D1 of a reinforcing member located closer to the hub of the wind turbine. The resulting maximum distance between two neighbouring reinforcing members may preferably be calculated based on the minimum of the two distances, i.e. distance D2, or based on the mean value of D1 and D2. It has been found that values of the resulting distance D fulfilling this relationship, there is a good balance between the reinforcing members' ability to take up the shear forces, the total weight of the wind turbine blade and the blade's stiffness. However, the maximum distance between two reinforcing members may in stead be based on other requirements, such as, but not limited to, a need for a particularly strong wind turbine blade design, e.g. when the wind turbine is intended to be subjected to repeatedly severe weather conditions, such as when erected at open sea.

In an embodiment of the invention, two or more reinforcing members may be positioned in certain sections of the blade only, possibly without any predetermined or calculated maximum distance.

In a blade with two or more reinforcing members, the members may be of the same type or may have different geometries, and possibly may be made from different materials. The members may be positioned so that they span the same two opposed corners, e.g. along the longitudinal extension of the blade, or they may alternate between the sets of opposed corners.

In an embodiment of the invention, the reinforcing members are located in positions wherein a substantial transverse distortion of the blade is expected or established.

In an embodiment of the invention, two reinforcing members may constitute the legs of an X-shaped reinforcing member, e.g. produced as an integral member, and interconnecting the upper part of the shell with the lower part of the shell at the respective connection points of the girders to the upper and lower parts of the shell.

The X-shaped reinforcing member may be made from two straight reinforcing members that are assembled to form the X-shaped reinforcing member. The X-shaped reinforcing member may preferably be assembled from plates of a fibre reinforced plastic material laminated to each other. Feet may be provided at the ends of the individual straight reinforcing members forming the legs of the X-shaped member, the feet facilitating connection, particularly by bonding means, to the respective surfaces of the shell or girder or both of the blade. However, the connections may be obtained in other ways, such as by secondary lamination, mechanical connection means, etc, or any combination of such connection measures.

Further, the X-shaped member may be made in one piece. The ends of the legs of the single pieced X-shaped member may preferably be connected with the girders by bonding. Bonding may be performed prior to connection of the girders to the inner surfaces of the blade shell. However, the reinforcing member and the girders may also be provided as a single integrated member, preferably of a fibre reinforced plastic, that is connected to the shell parts.

In an embodiment of the invention with two or more X-shaped reinforcing members, the members may be positioned in certain sections of the blade only and not at any predetermined or calculated distance. Particularly, but not exclusively, the X-shaped members may be located at positions wherein a substantial transverse distortion of the blade is expected or established.

During operation of the blade, only one of the legs of the X-shaped member may be subjected to a load, and this leg will be subjected to tension only whereby the material of the reinforcing member is utilized to a high degree, thus reducing the required material thickness of the member and consequently keeping the total weight of the blade at a minimum.

Assembly of a wind turbine blade with X-shaped members may be facilitated by assembly of the X-shaped members and the girders before assembly with the shell parts, or by manufacturing the X-shaped members and the girders in one piece, thus facilitating at least a better quality control of the parts during assembly.

A wind turbine blade with X-shaped members, a cavity may be provided between a member and a respective girder or the inner surface of a shell part. In order to facilitate the assembly of the reinforcing member with the girders or with the shell parts or with both, the cavity may be filled with a lightweight foamed material to facilitate positioning of the X-shaped member.

In an embodiment of the wind turbine blade according to the present invention, the blade is designed so that shear distortion occurs in one direction only so that a straight reinforcing member can be positioned so that it will be subjected to tension only.

The direction of shear distortion may be controlled by proper orientation of the layers of fibre reinforced plastic of the shell substantially in a single specific direction, or by proper positioning of the one or more girders in the blade, or by positioning the one or more girders at a specific angle in relation to the flapwise direction, or any combination of such measures.

A straight reinforcing member that is positioned so that it will be subjected to tension only keeps its end connections in substantially mutually fixed positions and thus prevents the distance between the connections from increasing thereby strengthening the shell against forces in the flapwise direction. Since the reinforcing member is required to have a high tensional strength only, i.e. the reinforcing member need not carry other loads; the reinforcing member is preferably thin so that its weight and cost are kept at a minimum.

Even though a straight reinforcing member may be subjected to tension only, the member may as well be capable of withstanding compression forces, e.g. the member may comprise a tube or a plate of a laminated or sandwiched construction that is capable of withstanding compression forces.

In an embodiment of the invention, the one or more reinforcing members may be individually designed so that the bending and torsion of the blade is coupled to withstand

the high loads of strong wind gusts. This leads to lower fatigue loads on the blade and also facilitate a higher energy output of the wind turbine. The individual design may include pre-tensioning of some of the reinforcing members.

Each of the reinforcing members may comprise one or more electro-mechanical transducers, such as piezoelectric transducers, that may change the extension of respective reinforcing members in certain directions in response to an individual control signal, such as a voltage, a current, an electric field, or a magnetic field, e.g. for imposing stresses on the members coupling the bending and torsion of the blade.

Below the invention will be described in more detail with reference to the exemplary embodiments illustrated in the drawings, wherein

Fig. 1 schematically illustrates in perspective a wind turbine blade and arrows indicating the directions of flapwise, edgewise, and torsional loads, respectively,

Fig. 2a is a schematic cross-section of a wind turbine blade with arrows indicating directions of transverse shear forces in the blade,

Fig. 2b schematically illustrates deformation of a cross-section of a wind turbine blade caused by transverse shear forces,

Fig. 3 is a schematic cross-section of a wind turbine blade with arrows indicating crushing pressure on the blade,

Fig. 4 is a schematic cross-section of a wind turbine blade with an X-shaped reinforcing member interconnecting two girders and the upper and lower part of the shell,

Fig. 5 is a schematic cross-section of a wind turbine blade with another X-shaped reinforcing member interconnecting two girders,

Fig. 6 is a schematic cross-section of a wind turbine blade with yet another X-shaped reinforcing member interconnecting two girders and the upper and lower part of the shell,

Fig. 7 is a schematic cross-section of a wind turbine blade with still another X-shaped reinforcing member interconnecting two girders and the upper and lower part of the shell,

Fig. 8 is a schematic cross-section of a wind turbine blade with a straight reinforcing member,

Fig. 9 schematically illustrates in perspective a wind turbine blade with part of the shell surface removed for making visible an internally positioned plurality of straight reinforcing members extending along crossing directions,

Fig. 10 schematically illustrates in perspective a wind turbine blade with part of the shell surface removed for making visible internally positioned two girders connected by an X-shaped reinforcing member extending along the longitudinal extension of the blade,

Fig. 11 is a schematic cross-section of a wind turbine blade with a reinforcing angle bar,

Fig. 12 is a schematic cross-section of a wind turbine blade with another reinforcing angle bar,

Fig. 13 is a schematic cross-section of a wind turbine blade with yet another reinforcing angle bar,

Fig. 14 is a schematic cross-section of a wind turbine blade with a plurality of reinforcing angle bars,

Fig. 15 schematically illustrates in perspective a wind turbine blade with an angle bar,

Fig. 16 is a schematic cross-section of another wind turbine blade with the angle bar of Fig. 15,

Fig. 17 schematically illustrates in perspective a wind turbine blade with still another angle bar,

Fig. 18 is a schematic cross-section perpendicular to the girder showing a wind turbine blade with an angle bar,

Fig. 19 is a schematic cross-section perpendicular to the girder showing another angle bar,

Fig. 20 is a schematic cross-section perpendicular to the girder showing yet another angle bar,

Fig. 21 shows the deformation of a conventional wind turbine blade at a sector near the root of the blade, and

Fig. 22 shows the deformation of a wind turbine blade according to the invention at a sector near the root of the blade.

The figures are schematic and simplified for clarity, and they merely show details which are essential to the understanding of the invention, while other details have been left out. Throughout, the same reference numerals are used for identical or corresponding parts.

The present invention will now be described more fully hereinafter with reference to the accompanying drawings, in which exemplary embodiments of the invention are shown. The invention may, however, be embodied in different forms and should not be construed as limited to the embodiments set forth herein. Rather, these embodiments are provided so that this disclosure will be thorough and complete, and will fully convey the scope of the invention to those skilled in the art. Like reference numerals refer to like elements throughout.

Fig. 1 schematically illustrates in perspective a wind turbine blade 1 and arrows indicating the directions of flapwise F, edgewise E, and torsional T loads, respectively. The cross-section S1 is shown in Figs. 2a+2b.

Fig. 2a is a schematic cross-section S1 of a wind turbine blade and arrows indicating directions C of transverse shear forces in the blade,

Fig. 2b schematically illustrates deformation of a cross-section S1 of a wind turbine blade 1 caused by transverse shear forces. The illustrated blade 1 is twisted clockwise by the transverse shear forces.

Fig. 3 is a schematic cross-section of a wind turbine blade 1 having a shell 2 with leading edge 3 and trailing edge 4. The wind turbine blade 1 has a box profile with two girders 5 and caps 10 and 11 of the shell 2 located between the girders. The aerodynamic and inertia forces working on a blade in operation induce a bending moment on the blade and create a crushing pressure indicated by arrows B. The crushing pressure is also referred to as the Brazier effect (reference is made to the article "Structural testing and numerical simulation of a 34 m composite wind turbine blade" by F. M. Jensen et.al. published by Elsevier in Composite Structures 76 (2006) 52-61).

Fig. 4 is a schematic cross-section of a wind turbine blade 20 with an X-shaped reinforcing member 24 interconnecting two girders 21 and the upper thickened cap part 22 and the lower thickened cap part 23 of the shell. The two girders 21 and thickened cap parts 22 and 23 of the blade constitute a box profile. The box profile is reinforced with X-shaped reinforcing member 24. In the illustrated embodiment, the reinforcing member 24 is connected to both of the girders 21 and to the inner surfaces of both the upper and lower parts 25 and 26 of the shell of the blade. In the illustrated embodiment, the parts 21, 24, 25 and 26 are connected to each other with bonding connections 27-30, respectively. The

X-shaped reinforcing member 24 comprises feet 31 each of which provides a large surface for bonding with the respective girder 21 and part 25, 26 of the shell. In the illustrated embodiment, the X-shaped reinforcing member 24 is made in one piece. Each leg of the X-shaped reinforcing member constitutes a straight reinforcing member. A foamed material 40 is located in the cavity between the member 24 and the inner surface of the cap 23. In the illustrated embodiment, the shape of the foamed material 40 matches the shape of the cavity whereby the material 40 may guide the positioning of the member 24 during assembly of the blade.

Fig. 5 is a front view of a box profile of a wind turbine blade 20 according to the invention. The box profile comprises two girders 21 and thickened caps 22 and 23 of the blade. In the illustrated embodiment, the blade has a box profile that is reinforced with two straight reinforcing members in the form of rods 24a and 24b. In Fig. 5, the rod 24a is positioned in front of the rod 24b. In the illustrated embodiment, the positions of the individual straight reinforcing members 24a, 24b may alternate along the longitudinal extension of the blade. In Fig. 5, the rod 24a connects the upper left corner 32 of the box profile with the lower right corner 33 of the box profile. The rod 24b connects the upper right corner 35 with the lower left corner 34 of the box profile. It should be noted that the rods 24a, 24b are not connected directly in the corners 32-35. In stead, the rods 24a, 25b are connected to the respective girders 21 proximate the inner surfaces of the respective shell parts 25 and 26. In the figure, the reinforcing members 24 connect both of the girders 21. In the illustrated embodiment, the reinforcing members 24 are mechanically connected to the girders 21 by leading rods 24a and 24b through suitable openings in the girders 21 and fastening them by means of a mechanical connection 36, such as a nut engaging with a threaded section of the end part of the rods 24a and 24b. The girders 21 further have retaining members 37 for guiding and supporting the connection 36.

Fig. 6 is a schematic cross-section of a wind turbine blade 20 with yet another X-shaped reinforcing member 24 interconnecting two girders 21 and the upper and lower caps 22, 23 of the shell. The two girders 21 and thickened cap parts 22 and 23 of the blade form a box profile. In the illustrated embodiment, the box profile is reinforced with an X-shaped reinforcing member 24 comprising two straight reinforcing members constituting the legs of the X-shaped member. Plate 24a constitutes one of the straight reinforcing members, and plates 24b, 24c constitute the other straight reinforcing member. Plate 24a connects the upper left corner 32 with the lower right corner 33 of the box profile. Plate 24b connects the upper right corner 35 with a first surface of plate 24a and is connected to the surface of plate 24a at connection 38. Plate 24c connects the lower left corner 34 of the box profile with a second side of plate 24a and is connected to the other surface of plate 24a at connection 39. The plates 24b and 24c are substantially aligned and co-operate to

connect the opposite set of corners 34, 35 of the box profile. The X-shaped reinforcing member further comprises anchors 41 for connection with the respective corners 32-35. In the illustrated embodiment, the anchors 41 are bonded to the inner surface of the box profile. The plates 24a - c are received between two receiving surfaces 42 of the anchors and the plates 24a – c are bonded or adhered to the anchors 41. Similar anchors are provided at connections 38 and 39.

Fig. 7 is a schematic cross-section of a wind turbine blade 20 with still another X-shaped reinforcing member 24 interconnecting two girders 21 and the upper part 25 and the lower part 26 of the shell. The two girders 21 and thickened caps 22 and 23 of the blade constitute a box profile. In the illustrated embodiment, the X-shaped reinforcing member 24 is made of two angle plates 43a, 43b. Angle plates 43a and 43b have a generally triangular shape. Each of the angle plates 43a, 43b has feet 44 and a projection 45 facilitating connection of the angle plates 43a, 43b. In the illustrated embodiment, the feet 44 of angular plates 43a, 43b are bonded to flanges of the girders 21 and to inner surfaces of the shell parts 25 and 26 of the blade at the corners 32-35 of the box profile. The projections 45 of the angular plates are bonded to each other at the connection 46. Further a foamed material 40 is provided, e.g., in a cavity defined between angular plate 43a and the girder 21. The foamed material 40 has a shape that matches the shape of the cavity and is used for guiding positioning of the plate member 43a during assembly.

Fig. 8 is a schematic cross-section of a wind turbine blade 20 with a straight reinforcing member 47. The two girders 21 and thickened cap parts 22 and 23 of the blade constitute a box profile. The box profile is reinforced with a single straight reinforcing member 47 in the form of plate 47. Plate 47 is a sandwich construction with outer layers 48 of fibre reinforced plastic on both sides of a foamed material 49. The straight reinforcing member 47 has feet 50 providing connection surfaces for bonding the member 47 to the respective girder 21 and part 25, 26 of the shell. The feet 50 are bonded to respective flanges of the girders 21 as well as to inner surfaces of the respective shell parts 25 and 26 so that the straight reinforcing member 47 connects corners 34 and 35 of the box profile. The plate 47 may provide reinforcement against tension forces and compression forces.

Fig. 9 schematically illustrates in perspective a wind turbine blade 20 with part of the shell surface removed for making visible an internally positioned plurality of straight reinforcing members 51, 52 extending transversely along crossing directions. The blade 20 is reinforced with two straight reinforcing members 51, 52 similar to the straight reinforcing member 47 shown in Fig. 8, i.e. each of the reinforcing members 51, 52 is a plate, e.g., of a sandwich construction. In the illustrated embodiment, the straight reinforcing members 51, 52 are positioned at a mutual distance D (not indicated) along the longitudinal extension of the blade 20. It is seen that the first reinforcing member 51 extends between

two diagonally opposed corners of the box profile and the second neighbouring reinforcing member 52 extends between the other two diagonally opposed corners of the box profile.

Fig. 10 schematically illustrates in perspective a wind turbine blade 20 with part of the shell surface removed for making visible internally positioned two girders 21 connected by an X-shaped reinforcing member 53 extending along the longitudinal extension of the blade 20. The blade 20 is reinforced with an X-shaped reinforcing member 53 connecting the corners of the box profile. The straight reinforcing member 53 is made in one piece and has feet 54 connected to flanges of the girders 21. The straight reinforcing member 53 and girders 21 are assembled before connection with the shell parts 25 and 26.

Fig. 11 is a schematic cross-section of a box profile of a wind turbine blade with a reinforcing angle bar 100 with a first leg 102 abutting the first girder 21a, and a second leg 104 abutting the lower cap 23 of the shell. The reinforcing angle bar 100 further comprises a plate 106 connected to the first leg 102 and the second leg 104 and protruding therefrom for further reinforcement of the blade 20. The plate 106 may for example extend centrally with relation to the first leg 102 and the second leg 104, or the plate may for example extend at a side edge of the first leg 102 and the second leg 104.

In the illustrated embodiment, the angle bar 100 is positioned at the connection between the girder 21a and the lower cap 23 of the shell between the girders 21a, 21b. The angle bar 100 reduces the change of the angle between the girder 21a and the shell 26 caused by transverse shear distortion of the blade 20. When the change of angle between the girder 21a and the shell 26 is reduced, the transverse distortion is also reduced.

The first leg 203 of the angle bar 100 abutting the girder 21a preferably constitutes a plate or flange with a surface contour that matches the contours of the girder 21a at the position of their interconnection. Likewise, the second leg 104 of the angle bar 100 abutting the cap 23 preferably constitutes a plate or flange with a surface contour that matches the contours of the cap 23 at the position of their interconnection. Preferably, the angle bar 100 with the plate is manufactured in one piece.

The reinforcing member may be subjected to tensile and compressive forces when the blade is loaded. To prevent the reinforcing member from buckling when subjected to compression forces, the member can be stiffened with flanges on top of the member or stringers on the side. Further, the member may constitute a sandwich construction with a foam material with laminates on each side.

Fig. 12 is a schematic cross-section of a box profile of a wind turbine blade 20 with another reinforcing angle bar 110 with a first leg 102 abutting the second girder 21b, and a second

leg 104 abutting the lower cap 23 of the shell. The reinforcing angle bar 110 further comprises a third leg 108 connected to the first leg 102 opposite the second leg 104 and abutting the upper cap 22 of the shell. The reinforcing angle bar 100 also comprises a plate 106 connected to the first leg 102, the second leg 104, and the third leg 106, and protruding therefrom for further reinforcement of the blade 20. The plate 106 may for example extend centrally with relation to the first leg 102, the second leg 104, and the third leg 106, or the plate may for example extend at a side edge of the first leg 102, the second leg 104, and the third leg 106. In the illustrated embodiment, the angle bar 100 is positioned between the girders 21a, 21b. The angle bar 100 reduces the change of the angle between the girder 21b and the lower cap 23 and of the angle between the girder 21b and the upper cap 22 caused by transverse shear distortion of the blade 20. When the change of the angles between the girder 21a and the upper cap 22 and the lower cap 23 is reduced, the transverse distortion is also reduced. Similar to the angle bar 100 shown in Fig. 12, the surfaces of the angle bar 110 match corresponding surfaces of the box profile.

Fig. 13 is a schematic cross-section of a box profile of wind turbine blade with yet another reinforcing angle bar 100 somewhat similar to the angle bar 100 shown in Fig. 11. The angle bar 100 illustrated in Fig. 13 has a first leg 102 abutting the second girder 21b, and a second leg 104 abutting the lower cap 23 of the shell. The reinforcing angle bar 100 further comprises a plate 106 connected to the first leg 102 and the second leg 104 and protruding therefrom for further reinforcement of the blade 20. The plate 106 may for example extend centrally with relation to the first leg 102 and the second leg 104, or the plate may for example extend at a side edge of the first leg 102 and the second leg 104.

In the illustrated embodiment, the angle bar 100 is positioned outside the internal volume defined by the box profile. The angle bar 100 reduces the change of the angle between the girder 21b and the shell 26 caused by transverse shear distortion of the blade 20. When the change of angle between the girder 21b and the shell 26 is reduced, the transverse distortion is also reduced.

Fig. 14 is a schematic cross-section of a wind turbine blade 20 with a plurality of reinforcing angle bars 100a, 100b similar to the angle bars shown in Figs 11 and 13.

Fig. 15 schematically illustrates in perspective a wind turbine blade 20 with a reinforcing angle bar 100 with a first leg 102 abutting the second girder 21b, and a second leg 104 abutting the lower part 26 of the shell. The reinforcing angle bar 100 further comprises a body plate 103 interconnecting the first leg 102 and the second leg 104. Thus, the first leg 102 and the second leg 104 are interconnected with the girder 21b and the shell 26, respectively, at some distance from the connection 30 between the girder 21b and the

lower part 26 of the shell. The reinforcing angle bar 100 with the body plate 103 extends in the longitudinal direction of the blade 20.

As shown in Fig. 16, in its operating position in the blade 20, the body plate 103 may be supported by foam 40 located in the volume defined between the girder 21b, the lower part 26 of the shell, and the body plate 103 to prevent buckling failure when loaded in compression. The body plate may be a sandwich construction or may have corrugations or stiffeners to prevent buckling failure. In Fig. 16, the girders 21a, 21b are sandwich constructions.

Fig. 17 is similar to Fig. 16 with the difference that the reinforcing angle bar with a body plate 103 has been substituted with the angle bar shown in Fig. 13. The centre positioning of the plate 106 with relation to the first leg 102 and the second leg 104 is clearly visible.

Fig. 18 is a schematic cross-section perpendicular to the girder showing a wind turbine blade 20 with the reinforcing angle bar 100 shown in fig. 1.

Fig. 19 is a schematic cross-section perpendicular to the girder showing a wind turbine blade 20 with another angle bar in which the plate 106 is positioned along a side of the first leg 102 and a side of the second leg 104.

Fig. 20 is a schematic cross-section perpendicular to the girder showing a wind turbine blade 20 with a reinforcing angle bar corresponding to the reinforcing angle bar of Fig. 19 however with a plate 106 that is a sandwich construction.

An embodiment of the invention was analysed with respect to increased strength as compared to a conventional wind turbine blade using numerical modelling of a 34 m wind turbine blade designed for use on a 1.5 MW wind turbine.

The numerical analysis included Finite Element analysis of a model containing more than 150 000 shell and 3D elements. Advanced software and algorithms were used in the analysis to account for the effect of nonlinear geometrical deformations.

The model of the blade has been verified with full-scale test of the blade ("Structural testing and numerical simulation of a 34 m composite wind turbine blade" by F. M. Jensen et. al. published by Elsevier in Composite Structures 76 (2006) 52-61). The blade was loaded with a combination of loads in both flapwise and edgewise direction that should simulate the operational loads of the blade.

The analysis showed a significant reduction of transverse shear distortion when the blade is equipped with the invention. Figs. 21 and 22 show the results of the analysis of a sector near the root of the blade.

The analysis shows a reduction of the transverse shear distortion of the profile and this increase the blade's resistance to the crushing pressure and thereby increases the ultimate strength of the wind turbine blade.

Furthermore, the aerodynamic efficiency of the blade is also improved since the designed shape of the blade profile is maintained to a higher degree than for a conventional blade.

The scope of the present invention is set out by the accompanying claim set. In the context of the claims, the terms "comprising" or "comprises" do not exclude other possible members or steps. Also, the mentioning of references, such as "a", "an", etc., should not be construed as excluding a plurality. Furthermore, individual features mentioned in different claims, may possibly be advantageously combined, and the mentioning of these features in different claims does not exclude that a combination of features is not possible and advantageous.

CLAIMS

1. A wind turbine blade comprising a shell, a first girder, and a reinforcing member for inhibiting transverse shear distortion of the blade, wherein the reinforcing member is connected to the first girder at a connection between the first girder and the shell at one of the upper part and lower part of the shell and wherein the reinforcing member is selected from the group consisting of

a) a reinforcing angle bar with a first leg abutting the first girder, and a second leg abutting the one of the upper part and lower part of the shell, and

b) a straight reinforcing member connected to the other one of the upper part and lower part of the shell at a distance from the girder.

2. A wind turbine blade according to claim 1, further comprising a second girder and wherein the reinforcing member is a first straight reinforcing member interconnecting the first and second girders between a connection between the first girder and the shell at one of the upper part and lower part of the shell and a connection between the second girder and the shell at the other one of the upper part and lower part of the shell.

3. A wind turbine blade according to claim 2, further comprising a second straight reinforcing member interconnecting the first and second girders between a connection between the first girder and the shell at the one of the upper part and lower part of the shell that is opposite the connection of the first straight reinforcing member to the first girder and a connection between the second girder and the shell at the other one of the upper part and lower part of the shell whereby the first and second straight reinforcing members form a cross.

4. A wind turbine blade according to any of the preceding claims, wherein the straight reinforcing member comprises at least one element selected from the group consisting of a plate, a wire, a rope, a tube, a textile and a fabric.

5. A wind turbine blade according to any of the preceding claims, comprising a plurality of straight reinforcing members positioned in spaced relationship along the longitudinal extension of the blade with a mutual distance that is less than 2xD, wherein D is the distance of opposing connections of one of the plurality of straight reinforcing members to the upper part and lower part of the shell, respectively.

6. A wind turbine blade according to any of the preceding claims, wherein at least one reinforcing member comprises a laminated plate.

7. A wind turbine blade according to claim 6, wherein the laminated plate is a sandwich construction.

8. A wind turbine blade according to claim 1, wherein the reinforcing member is a reinforcing angle bar further comprising a plate connected to the first and second legs and protruding therefrom.

9. A wind turbine blade according to claim 8, wherein the plate extends centrally with relation to the first and the second leg.

10. A wind turbine blade according to claim 8, wherein the plate extends at a side edge of the first and the second leg.

11. A wind turbine blade according to any of claims 8 – 10, wherein the reinforcing angle bar further comprises a body plate interconnecting its first and second legs.

12. A wind turbine blade according to any of claims 8 - 11, further comprising a third leg and abutting the one of the upper part and lower part of the shell opposite the second leg.

13. A wind turbine blade according to any of claims 8 – 12 as dependent on claim 2, wherein the reinforcing angle bar is positioned between the first and the second girder.

14. A wind turbine blade according to any of claims 8 – 12 as dependent on claim 2, wherein the reinforcing angle bar is positioned outside the volume defined between the first and the second girder.

15. A method of inhibiting transverse shear distortion in a wind turbine blade with a shell and a first girder wherein the first girder is connected to an upper part of the shell and a lower part of the shell, the method comprising the steps of

providing a straight reinforcing member with a first end and a second opposite end, and

connecting the first end to the first girder at the connection between the first girder and the shell at the upper part or the lower part of the shell,

and connecting the second end to the opposite part of the shell at a distance from the girder.

16. A method of inhibiting transverse shear distortion in a wind turbine blade with a shell and a first girder wherein the first girder is connected to an upper part of the shell and a lower part of the shell, the method comprising the steps of providing a reinforcing angle bar having a first leg and a second leg; and connecting the first leg to the first girder, and connecting the second leg to the upper part or the lower part of the shell.

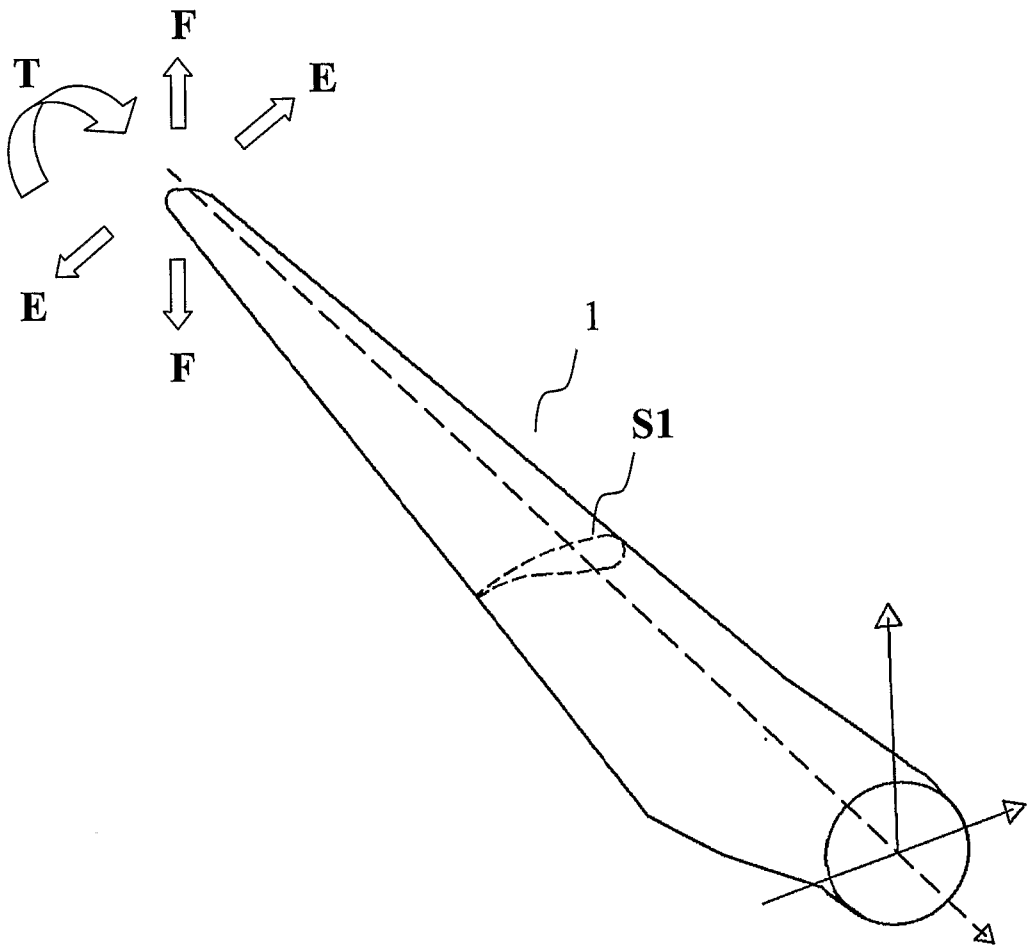

Fig. 1

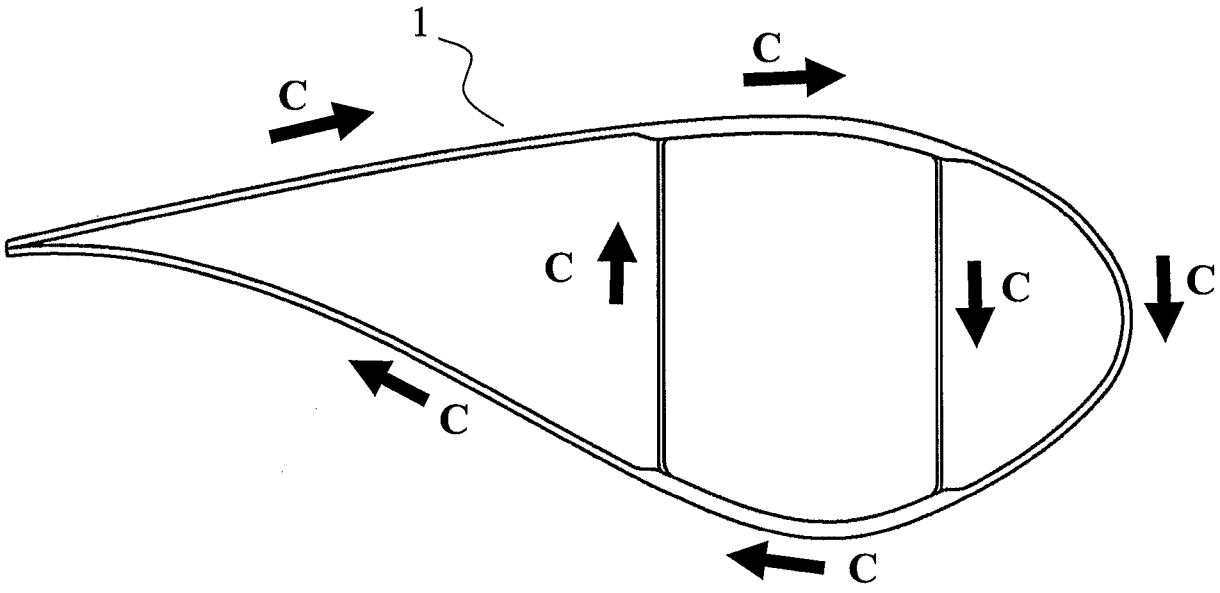

Fig. 2a

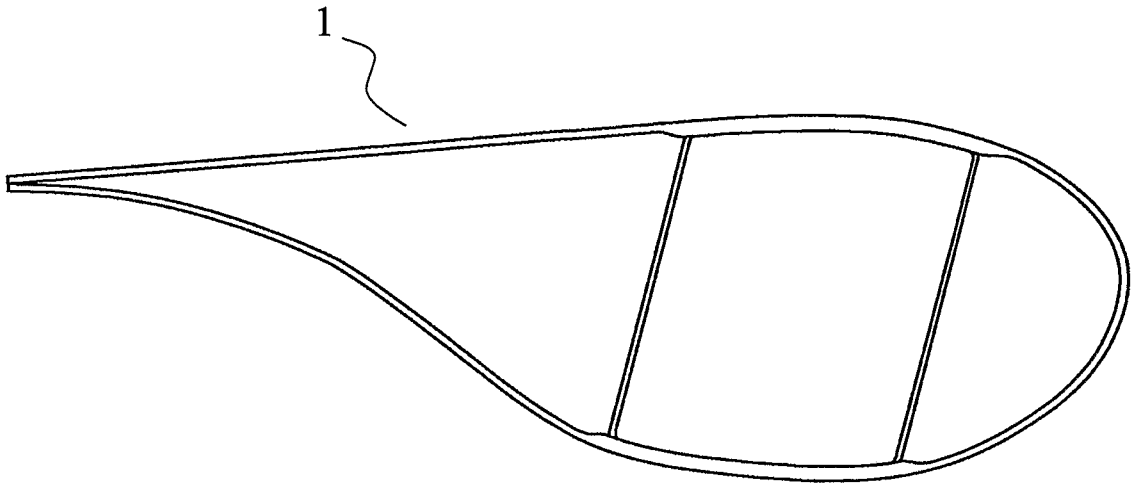

Fig. 2b

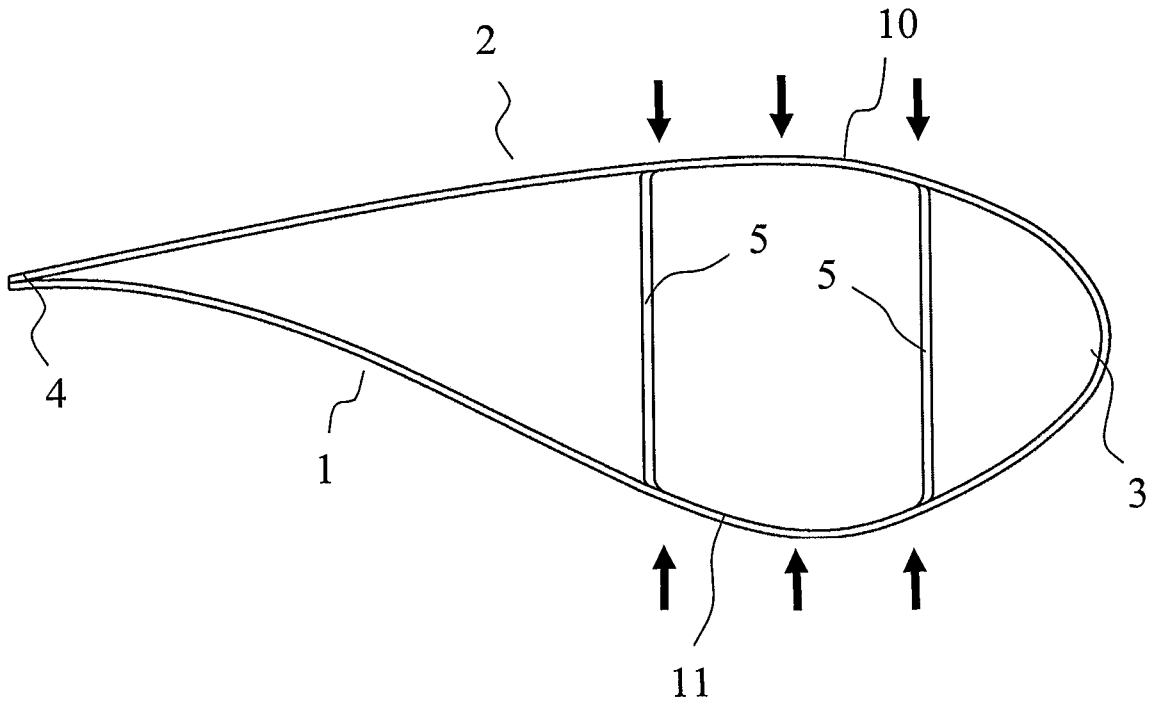

Fig. 3

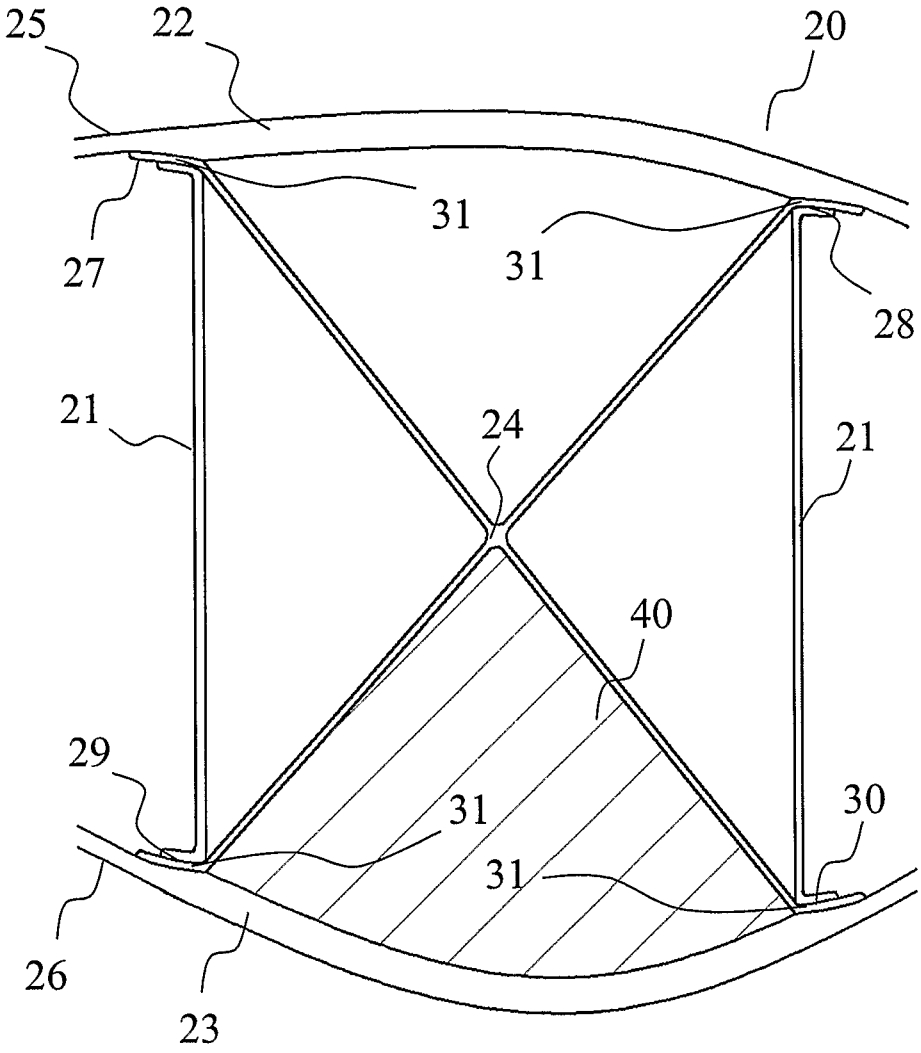

Fig. 4

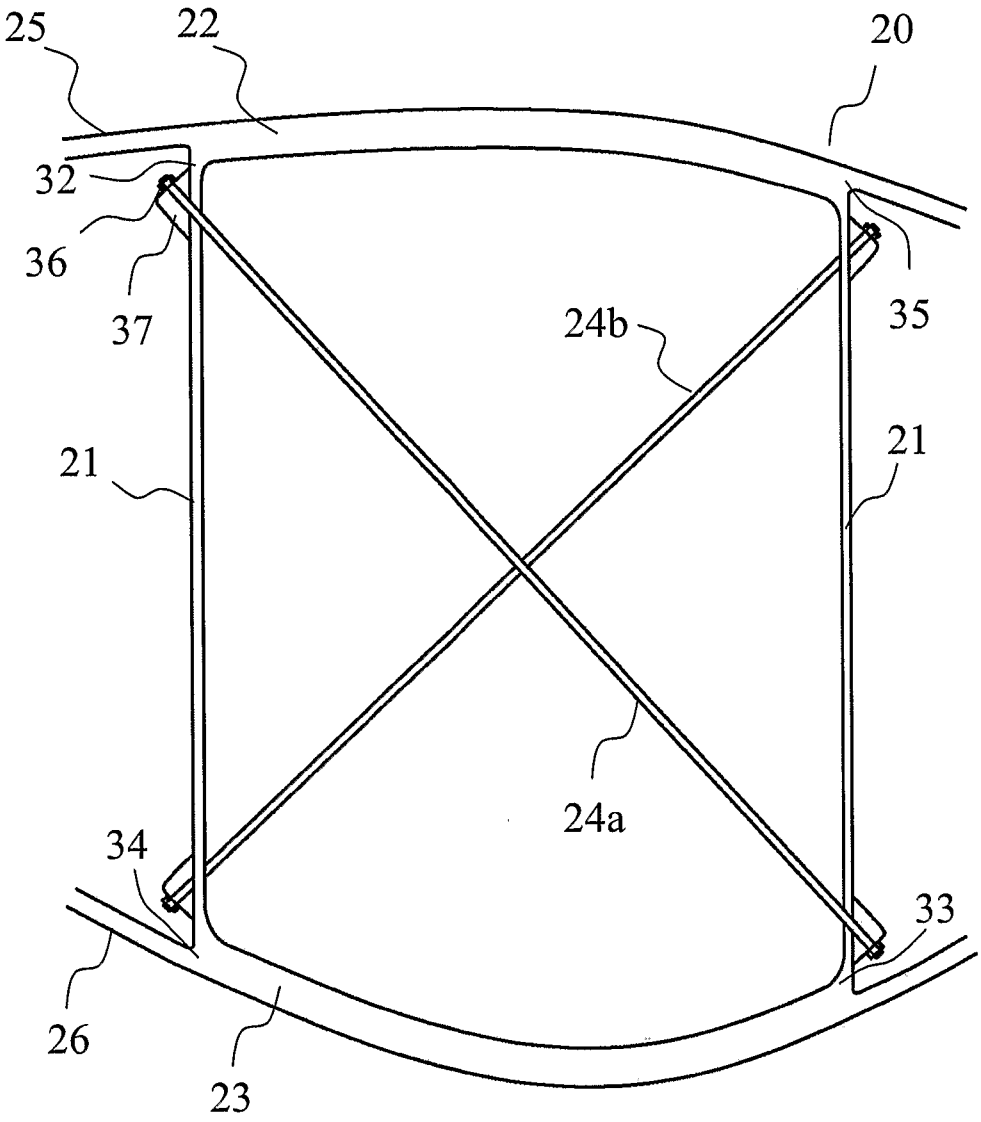

Fig. 5

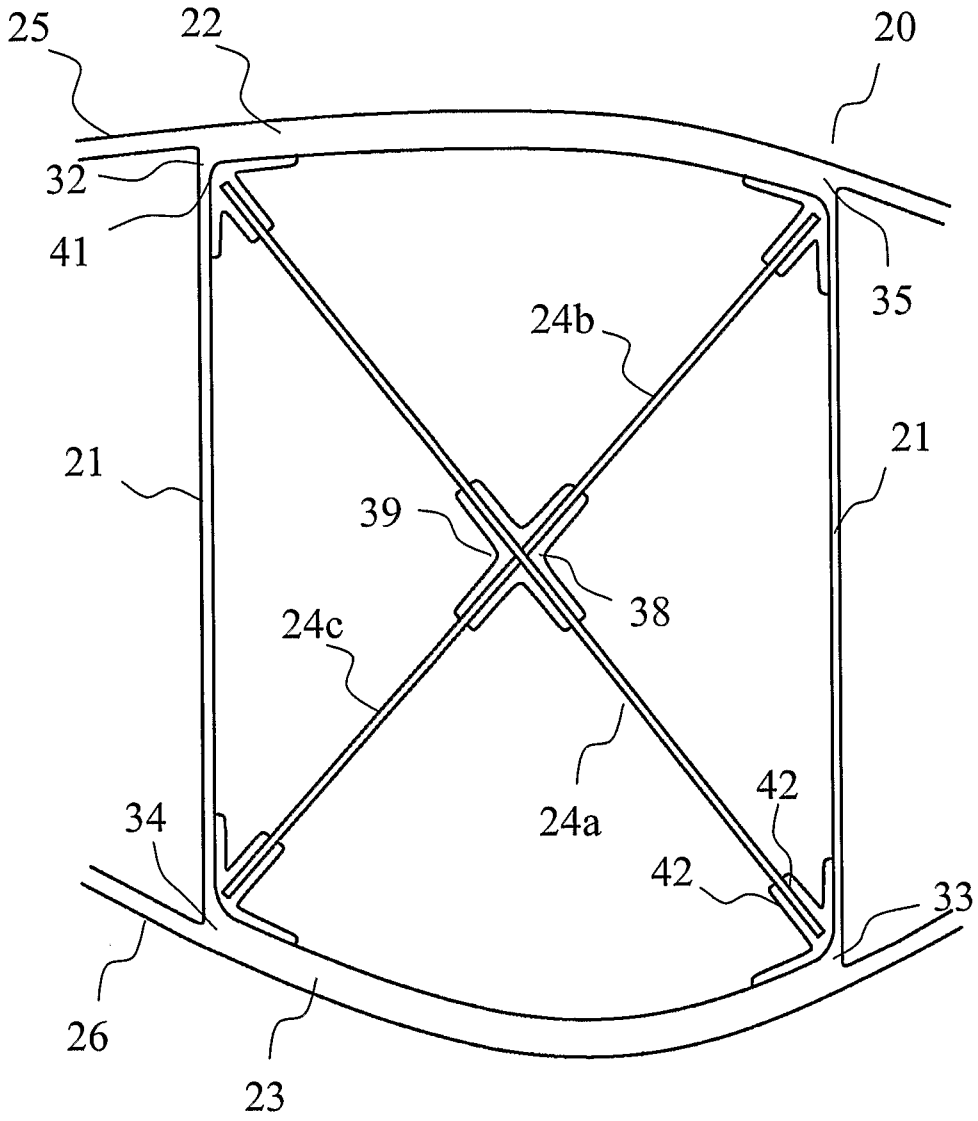

Fig. 6

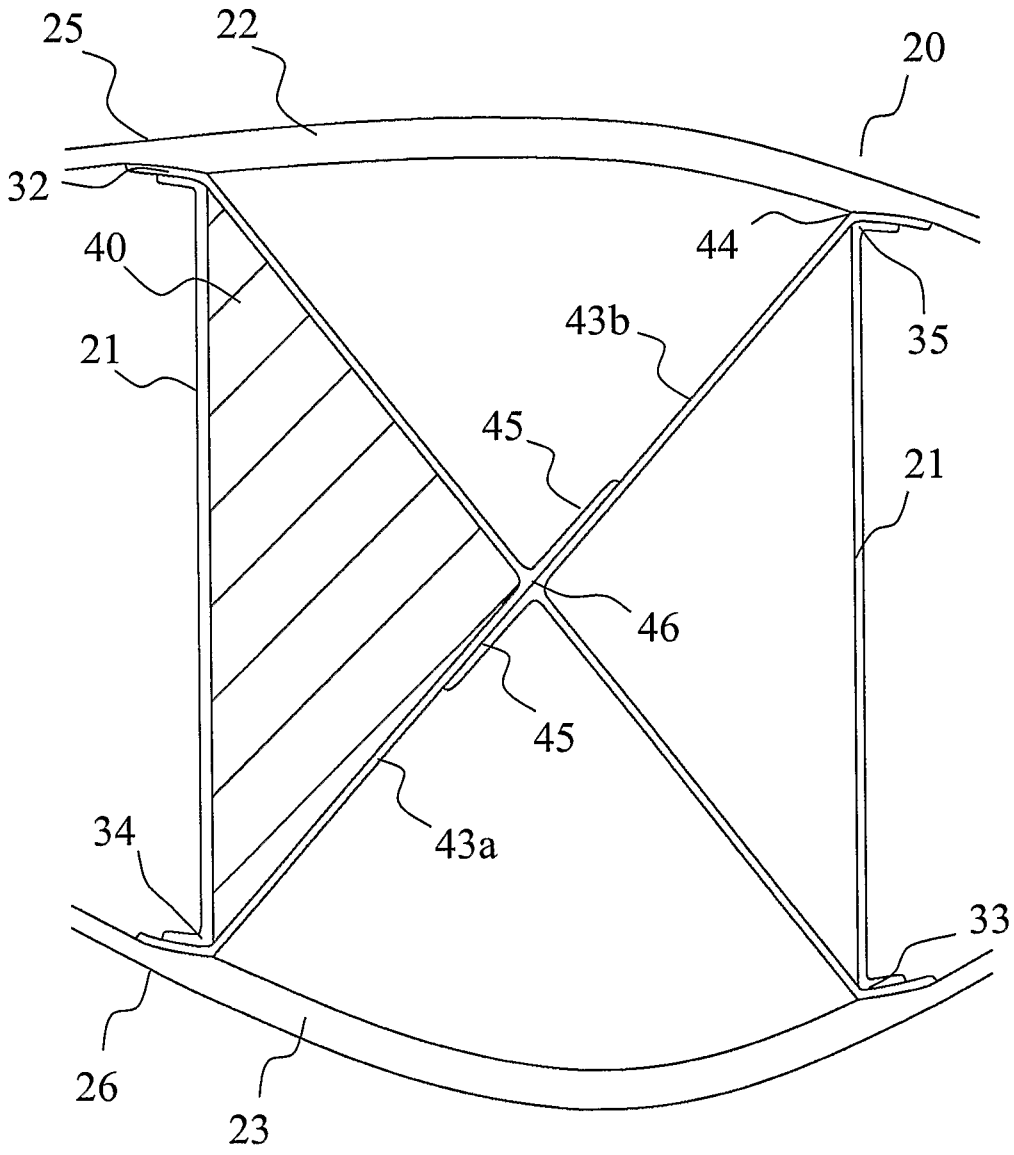

Fig. 7

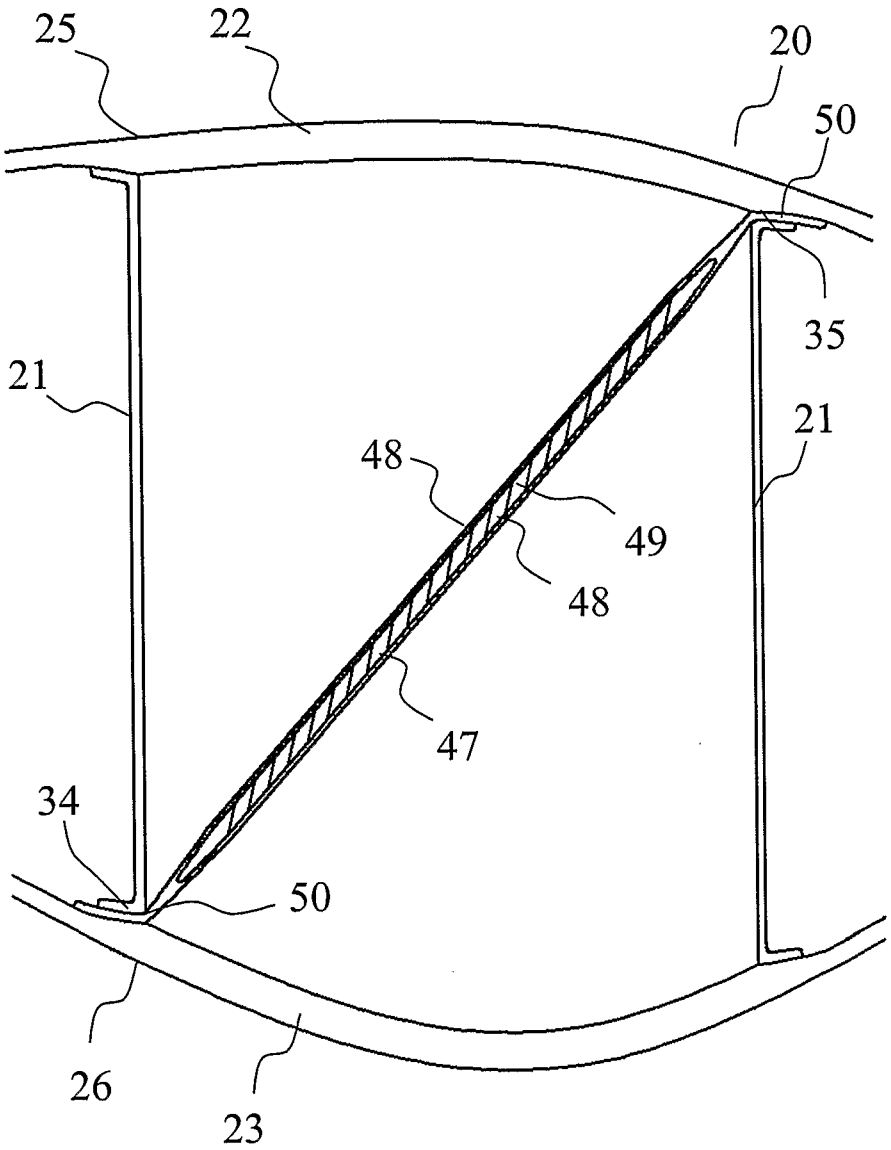

Fig. 8

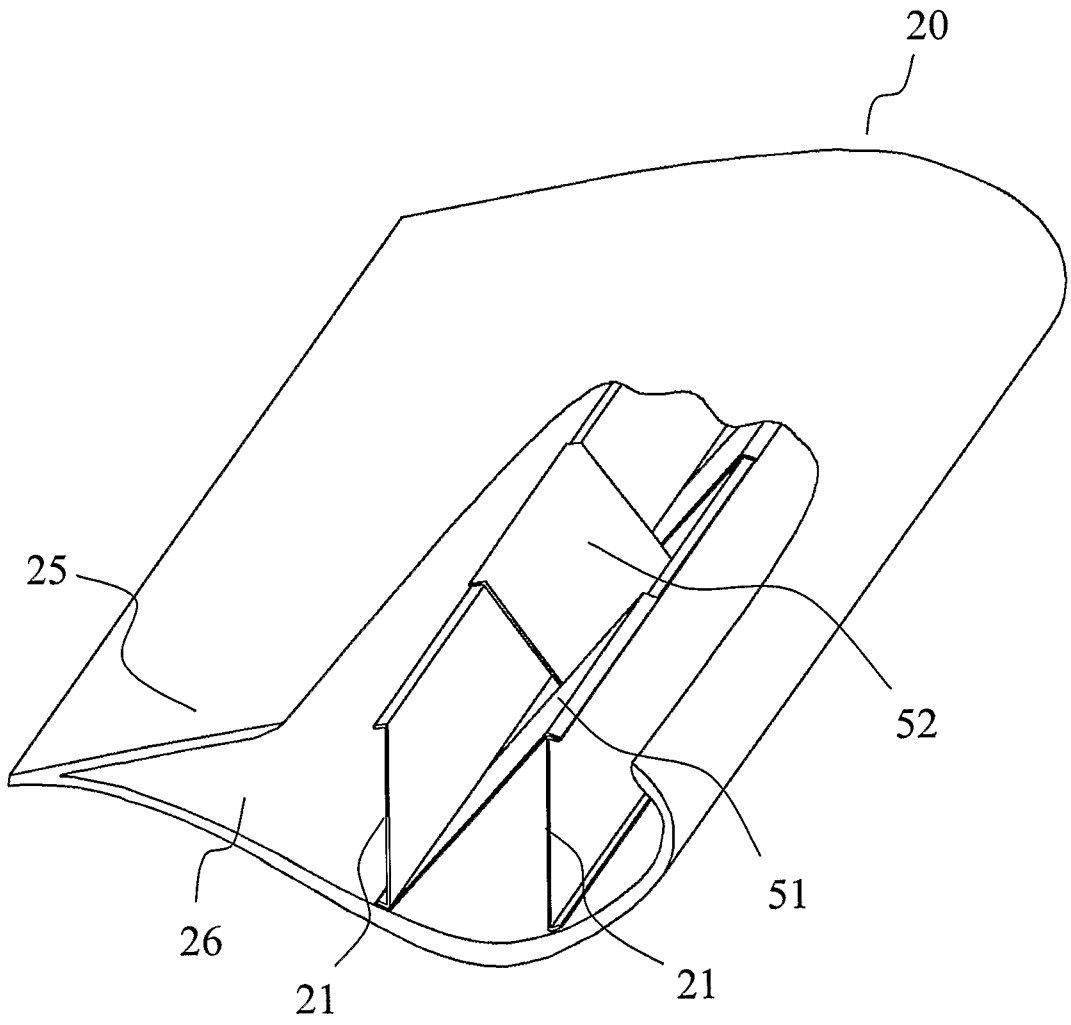

Fig. 9

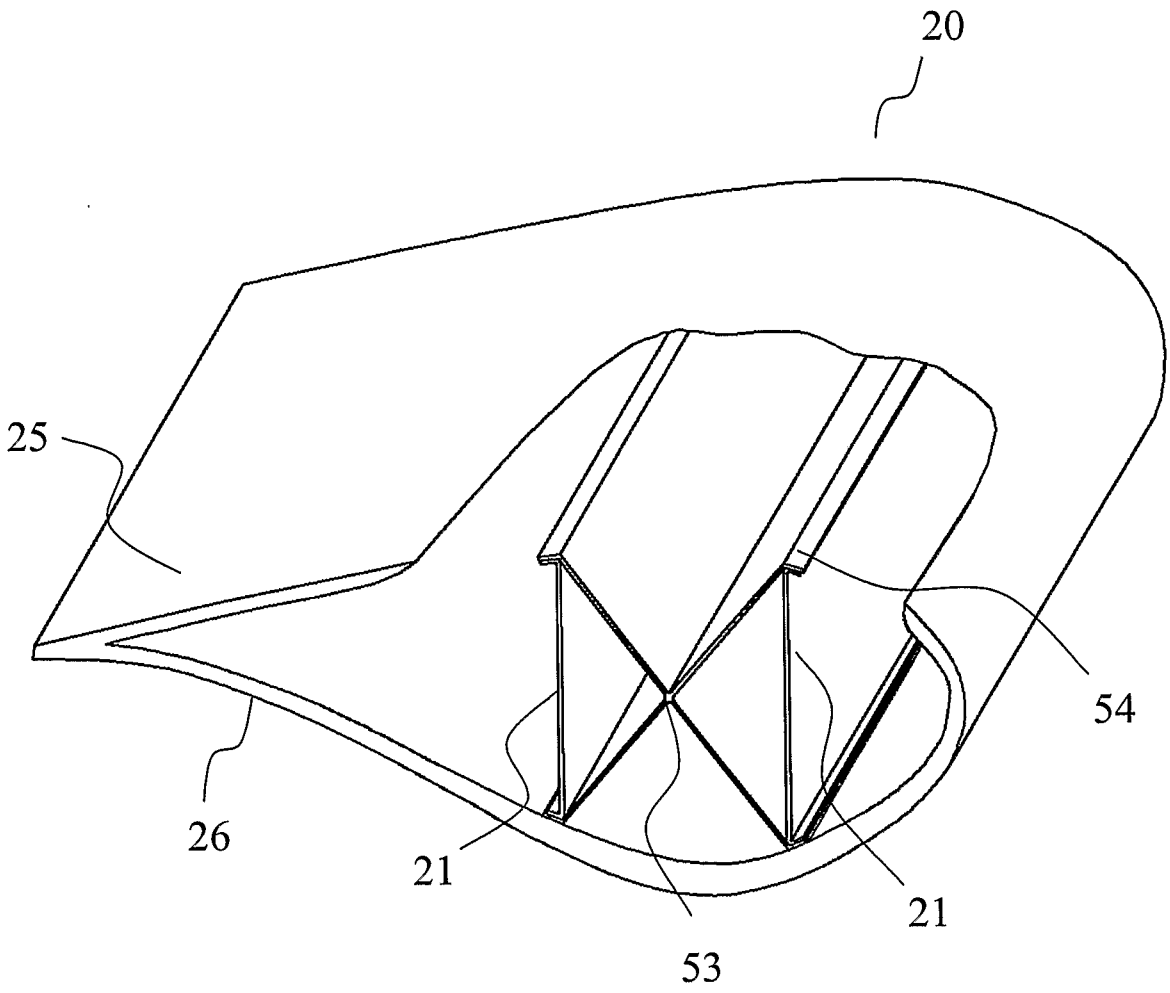

Fig. 10

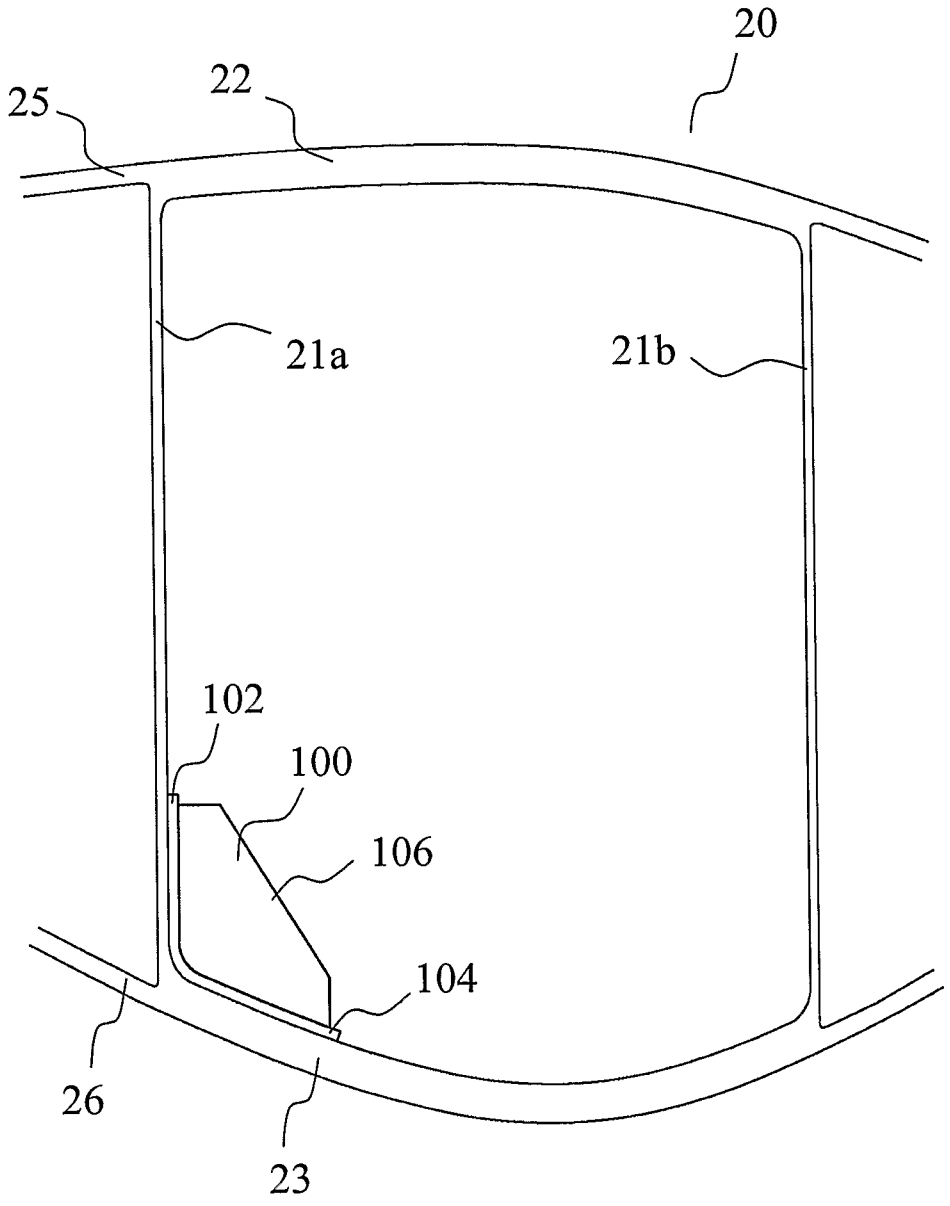

Fig. 11

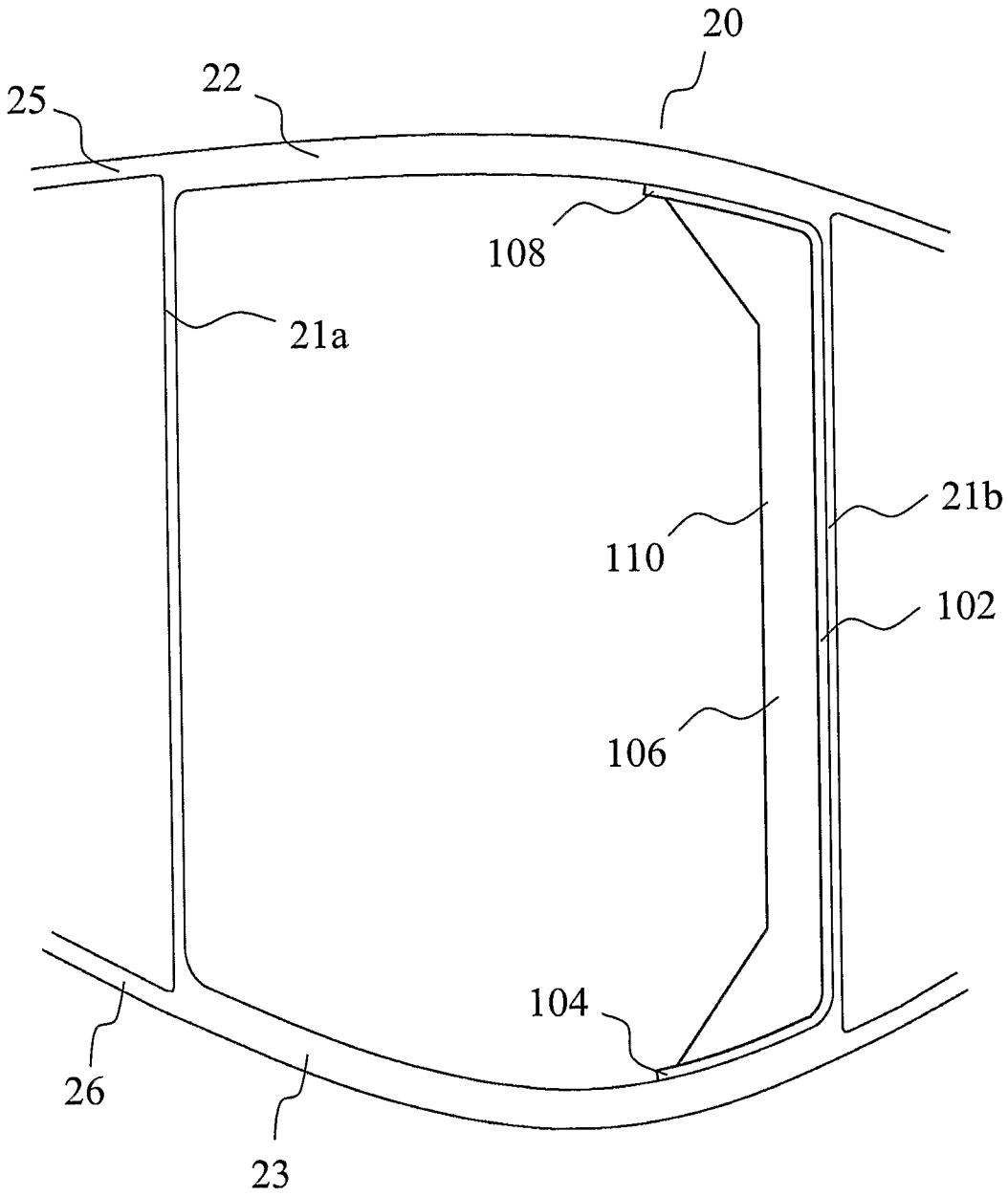

Fig. 12

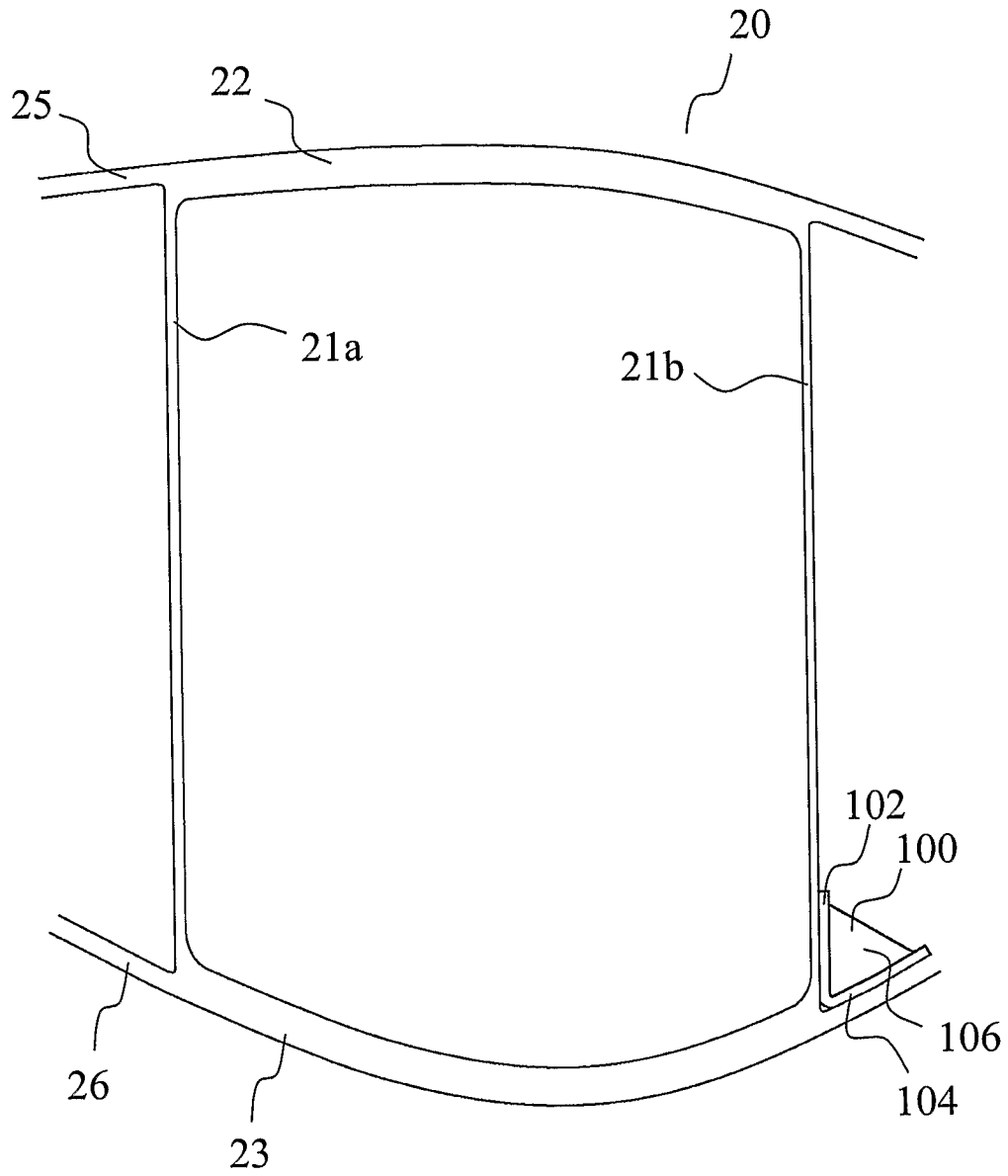

Fig. 13

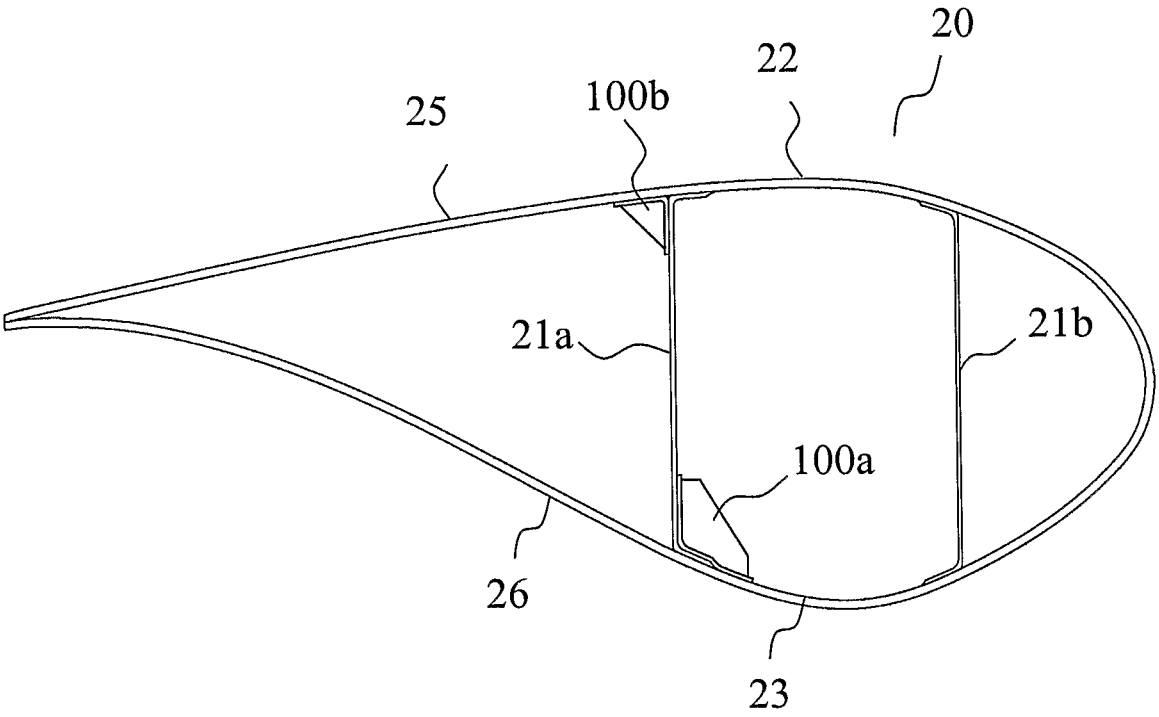

Fig. 14

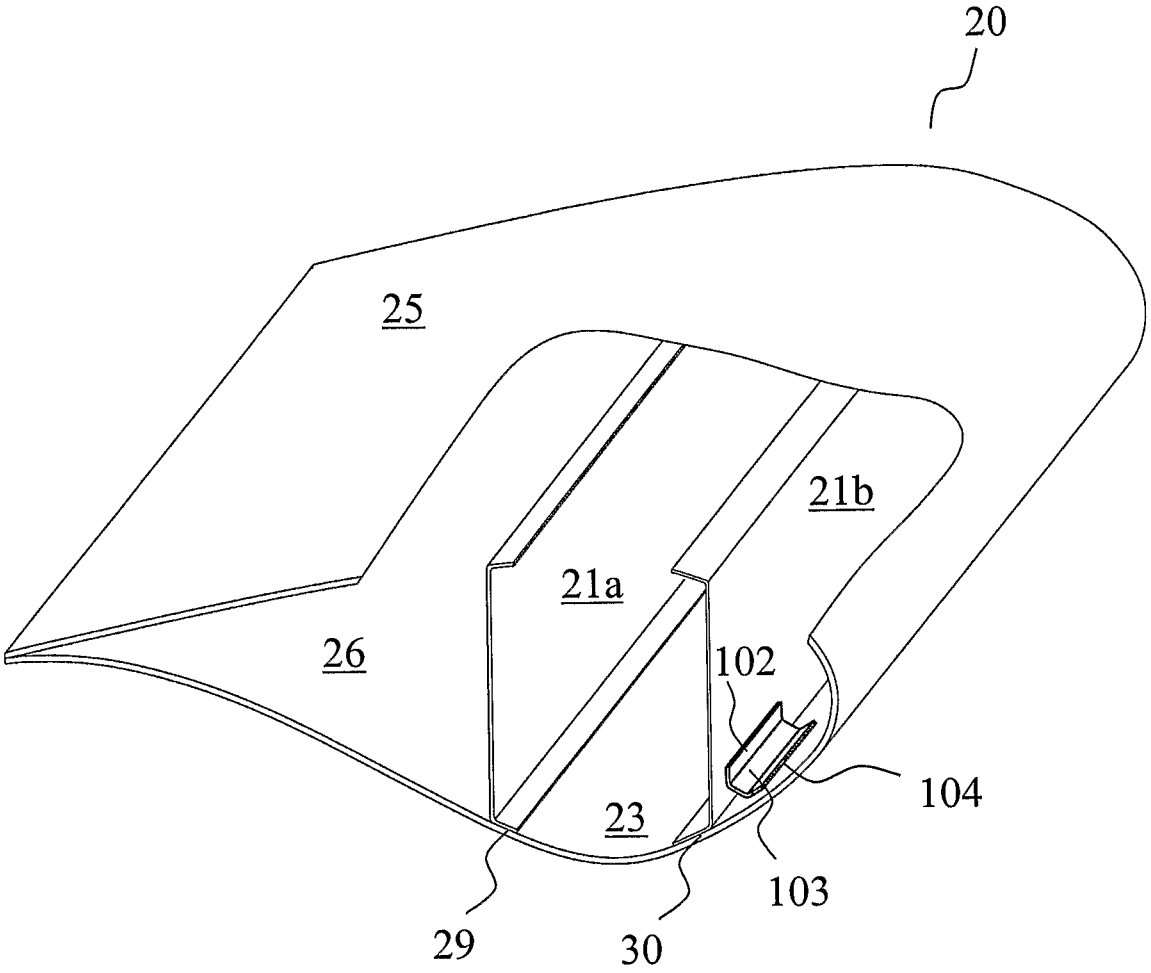

Fig. 15

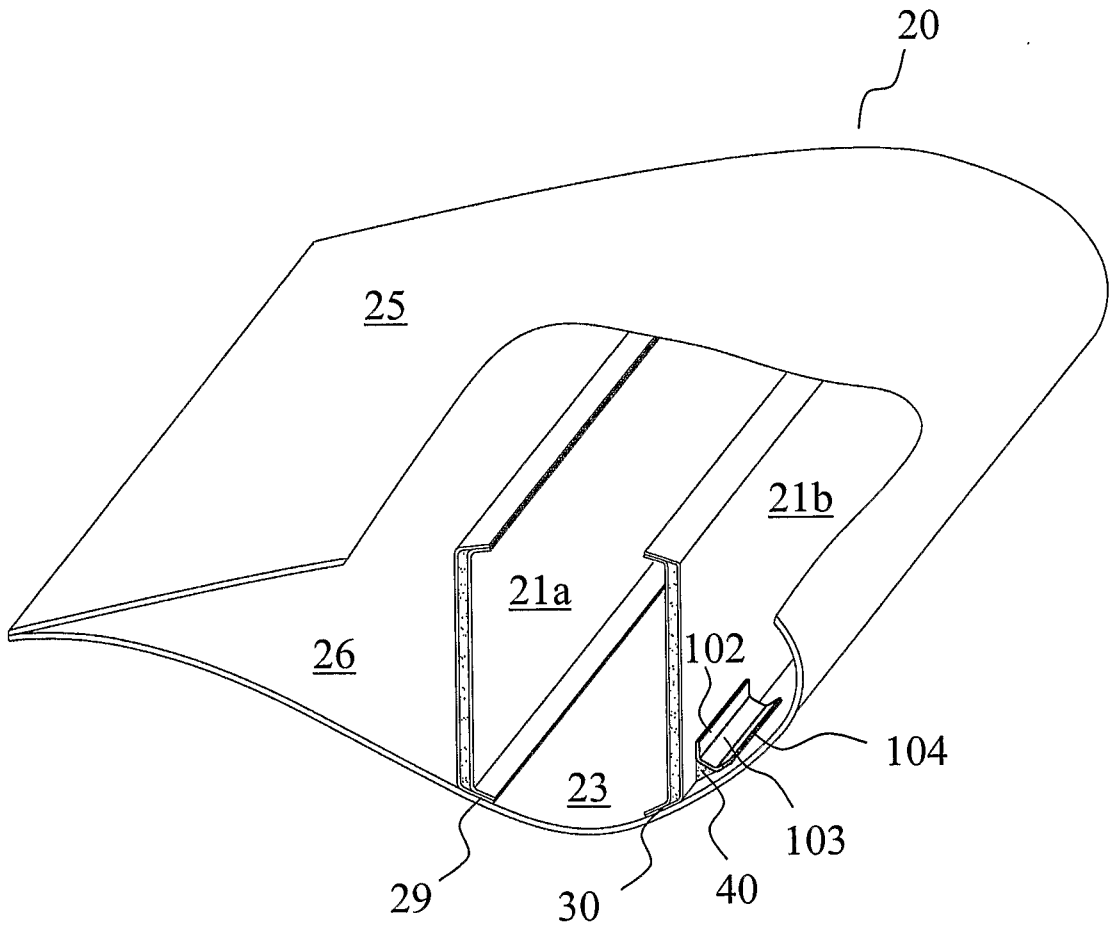

Fig. 16

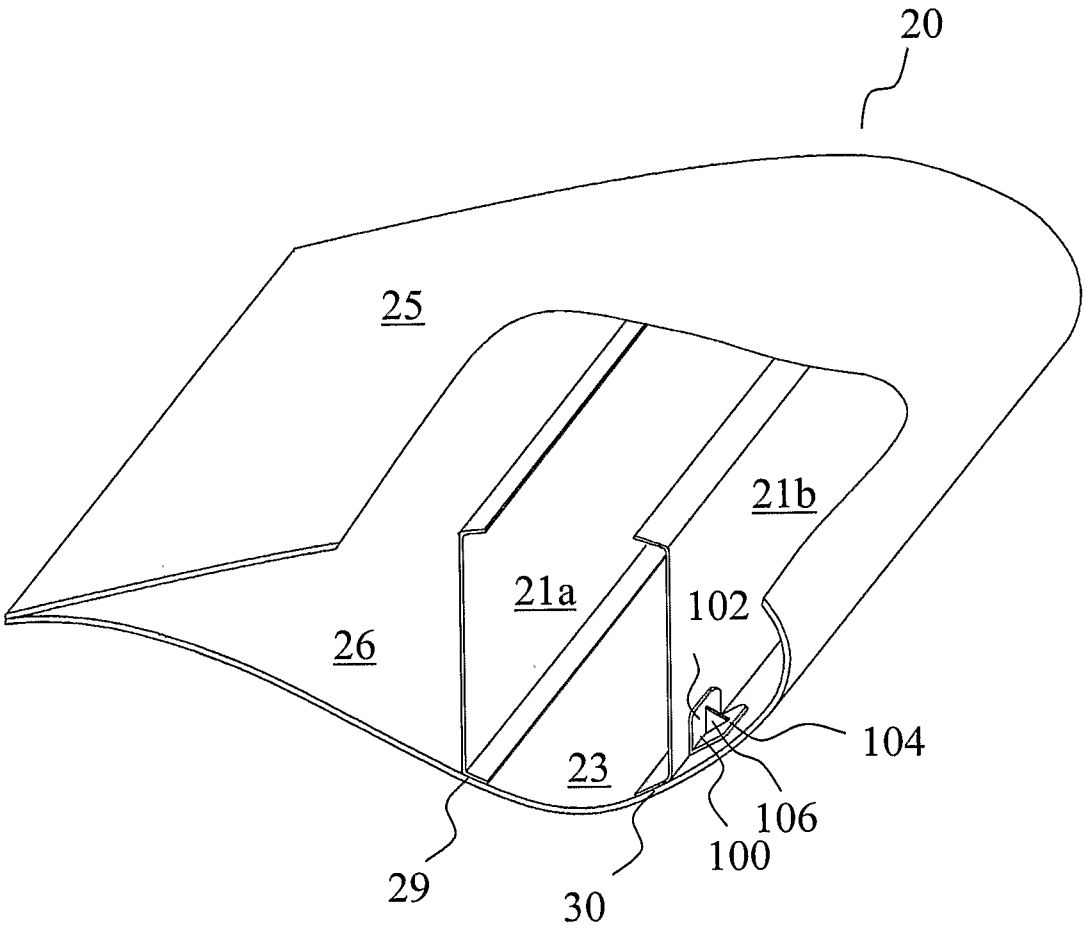

Fig. 17

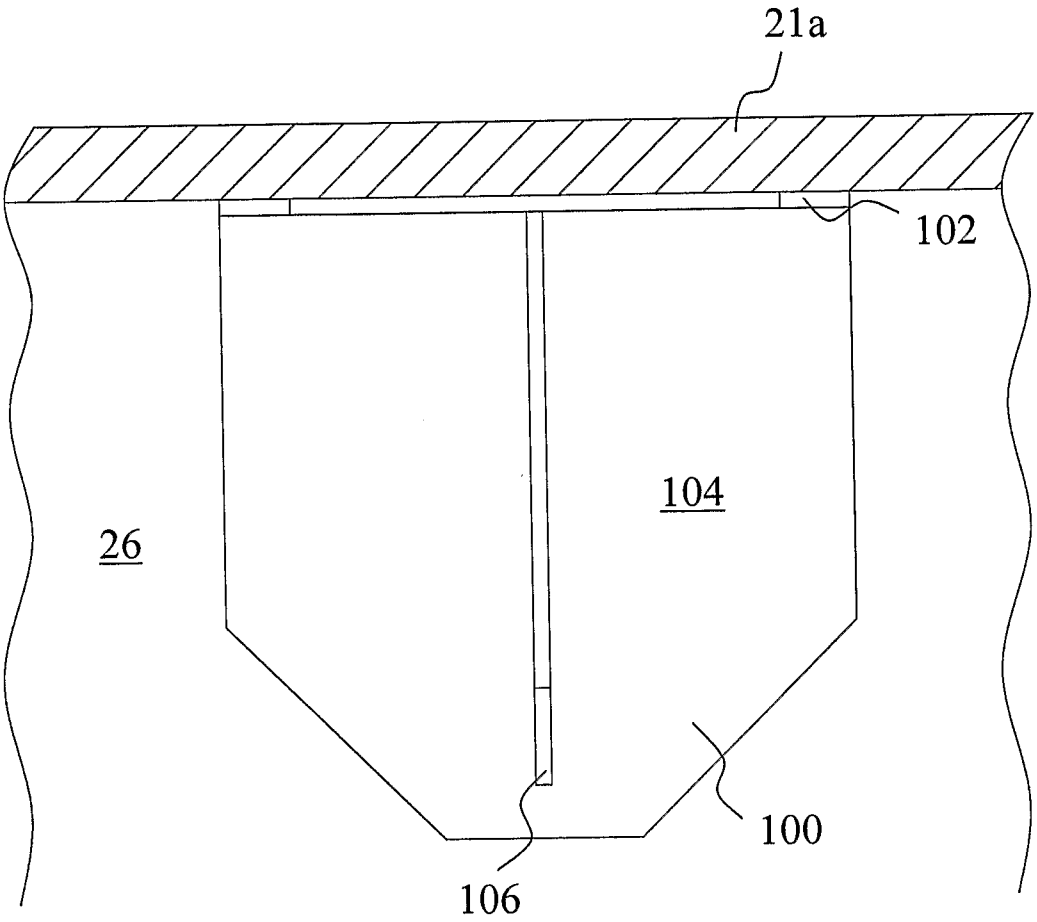

Fig. 18

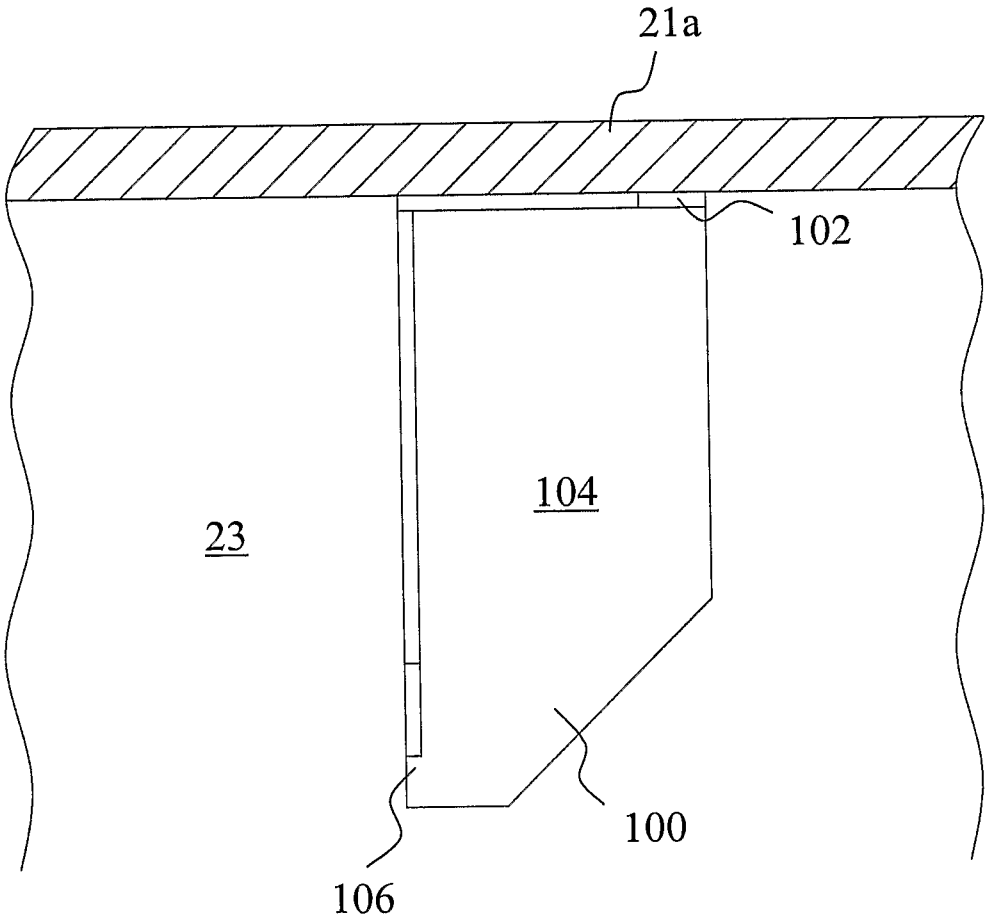

Fig. 19

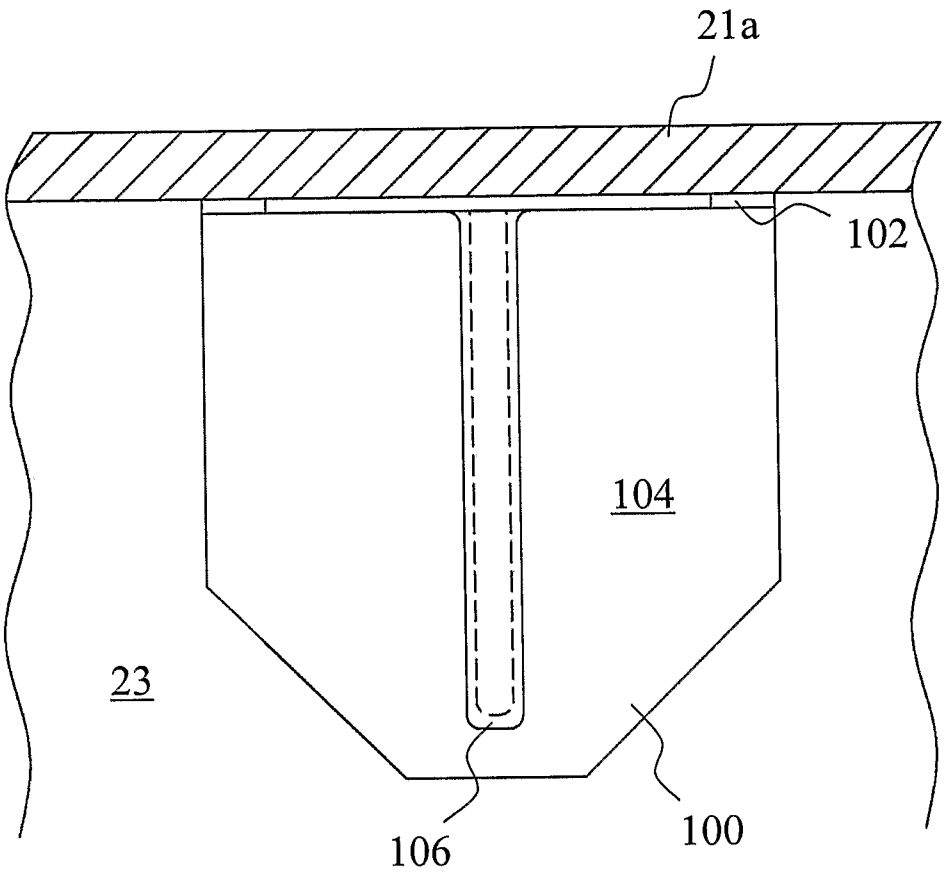

Fig. 20

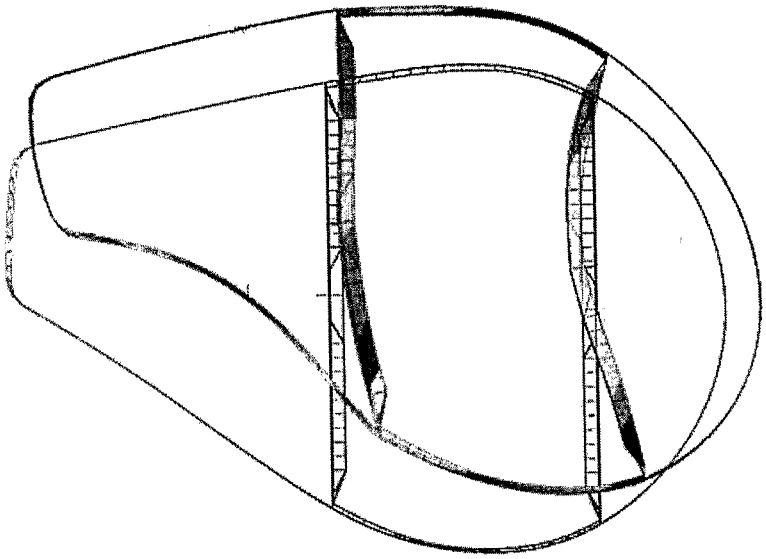

Fig. 21

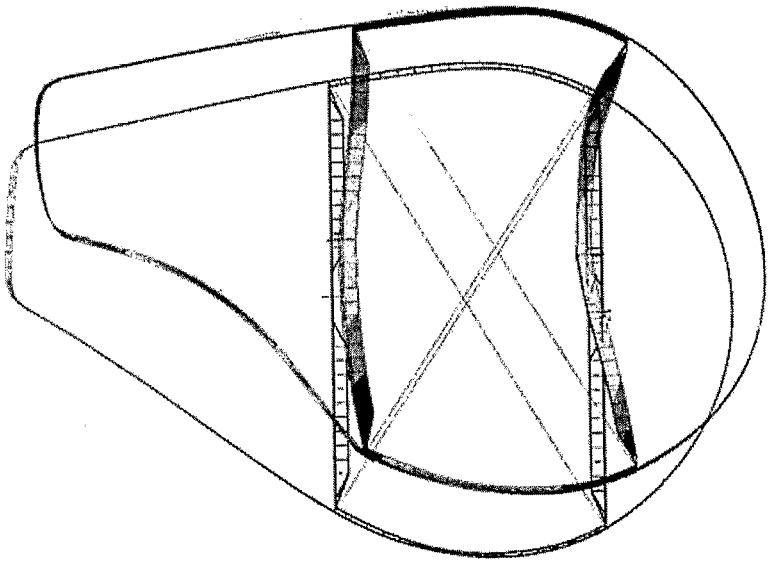

Fig. 22

Appendix B4 - “WO 2008-092451 Wind turbine blade(U-profile-patent D ”. Find M. Jensen

(12) INTERNATIONAL APPLICATION PUBLISHED UNDER THE PATENT COOPERATION TREATY (PCT)

(19) World Intellectual Property Organization
International Bureau

(43) International Publication Date
7 August 2008 (07.08.2008)

PCT

(10) International Publication Number
WO 2008/092451 A2

(51) International Patent Classification:
F03D 1/06 (2006.01) *F03D 3/06* (2006.01)

(21) International Application Number:
PCT/DK2008/000040

(22) International Filing Date: 29 January 2008 (29.01.2008)

(25) Filing Language: English

(26) Publication Language: English

(30) Priority Data:
PA 2007 00134 29 January 2007 (29.01.2007) DK

(71) Applicant *(for all designated States except US)*: **DANMARKS TEKNISKE UNIVERSITET** [DK/DK]; Anker Engelundsvej 1, Bygning 101A, DK-2800 Kgs. Lyngby (DK).

(72) Inventor; and

(75) Inventor/Applicant *(for US only)*: **JENSEN, Find, Mølholt** [DK/DK]; Emilsgave, 8, DK-4130 Viby Sjaelland (DK).

(74) Agent: **ALBIHNS A/S**; Havneholmen 29, bygn. 2, 3. sal, DK-1561 København V (DK).

(81) Designated States *(unless otherwise indicated, for every kind of national protection available)*: AE, AG, AL, AM, AO, AT, AU, AZ, BA, BB, BG, BH, BR, BW, BY, BZ, CA, CH, CN, CO, CR, CU, CZ, DE, DK, DM, DO, DZ, EC, EE, EG, ES, FI, GB, GD, GE, GH, GM, GT, HN, HR, HU, ID, IL, IN, IS, JP, KE, KG, KM, KN, KP, KR, KZ, LA, LC, LK, LR, LS, LT, LU, LY, MA, MD, ME, MG, MK, MN, MW, MX, MY, MZ, NA, NG, NI, NO, NZ, OM, PG, PH, PL, PT, RO, RS, RU, SC, SD, SE, SG, SK, SL, SM, SV, SY, TJ, TM, TN, TR, TT, TZ, UA, UG, US, UZ, VC, VN, ZA, ZM, ZW.

(84) Designated States *(unless otherwise indicated, for every kind of regional protection available)*: ARIPO (BW, GH, GM, KE, LS, MW, MZ, NA, SD, SL, SZ, TZ, UG, ZM, ZW), Eurasian (AM, AZ, BY, KG, KZ, MD, RU, TJ, TM), European (AT, BE, BG, CH, CY, CZ, DE, DK, EE, ES, FI, FR, GB, GR, HR, HU, IE, IS, IT, LT, LU, LV, MC, MT, NL, NO, PL, PT, RO, SE, SI, SK, TR), OAPI (BF, BJ, CF, CG, CI, CM, GA, GN, GQ, GW, ML, MR, NE, SN, TD, TG).

Published:
— *without international search report and to be republished upon receipt of that report*

(54) **Title:** WIND TURBINE BLADE

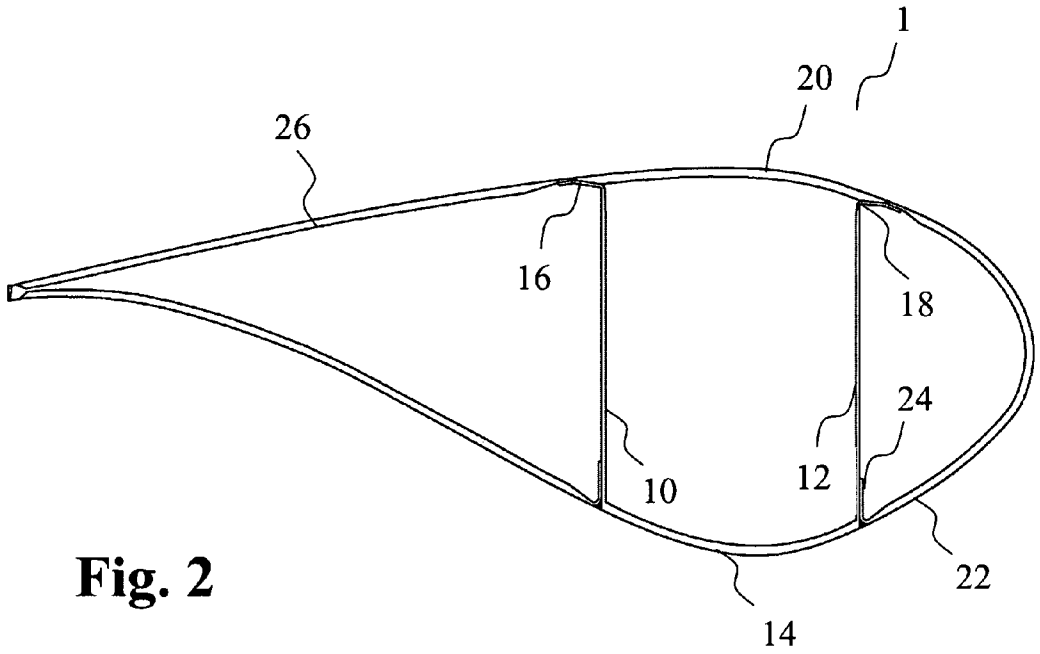

Fig. 2

(57) **Abstract:** The invention relates to a blade for a wind turbine, particularly to a blade that may be produced by an advanced manufacturing process for producing a blade with high quality structural components. Particularly, the structural components, which are preferably manufactured from fibre reinforced plastic material, will have a high level of stretched fibres as well as a far better controlled resin distribution and content and also a low void content.

WO 2008/092451 A2

WIND TURBINE BLADE

The present invention relates to a blade for a wind turbine, particularly to a blade that may be produced by an advanced manufacturing process for producing a blade with high quality structural components. Particularly, the structural components, which are preferably manufactured from fibre reinforced plastic material, will have a high level of stretched fibres as well as a far better controlled resin distribution and content and also a low void content.

A wind turbine blade normally consists of an aerodynamic shell and an internal girder such as a beam or a spar. Often two girders are used, and along with the shell the girders can be said to form a box profile. The top and bottom of the box profile are often referred to as the caps. Some types of blades are designed with a spar in the form of a box profile which is manufactured separately and bonded in between prefabricated surface shells.

The caps are the main load bearing elements in the blade as they under normal circumstances are designed to carry the bending moment generated by the flapwise load.

Therefore there is a massive material concentration in the caps making them rather thick and heavy. In an attempt of reducing the weight of the caps, the substitution of glass fibres in the caps with carbon fibres has until now been quite difficult because carbon fibres must be used with much more care in a production process to obtain the full potential of this material in terms of load carrying effect. Due to the fact that very large moulds are needed for the shells and girders of known wind turbine blades, both the handling of the material and methods of curing has not been adequate for the use of carbon fibres, resulting in inferior quality laminates with unwanted crimped fibres and too high void and resin contents.

During normal operation, a wind turbine blade is primarily loaded at an angle to the flapwise directions by aerodynamic and inertia forces.

This load is typically resolved into its components in the flapwise and edgewise directions. By flapwise direction is meant a direction substantially perpendicular to a transverse axis through a cross-sectional cut of the blade. Alternatively, the flapwise direction may be construed as the direction (or the opposite/reverse direction) in which the aerodynamic lift acts on the profile. The flapwise and edgewise directions are illustrated by way of example as indicated by arrows F and E in Fig. 1.

The flapwise load bending the blade from the Pressure side of the blade to the Suction side, see Fig. 1 - the upper side US will be the suction side of the blade and the lower side LS will be the pressure side, when the blade is in normal operation, is the most severe load. This load case is referred to as the PTS load. The flapwise load in the

opposite direction, from the Suction side of the blade To the Pressure side - STP load, is typically approximately 30 % less than the PTS load. In the PTS load case the cap on the upper side, see ref. US in Fig. 1, of the profile is in compression.

Fibre reinforced plastic used in wind turbine blades are layered materials and are more susceptive to compression forces than isotropic materials. This is because the fibres as a single fibre or a small bundle can buckle inside the laminate. This phenomenon is referred to as micro buckling and when the fibre or the bundle has buckled its load bearing capability is much smaller. Other fibres in the laminate have to carry the load, but if the laminate is further stressed, these fibres can also succumb to the micro buckling, and a global failure of the laminate can be the result. Carbon fibre reinforced plastic (CFRP) is very prone to this type of defects, if the manufacture of the laminate has not been carried out according to high manufacturing standards. Several attempts to produce a blade with carbon fibres in the load bearing parts have resulted in failure of the blade, because it was not possible to achieve the quality of the laminate necessary for the use of carbon fibres.

Furthermore, the cap in the upper part of the blade has only a very small transverse curvature, i.e. a very large radius of curvature which makes it particularly exposed deflections, also denoted buckling. The use of carbon fibres and high quality laminates facilitates a thinner cap, but this makes the cap more sensitive to buckling caused by compression forces.

The cap in the lower part of the blade, c.f. ref. LS in Fig. 1, is loaded in tension in the PTS load case, and fibre reinforced plastics can easily cope with this type of load.

In the STP load case, the cap in the lower part of the blade is subjected to compression forces, however this load is typically smaller compared to the load in the upper cap and further the lower cap has a much smaller radius of curvature which, as mentioned, increases the resistance to buckling failures.

For the manufacture of the laminates of wind turbine blades different methods are known in the industry. An older method comprises a wet lay up technique, where fabrics of fibreglass were laid into a mould and wetted manually with resin, and then built layer by layer. More recent methods which are now mainly used within the industry comprise manufacturing using a prepreg material or a resin infusion process.

Prepreg material is fabrics of fibres, mainly fibreglass or carbon fibres, that are wetted and consolidated with high viscosity resin. Such a material is more difficult to handle and position because it is stiff and heavy, however it is advantageous in that the resin is distributed optimally and the resin content can be thoroughly controlled which facilitates manufacturing of laminates with lower weight.

The resin infusion process involves the build-up of the layers of fabric on top of each other and then covering the layers of fabric with a thin plastic sheet material. Then

resin is delivered through inlets in the mould and/or in the plastic sheet and drawn into the layers of fabric by vacuum and thereby wetting the fibres. This is an economically attractable way of producing laminates, but the method has the drawbacks that the resin content may vary unsatisfactory throughout the part and further the void content is higher in comparison to laminates made of prepregs.

As the individual fibre mats or prepregs are typically quite large and heavy, they are difficult to place accurately in a mould and it is further difficult to obtain the desired level of stretched fibres in the laminate. The most advanced method of placing fibre mats or prepregs utilize a machine that place pre-cut fibre mats or prepregs from a roll into the mould which very often requires assistance from manual labour. Although such machines may improve the quality of the laminate, neither the prepreg method nor the resin infusion process provides an optimal laminate.

The evacuation of trapped air and the consolidation of the laminates are known to be improved if an autoclave is used subsequent to either of the described processes, but it is not economically feasible to construct autoclaves that are able to house the often very large moulds that are necessary in the wind turbine industry.

In a presently available and commonly used technique for the manufacture of wind turbine blades, the assembly between the shell parts and the one or more internal girders is as follows: the lower shell part is prepared for the bonding phase when it sits in the mould curing. Adhesive is applied on the inner surface of the lower shell part beneath the intended position(s) of the girder(s) and afterwards the girder(s) is/are placed on the adhesive. The girder(s) is/are now bonded to the lower shell. For the next step, adhesive is applied on the bonding flanges on top of the girders and in the trailing and leading edge sections of the lower shell part. The upper shell part is then placed on top of both the girder(s) and the lower shell part and kept in that position until the adhesive has cured. With this process it is often difficult to achieve a correct alignment of the leading edge of the lower and upper shell parts. If a correct alignment is not achieved the resulting aerodynamic shape of the blade is compromised and consequently a less stable blade with a lower operating power output is produced.

Presently, there is a need for a wind turbine blade that overcomes the disadvantages of the currently available techniques as described and may be manufactured with a significantly better quality than achieved in previously provided blades.

It is therefore an object of the present invention to provide a wind turbine blade with increased strength, yet still with a reduced weight in comparison to currently available blades and at a lower manufacturing cost.

It is also an object of the present invention to provide a wind turbine blade which facilitates the use of advanced fibre materials such as carbon fibres.

It is another object of the present invention to provide a wind turbine blade of better quality due to more homogenous material distribution and thus with an improved reliability of the blade profile.

It is another object of the present invention to provide a wind turbine blade with a leading edge without deviation from the optimal shape.

It is yet another object of the present invention to provide a wind turbine blade with increased aerodynamic performance and thereby a higher power output.

It is another object of the present invention to provide alternatives to the prior art.

In particular, it may be seen as an object of the present invention to provide a wind turbine blade that solves the above mentioned problems of the prior art by providing a blade made from combinations of novel and inventive components e.g. such as described by way of the examples in the following disclosure.

According to the present invention, the above-mentioned and other objects are fulfilled by a wind turbine blade comprising

a girder substantially shaped as a U-profile,

a first shell part,

a second shell part, and

a box cap part,

wherein the girder and the box cap part constitutes, when assembled, a load carrying box profile of the blade and wherein the bottom part of the U-profile and the box cap part conform to the outer surface of the blade , and wherein the box cap part, the first shell part and the second shell part are connected to the girder.

For example in one embodiment, the first shell part constitutes a leading edge section of the blade and the second shell part constitutes a trailing edge section of the blade and the bottom part of the U-profile constitutes a part of the outer surface of the blade substantially opposite the box cap part, and

in another embodiment, the first shell part constitutes an upper shell part of the blade and the second shell part constitutes a lower part of the blade.

Thus, the above described objects and several other objects are obtained in a first aspect of the present invention by providing a wind turbine blade comprising individual components in the forms of

- a girder substantially shaped as a U-profile,
- a leading edge section,
- a trailing edge section, and

- a box cap part,

wherein the girder and the box cap part constitutes, when assembled, a load carrying box profile of the blade and wherein the bottom part of the U-profile constitutes a first part of the outer surface of the blade and wherein the box cap part constitutes a second part of the outer surface of the blade, substantially opposite to the first part, and wherein the box cap part, the trailing edge section and the leading edge section are connected to the girder.

The girder substantially shaped as a U-profile is hereinafter referred to as the U-profile. The U-profile is provided to primarily strengthen and/or reinforce the blade in its longitudinal direction and is preferably of a fibre reinforced plastic material or other suitable material. In this application a U-profile should be construed as an elongate constructional element capable of taking up loads, such as a beam or a spar comprising two parallel sides and a third substantially transverse "side" connecting the parallel sides. In embodiments of the invention, the U-profile component may itself comprise individual parts. Preferably, in such embodiments, the U-profile is assembled with two parallel sides connected by a transverse "side" in the shape of another, geometrically reversed but otherwise similar, box cap part. The U-profile may substantially extend along the length of the blade. However, it may also be preferred to provide the blade with two or more separated U-profiles in the longitudinal direction of the blade, especially for facilitating handling or transporting purposes.

The first part of the outer surface of the blade constituted by the bottom part of the U-profile may preferably be a cap part of the blade.

The second part of the outer surface of the blade that is substantially opposite to the before mentioned first part, may preferably be another cap part of the blade. In this context, substantially opposite refers to positions at the other side of the profile chord of the blade. The profile chord of the blade is an imaginary surface that contains the leading edge and the trailing edge of the blade and extends therebetween.

The box cap part, the trailing edge section and the leading edge section may preferably be connected to the U-profile and/or with each other. The connections, or joints, may be established by bonding, laminating or mechanical means.

When the U-profile and the box cap part are joined, they constitute the load carrying box profile of the blade. Particularly, with the configuration of the components according to the first aspect, the load bearing fibres in the cap parts are situated to the outermost part of the blade where they provide the most efficiency in counteracting the bending moment of the blade.

According to the first aspect the leading edge section may preferably be made in one piece by traditional laminating techniques. The section is much smaller than compared

to the upper and lower shells of a conventional blade and this facilitates an improved possibility for controlling the laminate's quality during manufacture. Another important benefit is that no joining is necessary in the leading edge whereby the shape of the leading edge is not compromised due to misaligned assembly, thus eliminating the risk of deviation from the optimal profile as often seen on conventional blades. The result is that the optimal power output of the blade in operation is maintained.

According to the first aspect the trailing edge section may also be manufactured in one piece. This will avoid the normally necessary bonding connection in the trailing edge that often cause fractures in conventional blades. However, the trailing edge section may also be manufactured in two pieces that are joined in the trailing edge before the section is assembled with the other components. The access to the trailing edge in this situation is much better compared to the conventional blades and this facilitates the provision of a higher quality the trailing edge joint, avoiding many of the failures experienced in the conventional wind turbine blades. As with the leading edge section, the dimensions of the trailing edge section, whether the part is made in one or more pieces, are much smaller than compared to those of the upper and lower shells of conventional blades and this makes quality control much easier.

Each of the individual components according to the first aspect of the present invention may, due to their dimensions, be manufactured using an autoclave for improving the quality as previously described. Preferably, however, it is the box cap part and the U-profile that is subjected to use in an autoclave. The laminate of the component in the relevant mould is covered by a bag that is put under vacuum. The laminate and the mould are placed in the autoclave, which is pressurized and heated during the cure of the laminate. This result in a laminate with fully wetted fibres, an improved distribution of resin, low resin content and a very low void content.

According to the embodiments of first aspect of the invention, the individual components may preferably be manufactured separately. The individual components may then subsequently be bonded or laminated together to form a complete blade. The provision of a blade made from smaller individual components means that the components may be manufactured in moulds of a size that may fit in autoclaves that are economically feasible. Consequently, the provision of a blade constructed of individual components facilitates the use of an autoclave in the manufacturing of components for the blade which in turn produces blades of a higher quality than with the known techniques.

In embodiments, one or more of the individual components is/are at least partly made of a carbon fibre reinforced plastic material. As the use of an autoclave is facilitated by the invention it is particularly, but not exclusively, preferable to use carbon fibres for reinforcing the plastic materials of the components according to the invention

because it is possible to fulfil the demands in terms of level of stretched fibres, controlled resin distribution and content and also low void content. Particularly, it may be advantageous to manufacture the box cap part in an extra good quality as the box cap part may constitute the cap part of the blade and an improved capability of taking up compression forces in the blade is therefore clearly beneficial.

In embodiments, the box cap part has a radius of curvature of at least 2 Meters. However, in certain embodiments the box cap part is completely linear or flat. The box closing may preferably be so designed that it is possible to produce the part on a nearly flat table or mould, further facilitating the use of an autoclave, and also makes it much easier to place plastic material in the mould of the box cap part. The easy access to the mould facilitates manufacture of the box cap part with accurate placing of the material, stretching of the fibres and also allows for a preferably mechanical pressurisation of the fibre material during the lay-up. Such a pressurisation will further lower the void content if prepreg materials are used. A nearly flat mould is particularly suited in connection with use of machines for laying up of fibres due to the unhindered access from the sides. The use of machines may further improve the level of stretched fibres and reduce the void content. The box cap part according to the invention may also be well suited for adjustments or adaptations subsequent to curing using CAD/CAM milling machines. With these machines, narrow tolerances in regard to width, length and thickness of the box cap part may be achieved. It may also be possible to shape the edges of the closing part so that they are prepared for connections with the other components. One particularly suitable type of joint for load transfer is a scarf joint used for bonding of the closing part to the other parts. However, any suitable type of joint may be applied.

Another advanced method of manufacturing the box closure part is by pultruding, wherein yarns of fibres are drawn thought a matrix which has the shape of a cross-section of the box closure part. In the matrix resin is added and cured as the complete part is drawn continuously from the matrix. This method has the potential of achieving the highest quality possible for fibre reinforced plastics.

In embodiments, one or both of the sides of the U-profile comprise a sandwich construction. However, one or both sides may be made as a single skin laminate but as the girder is subjected to compression forces, sandwich construction is a particularly useful solution enabling the sides to take up such forces. As the connection with the box cap part are typically at the end of the U-profile, the girders' resistance to deflection/buckling is not compromised, as it would be by joints positioned e.g. at the middle of their span.

In embodiments, the U-profile further comprises connection means at an end region of the sides thereof. In embodiments, the connection means comprises a flange integrated with the end region of the side(s). The flange may serve as a connection

surface for bonding, laminating or mechanically fastening the girder to the respective other components. However, the flange and other suitable connection means may also be attached to the girder in stead of being integrated therewith.

In other embodiments, the box cap part may further comprise one or more stiffening means provided in the longitudinal direction of the blade. Particularly, when the box cap part constitutes a cap part of the blade it may be designed to have increased resistance against global deflection/buckling. A simple way to do this is to connect one or more stiffeners to the inner surface of the cap part in the along at least a part of the length of the blade. The stiffener may be of any suitable shape. Alternatively, the one or more stiffeners may be made integral with the box cap part. The caps' resistance to deflection/buckling may also be increased with the use of a sandwich construction or a hollow profile with internal stiffeners. These features may advantageously be included in the manufacture of the box cap part and the U-profile. The stiffeners may comprise any suitable material but are preferably made of same material as the main part itself.

At least some of the above described objects and other objects are obtained in a second aspect of the present invention by providing a box profile structure for a wind turbine blade comprising

- a girder substantially shaped as a U-profile, and
- a box cap part,

wherein the U-profile and the box cap part constitutes, when assembled, a load carrying box profile of the blade and wherein a bottom part of the U-profile conforms with, at least a part of a first shell part of the blade and wherein the box cap part conforms with at least a part of a second shell part of the blade.

The substantially U-shaped girder and the box cap part according to the second aspect of the invention may preferably be manufactured and assembled and/or connected by the methods and of the materials as described above with respect to the first aspect of the invention.

With this configuration the load carrying box profile may be assembled separately and subsequently bonded in between two shell parts. The shell parts will then cover the complete surface of the box profile and surround the U-shaped girder and the box cap part completely. This facilitates that shell parts from a conventionally manufactured blade maybe used with the novel box cap part and the U-profile.

Thus, in embodiments, a wind turbine blade comprising at least one box profile structure according to the second aspect of the invention as well as first and second shell parts is provided.

In accordance with a third aspect of the invention, a method is provided the steps of

producing a girder substantially shaped as a U-profile with a bottom conforming to a predetermined aerodynamic profile,

producing a first shell part having the shape of a part of the predetermined aerodynamic profile,

producing a second shell part having the shape of a part of the predetermined aerodynamic profile, and

producing a box cap part having the shape of a part of the predetermined aerodynamic profile,

connecting the box cap part to the girder thereby forming a load carrying box profile of the blade, and

connecting the first shell part and the second shell part to the girder. Below the invention will be described in more detail with reference to the exemplary embodiments illustrated in the drawings, wherein

Fig. 1 is a schematic, perspective view of a wind turbine blade indicating the directions of the flapwise and edgewise loads as well as an upper and lower side of the blade.

Fig. 2 shows a schematic cross sectional view of a first embodiment of a wind turbine blade according to the first aspect of the present invention.

Fig. 3a shows a schematic, cross sectional view of a blade and an enlarged detail of the box cap part provided with a stiffener in the form of a corrugated plate.

Fig. 3b shows a schematic, cross sectional view of a blade and an enlarged detail of the box cap part provided with a stiffener in the form of a top hat profile.

Fig. 4 shows a schematic view of a blade and an enlarged detail of the box cap part provided with a stiffener in the form one or more I-profiles.

Fig. 5 shows a schematic, cross sectional view of a blade wherein the box cap part is of a sandwich construction.

Fig. 6 shows a schematic, cross sectional view of a blade with a reinforcing member connected to the box profile,

Fig. 7 shows a schematic cross sectional view of an embodiment of a wind turbine blade according to a second aspect of the present invention.

Fig. 8 shows a schematic, cross sectional view of how the connections between the different components may be provided with a protective covering.

Figs. 9-12 show details of different solutions for connecting an upper part of the trailing edge section with the box cap part and with the U-shaped girder. Figs. 9 – 12

are also representative for the connecting of an upper part of the leading edge section with the box cap part and the U-shaped girder.

Figs. 13-15 show details of different solutions for connecting a lower part of the trailing edge section with the U-shaped girder. Figs. 13 – 15 are also representative for the connecting of an upper part of the leading edge section with the U-shaped girder.

Fig. 16 shows an alternative embodiment of the invention according to the first aspect of the invention.

The drawings are schematic and simplified for clarity, and they merely show details which are essential to the understanding of the invention, while other details have been left out. Throughout, the same reference numerals are used for identical or corresponding parts.

The present invention will now be described more fully hereinafter with reference to the accompanying drawings, in which exemplary embodiments of the invention are shown. The invention may, however, be embodied in different forms and should not be construed as limited to the embodiments set forth herein. Rather, these embodiments are provided so that this disclosure will be thorough and complete, and will fully convey the scope of the invention to those skilled in the art. Like reference numerals refer to like elements throughout.

Fig. 1 shows a wind turbine blade 1 in perspective and indicates the directions of the flapwise and edgewise loads by arrows F and E respectively. An upper and a lower side of the blade is denoted US and LS. The upper side US will be the suction side of the blade and the lower side LS will be the pressure side, when the blade is in normal operation.

In Fig. 2 a cross sectional view of wind turbine blade 1 is shown. The wind turbine blade 1 comprises a girder. The girder of the embodiment shown in Fig. 1 is U-shaped and comprises two vertical girder parts 10, 12 and a bottom girder part 14 constituting a part of the outer surface of the blade 1. The three parts 10, 12, 14 are typically made integral with each other by a moulding process in which the U-shaped girder is made as an individual component. However, the various girder parts 10, 12, 14 can be made as separately produced parts assembled to form the U-shaped girder as previously described and as illustrated by way of example in Fig. 16.

The upper ends of the girder parts 10, 12 are provided with flange parts 16, 18 to which a box cap part 20 is connected as shown in Fig. 16 and shown in more detail in Fig. 8. The box cap part 20 is formed so as to constitute the outer surface of the blade. Similarly, the girder part 14 constitutes also an outer surface of the blade.

The blade further comprises a leading edge section 22. The leading edge section 22 is shaped as an open profile defining the leading edge section of the blade and is attached to the flange 18 of the girder 12 at the upper side of the profile and attached to the girder 12 by a flange 24 in a region in vicinity of the lower side of the blade.

The flanges 18, 16 are shown as outward pointing flanges; the flange 16 points towards the trailing edge and the flange 18 points towards, the leading edge. These flanges may instead be inwardly pointing flanges so that the flange 18 e.g. points in the direction of the trailing edge or a combination of inwardly and outwardly pointing flanges may be provided.

The leading edge section 22 is preferably attached to the girder 12 by a adhering technique in which e.g. resin is applied to the surfaces to be adhered which in turn are pressed against each other.

Similarly, the trailing edge section 26 is shaped as an open profile defining the trailing edge of the blade and attached to the girder 10 in a manner similar to the manner according to which the leading edge section 22 is attached to the girder 12.

It should be noticed, that although the box cap part is shown as constituting an upper surface part of the outer surface the girder can be geometrically reversed in such a manner that the girder part 14 constitutes an outer surface part of the upper surface and the box cap part 20 constitutes an outer surface part of the lower surface.

The girder with box cap part extends along the length of the blade. Typically, the girder with box cap part extends through-out the entire span of the wing. However, the load on the tip of the blade is typically low and the size of the tip is typically small allowing the tip to be formed without any girder parts 10, 12, 14 and box cap part 20. Thus, the girder parts with box cap part may in some preferred embodiments extend only to an extent where the load carrying effect of the girder with box cap part plays a role. It has been found that an extension of at least 70%, such as at least 80%, preferably at least 90% or even at least 95% of the lengthwise extension of the blade is sufficient to provide a suitable stiffness of the blade.

In embodiments where the girder with box cap part does not extend through-out the whole lengthwise extension of the blade, the tip may preferably be made as a single piece which is attached to the girder.

In Fig. 3a is shown a reinforcement of the box cap part 20 in the form of a stiffener in the lengthwise direction of the blade, in Fig. 3a provided as a corrugated plate 30. The plate 30 may comprise any suitable shape, size and number of corrugations and be of a fibre reinforced plastic or a lightweight metal such as aluminium. In Fig. 3a, a number of three corrugations are shown. A corrugation 31 is shown enlarged in detail. The cavities 32 created by the corrugations may be filled with a lightweight foamed material (not shown). The reinforcement may also, or additionally, be provided on the

opposite girder part 14. The plate 30 may be adhered, bonded or mechanically attached to the parts 14, 20. The reinforcement may also be integrated with either of the parts 14, 20 during their manufacture.

Fig. 3b is substantially identical to Fig. 3a, but shows a reinforcement of the box cap part 20 in the form of a stiffener in the lengthwise direction of the blade, in Fig. 3b provided as a top hat profile 30b. The top hat profile 30b may be of any suitable shape and size and be of a fibre reinforced plastic or a lightweight metal such as aluminium. The top hat profile 30b is shown enlarged in detail. The cavity 32 created by the top hat may be filled with a lightweight foamed material (not shown). The top hat profile may also be used in connection with making the box cap part at least partly as a sandwich construction. This kind of reinforcement may in an identical manner also, or additionally, be provided on the opposite girder part 14. The top hat profile 30b may be adhered, bonded or mechanically attached to the parts 14, 20. In Fig. 3b, the top hat profile is shown without any bonding "feet" for the attachment to the box cap part 20. However, it may comprise such bonding "feet" or it may alternatively be made integral with the parts 14, 20. One or more such top hat profiles may be provided.

Fig. 4 substantially corresponds to Fig. 3a+b except that the stiffener in the lengthwise direction of the blade is provided as I-profiles, in Fig. 4 shown on the box cap part 20. One I-profile 33 is shown enlarged in detail. The one or more I-profiles 33 may be of any suitable size and be of a fibre reinforced plastic or a lightweight metal such as aluminium or other materials. Like in Fig. 3 the I-profiles may also, or additionally, be provided on the opposite girder part 14. They may be adhered, bonded or mechanically attached to the parts 14, 20. The I-profiles may also be integrated with either of the parts 14, 20 during their manufacture e.g. by lamination.

In Fig. 5 is shown a blade having a box cap part 34 of a sandwich construction. Box cap part 34 is shown as consisting of outer layers 35, 36 of fibre reinforced plastic on both sides of a foamed material 37. Even though the laminate may be made thinner by using carbon fibres, it may simultaneously be more sensible to buckling caused by compression forces. Thus, a sandwich construction enables the box cap part 35 with a high resistance against buckling from the compression forces therein. The space between the outer layers 35, 36 may in embodiments further comprise one or more "internal" stiffeners in the blade's lengthwise direction. In these embodiments foamed material 37 may be provided in sections between the stiffeners. The stiffeners may comprise any suitable shape, size and material, preferably substantially corresponding to the choices of the above described "external" reinforcements of the parts 14, 20.

Fig. 6 shows a transverse cross-section through the blade 1 with an internal reinforcing member 40 of the box profile. In the illustrated embodiment, the reinforcing member 40 is a plate preferably with one or more cut-outs for weight

saving purposes. The reinforcing member 40 supports the box cap part 20 and prevents the box cap part 20 from buckling like the reinforcements shown in Figs. 3 - 5. The plate 40 also facilitates assembly of the box profile and secures a strong connection between the box profile parts. The plate 40 further reinforces the web, i.e. the vertical girder parts 10, 12, of the box profile preventing buckling failure of the box profile.

Preferably, the blade 1 has a plurality of reinforcing members 40 positioned spaced apart in appropriate positions along the longitudinal direction of the blade 1. The reinforcing member 40 can be made of any suitable material, and preferably the reinforcing member 40 is made of the same material as the blade 1. Further, the reinforcing member 40 can be made as a sandwich construction. The reinforcing member 40 may be reinforced with stringers or flanges to avoid buckling failure of the member. The reinforcing member 40 can be fastened with any suitable method, and preferably the reinforcing member 40 is bonded or laminated to the box profile. An edge of the reinforcing member 40 may be provided with bonding flanges for this purpose. In Fig. 7 an embodiment of the wind turbine blade according to a second aspect of the present invention is shown. Also in this embodiment, the girder comprises girder parts 10, 12, 14 similar to the girder parts shown in Fig. 2. Furthermore, a box cap part 20 is provided similar to the box cap part of Fig. 2. The box cap part 20 is connected to the girder part 10, 12 in a manner similar to the manner disclosed above in connection with Fig. 2.

The box cap part 20 and the girder part 14 have each a shape conforming to the outer surface parts of the blade. These parts are covered by two shell parts, an upper shell part 26 and a lower shell part 28 that defines the shape of the leading and trailing edges of the blade. The U-profile, box cap part 20 and upper and lower shell parts 26, 28 are preferably manufactured as individual components which are assembled into a blade. As previously described, the U-profile may itself comprise individual parts. Particularly, the girder part 14 of the U-profile may be another box cap part 20b similar, but typically with a different radius of curvature, to box cap part 20, see Fig. 16. The box cap part 20, and possibly also 20b, may preferably initially be connected to the girder parts 10, 12 and there after the two shell parts 26, 28 are subsequently connected thereto while simultaneously bonding or adhering the two shell parts 26, 28 at their trailing and leading edges.

The regions 30, 32 of the upper and lower shell parts where they are attached to the box part closing 20 and girder part 14 respectively, are in general thinner than the remaining regions of the shell parts.

Also in this embodiment, the box cap part 20 and the girder may be geometrically reversed so the box cap part 20 is located at the lower side and the girder part 14 located at the upper side of the blade. Furthermore, the longitudinal extension of the

girder with box cap part 20 in this embodiment may typically be the same as the extension of the girder with box cap part of Fig. 2.

In Fig. 8 is shown how the connections between the different components may subsequent to the assembly be provided with a protecting surface. In Fig. 8, the connection between trailing edge section 26, box cap part 20 and girder part 10 is shown as an example. Although the girder part 14 and the box cap part 20 as e.g. disclosed in Fig. 2 may constitute parts of the outer surfaces of the blade, these connections may be coated once the blade is assembled typically in order to provide a smooth transition between for instance the trailing edge section 26 or the leading edge section 22 and the box cap part 20 and/or the girder part 14. Such a coating is typically a surface finish which does not change any of the structural characteristics of the profile. The coating may also comprise adapted thin sheets or skins 38, or similar, of fibre reinforced plastic material that is laminated to the surfaces as an effective measure to protect the joints.

Figs. 9 - 12 show ways of connecting the upper part of the trailing edge section, box cap part and the U-profile. The connections may be made in several ways, and may primarily depend on the method used for the overall assembly of the blade components. Even though the details are only shown and described for the trailing edge section, they are also applicable for the leading edge section.

The laminate of the trailing edge section and box cap part may be bonded end to end on top of the flange on the U-profile as shown in Fig. 9. This solution demands a wide flange on the U-profile, but is advantageous in that the components may be assembled in any sequence desired.

The box cap part may be bonded on top of the U-profile before the trailing edge section is bonded on top of the box cap part as shown in Fig. 10. This solution has the advantage that the box profile may be assembled before the other components are bonded to the profile.

The trailing edge section and/or the leading edge section may be bonded on top or the side of an end region of the U-profile before the box cap part is bonded on top of the leading and trailing edge sections as shown in Figs. 11 and 12.

Figs. 13 – 15 show ways of connecting the lower part of trailing edge section and the U-profile. The connections may be made in several ways, and may primarily depend on the method used for the overall assembly of the blade components. Even though the details are only shown and described for the trailing edge section, they are also applicable for the leading edge section.

The laminate in the lower part of the trailing edge section is made with a flange, which makes it possible to bond the section to the side of the U-profile as shown in

Fig. 13. This solution makes it easy to align the two parts, and make a joint without any unevenness.

The laminate in lower part of the trailing edge section is bonded on top on the outside on the cap part of the U-profile as shown in Fig. 14. This solution facilitates an easier manufacturing of the trailing edge section. A further, substantially V-shaped bonding member may bond the inner surface of the trailing edge section and the side of the U-profile as shown in Fig. 15.

In Fig. 16 is shown an embodiment wherein the girder part 14 is equivalent to another box cap part 20b, similar to box cap part 20 but only reversed, thus facilitating another sequence of assembling the individual components.

Although the present invention has been described in connection with the specified embodiments it should not be construed as being in any way limited to the presented examples. The scope of the present invention is set out by the accompanying claim set. In the context of the claims, the terms "comprising" or "comprises" do not exclude other possible elements or steps. Also, the mentioning of references such as "a" or "an" etc. should not be construed as excluding a plurality. The use of reference signs in the claims with respect to elements indicated in the drawings shall also not be construed as limiting the scope of the invention. Furthermore, individual features mentioned in different claims, may possibly be advantageously combined, and the mentioning of these features in different claims does not exclude that a combination of features is not possible and advantageous.

CLAIMS

1. A wind turbine blade comprising

a girder substantially shaped as a U-profile,

a first shell part,

a second shell part, and

a box cap part,

wherein the girder and the box cap part constitutes, when assembled, a load carrying box profile of the blade and wherein the bottom part of the U-profile and the box cap part conform to the outer surface of the blade , and wherein the box cap part, the first shell part and the second shell part are connected to the girder.

2. A wind turbine blade according to claim 1, the first shell part constitutes a leading edge section of the blade and the second shell part constitutes a trailing edge section of the blade and wherein the bottom part of the U-profile constitutes a part of the outer surface of the blade substantially opposite the box cap part.

3. A wind turbine blade according to claim 1, the first shell part constitutes an upper shell part of the blade and the second shell part constitutes a lower part of the blade.

4. A wind turbine blade according to any of the preceding claims, wherein the individual components are manufactured separately.

5. A wind turbine blade according to claim 4, wherein at least some of the individual components are at least partly made of a carbon fibre reinforced plastic material.

6. A wind turbine blade according to any of the preceding claims, wherein the box cap part has a radius of curvature of at least 2 Meters.

7. A wind turbine blade according to any of the preceding claims, wherein one or both of the sides of the girder comprise a sandwich construction.

8. A wind turbine blade according to any of the preceding claims, wherein the girder further comprises connection means at an end region of the sides thereof.

9. A wind turbine blade according to claim 6, wherein the connection means comprises a flange integrated with the end region.

10. A wind turbine blade according to any of the preceding claims, wherein the box cap part further comprises one or more stiffening means provided in the longitudinal direction of the blade.

11. A wind turbine blade according to any of the preceding claims, further comprising a reinforcing member positioned inside the box profile and extending transversal to the longitudinal extension of the blade.

12. A wind turbine blade according to claim 11, wherein the reinforcing member is a plate.

13. A wind turbine blade according to claim 11 or 12, further comprising a plurality of the reinforcing members positioned spaced apart in appropriate positions along the longitudinal direction of the blade.

14. A method of producing a wind turbine blade comprising the steps of

producing a girder substantially shaped as a U-profile with a bottom conforming to a predetermined aerodynamic profile,

producing a first shell part having the shape of a part of the predetermined aerodynamic profile,

producing a second shell part having the shape of a part of the predetermined aerodynamic profile, and

producing a box cap part having the shape of a part of the predetermined aerodynamic profile,

connecting the box cap part to the girder thereby forming a load carrying box profile of the blade, and

connecting the first shell part and the second shell part to the girder.

15. A method according to claim 14, wherein the first shell part constitutes a leading edge section of the blade and the second shell part constitutes a trailing edge section of the blade and wherein the bottom part of the U-profile constitutes a part of the outer surface of the blade substantially opposite the box cap part.

16. A method according to claim 14, the first shell part constitutes an upper shell part of the blade and the second shell part constitutes a lower part of the blade.

17. A method according to any of claims 14 - 16, wherein the individual components are manufactured separately.

18. A method according to any of claims 14 - 17, wherein one or more of the individual components are at least partly made of a carbon fibre reinforced plastic material.

19. A method according to any of claims 14 -18, wherein the box cap part has a radius of curvature of at least 2 Meters.

20. A method according to any of claims 14 - 19, wherein one or both of the sides of the girder comprise a sandwich construction.

21. A method according to any of claims 14 - 20, wherein the girder further comprises connection means at an end region of the sides thereof.

22. A method according to claim 21, wherein the connection means comprises a flange integrated with the end region.

23. A method according to any of claims 11 - 19, wherein the box cap part further comprises one or more stiffening means provided in the longitudinal direction of the blade.

24. A method according to any of claims 11 - 23, further comprising the step of positioning a reinforcing member inside the box profile that extends transversal to the longitudinal extension of the blade.

25. A method according to claim 24, wherein the reinforcing member is a plate.

26. A method according to claim 24 or 25, further comprising the step of positioning a plurality of the reinforcing members spaced apart in appropriate positions along the longitudinal direction of the blade.

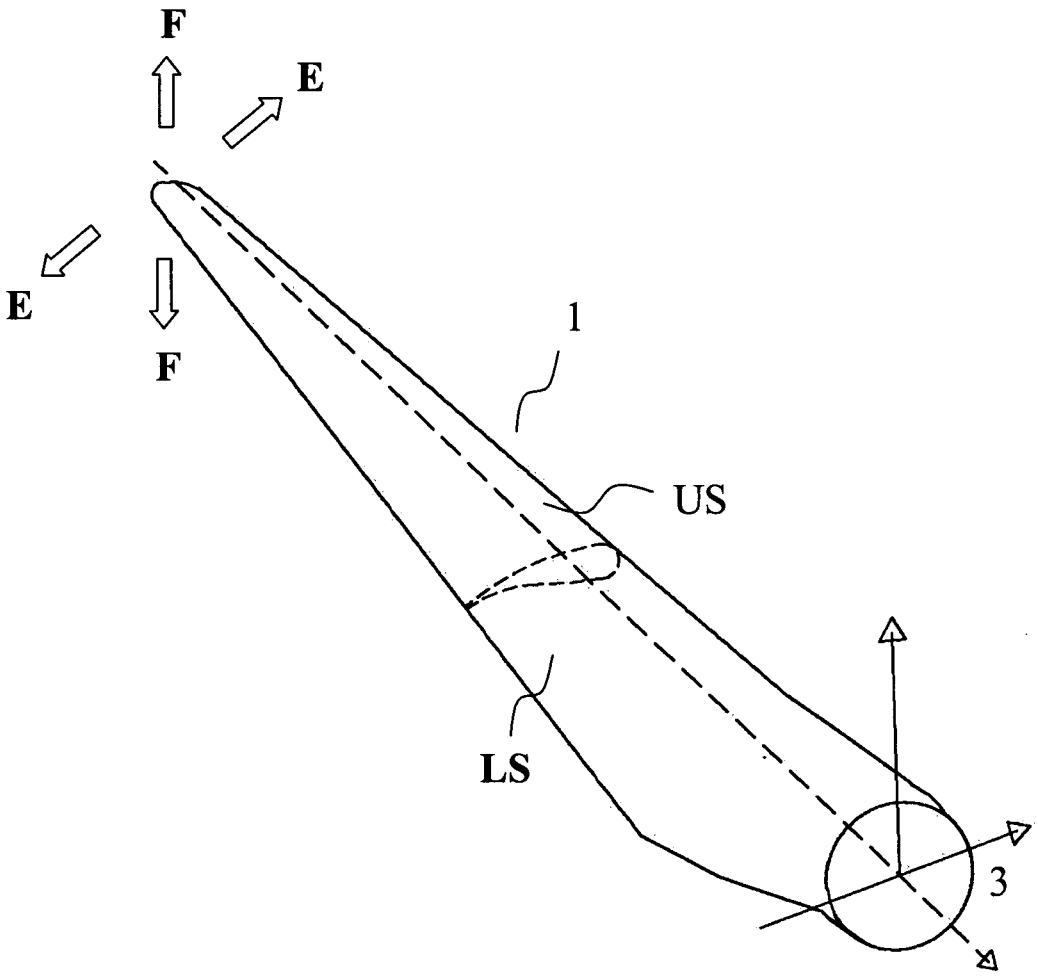

Fig. 1

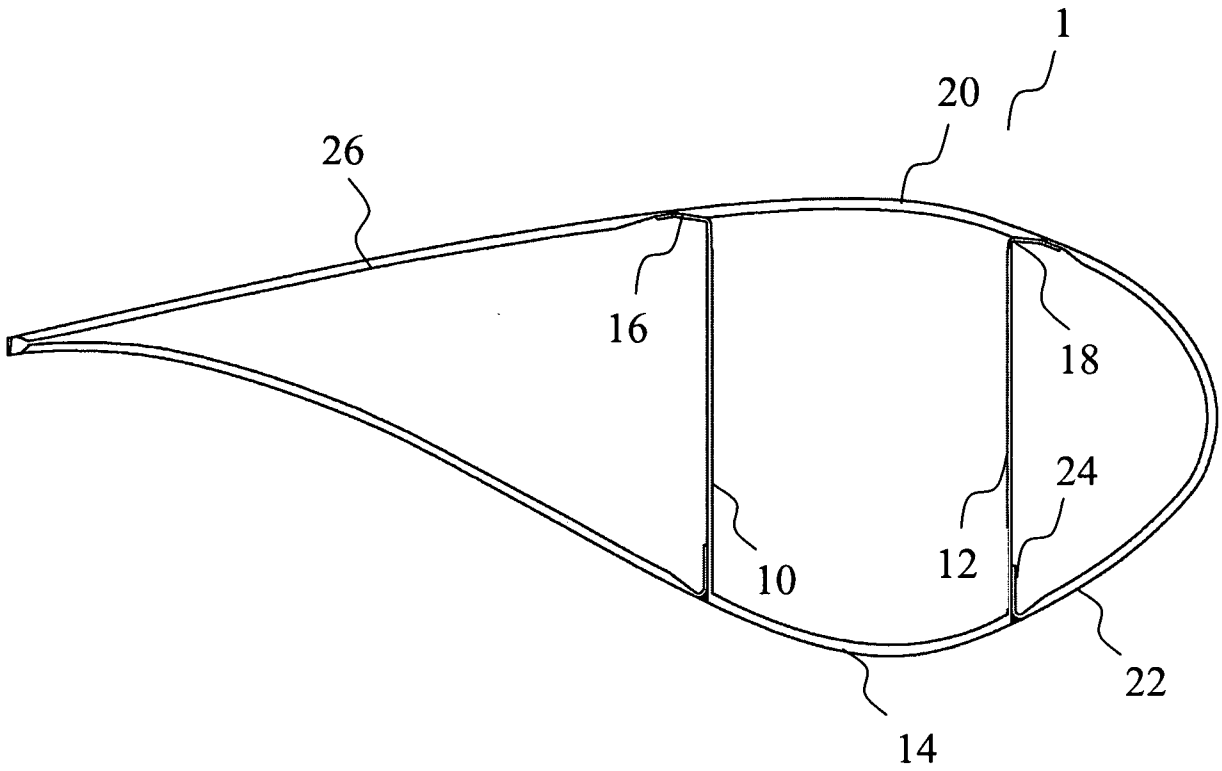

Fig. 2

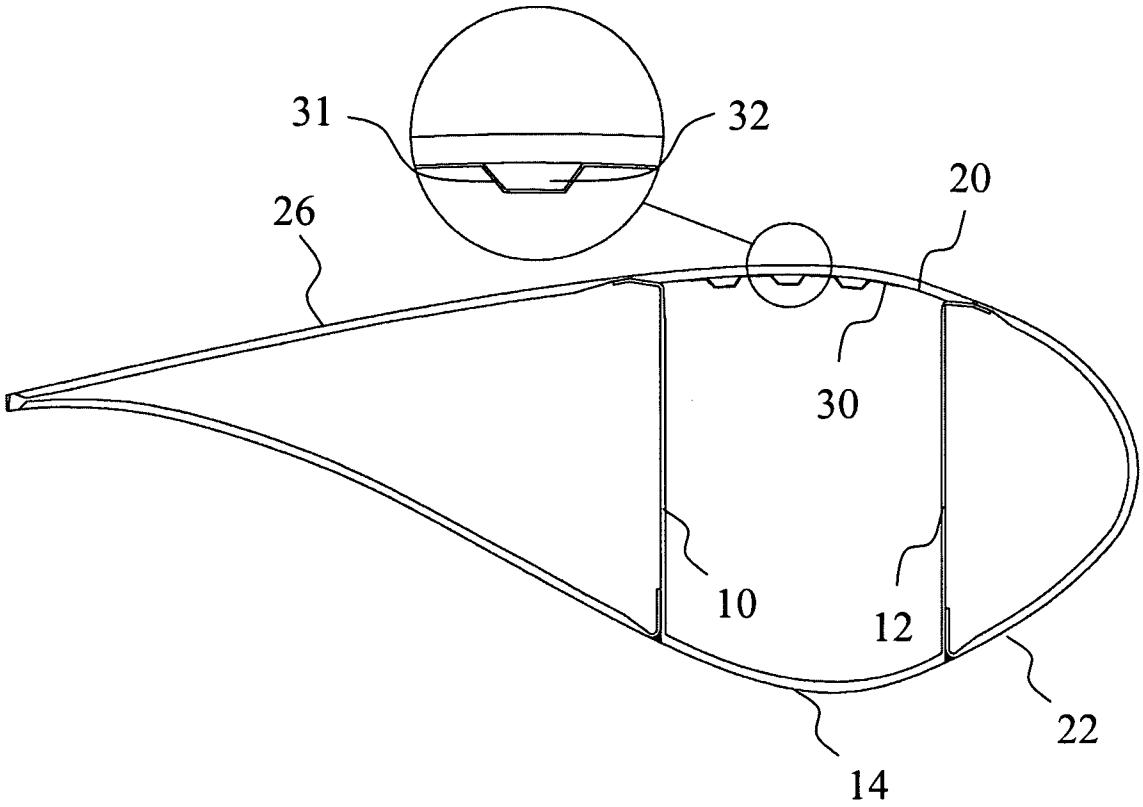

Fig. 3a

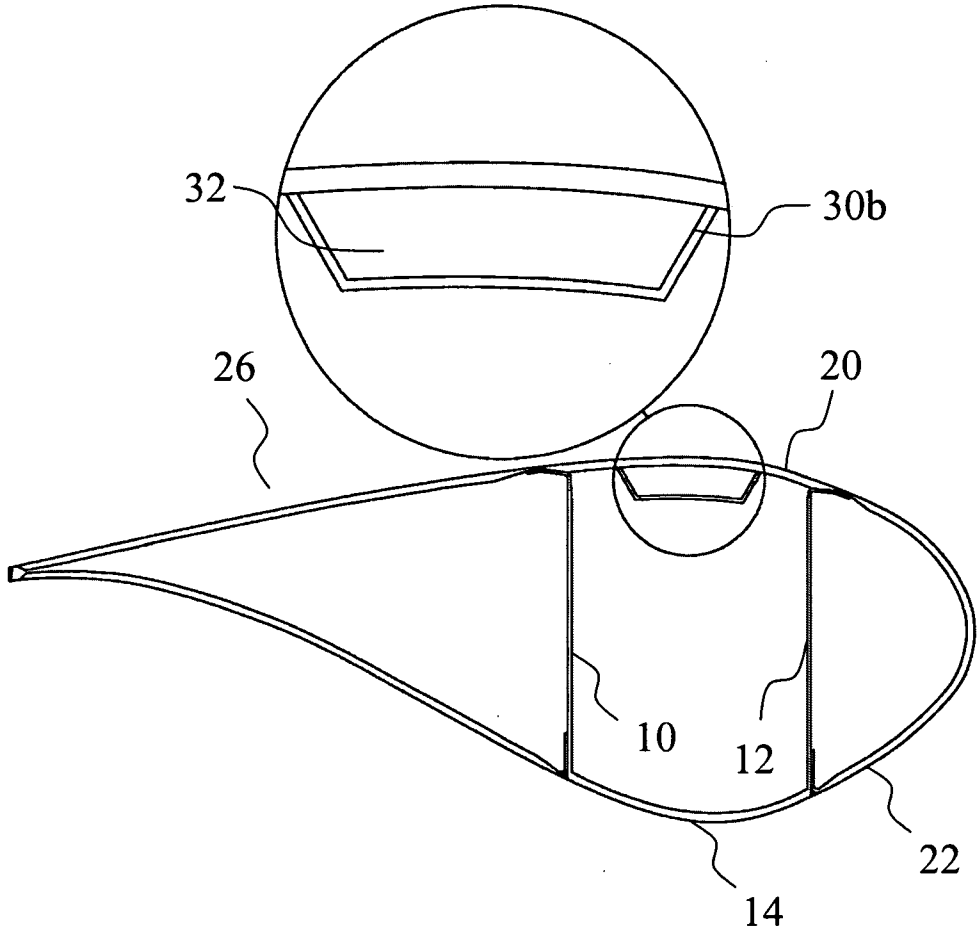

Fig. 3b

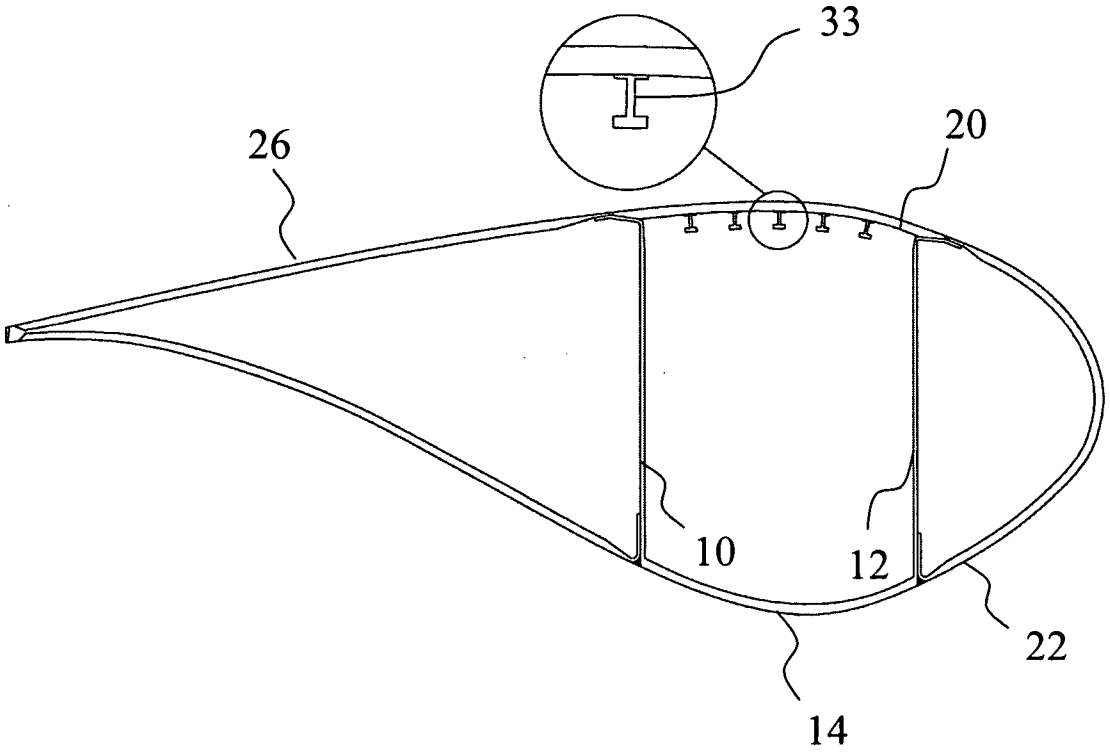

Fig. 4

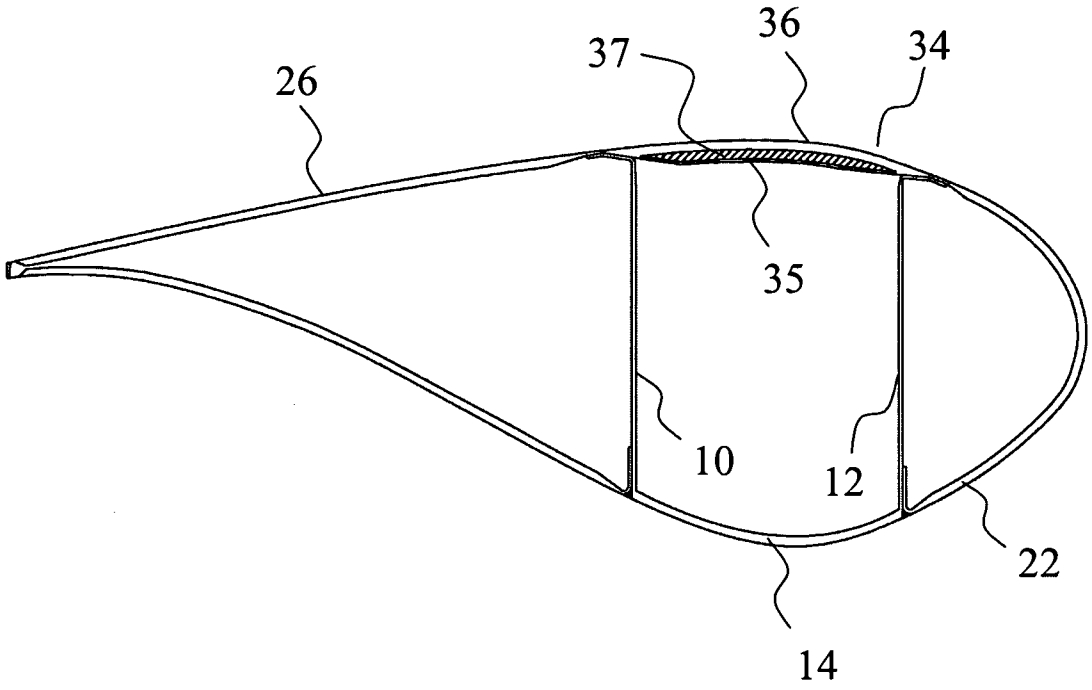

Fig. 5

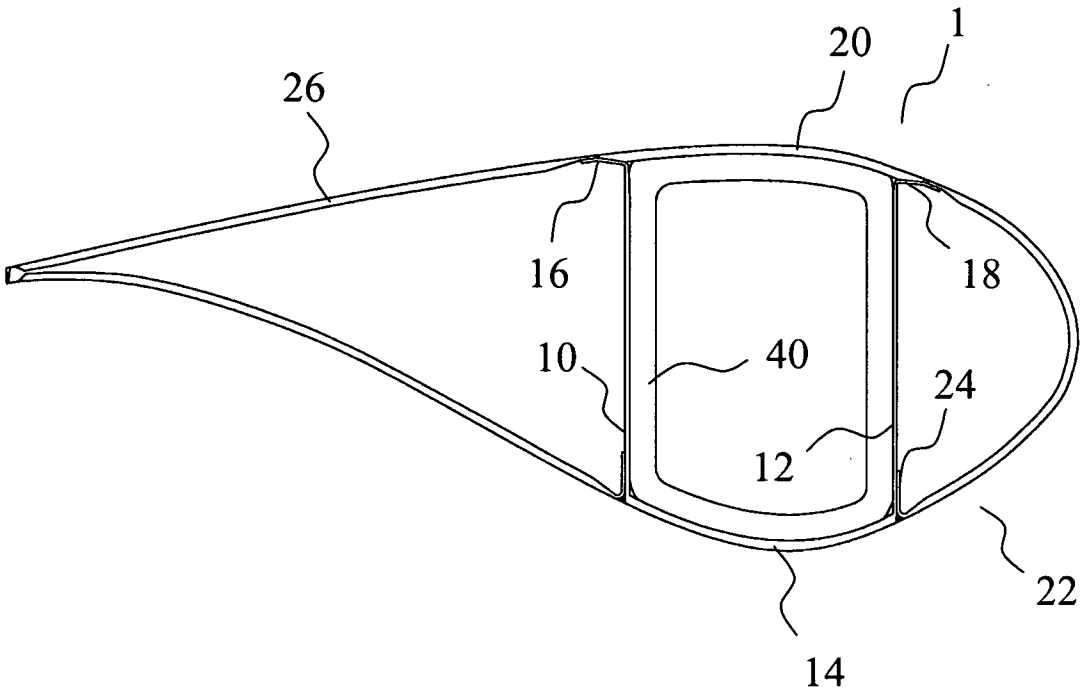

Fig. 6

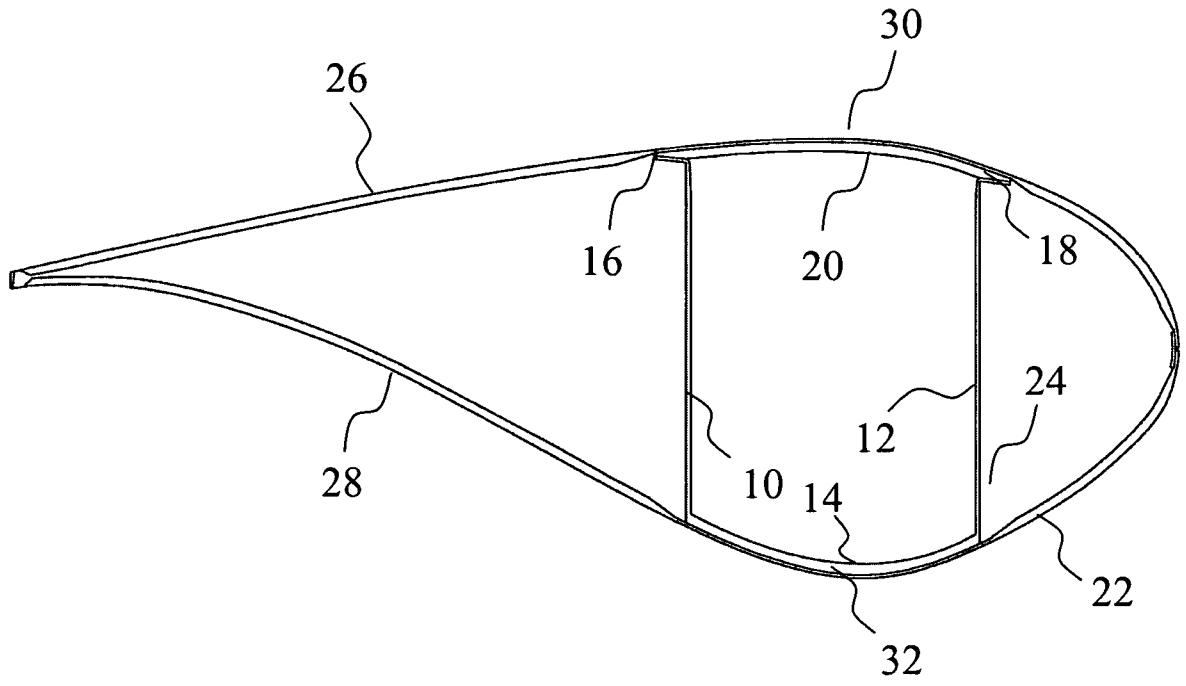

Fig. 7

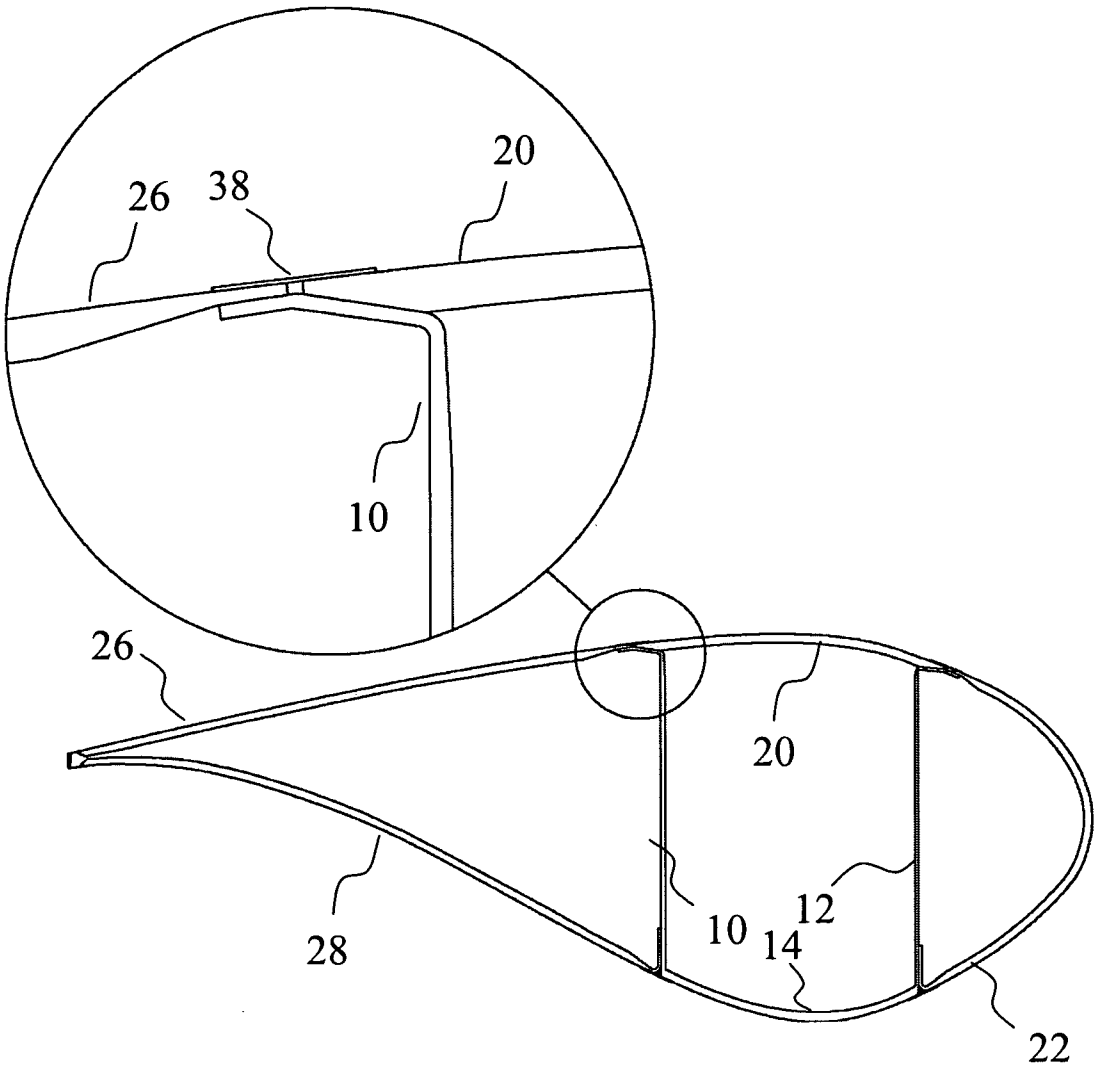

Fig. 8

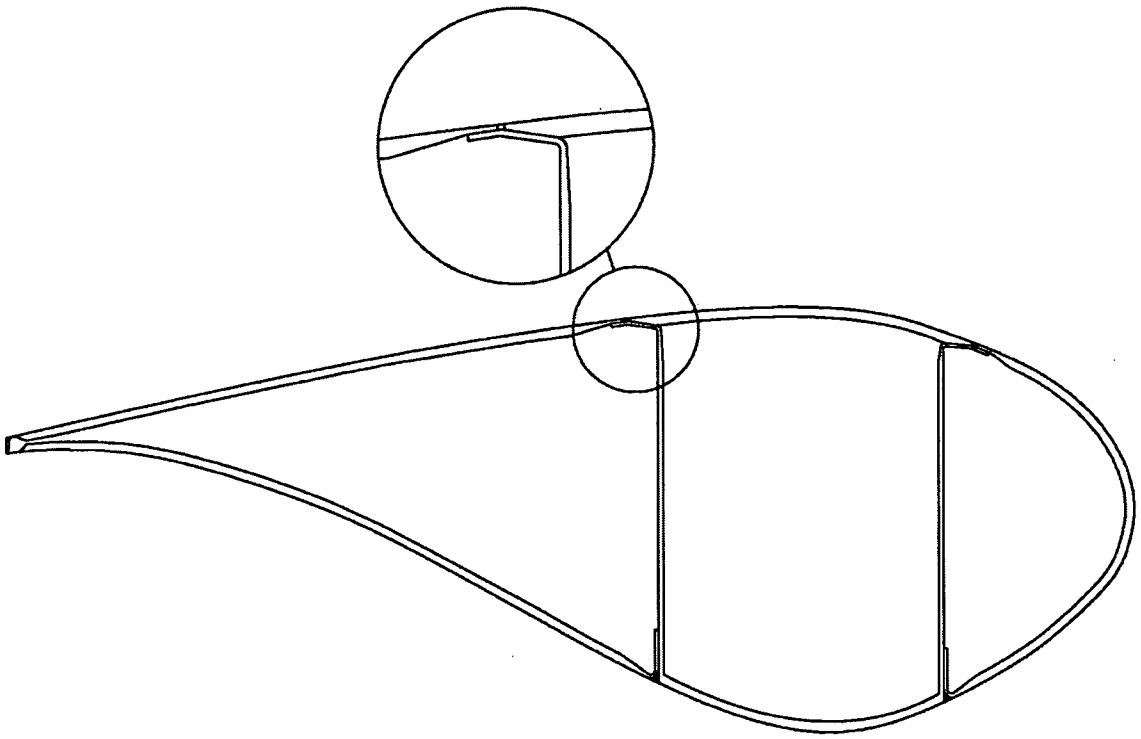

Fig. 9

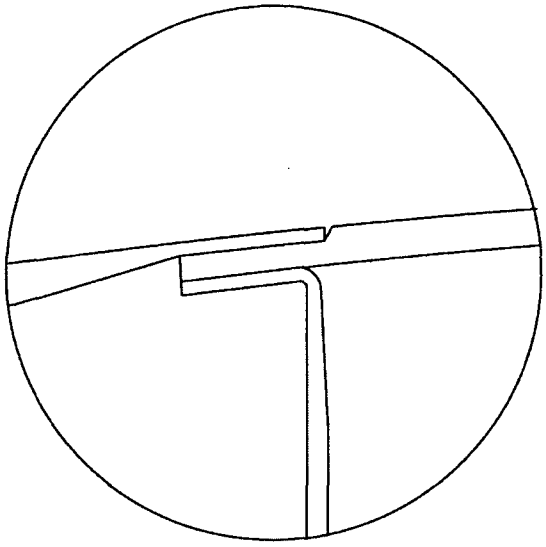

Fig. 10

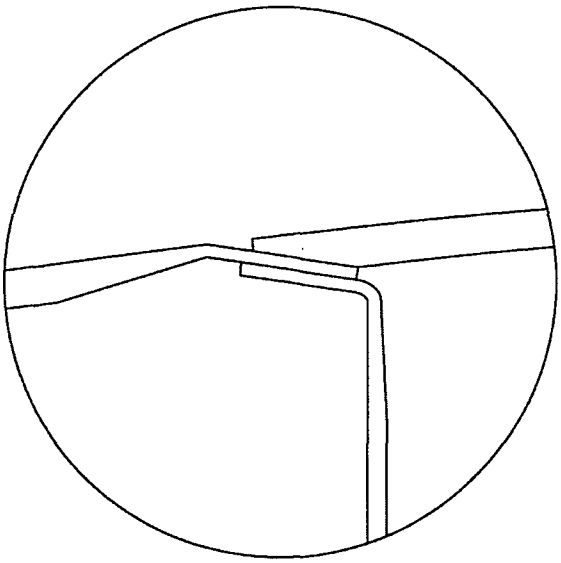

Fig. 11

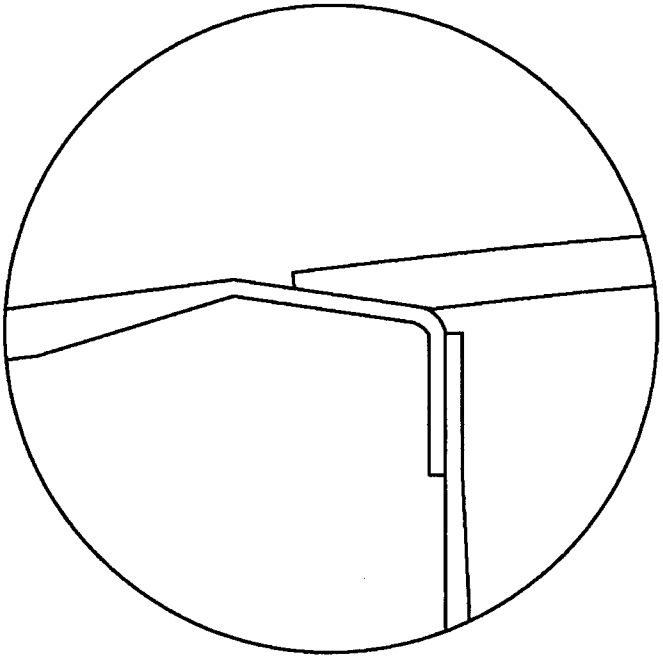

Fig. 12

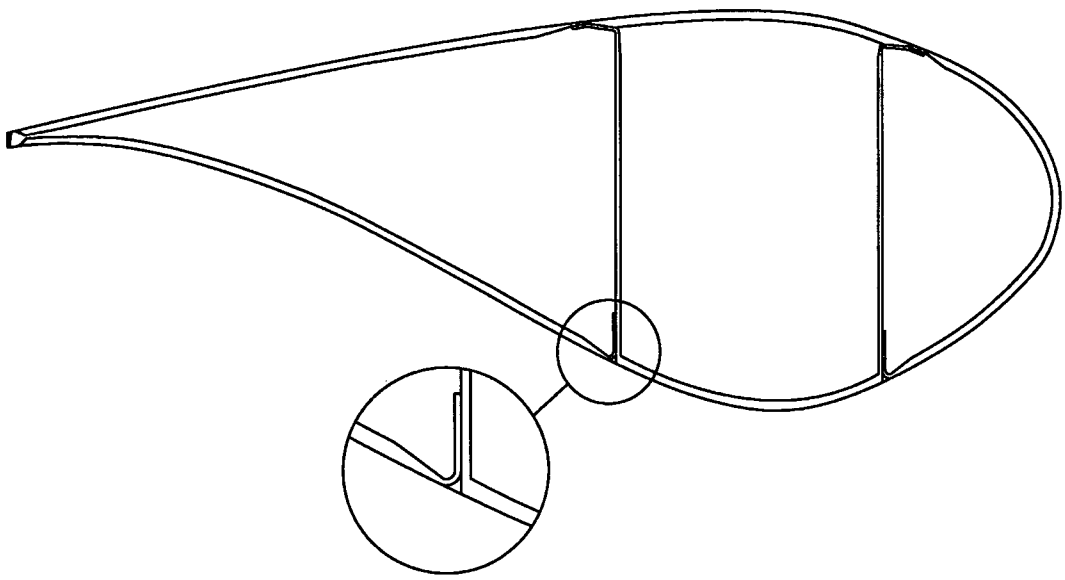

Fig. 13

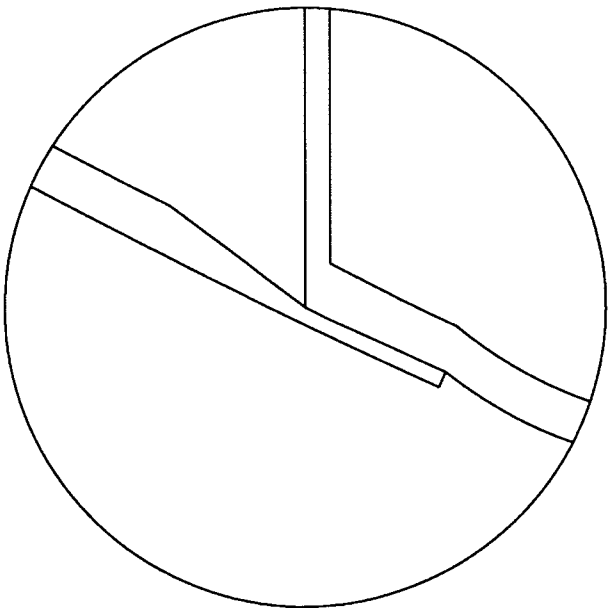

Fig. 14

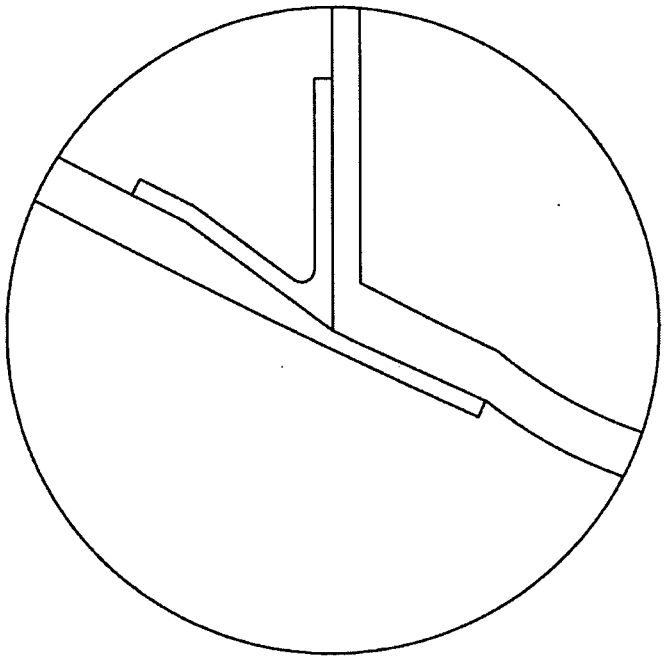

Fig. 15

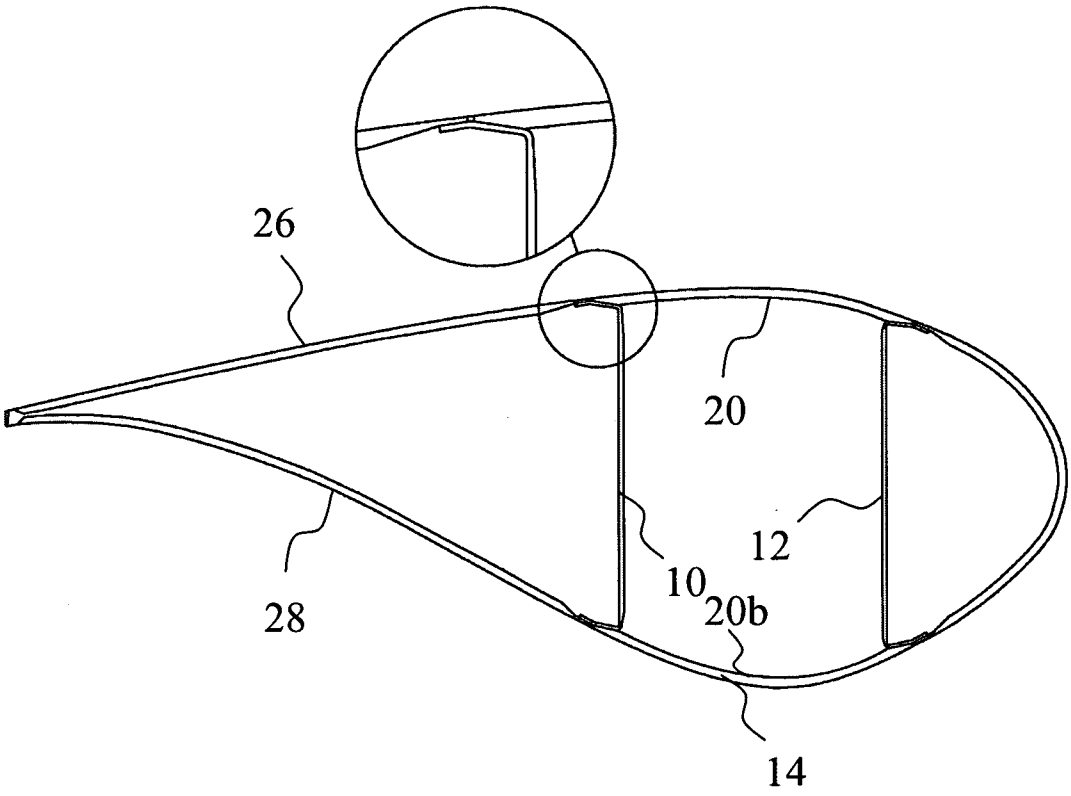

Fig. 16

Risø's research is aimed at solving concrete problems in the society.

Research targets are set through continuous dialogue with business, the political system and researchers.

The effects of our research are sustainable energy supply and new technology for the health sector.